Radioimmunotherapy with Yttrium Macrocycles

Norman

Radioimmunotherapy with Yttrium Macrocycles

by

Timothy John Norman B.Sc. (Hons.)

University of Durham Chemistry Department

A Thesis submitted for the degree of Doctor of Philosophy

September 1994

DECLARATION

The contents of this thesis represents the work of the author unless otherwise acknowledged by reference. The thesis describes results of research carried out in the Department of Chemistry at the University of Durham, at Celltech Ltd., Slough, and at the Medical Research Council's Radiobiology Unit, Harwell between October 1991, and September 1994. It has not been submitted for a degree at this or any other university.

STATEMENT OF COPYRIGHT

ACKNOWLEDGEMENTS

I would like to express my sincere thanks to my supervisor Prof. David Parker for his enthusiastic support and guidance through the course of my work. I am also indebted to Alice Harrison of the MRC Radiobiology Unit in Harwell for providing all the radiochemical and biodistribution data, and to Dr. D. King for the hospitality and assistance given during my time at Celltech. Others who deserve thanks include Lenny Lauchlan who guided me through the exciting world of HPLC, and all the members past and present of the research group.

Last but no means least, I would like to thank my family and my wife Karen for their support and encouragement throughout my research and the typing of this thesis. Thank you !

ABSTRACT

RADIOIMMUNOTHERAPY WITH YTTRIUM MACROCYCLES

Timothy John Norman (September 1994)

Monoclonal antibody fragments (Fab') which recognise tumour-associated antigens provide an ingenious means of selectively targeting a therapeutic radionuclide to a tumour for radioimmunotherapy. The radionuclide yttrium-90, a long range β^- emitter, was chosen to deliver a sterilising dose of radiation to the tumour.

A selection of novel functionalised macrocyclic ligands based on a 1,4,7,10-tetraazacyclododecane skeleton have been synthesised, and the stabilities of their yttrium (III) and gadolinium (III) complexes studied *in vitro* through association and dissociation measurements, and *in vivo* through animal biodistribution studies. The radiolabelled complexes do not dissociate *in vivo*.

Maleimides are compounds which are capable of selectively reacting with a thiol of an antibody fragment. Selective functionalisation of one of the yttrium binding macrocyclic ligands with either one or three maleimides has been carried out, and the resulting compounds conjugated to tumour seeking humanised antibody fragments. Subsequent radiolabelling with ^{90}Y, gave the desired tumour targeting drug for use in radioimmunotherapy.

Acridines are a class of intercalating agents which are capable of reversibly binding to DNA. A maleimide functionalised ligand derivatised with acridine was formed. Conjugation of this compound to antibody fragments capable of entering a tumour cell, may permit drug binding to tumour cell DNA, and thus enhance the targeting efficacy of the radiolabelled conjugate.

ABBREVIATIONS

DMF	Dimethylformamide
DMSO	Dimethylsulphoxide
TFA	Trifluoroacetic acid
BOC	t-Butoxycarbonyl
BOCON	2-(t-Butoxycarbonyloxyimino)-2-phenylacetonitrile
DCC	Dicyclohexylcarbodiimide
EDC	1-(3-Dimethylaminopropyl)-3-ethylcarbodiimide
β-ME	β-Mercaptoethylamine
PBS	Phosphate Buffered Saline
SDS	Sodium Dodecylsulphate
Tris	Tris[hydroxymethyl]amino-methane
HOBT	Hydroxybenzotriazole
DOTA	1,4,7,10-tetraazacyclododecane-1,4,7,10-tetraacetic acid
EDTA	Ethylenediamine-tetraacetic acid
DTPA	Diethylenetriamine-pentaacetic acid
m.p.	Melting Point
t.l.c.	Thin Layer Chromatography
T_R	Retention time
IR	Infra-Red
UV	Ultra-Violet
HPLC	High Performance Liquid Chromatography
NMR	Nuclear Magnetic Resonance
FAB	Fast Atom Bombardment
DCI	Desorption Chemical Ionisation
V.T.	Variable Temperature
IgG	Immunoglobulin G antibody
Ab	Antibody
Fab'	Antibody fragment
DNA	Deoxyribonucleic acid
RNA	Ribonucleic acid

TABLE OF CONTENTS

Chapter 1

Introduction

1.1 INTRODUCTION

The work described herein could be described as a fusion of both clinical oncology and synthetic chemistry, and it is this multidisciplinary approach which leads us to draw on the resources not only of a chemistry department, but also on the expertise of the Medical Research Council's Radiobiology Unit at Harwell, and on the biological skills of my sponsors Celltech Ltd.. It is this blurring of the so often too rigid boundaries of science which may in the future lead to both novel and improved approaches to medicine, and science in general.

Effective methods for the radioimmunotherapy of cancer have been explored with a view to employing the cytotoxic properties of particulate radiation in the selective irradiation of cancerous tissues. The term 'radioimmunotherapy' is self explanatory in that the term 'radio' refers to the use of radiation, and 'immuno' refers to the use of some form of immunological approach, in our case the exploitation of the selective and precise nature of antibody-antigen recognition of the human immune system, and finally 'therapy' infers the therapeutic benefit of this approach.

1.2 CANCER

"*Cancer, created by life itself,*
exists within life,
Yet in the end makes life untenable." [1]

Cancer can be thought of as a departure from the constraints of normal cell growth control.[1,2] The extent and rate to which healthy cells grow is normally controlled. Cancerous cells however, do not appear to respond to normal growth control mechanisms, and spread chaotically with no apparent consideration for their immediate environment. This often leads to a swelling called a tumour.

There are two distinct forms of tumours; benign, which do not spread, but merely confine themselves within a capsule, and the more dangerous malignant tumour. Malignant tumours shed cells into the blood and lymphatic streams which subsequently localise in other organs leading to the formation of secondary (metastatic) tumours.

Cancer is caused initially by the damage / mutation of a cell's DNA. This damage can be attributed to a number of factors such as exposure to radiation, certain chemicals, and specific viruses, but it may be many years until these dormant cells become active and develop into a tumour.

1.3 THE PREVALENCE OF CANCER

Cancer is a very common disease being the cause of death for a high proportion of people, and is classified according to the organ from which it originates. The incidence rates of cancers are highly age and sex specific. For instance, there is a logarithmic increase with age for the incidence of cancer of the lung and colon, whereas the number of cases of cancer of the testes peaks in men of 32 years old.[2] Many cancers such as lung, stomach and liver cancer are also more common in men, although many of these different rates can be attributed to working environments, and social habits such as smoking, eating and drinking.

1.4 THE TREATMENT OF CANCER

1.4.1 Surgery

There are two principal options for the treatment of cancer: surgery and therapy. Surgery is the front line approach to cancer, being however only effective

and practical in the removal of large easily accessible tumours, usually of a benign nature. More inaccessible and dispersed malignant tumours (metastases) require a different approach.

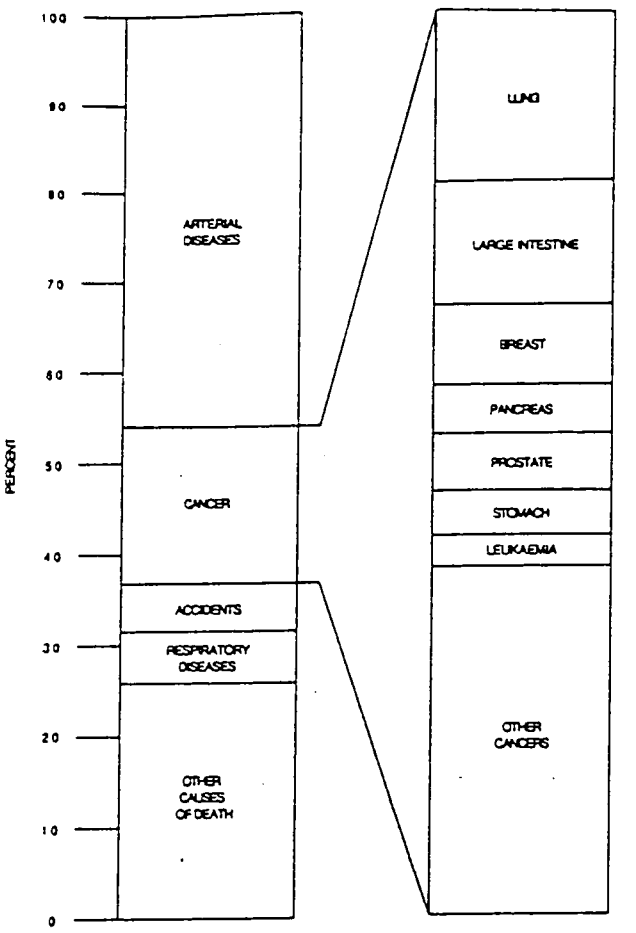

Figure 1.1 : *The incidence of cancer in the USA in 1975.*[3]

1.4.2 Chemotherapy[1,2,4,5]

It is in the treatment of metastatic tumours where chemotherapeutic drugs come into their own. As yet, chemotherapy is crude with little or no distinction between its action on cells of a specific tumour, and normal cells of the rest of the body. The potency of most conventional chemotherapeutic drugs can be attributed to their action on the DNA of rapidly dividing cells. It is at the point of division that

cells are at their most vulnerable. Unfortunately, tumour cells are not necessarily dividing faster than all those in healthy tissues, and thus cells such as the bone marrow and the mucosa of the gastro-intestinal tract are also vulnerable, leading to undesirable toxic side effects. It is this current problem of selectivity which needs to be surmounted.

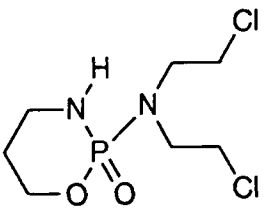

Cyclophosphamide

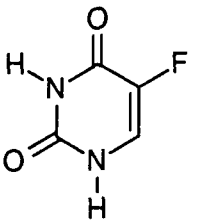

5-Fluorouracil

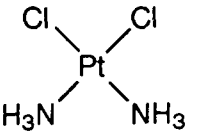

Cisplatin

Figure 1.2 : *Examples of some chemotherapeutic drugs currently in use.*

The mode of action of chemotherapeutics varies. Cyclophosphamide, a DNA alkylating agent causes intermolecular cross linking in DNA hence inhibiting replication, 5-Fluorouracil fraudulently incorporates into DNA halting further synthesis, and the drug Cisplatin has had remarkable success with testicular cancer owing to its guanine binding ability.

1.4.3 Radiotherapy[1]

An alternative approach to the cytotoxic effects of chemotherapeutics is the effect of radiation. Again cells are more sensitive to radiation damage when they are dividing, or when immature. The magnitude and nature of damage caused to a cell will depend on the amount of energy absorbed, and the nature of the absorbing tissue. Irradiation of a cell can damage its membrane, or cytoplasm, but more importantly its nuclear DNA which contains the biological coding for replication. Damage can be observed as a swelling of the cell as the damaged membrane allows extra fluid in, by a cloudiness of the cytoplasm indicating damage to its components

(e.g. mitochondria), and by fragmentation of the chromosomes. Although other forms of damage will also lead to immediate cell death, it is this multiple cleavage of the chromosomal DNA which is most important, as a toxic dose of radiation which acts directly on the DNA must affect the whole cell since it is the DNA which regulates the cell's life.

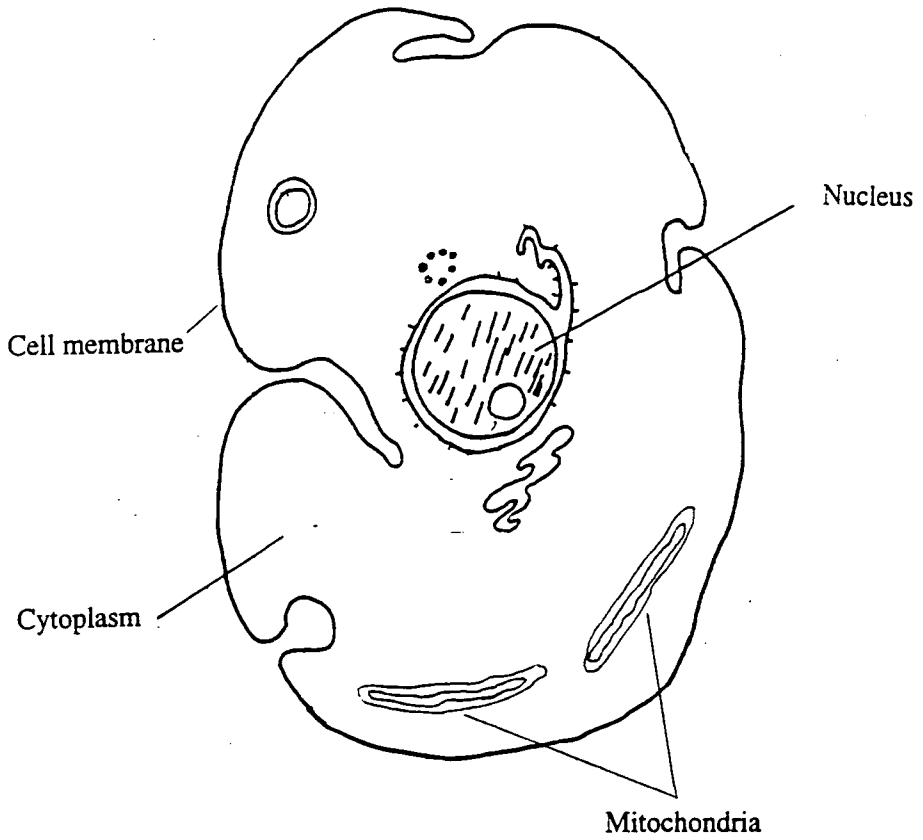

Figure 1.3 : *The structure of a human cell.*

Conventional radiotherapy relies on the use of external radiation sources such as a linear accelerator (which produces therapeutic X-rays or β^- particles), the more powerful betatron (produces β^- particles), or radioactive cobalt (produces γ rays). For the treatment of a deep tumour, e.g. cancer of the lung (approx. 10-15 cm deep), a radiation energy of 4 MegaVolts could be required because, as Figure 1.4 shows, the percentage of administered radiation reaching a tumour may be small, as the majority of the radiation is absorbed by the intervening healthy tissue.

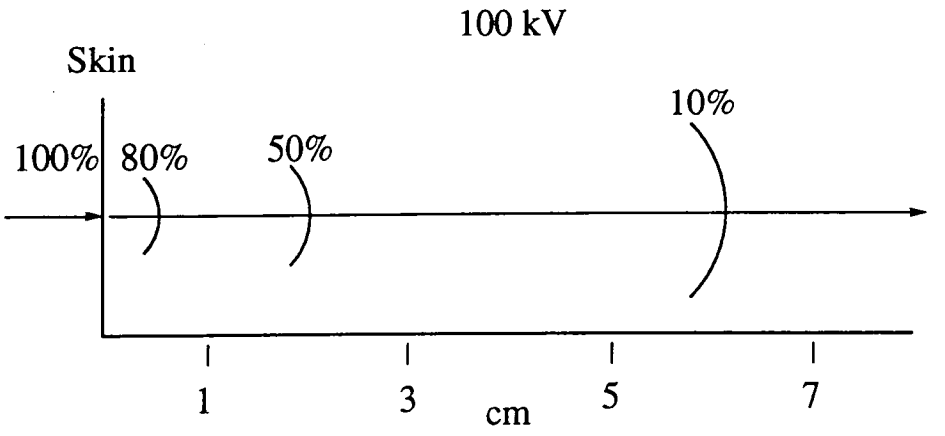

Figure 1.4 : *A depth-dose profile for a 100 kV source, showing the relationship between the depth of radiation penetration and the fraction of the total dose received. (Source : ref. 1)*

The use of lead blocks and templates is necessary to localise the radiation dose to a small area, but clearly the inherent problem with this approach is that in order to reach a deep seated cancer, the radiation must first pass through, and damage healthy tissues. In fact, irradiation of a tumour can later lead to the onset of another different tumour, caused ironically by the very radiation which was supposed to cure the patient. Again, as with chemotherapy, what is required is some degree of tissue specificity.

1.5 ANTIBODIES AND ANTIGENS

1.5.1 Cell Surface Antigens

The surface of a cell contains a mosaic of different glycoproteins and glycolipids.[2,6] Some of these molecules are shared by many types of cells, and others are more specific, in some cases being limited to one particular type of cell. If

these molecules elicit a response from the human immune system, i.e. if they stimulate the production of antibodies they are classed as antigens.

Tumour cells, although similar in many ways to normal cells, do exhibit some crucial differences. When a cell becomes malignant it may express a tumour-specific antigen on its surface. Being able to make use of this important difference between healthy and cancerous cells may enable us to target tumours.

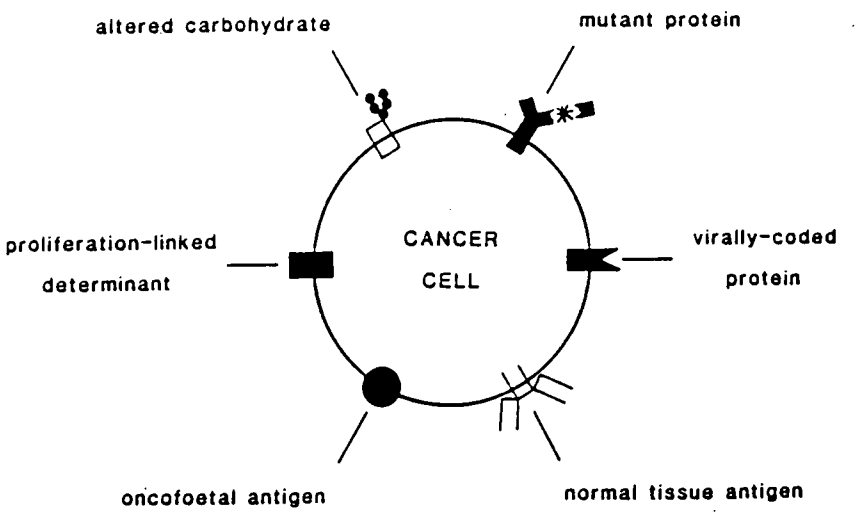

Figure 1.5 : *Possible antigenic targets on the surface of a cancer cell.*

(Source : ref. 2)

Each particular antigen on the cell surface will have its own complement antibody to which it will bind to in a "lock and key" manner.

1.5.2 Antibodies [2,4,6]

An antibody (or Immunoglobulin) is a protein synthesised by the immune system in response to a foreign material (antigen). The most common type of antibody found in the blood stream is Immunoglobulin G (IgG). This antibody has an overall mass of 150,000 Daltons with a complex folded three-dimensional

structure, approximated to a 'Y' shape in two dimensions. The antibody comprises of four polypeptide chains: two identical heavy chains (H) (50,000 Da) held together by a disulphide bond in the hinge region, and two identical light chains (L) (25,000 Da) each joined by a disulphide bond to one of the heavy chains.

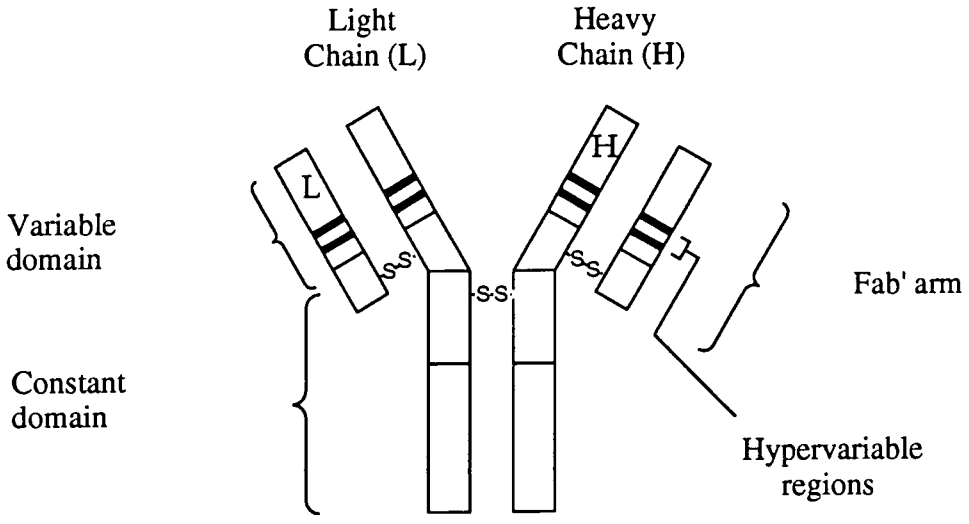

Figure 1.6 : *The structure of a typical IgG antibody.*

In the variable domains of each of the four chains exist hypervariable regions which form an antigen binding site (seven amino acid sequence) at the end of each Fab' arm. It is this site ("key") which is responsible for binding to the hapten ("lock") on the antigen (Figure 1.7).

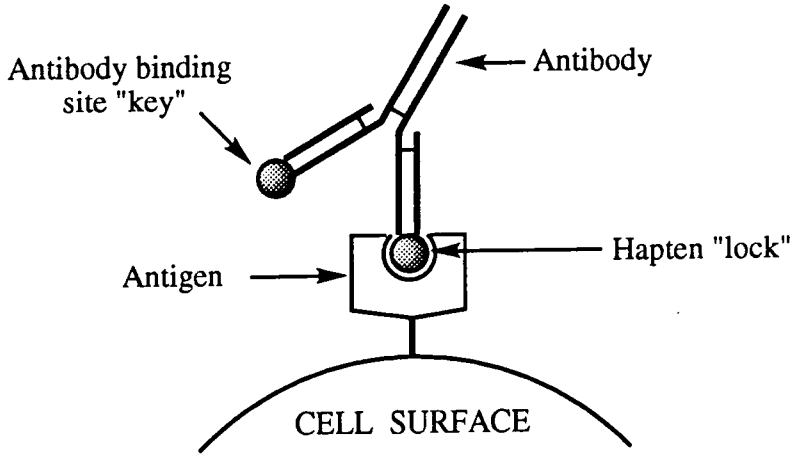

Figure 1.7 : *The specificity of antibody-antigen binding.*

1.6 ANTIBODIES FOR TUMOUR TARGETING

1.6.1 Radioimmunotherapy

Tumour targeting may be achieved through the judicious use of an antibody specifically designed to bind only to a tumour associated antigen. It was as long ago as 1957 that Pressman [7] conceived this idea of a "magic bullet" approach to the treatment of cancer utilising the property of an antigen-antibody interaction, but it was not until Köhler's and Milstein's discovery of hybridoma technology in 1975 [8] that antibodies of a sufficiently high tumour specificity became available to test Pressman's theories.

This is the basis of my work, the intention being to inject into a patient's bloodstream a radiation source (radionuclide) bound to a tumour specific antibody which will in turn bind only to the tumour. In this way we hope to localise radiation damage solely to the target tumour, and hence negate the need for high doses of deeply penetrating external radiation. This use of antibodies in conjunction with a therapeutic radionuclide is known as "radioimmunotherapy".

In its simplest form, something of the nature shown below is a synthetic target.

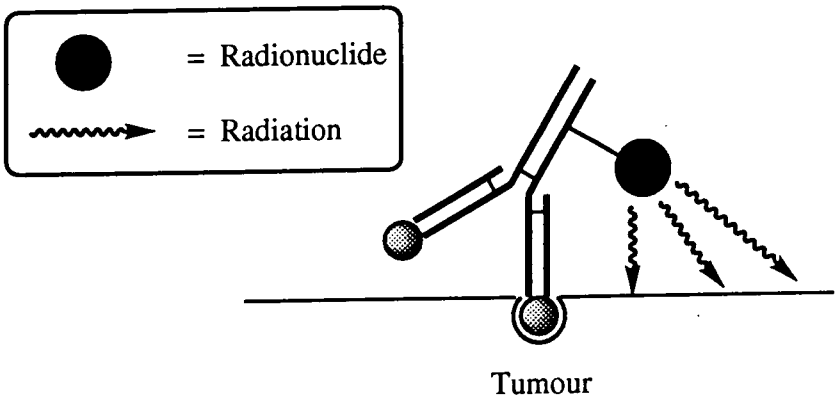

Figure 1.8 : *The principle of radioimmunotherapy.*

1.6.2 Polyclonal Antibodies

Unfortunately, tumour cells have many differing antigens on their surfaces, some found on many tissues, and others found only on tumours. In response to the presence of these antigens the immune system will produce a variety of antibodies ("polyclonal"), each specific for an individual antigen on the tumour cell's surface. For radioimmunotherapy we are interested only in tumour specific antibodies, and as it is not possible to separate these from the rest of the polyclonal mixture, an alternative approach to obtaining pure "monoclonal", tumour-specific antibodies is required.

1.6.3 Monoclonal Antibodies[9]

In 1975 Köhler and Milstein discovered [8] that if they fused a mouse myeloma cell (a malignant mouse lymphocyte with the capacity for continuous proliferation) with a healthy lymphocyte from the spleen of a mouse immunised against a specific antigen (which will therefore produce antibodies specific to that antigen), the resulting hybrid species retained the abilities of its parents in that it continuously produced large quantities of an identical "monoclonal" murine antibody. Using this technique, any antibody can be produced for any given antigen, e.g. those found only on a tumour cell. Köhler and Milstein's technique for monoclonal antibody production is shown in Figure 1.9.

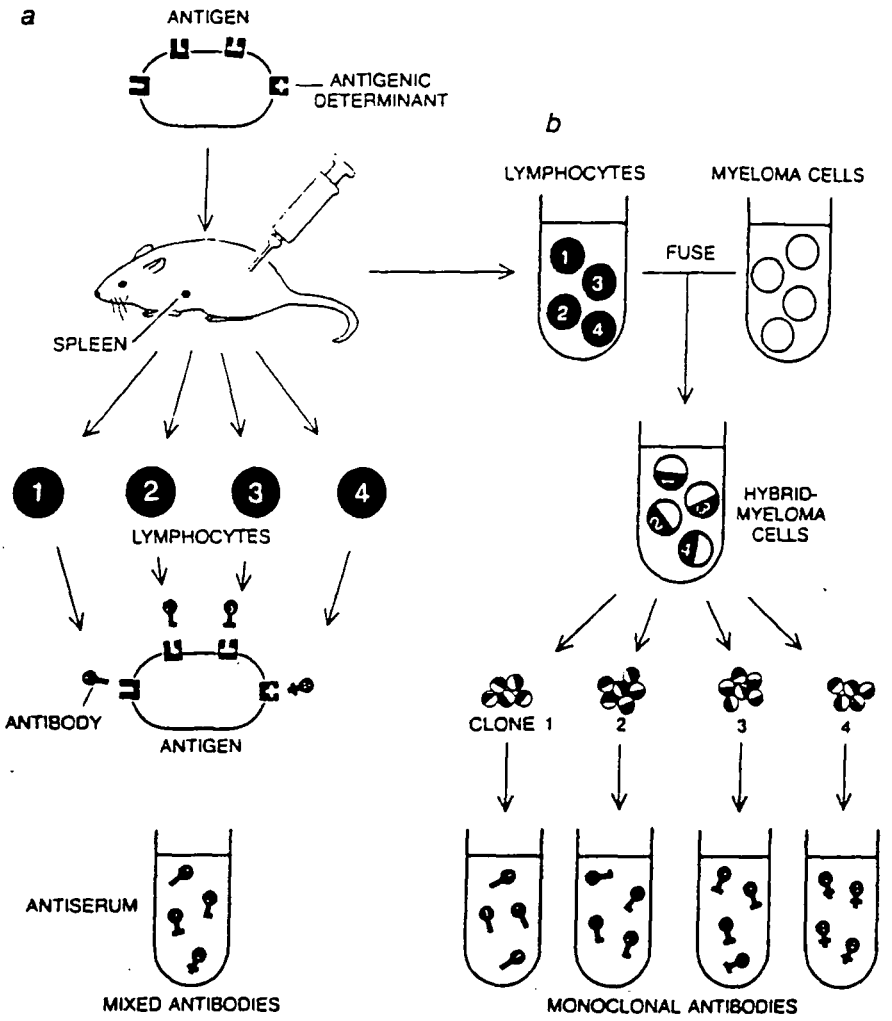

Figure 1.9 : *Monoclonal antibody production. (Source : ref. 9)*

1.6.4 Chimeric Antibodies

There is a fundamental flaw in the use of monoclonal mouse antibodies in humans in that they are themselves immunogenic, invoking an immune response (a HAMA response = Human Anti Murine Antibody) which will seriously damage the efficacy of immunotherapy, and can produce allergic side effects.[10,11] Unfortunately, production of a monoclonal human antibody in an analogous manner proved both experimentally difficult and ethically unsound, as the only source of

these antibodies is from the spleen of cancer victims. An alternative approach had to be found.

Chimeric antibodies appear to be one solution to the problem.[12,13] Using modern genetic engineering techniques it is now possible to introduce the human coding for the constant region of an antibody (it had been shown that it was the constant region of the murine antibodies which was the most immunogenic) into a mouse myeloma cell, and obtain large quantities of a monoclonal antibody with a human constant region and a mouse variable region, retaining the original antigen binding specificity, but being substantially less immunogenic.[14] More recently geneticists have gone one step further to the goal of a human monoclonal antibody in the production of a "humanised" antibody. This antibody has both human constant and variable regions, but the binding sites of the hypervariable regions remain murine in their nature, and has been shown to elicit a minimal immune response.[15,16]

1.6.5 Antibody Fragments[4]

For radioimmunotherapy, as well as not invoking an immune response, antibodies must satisfy certain criteria with regards to their rate and ability to penetrate tissues, and their rate of clearance from non-target tissues. These processes are essentially size and shape dependent, the smaller the antibody or fragment thereof, the faster its distribution around the body.

The antigen binding sites of an antibody are found in the hypervariable regions of the two Fab' arms. Thus, from the point of view of radioimmunotherapy, the constant region of an antibody becomes superfluous. Using the protease enzyme papain, an antibody can be selectively cleaved in the hinge region, yielding two Fab' fragments (and also an Fc fragment) (Figure 1.10), which have been shown to retain their binding affinity, and as a bonus show less of an immune response than the intact, parent antibodies.

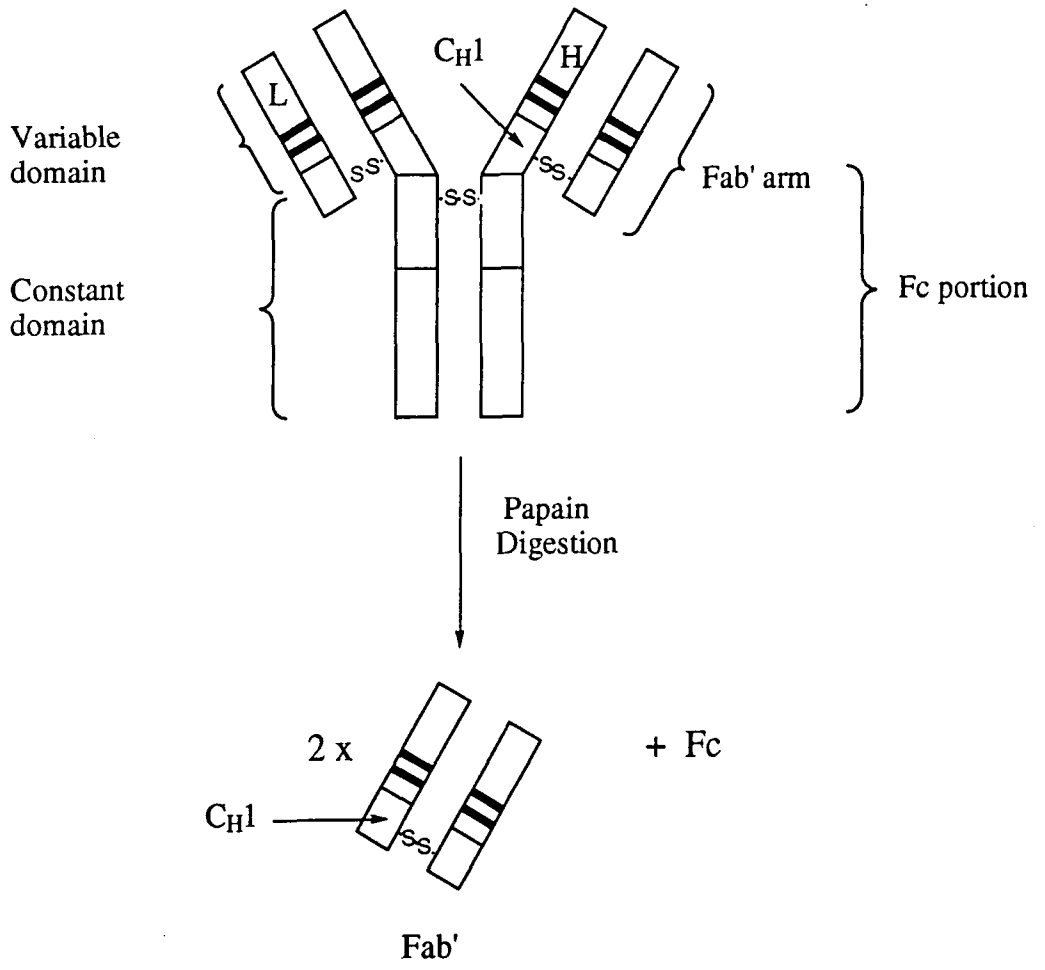

Figure 1.10 : *Papain site-selective digestion of IgG.*

As a result of their diminished size, Fab' fragments are able to localise more quickly, penetrate more deeply (thus improving access to more hindered regions of a tumour), and significantly reduce the time for unbound antibody to clear from non-target tissues thereby reducing irradiation of healthy tissues.[17] As a consequence, it would appear that the future of radioimmunotherapy lies in the use of either chimeric or humanised monoclonal antibody fragments.

1.7 CHOICE OF RADIONUCLIDE FOR RADIOIMMUNOTHERAPY

There are a number of radioinuclides available for therapy, the choice of which depends on the tumour morphology and the radionuclide's properties.

1.7.1 Tumour Morphology[18]

Densely packed tumours are often poorly vascularised resulting in a complicated pattern of diffusion gradients guiding radiolabelled antibodies through the tumour. As a consequence of this, and the lack of uniformity of antigen expression on tumours ('cold spots' occur where no antigens are found), some tumour cells will remain unbound by radiolabelled antibodies, and hence require efficient cross-fire from neighbouring cells to receive a sterilising dose of radiation. This necessitates the use of a long range β^- emitter (see Figure 1.11).

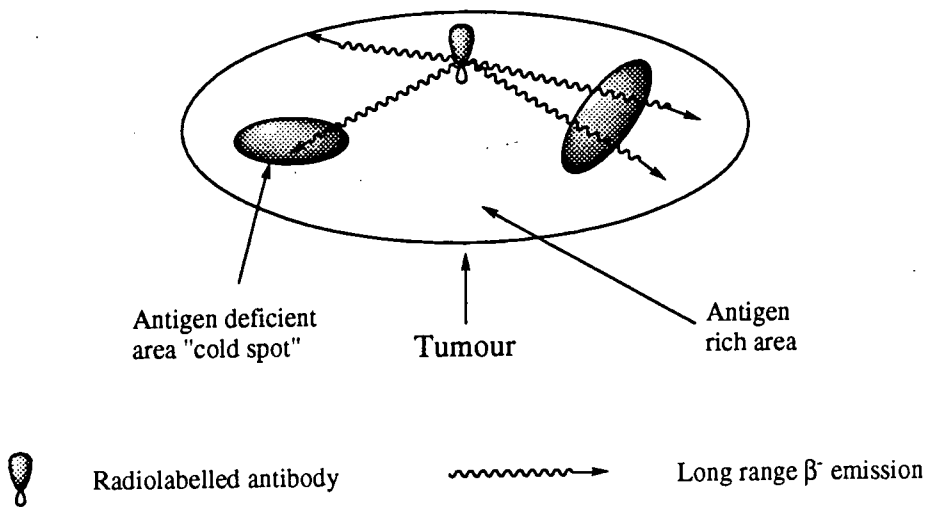

Figure 1.11 : *The importance of long range β^- emission in the treatment of a tumour with non-uniform antigen expression.*

If however the target is single circulating cancer cells such as those found in leukaemia, then a short range (0.1 mm) β^- emitter or an α emitter is required as long range emission could damage surrounding healthy cells. The need for short rather than long range emission can be seen in Figure 1.12.

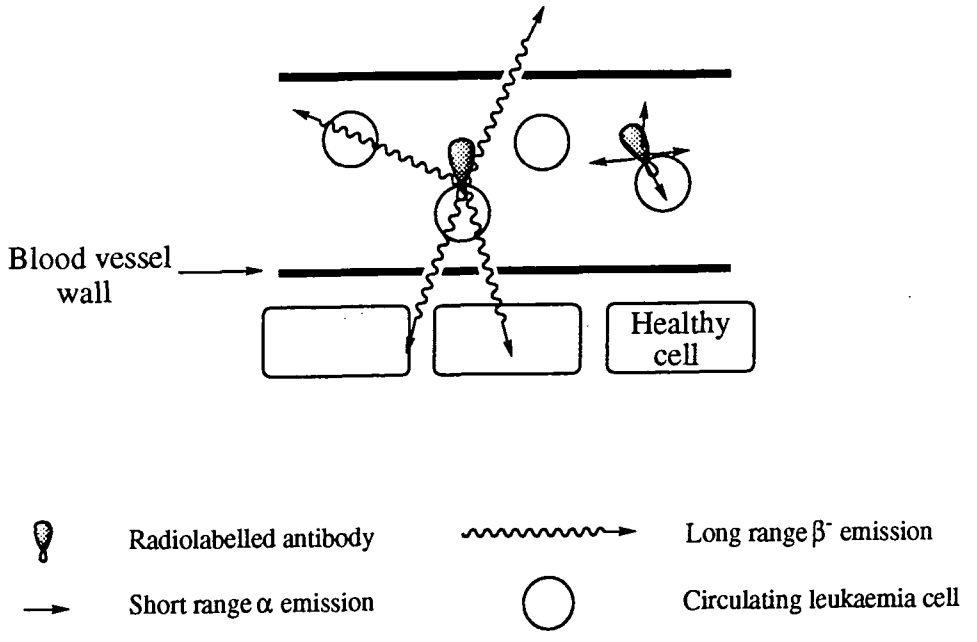

Figure 1.12 : *A short range emitter is required to minimize irradiation of healthy cells when treating circulating leukaemia cells.*

1.7.2 Radionuclide's Properties

The aim of radioimmunotherapy is to deliver to the target as great a dose of sterilising radiation over as short a time as possible, so as to effect efficient DNA double strand cleavage. Suitable radioisotopes are either α and β^- emitters with little or no γ component. To be useful, the radioisotope must comply to some exacting criteria. Firstly, it must be cheap, readily available, of a high chemical purity, and free from "cold" isotopes. It must be amenable to attachment to an antibody and decay to a stable daughter.

Also of prime importance is the half life ($t_{1/2}$). This should be in the region of 10 to 200 hours; sufficiently long to allow transport to the target, yet not so long as to deliver its radiation dose over too long a period. A list of possible radionuclides along with their properties is given below in Table 1.1.

Radionuclide	$t_{1/2}$ (hours)	β^-max (MeV) %	Mean range (mm)[b]
^{90}Y	64	2.25 (100%)	3.9
^{67}Cu	62	0.40 (45%) 0.48 (3%) 0.58 (20%)	0.2
^{186}Re	90	1.07 (74%) 0.93 (21%)	1.1
^{188}Re	17	1.96 (18%) 2.12 (80%)	3.3
^{131}I	193	0.61 (90%)	0.4
^{111}Ag	179	1.04 (93%) 0.69 (6%)	1.1
^{161}Tb	166	0.45 (26%) 0.57 (64%) 0.58 (10%)	0.3
^{199}Au	75	0.25 (22%) 0.30 (72%)	0.1
^{212}Bi	1.01	7.2[a]	0.1
^{211}At	7.21	6.8[a]	0.1

a) The α particle energy.

b) 0.1 mm is approximately equal to 10 cell diameters.

Table 1.1 : *Possible candidates for use in radioimmunotherapy.*

The following conclusions can be drawn. Copper-67 with its low β^- energy may be suitable for the treatment of leukaemia and small metastases,[19] but is expensive and difficult to obtain carrier-free. The two isotopes of rhenium (186 and 188) require a complex prelabelling protocol, whilst the relative ease of dehalogenation of iodine-131 *in vivo* poses practical problems for its use. A stable complex of silver-111 is as yet to be found,[20] terbium-161 is difficult to obtain carrier-free, whilst complex stability rules out the use of gold-199.

Of the α emitters, only ^{211}At and ^{212}Bi are plausible candidates,[21,22,23] but the ease of dehalogenation of the former, and the shortness of the half life of the latter may rule these out.

1.7.3 Yttrium-90 for Radioimmunotherapy

Of the original candidates proposed for radioimmunotherapy only ^{90}Y remains. It can be produced cheaply and in high chemical and radiochemical purity from a ^{90}Sr generator and decays ($t_{1/2}$ 64 hours) with a single high energy β^- emission to a stable zirconium daughter.

$$^{90}_{39}Y \xrightarrow{\beta^-} {}^{90}_{40}Zr$$

It is the long path length (4mm) of this β^- emission which makes ^{90}Y ideally suited for the treatment of densely packed tumours. The combination of all these points makes ^{90}Y the obvious choice for radioimmunotherapy, although it must be noted that because of a similar coordination chemistry to Ca^{2+}, free $^{90}Y^{3+}$ will preferentially localise in the bones, the radiotoxic effect of which has potentially fatal repercussions (myelosuppression, a reduction of the body's immune system due to damage of the bone marrow will result).

1.8 BIFUNCTIONAL COMPLEXING AGENTS FOR YTTRIUM

1.8.1 Requirements

Being a metal, yttrium cannot be directly attached to an antibody, but must first be bound by a metal complexing agent which has been functionalised in such a way as to enable it to be covalently bound to an antibody. This type of moiety is referred to as a "bifunctional complexing agent" because of its dual role in binding both the desired radionuclide and the antibody. Initial attempts to synthesise bifunctional complexing agents for yttrium centred around the use of functionalised EDTA[24,25] and DTPA.[26,27]

The earliest documented example of a bifunctional complexing agent however, was in 1968 when Benisek and Richards bound transition metals to hen egg white lysozyme using picolinimidate (Figure 1.13).[28]

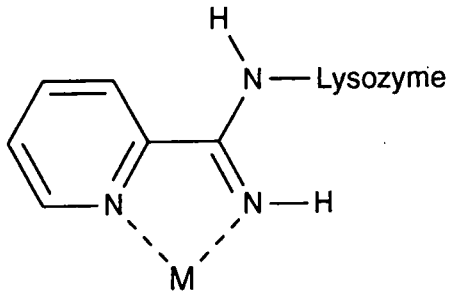

Figure 1.13

As a result of the toxicity of yttrium-90 *in vivo*, any proposed bifunctional complexing agent for $^{90}Y^{3+}$ must satisfy two important criteria. Firstly the metal complex formed must be kinetically stable with respect to acid and cation catalysed dissociation *in vivo* (there are regions of pH as low as 2 in the stomach and liver, and cation concentrations in serum are high $[Ca^{2+}]$ = 1.25 mM, $[Zn^{2+}]$ = 0.01 mM). Secondly radiolabelling of the complexing agent must be efficient (in excess of 90% in < 30 min.) under conditions compatible with antibody integrity (pH 4-7.5, 4-40°C),

and under concentrations mirroring those to be found in an antibody conjugate (5 to 10 μM).

Although a group three element, the coordination chemistry of yttrium resembles that of the lanthanides. This can be attributed to its possessing a similar charge density and ionic radius (1.07 Å for a coordination of 9) because of the "Lanthanide Contraction".[29] The variation of the ionic size with coordination number for yttrium and the lanthanides highlights this similarity, and is shown below in Figure 1.14.

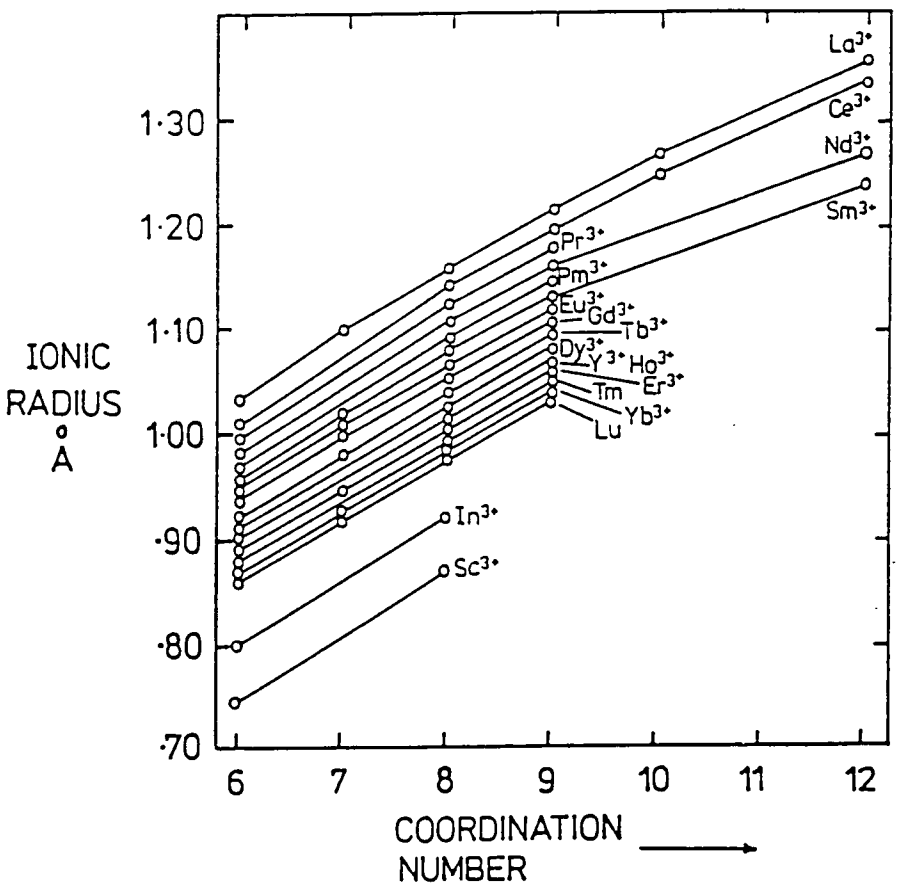

Figure 1.14 : *Effective Ionic Radii vs Coordination Number for yttrium and the lanthanides.*

Yttrium shows a preference for ligands containing hard nitrogen or oxygen donors which form 8 or 9 coordinate complexes (Figure 1.15).

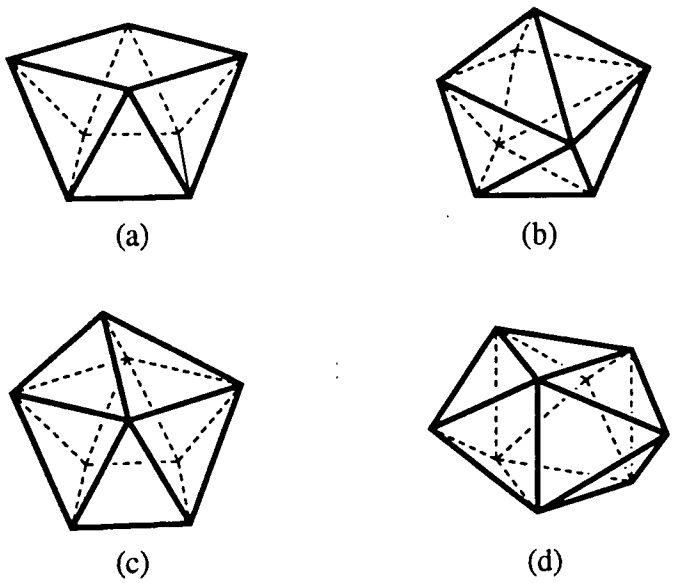

Figure 1.15 : *8 coordinate (a) square antiprismatic and (b) dodecahedral and 9 coordinate (c) monocapped square antiprism and (d) tricapped trigonal prism geometries of yttrium.*

Considering initially only the metal complexing part of a suitable bifunctional linker (the mode of linkage to the antibody will be discussed later in Section 1.9), there are two principal types of ligands available: *acyclic*, and *macrocyclic.*

1.8.2 Acyclic Complexing Agents

The most commonly used acyclic complexing agents are derivatives of EDTA **(I)** [25,30] and DTPA (**(II)**, **(III)**, and **(IV)**).[27,31] EDTA **(I)** being only hexadentate (yttrium requires octadentate coordination) was found to form yttrium complexes that were too unstable for use *in vivo* (log K_{ML} = 18.1). DTPA **(IIIa)** however is ideally suited to bind Y^{3+} in that it provides eight donor atoms (3 nitrogens and 5 oxygens) and was shown to form a very thermodynamically stable complex with yttrium (log K_{ML} = 22.1).[32] This high stability can be accounted for by virtue of the "chelate effect" [33] whereby there is a favourable entropy term in the displacement of nine water molecules surrounding the yttrium cation by one chelating ligand.

$$DTPA^{5-} + Y(H_2O)_9^{3+} \rightleftharpoons Y.DTPA^{2-} + 9\,H_2O$$

Although the thermodynamic stability of the complex was found to be reasonably high in *serum* studies, with 8% dissociation over 24 hours,[34] this did not take into account regions of low pH and high cation concentration *in vivo*. As the primary route for DTPA metal complex dissociation is acid catalysed (complex is sufficiently flexible to permit protonation of one of the binding nitrogen atoms), the *in vivo* stability was accordingly found to be appreciably lower than that found in serum studies.

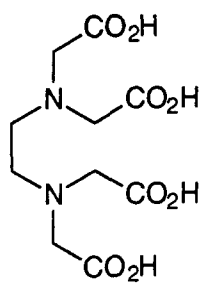

(I)

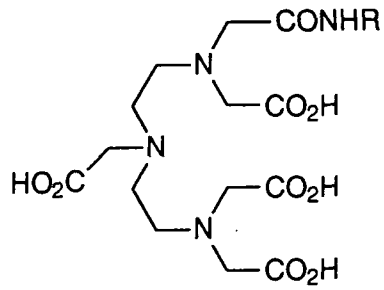

(II)

In the first attempts to use functionalised DTPA, the so called DTPA anhydride product (**II**) showed stability results poorer than DTPA owing to the replacement of one carboxylate donor by an amide. A study in human serum (37°C, pH 7.4) highlighted this point when backbone functionalised DTPA (**IIIb**) was shown to dissociate 45 times more slowly than (**II**).[35] DTPA derivatives (**IIIb**) also showed slightly enhanced *in vivo* stability compared to DTPA (**IIIa**) due to the extra complex rigidity imparted by the side chains. Further backbone functionalisation as in (**IV**) sterically hinders the breakage of metal chelate rings and improves the orientation of the chelating groups,[36] further increasing complex stability.[23]

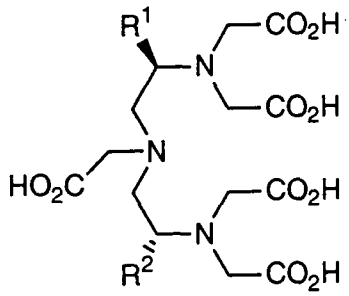

(III)

(a) $R^1 = R^2 = H$

(b) R^1 = H or Me

R^2 = 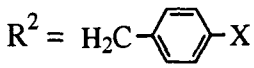

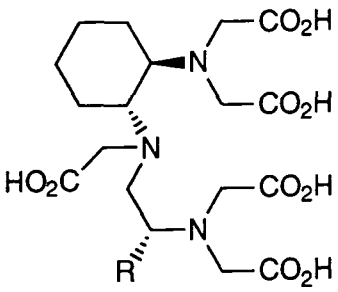

(IV)

R = H or 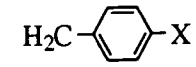

X = NO_2 or NCS

Unfortunately, these derivatives were still not of sufficient stability for safe *in vivo* use, thus ruling out DTPA based radioimmunotherapy, as significant quantities of yttrium would build up in the bone.

Other related acyclic chelating agents include (**V**) BOPTA, developed by Bracco of Italy for use with gadolinium in magnetic resonance imaging (MRI), and EGTA (**VI**) and TTHA (**VII**) [37] also considered for use in MRI. Although (**V**) forms a relatively stable Gd complex (log K_{ML} = 22.5), the corresponding yttrium complex

(like those of EGTA (**VI**) and TTHA (**VII**)) is not sufficiently stable with respect to acid-catalysed dissociation to allow safe *in vivo* use.

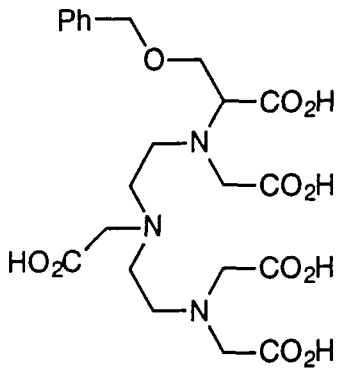

(V)

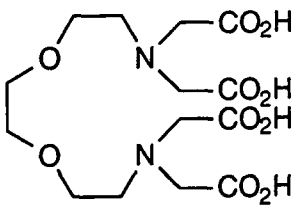

(VI)

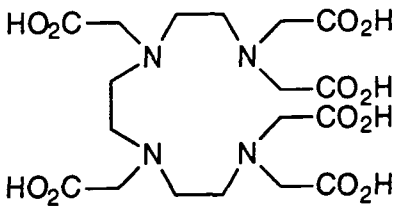

(VII)

Although backbone functionalised DTPA derivatives do go some way to improving kinetic stability, a further enhancement is still needed to warrant use with $^{90}Y^{3+}$.

1.8.3 Macrocyclic Complexing Agents

Although acyclic yttrium complexes, specifically those based on DTPA, have been shown to exhibit high thermodynamic stability, their use in therapy is compromised by their inherent lack of kinetic stability. Macrocyclic complexing agents however have been shown to display both the required thermodynamic and more importantly, *kinetic* stability.

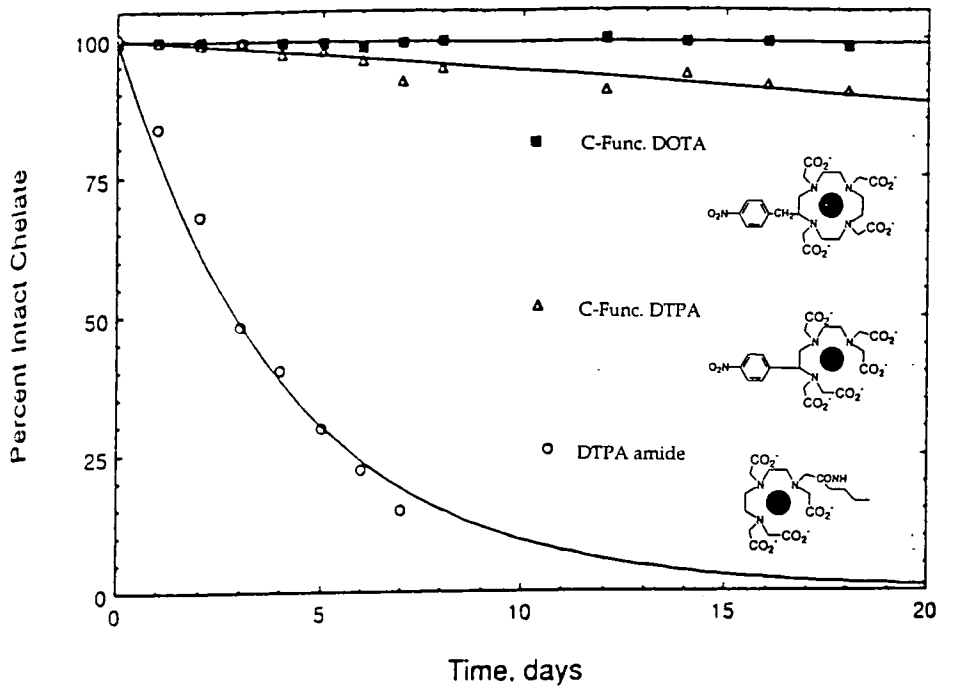

Figure 1.16 : *Loss of yttrium from acyclic and macrocyclic chelates in serum (37°C, pH 7.4), showing the enhanced stability of a macrocyclic complex. (Source : ref. 34).*

As mentioned earlier, yttrium requires an octadentate ligand containing hard nitrogen or oxygen donors. Yttrium also shows a preference for ligands which will form complexes of a square antiprismatic or dodecahedral geometry. With this in mind, a number of tetra-aza cycles of varying ring size and varying functionality have been synthesised, the most important being 12-membered 1,4,7,10-tetra azacyclododecane-1,4,7,10-tetraacetic acid (DOTA) (**VIIIa**) [38] and its derivatives,[39,40] 13-membered 1,4,7,10-tetraazacyclotridecane-1,4,7,10-tetraacetic acid (TRITA) (**IXa**) and its derivatives,[41] and 14-membered 1,4,8,11-tetra azacyclotetradecane-1,4,8,11-tetraacetic acid (TETA) (**Xa**) [42] and its derivatives.

Stability constants {298K, I = 0.1 [NMe_4NO_3]} for the formation of 1:1 complexes of yttrium with DOTA (**VIIIa**), TRITA (**IXa**) and TETA (**Xa**) were shown to be $[Y.DOTA]^-$ = 24.9, $[Y.TRITA]^-$ = 19.6 and $[Y.TETA]^-$ = 16.3. The rate of dissociation of yttrium from preformed complexes of DOTA and TRITA was also

compared (pH 3.6, OAc^- buffer), and showed that whilst no dissociation was observed for $[Y.DOTA]^-$, the half life of $[Y.TRITA]^-$ was only 5 minutes.[43]

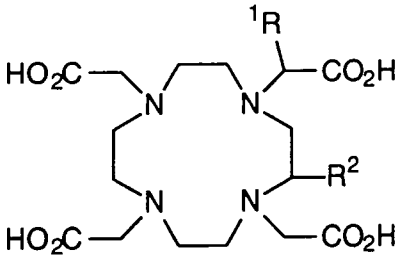

(VIII)

(a) $R^1 = R^2 = H$

(b) $R^2 = H$, $R^1 =$ 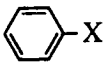

or $R^1 = H$, $R^2 =$ 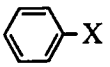

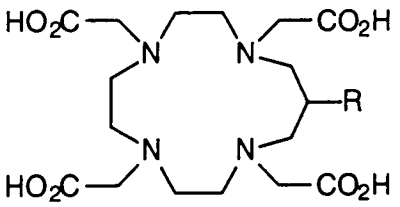

(IX)

(a) R = H

(b) R = 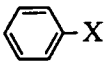

(c) R = 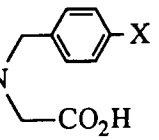

X = NO_2, NCS

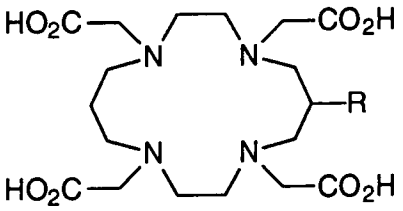

(X)

(a) R = H

(b) R = 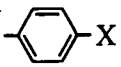

(c) R = 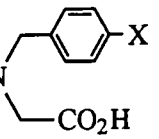

X = NO_2, NCS

Unlike crown ethers,[44] the variation in the thermodynamic stabilities of yttrium complexes of DOTA, TRITA and TETA complexes is not ring size dependent. Indeed the cavity formed in the plane of the four ring nitrogen donors is too small (DOTA radius 0.56 Å [45]) to accomodate the yttrium (III) cation (radius 1.07 Å coordination 9). A metal ion will essentially sit above the N_4 ring plane whilst the four pendent ligating arms encapsulate the cation from above forming a nearly spherical cage-like structure.[46] This has been shown to be the case in the

solid state for both europium and yttrium complexes of DOTA, both being nine coordinate (8 coordinate DOTA + 1 water molecule) with a mono-capped square antiprism structure.[47]

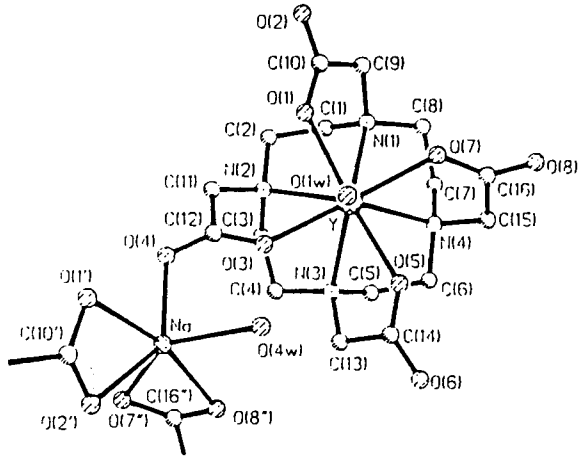

Figure 1.17 : The molecular structure of $Na[Y.DOTA.H_2O].4H_2O$.

The relative thermodynamic stability of the 12, 13, and 14 ring metal complexes may then be related to the degree of steric crowding and torsional strain of the five and six membered chelate rings of the complexes. The six membered propylenediamine chelates found in complexes of TRITA and TETA possess unfavourable eclipsing interactions between CH_2 groups compared to the five membered chelates in DOTA complexes. These five membered chelates of DOTA are also better suited (have a better chelate "bite") to the ionic radius of yttrium as a five ring chelate favours binding to larger metal ions in higher coordination. Six ring chelates on the other hand favour smaller low coordination cations.[48] It is for these reasons that of the three ligands, DOTA forms the most thermodynamically stable yttrium complex.

As the primary route for yttrium dissociation is acid catalysed, it would be reasonable to expect from an electrostatic point of view that complexes with overall charge neutrality would be less susceptible to acid catalysed dissociation. Taking this into consideration, three neutral complexes of 1-oxa-4,7,10-triaza cyclododecane-

4,7,10-triacetic acid (ODOTRA) **(XI)**, 4-(N-benzyl-N-methylcarboxamidomethyl)-4,7,10-tetraazacyclo dodecane-1,4,7-triacetic acid (DOTA-BMA) **(XII)** and 1,7-dioxa-4,10,13-triazacyclopentadecane-4,10,13-triacetic acid (DTCTA) **(XIII)** were synthesised.[49]

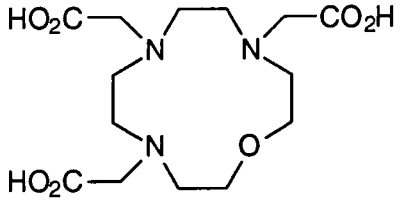

(XI)

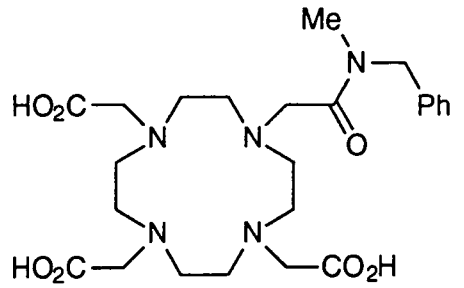

(XII)

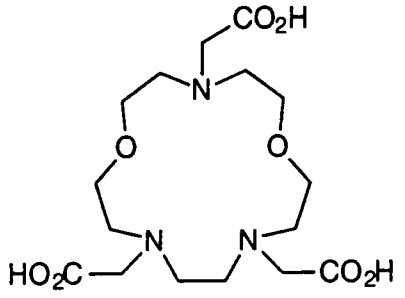

(XIII)

Both [Y.**(XI)**] and [Y.**(XIII)**] were found to be unstable with respect to trans-complexation by DTPA (pH 5.5, 500 fold excess of DTPA), undergoing complete dissociation in 48 hours, whilst the yttrium complex of DOTA-BMA **(XII)** was stable.

For a ligand to be suitable, it must complex yttrium efficiently. The rate of yttrium complexation for ligands **(VIII)** to **(XIII)** was examined and the results shown in Table 1.2.

[Ligand] / 10^{-6} mol dm^{-3}	Ligand					
	VIIIa	**IXa**	**Xa**	**XI**	**XII**	**XIII**
5	84				48	
10	98				81	0
100	99			0	94	10
500	>99.5	13	0	31	-	72
1000	>99.5	52	0	82	98	86

Table 1.2 : *Labelling efficiencies for $^{90}Y^{3+}$ complexation (30 min., pH 5.5, 0.1 mol dm^{-3} NH_4OAc, 310K).* [50]

The poor labelling efficiency and complex kinetic instability of TRITA **(IXa)**, and the obvious lack of labelling and poor complex thermodynamic stability of TETA **(Xa)** essentially rules them out. ODOTRA **(XI)** labels poorly, whilst the yttrium complex of DTCTA **(XIII)** was found to be kinetically unstable. Only DOTA **(VIIIa)** and the amide DOTA-BMA **(XII)** appear to label sufficiently well and exhibit adequate complex stability for use in radioimmunotherapy.

The poor labelling of TRITA **(IXa)** by yttrium has led one group to investigate the use of TRITA attached to a flexible pendent carboxylic acid donor **(IXc)**,[41] which it was postulated would loosely capture Y^{3+} ions, and consequently increase the metal ion concentration in the immediate vicinity of the ligand binding site, thereby increasing the complexation rate. Although this approach has proven successful, apparently without further loss of complex stability, it must be noted that Cox *et al* showed $[Y.TRITA]^-$ to be essentially too kinetically unstable to warrant its use.[43] Similarly, in an attempt to obtain complexation rates closer to those oberved

for acyclic complexing agents such as DTPA (**IIIa**), one group synthesised the larger more flexible ligands PEPA (**XIV**) and HEHA (**XV**).[32]

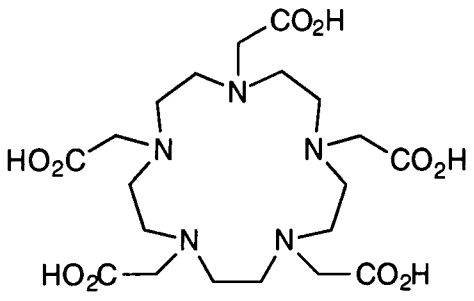

(**XIV**)

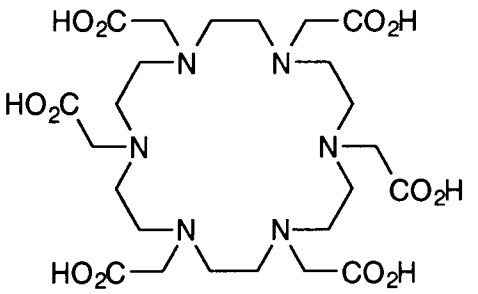

(**XV**)

Yttriuim labelling of PEPA (**XIV**) and HEHA (**XV**) was shown to be 100 times faster than for DOTA (**VIIIa**), and only 10 times slower than for DTPA (**IIIa**). The thermodynamic stabilities of the corresponding yttrium complexes {298K, I = 0.20 [$NaNO_3$]} were found to be log K_{ML} = 16.07 and 24.04 respectively. Although HEHA shows a 100-fold increase in complexation rate, and an yttrium complex thermodynamic stability comparable to that of $[Y.DOTA]^-$, the more crucial kinetic stability has as yet not been published. It would seem plausible however, that such a flexible and anionic metal complex would suffer from the same inherent lack of kinetic stability as observed for acyclic ligands such as DTPA.

It would seem therefore that the choice of ligand for a bifunctional complexing agent lies in the use of DOTA and perhaps other 12-membered macrocyclic tetra-aza ligands with four pendent ligating arms (e.g. DOTA-BMA).

1.9 YTTRIUM COMPLEX CONJUGATION TO AN ANTIBODY

Once the metal complexing part of a bifunctional complexing agent has been chosen, it must then be joined to an antibody. Introduction of a reactive functional group onto the complexing agent allows conjugation to the antibody.

Reactive functional groups which can be introduced onto the ligand are generally of two types; those which will react with the ε-amino groups of lysine residues on the antibody, and those which are able to react with free thiol groups on the antibody. Macrocycles functionalised with examples of these reactive functional groups can be seen below.

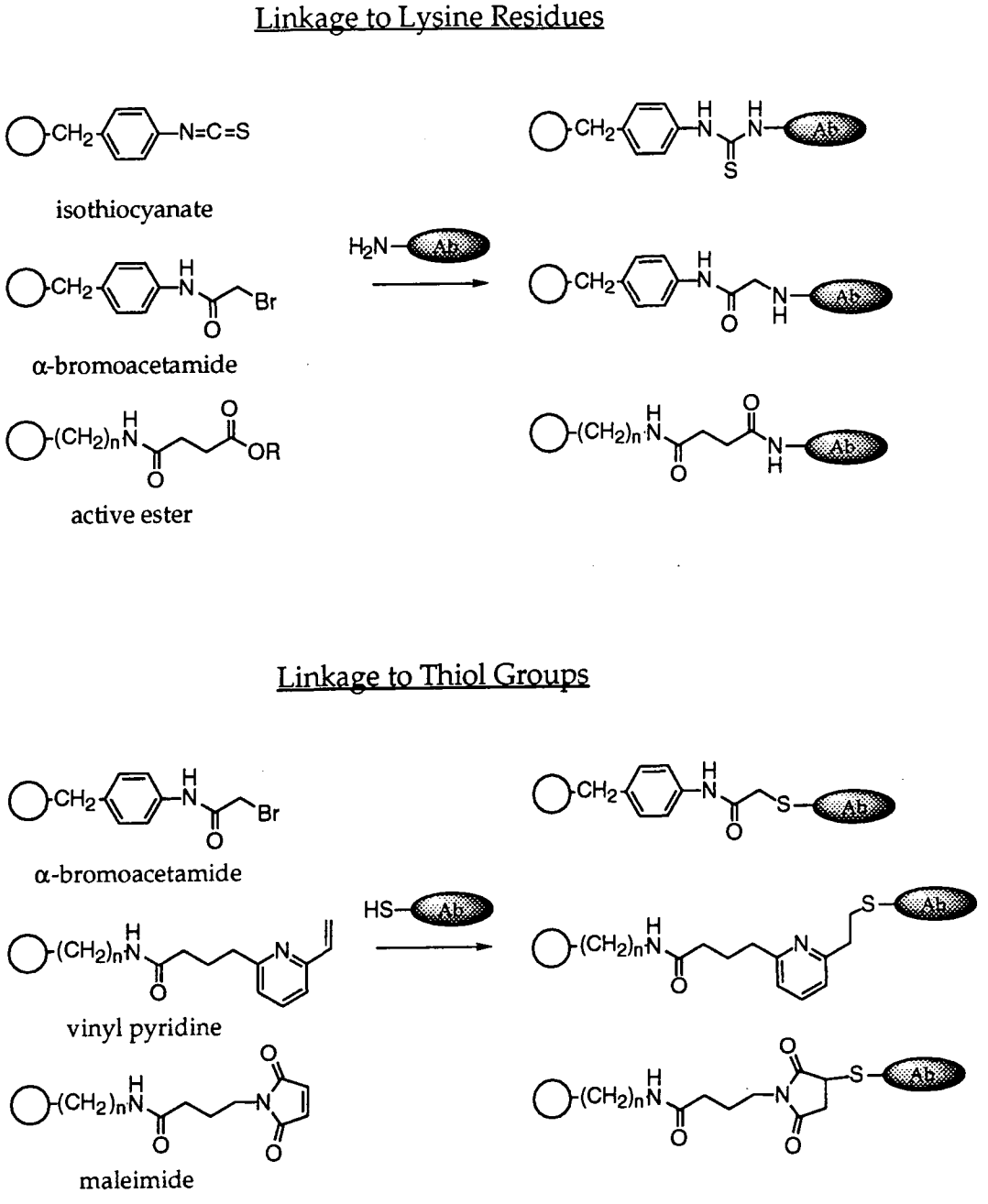

Figure 1.18 : *Antibody conjugation via an amino or thiol residue.*

An example of the use of a bifunctional complexing agent can be seen below where DTPA, backbone functionalised with an isothiocyanate moiety, is conjugated to an antibody via a ε-amino lysine residue, and subsequently radiolabelled.

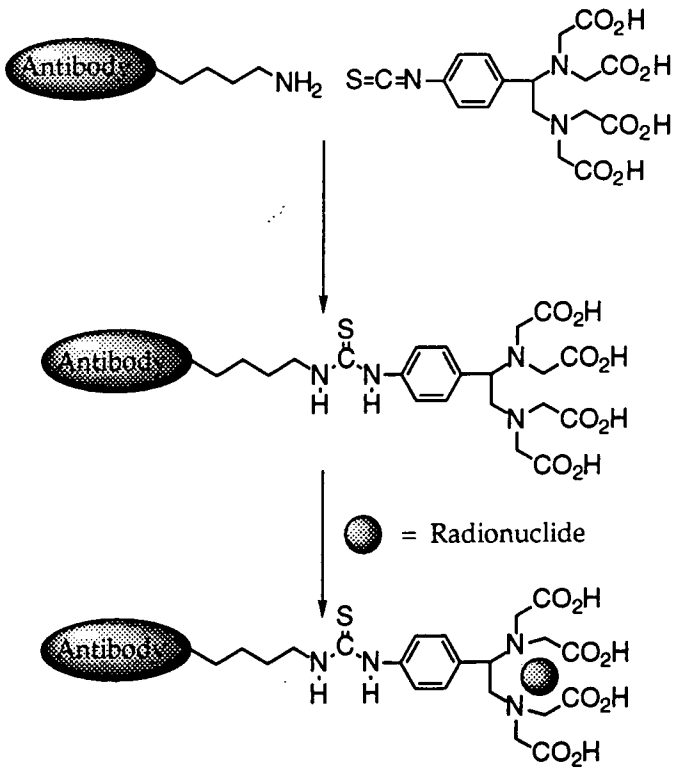

Figure 1.19 : *The use of a bifunctional complexing agent to radiolabel an antibody.*

1.10 TARGETING METAL COMPLEXES IN VIVO - AN OVERVIEW

The use of antibodies for targeting, although very specific, is only applicable for cells and tissues expressing a unique surface antigen. For this reason, and also for reasons of simplicity, other techniques are being pursued for the targeting of tissues and tumours for both imaging and therapy.

1.10.1 Tissue Targeted Complexes

In general, the biodistribution of a given metal complex is determined both by blood perfusion and by the size, charge, lipophilicity, redox properties, and specific binding interactions of the metal complex.

Solely on the basis of size, ^{99m}Tc ($t_{1/2}$ 6 hours, Eγ) particulates are used to assess disease state and blood perfusion throughout the body. These technetium particulates consist of a range of large molecules, colloids or microspheres whose size determines their biological fate. Particles of size >15 μM (but < 100 μM) are trapped purely by a mechanical process in the lung capillaries allowing evaluation of pulmonary perfusion (^{99m}Tc-MAA (macroaggregated albumin) is marketed for this purpose), whilst particles below 1-10 μM in size (^{99m}Tc-albumin colloid) are taken up by the liver, spleen, and bone marrow.

TcO(HM-PAO) and TcO(L,L-ECD) [51] are both used as a cerebral perfusion agents for brain imaging. These charge neutral metal complexes are able to cross the blood-brain barrier (BBB) where TcO(HM-PAO) is transformed, perhaps by intracellular glutathione, to a more hydrophilic species which is unable to diffuse back across the lipophilic BBB,[52] whilst one of the two esters of TcO(L,L-ECD) is enzymatically hydrolysed to give the monoanionic carboxylate complex which is also unable to diffuse back across the BBB. Thus, through the use of lipophilicity and charge, brain localisation can be achieved permitting successful imaging.

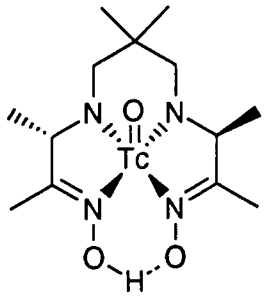

TcO(HM-PAO)

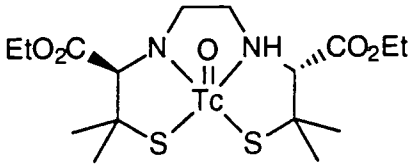

TcO(L,L-ECD)

Cu(PTSM) is a heart and brain imaging agent [53] which utilises the redox property of Cu(II). The neutral lipophilic complex is taken up by the heart and brain, where intracellular glutathione reduces the neutral copper (II) complex to the unstable anionic copper (I) complex which then deposits its ^{62}Cu radiolabel ($t_{1/2}$ 9.7 min., β^+) in the cell.

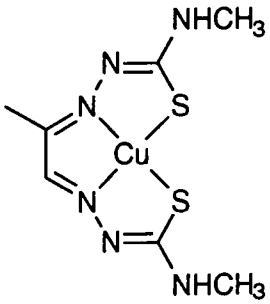

Cu(PTSM)

Nitroimidazoles tend to localise in oxygen-deficient regions such as those found in tumours and damaged heart tissue where they are substrates for reductase enzymes. The reduced product is then less able to diffuse out of the cell and therefore builds up there. TcO(PnAO)-1-(2-nitroimidazole) is a nitroimidazole-technetium complex conjugate which has shown promise for imaging of diseased heart tissue.[54]

Technetium phosphonate complexes are used as bone and myocardial infarct imaging agents. A diphosphonate ligand, such as HMDP, complexes ^{99m}Tc forming a 1:1 oligomer in which each technetium atom is bound by two diphosphonate ligands, and each phosphonate is coordinated to two technetium centres.[55] The

complex will localise in bone due to the tridentate binding of the coordinated diphosphonate ligand to calcium in actively growing bone.[56] Similarly, the metal complex will target infarcted heart muscle due to calcium deposits in the muscle.

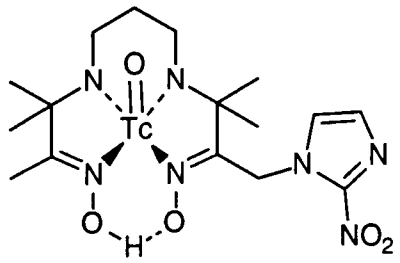

TcO(PnAO)-1-(2-nitroimidazole)

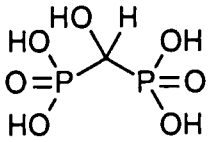

HMDP

Muscarinic acetylcholine receptors (mAChR) in the brain can also be targeted using $TcO(N_2S_2)$-quinuclidinol, a technetium radiolabelled portion of a high affinity ligand for mAChR. Unfortunately, a three fold decrease in affinity for the receptors is observed as compared to the intact ligand from which it was derived.

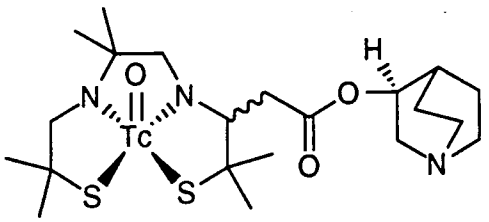

$TcO(N_2S_2)$-quinuclidinol

It can be shown therefore, that a number of different properties can be utilised to effect specific tissue targeting. Technetium particulates localise due to their size, TcO(HM-PAO) and TcO(L,L-ECD) localise because of their lipophilicity and charge, Cu(PTSM) and TcO(PnAO)-1-(2-nitroimidazole) show selectivity because of their redox properties, whilst technetium phosphonates and $TcO(N_2S_2)$-quinuclidinol, selectively target because of their ability to bind to their respective targets.

1.10.2 Tumour Targeted Complexes

Non-antibody based tumour targeting compounds have been investigated because their small size permits rapid biodistribution and tumour localisation without significant liver localisation.

The anti-cancer drug Bleomycin for example has the unusual property of accumulating in some types of cancer cells. For this reason, Meares and Wensel attached to it an ^{111}In-EDTA complex for the purpose of tumour imaging.[57]

^{186}Re labelled progestin (11β-ReO(N_2S_2)-progestin) is another diagnostic imaging agent, designed to bind to steroid positive tumours.[58] It was shown to have enhanced binding to the tumour compared to progestin itself, but non-specific binding was too high for the complex to be of significant use.

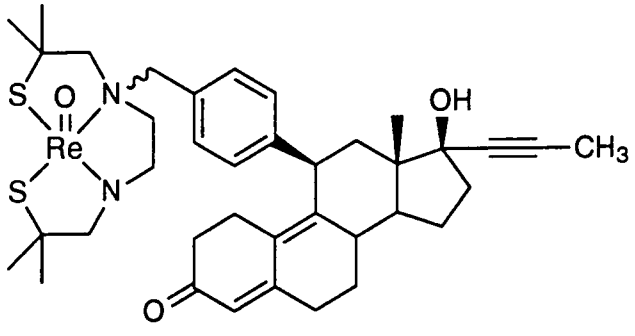

11β-ReO(N_2S_2)-progestin

It has been postulated that instead of an intact antibody or a fragment thereof, only the amino acid sequence concerned with receptor binding may be required for tumour localisation. ^{111}In-DTPA-octreotide is a somatostatin receptor binding radiopharmaceutical with less than 10% non-specific binding.[59] This has allowed ^{111}In based imaging of somatostatin-positive tumours using only an eight amino acid sequence.

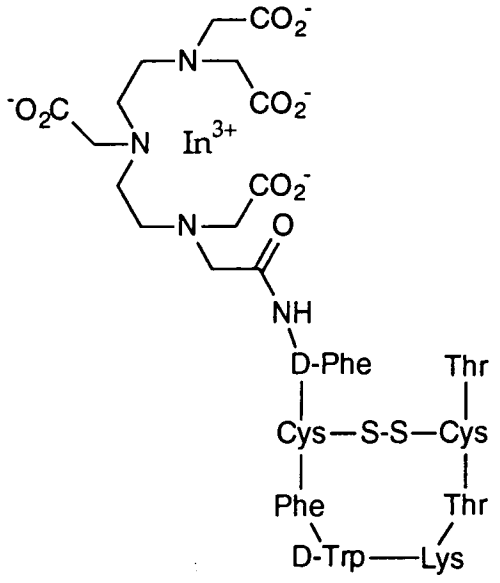

In-DTPA-D-Phe-octreotide

Similarly, the same octreotide amino acid sequence has been conjugated to ^{90}Y radiolabelled DOTA and TRITA for tumour therapy, and to backbone functionalised ^{111}In-DTPA for tumour imaging.[60]

1.10.3 Antibody Based Tumour Targeting

The forerunners of radiolabelled antibodies were radiolabelled proteins. Indium-111 labelled DTPA and EDTA were conjugated in an similar way as for antibodies, to proteins such as human serum albumin, and fibrinogen for use as biological probes.[30,61]

Since then, antibodies such as those specific for colorectal carcinoma, the human interleukin 2 receptor, or antibody Fab' fragments to canine cardiac myosin (for myocardial infarction location) have been successfuly conjugated to EDTA and DTPA giving site-specific imaging or therapy when labelled with indium-111 [62,63,64,65] or bismuth-212 [21] respectively. Macrocyclic metal complexes have also been conjugated to antibodies, showing promising results with indium-111 labelled

NOTA,[66] copper-67 and 64 labelled tetraaza cycles,[67,68] and yttrium-90 labelled DOTA.[69]

Other interesting approaches to the radiolabelling of antibodies include a first attempt to attach a radiolabelled carborane ligand; a so called Venus Flytrap Cluster (VFC), to a tumour localising antibody,[70] and the ^{99m}Tc labelling of antibodies using an imaginative thiolactone based bifunctional complexing agent.[71] The novel VFC showed excellent *in vivo* stability and tumour localisation, and although only labelled with ^{57}Co, there is scope for alteration to allow the synthesis of ^{67}Cu labelled clusters for use in radioimmunotherpy provided the forward rate of copper complexation is sufficiently fast under ambient conditions. The ^{57}Co cluster is shown below in Figure 1.20.

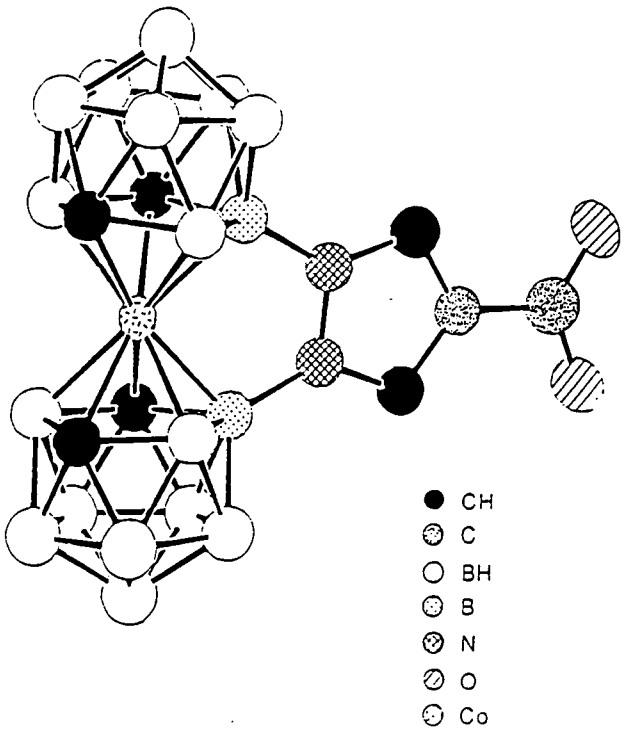

Figure 1.20 : *The VFC to which an antibody can be conjugated.*

In the technetium labelled antibody, the thiolactone on reaction with a ε-amino lysine residue of an antibody liberates a diamino-dithiol technetium binding ligand

which on addition of ^{99m}Tc glucoheptanonate yields a stable radiolabelled product which has shown good *in vivo* stability.

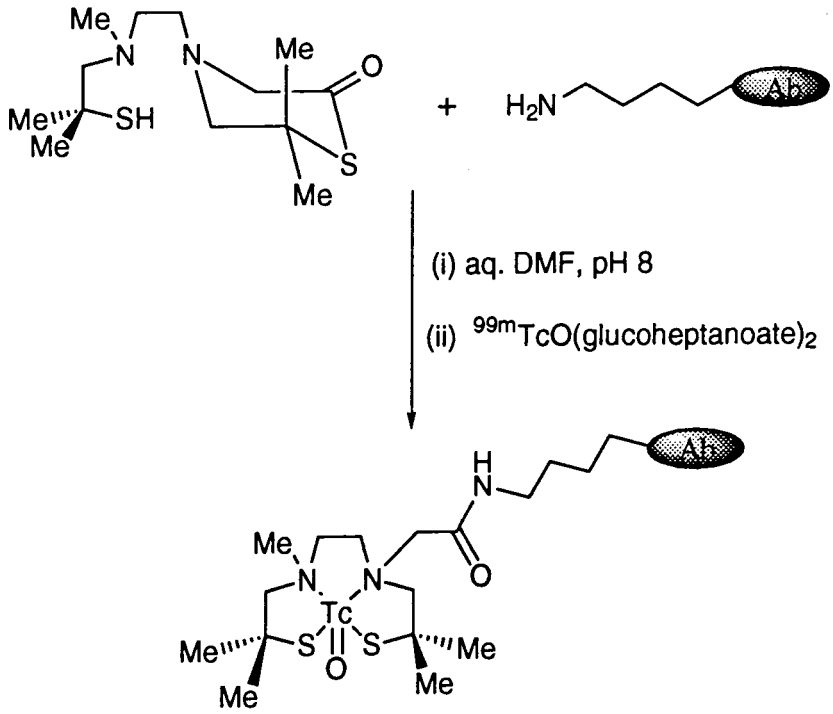

Figure 1.21 : *The use of a thiolactone bifunctional complexing agent to label an antibody with ^{99m}Tc.*

1.11 SCOPE OF THIS WORK

The majority of this thesis is concerned with the synthesis of a number of ligands for yttrium and gadolinium, and with the testing of their suitability for safe *in vivo* use. The rate of both yttrium complexation and decomplexation will be examined, along with a detailed biodistribution study of the metal complexes to determine of *in vivo* stability, and the rate and mode of clearance from the body. Once chosen, a suitable ligand will then be functionalised to permit its conjugation to

one or more antibody fragments, or to a tumour localising moiety such as a nitroimidazole.

The functionalised ligands once conjugated to antibodies will then be tested to determine antibody immunoreactivity, and most importantly tumour localising ability. Finally, the use of DNA binding intercalators will be discussed with a view to their incorporation into antibody conjugates to bring the complexed radionuclide into closer proximity to its target, the chromosomal DNA of tumour stem cells.

1.12 REFERENCES

1 L. G. Capra, "Care of the Cancer Patient", Macmillan, 1986.

2 "Introduction to the Cellular and Molecular Biology of Cancer", ed. L. M. Franks and N. Teich, Oxford Science Publications, 1988.

3 J. Cairns, *Sci. Amer.*, 1975, **233**, 64.

4 "Molecular Foundations of Oncology", ed. S. Broder, Williams & Wilkins, 1991.

5 "Chemistry of Antitumour Agents", ed. D. E. V. Wilman, Blackie & Son Ltd., 1990.

6 L. Stryer, "Biochemistry 2nd Edition", W. H. Freeman and Company, 1981.

7 D. Pressman, *Ann. N.Y. Acad. Sci.*, 1957, **69**, 644.

8 G. Köhler and C. Milstein, *Nature,* 1975, **256**, 495.

9 C. Milstein, *Scientific American*, 1980, **243 (4)**, 56.

10 J. C. Reynolds, S. DelVecchio, H. Sakahara, et al, *Nucl. Med. Biol.*, 1989, **16**, 121.

11 E. Seccamani, M. Tattanelli, M. Mariani, E. Spranzi, G. A. Scassellati, A. G. Siccaridi, *Nucl. Med. Biol.*, 1989, **16**, 167.

12 S. L. Morrison, M. J. Johnson, L. A. Herzenberg and V. T. Oi, *Proc. Nat. Acad. Sci. N.Y.*, 1984, **81**, 6851.

13 J. L. Marx, *Science*, 1985, **229**, 455.

14 A. F. LoBuglio, et al., *Proc. Nat. Acad. Sci. N.Y.*, 1989, **86**, 4220.

15 L. Reichmann, M. R. Clark, H. Waldmann, and G. Winter, *Nature*, 1988, **332**, 323.

16 C. Queen, W. P. Schneider, H. E. Selick, et al, *Proc. Natl. Acad. Sci USA*, 1989, **86**, 10029.

17 A. Skerra and A. Pluckthun, *Science*, 1988, **40**, 1038.

18 J. L. Humm, *J. Nucl. Med.*, 1986, **27(9)**, 1490.

19 J. R. Morphy, D. Parker, R. Kataky, A. Harrison, M. A. W. Eaton, A. T. Millican, A. Phipps, C. Walker, *J. Chem. Soc., Chem. Commun.*, 1989, 792.

20 A. S. Craig, R. Kataky, R. C. Mathews, D. Parker, G. Ferguson, A. Lough, H. Adams, N. Bailey, and H. Schneider, *J. Chem. Soc., Perkin Trans. 2*, 1990, 1523.

21 R. W. Kozak, R. W. Atcher, O. A. Gansow, A. M. Freidman, J. J. Hines, and T. A. Waldman, *Proc. Nat. Acad. Sci. USA*, 1986, **83**, 474.

22 K. Kumar, M. Magerstädt, and O. A. Gansow, *J. Chem. Soc., Chem. Commun.*, 1989, 145.

23 M. W. Brechbiel, C. G. Pippin, T. J. McMurry, D. Milenc, M. Roselli, D. Colcher, and O. A. Gansow, *J. Chem. Soc., Chem. Commun.*, 1991, 1169.

24 S. M. Yeh, D. G. Sherman, and C. F. Meares, *Anal. Biochem.*, 1979, **100**, 152.

25 J. Altman, N. Shoef, M. Wilchek, and A. Warshawsky, *J. Chem. Soc. Perkin Trans. 1*, 1983, 365.

26 G. E. Krejcarek and K. L. Tucker, *Biochem. Biophys. Res. Communn.*, 1977, **77**, 581.

27 M. W. Brechbiel, O. A. Gansow, R. W. Atcher, J. Schlom, J. Esteban, D. E. Simpson and D. Colcher, *Inorg. Chem.*, 1986, **25**, 2772.

28 W. F. Benisek and F. M. Richards, *J. Biol. Chem.*, 1968, **243**, 4267.

29 F. A. Cotton, and G. Wilkinson, "Advanced Inorganic Chemistry., Fifth Edition", Wiley Interscience, 1988, 955-956. and R. D. Shannon, *Acta. Crystallogr. Sect. A*, 1976, 751.

30 M. W. Sundberg, C. F. Meares, D. A. Goodwin, and C. I. Diamanti, *Nature*, 1974, **250**, 587.

31 D. J. Hnatowich, W. W. Layne, R. L. Childs, D. Lanteigne, M. A. Davis, T. W. Griffin, and P. W. Doherty, *Science*, 1983, **220**, 613.

32 M. Kodama, T. Koike, A. B. Mahatma, and E. Kimura, *Inorg. Chem.*, 1991, **30**, 1270.

33 F. A. Cotton, and G. Wilkinson, "Advanced Inorganic Chemistry., Fifth Edition", Wiley Interscience, 1988, 45-47.

34 D. J. Hnatowich, *Nucl. Med. Biol.*, 1986, **13**, 253.

35 M. K. Moi, C. F. Meares, and S. J. DeNardo, *J. Am. Chem. Soc.*, 1988, **110**, 6266.

36 A. S. de Sousa, G. J. B. Croft, C. A. Wagner, J. P. Michael, and R. D. Hancock, *Inorg. Chem.*, 1991, **30**, 3525.

37 C. A. Chang, H. G. Brittain, J. Tesler, and M. F. Tweedle, *Inorg. Chem.*, 1990, **29**, 4468.

38 J. F. Desreux, *Inorg. Chem.*, 1980, **19**, 1319.

39 D. Parker, *Chem. Soc. Rev.*, 1990, **19**, 271.

40 J. P. L. Cox, A. S. Craig, I. M. Helps, K. J. Jankowski, D. Parker, M. A. W. Eaton, A. T. Millican, K. Millar, N. R. A. Beeley, and B. A. Boyce, *J. Chem. Soc. Perkin Trans. 1*, 1990, 2567.

41 K. Takenouchi, K. Watanabe, Y. Kato, T. Koike, and E. Kimura, *J. Org. Chem.*, 1993, **58**, 1955.

42 H. Stetter, and W. Frank, *Angew. Chem., Int. Ed. Engl.*, 1976, **15**, 686.

43 J. P. L. Cox, K. J. Jankowski, R. Kataky, D. Parker, N. R. A. Beeley, B. A. Boyce, M. A. W. Eaton, K. Millar, A. T. Millican, A. Harrison, and C. Walker, *J. Chem. Soc., Chem. Commun.*, 1989, 797.

44 J. Massaux, and J. F. Desreux, *J. Am. Chem. Soc.*, 1982, **104**, 2967.

45 J. F. Desreux, *Inorg. Chem.*, 1980, **19 (5)**, 1319.

46 M. Spirlet, J. Rebizant, M. Loncin, and J. F. Desreux, *Inorg. Chem.*, 1984, **23**, 4278.

47 C. A. Chang, L. C. Francesconi, M. F. Malley, K. Kumar, J. Z. Gougoutas, M. F. Tweedle, D. W. Lee, and L. J. Wilson, *Inorg. Chem.*, 1993, **32**, 3501. and D. Parker, K. Pulukkody, F. C. Smith, A. Batsanov, and J. A. K. Howard, *J. Chem. Soc. Dalton Trans.*, 1994, 689.

48 M. F. Loncin, J. F. Desreux, and E. Merciny, *Inorg. Chem.*, 1986, **25**, 2646.

49 J. P. L. Cox, Ph. D. Thesis, University of Durham, 1989.

50 C. J. Broan, J. P. L. Cox, A. S. Craig, R. Kataky, D. Parker, A. Harrison, A. M. Randall, and G. Ferguson, *J. Chem. Soc. Perkin Trans. 2*, 1991, 87.

51 S. Z. Lever, K. E. Baidoo, and A. Mahmood, *Inorg. Chim. Acta.*, 1990, **176**, 183.

52 S. Jurisson, E. O. Schlemper, D. E. Troutner, L. R. Canning, D. P. Nowotnik, and R. D. Neirinckx, *Inorg. Chem.*, 1986, **25**, 543.

53 E. K. John, and M. A. Green, *J. Med. Chem.*, 1990, **33**, 1704.

54 R. J. DeRocco, A. Bauer, B. L. Kuczynski, J. P. Pirro, K. Linder, R. K. Narra, and A. D. Nunn, *J. Nucl. Med.*, 1992, **33**, 865.

55 K. Libson, E. Deutsch, B. L. Barnett, *J. Am. Chem. Soc.*, 1980, **102**, 2476.

56 C. L. De Ligny, W. J. Gelsema, T. G. Tji, Y. M. Huigen, and H. A. Vink, *Nucl. Med. Biol.*, 1990, **17**, 161.

57 C. F. Meares, and T. G. Wensel, *Acc. Chem. Res.*, 1984, **17**, 202.

58 J. P. D. Zio, R. Fiaschi, A. Davison, A. G. Jones, and J. A. Katzenellenbogen, *Bioconjugate Chem.*, 1991, **2**, 353.

59 E. P. Krenning, W. H. Bakker, P. P. M. Kooiji, W. A. P. Breeman, H. Y. Oei, M. deJong, J. C. Reubi, T. J. Visser, C. Bruns, D. J. Kwekkeboom, A. E. M. Reijs, P. M. Van Hagen, J. W. Koper, and S. W. J. Lamberts, *J. Nucl. Med.*, 1992, **33**, 652.

60 E. P. Appl. 515,313 (Cl. C07K7/26).

61 C. F. Meares, D. A. Goodwin, C. S-H. Leung, A. Y. Girgis, D. J. Silvester, A. D. Nunn, and P. J. Lavender, *Proc. Natl. Acad. Sci. USA*, 1976, **73**, 3803.

62 B. A. Khaw, J. T. Fallon, H. W. Strauss, and E. Haber, *Science*, 1980, **209**, 295.

63 C. F. Meares, M. J. McCall, D. T. Reardan, D. A. Goodwin, C. I. Diamanti, and M. McTigue, *Anal. Biochem.*, 1984, **142**, 68.

64 V. L. Alvarez, M. Wen, C. Lee, A. D. Lopes, J. D. Rodwell, and T. J. McKearn, *Nucl. Med. Biol.*, 1986, **13**, 347.

65 D. A. Scheinberg, M. Strand, and O. A. Gansow, *Science*, 1982, **215**, 1511.

66 A. S. Craig, I. M. Helps, K. J. Jankowski, D. Parker, N. R. A. Beeley, B. A. Boyce, M. A. W. Eaton, A. T. Millican, K. Millar, A. Phipps, S. K. Rhind, A. Harrison, and C. Walker, *J. Chem. Soc., Chem. Commun.*, 1989, 794.

67 M. K. Moi, C. F. Meares, M. J. McCall, W. C. Cole, and S. J. DeNardo, *Anal. Biochem.*, 1985, **148**, 249.

68 J. R. Morphy, D. Parker, R. Kataky, M. A. W. Eaton, A. T. Millican, R. Alexander, A. Harrison, and C. Walker, *J. Chem. Soc. Perkin Trans. 2*, 1990, 573.

69 A. Harrison, C. A. Walker, D. Parker, K. J. Jankowski, J. P. L. Cox, A. S. Craig, J. M. Sansom, N. R. A. Beeley, B. A. Boyce, L. Chaplin, M. A. W. Eaton, A. P. H. Farnsworth, K. Millar, A. T. Millican, A. M. Randall, S. K. Rhind, D. S. Secher, and A. Turner, *Nucl. Med. Biol.*, 1991, **18**, 469.

70 R. J. Paxton, B. G. Beatty, M. F. Hawthorne, A. Varadarajan, L. E. Williams, F. L. Curtis, C. B. Knobler, J. D. Beatty, and J. E. Shilvey, *Proc. Natl. Acad. Sci. USA*, 1991, **88**, 3387.

71 S. Z. Lever, K. E. Baidoo, A. V. Kramer, and H. D. Burns, *Tet. Lett.*, 1988, **29**, 3219.

Chapter 2

Ligand Design and Synthesis

2.1 INTRODUCTION

Chapter 1 (Section 1.8) discussed the need for high complex stability when using yttrium-90 complexes conjugated to antibody fragments for radio immunotherapy. At the outset of this work, and of the ligands discussed so far, DOTA (**VIIIa**) and also the mono-amide functionalised DOTA-BMA (**XII**) (Section 1.8.3), both based on the 1,4,7,10-tetraazacyclododecane ($12N_4$) skeleton showed the greatest promise for radioimmunotherapy, forming very stable yttrium complexes with little indication of decomplexation of the highly toxic free $^{90}Y^{3+}$ cation.

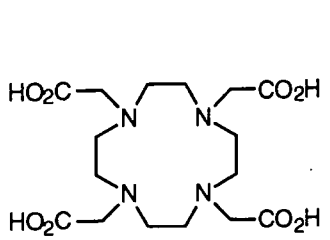

DOTA

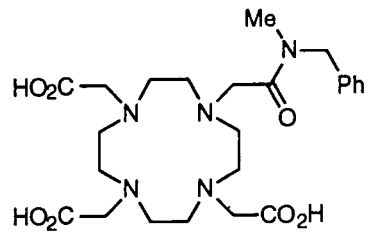

DOTA-BMA

2.2 COMPLEX NEUTRALITY

Although radioimmunotherapy was the primary objective of the research, an additional goal was to covalently attach to an yttrium-90 complex, tumour localising moieties such as 2-nitroimidazoles.

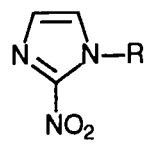

A 2-Nitroimidazole

These have been shown to localise in oxygen deficient cells such as those found in the dead core of solid tumours, or in ischaemic heart tissue. It was hoped

that conjugation of such a molecule to an yttrium-90 complex would facilitate uptake of the metal complex into the tumour (see also Chapter 3, Section 3.8).

To be most effective, 2-nitroimidazole must first be internalised into the tumour cell by diffusing through the cell wall (Section 1.10.1). Unless an active uptake mechanism operates, only a charge neutral compound is able to do this. For this reason, and to reduce acid or cation promoted metal dissociation, conjugation to a *charge neutral* yttrium complex such as [Y.DOTA-BMA] is essential.

With this in mind it should be noted that, because of the so called "lanthanide contraction", many of the $12N_4$ functionalised ligands that form neutral complexes with Gd^{3+}, and have been studied as paramagnetic contrast agents for Magnetic Resonance Imaging (MRI) (see Section 2.13), may also be potentially useful as ligands for yttrium. The thermodynamic stability of $[Gd.DOTA]^-$ ($\log K_{ML} = 25.8$) is almost identical to that of $[Y.DOTA]^-$ ($\log K_{ML} = 24.9$ [1]).

Complex	$\log K_{ML}$	$k_{obs} \times 10^3$ (s^{-1})	Overall Charge
[Gd.DO3A]	21.1	2.4	0
[Gd.DO3MA]	25.3	0.162	0
[Gd.HP-DO3A]	23.8	31×10^{-3}	0
[Gd.DOTA-PA]	20.1	-	0
[Gd.A]	25.9	-	0
[Gd.B]	26.4	-	0
$[Gd.DOTA]^-$	25.8	0.84×10^{-3}	-1
$[Gd.DTPA]^{2-}$	22.5	> 5	-2
$[Gd.EDTA]^-$	17.3	-	-1

Data taken from references 2, 3, 4, 5, 6, 7, 8, 9 and 10.

Table 2.1 : *Stability constants (I = 0.1 [NMe_4Cl or NMe_4NO_3]), and relative rates of acid catalysed dissociation (pH 1.0) at 298 K.*

A number of the neutral gadolinium complexes that have been synthesised as contrast agents for MRI incorporate a pendent amide and are shown in Figure 2.1 & Table 2.1 (anionic $[Gd.DOTA]^-$, $[Gd.DTPA]^{2-}$ and $[Gd.EDTA]^-$ are given for comparison).

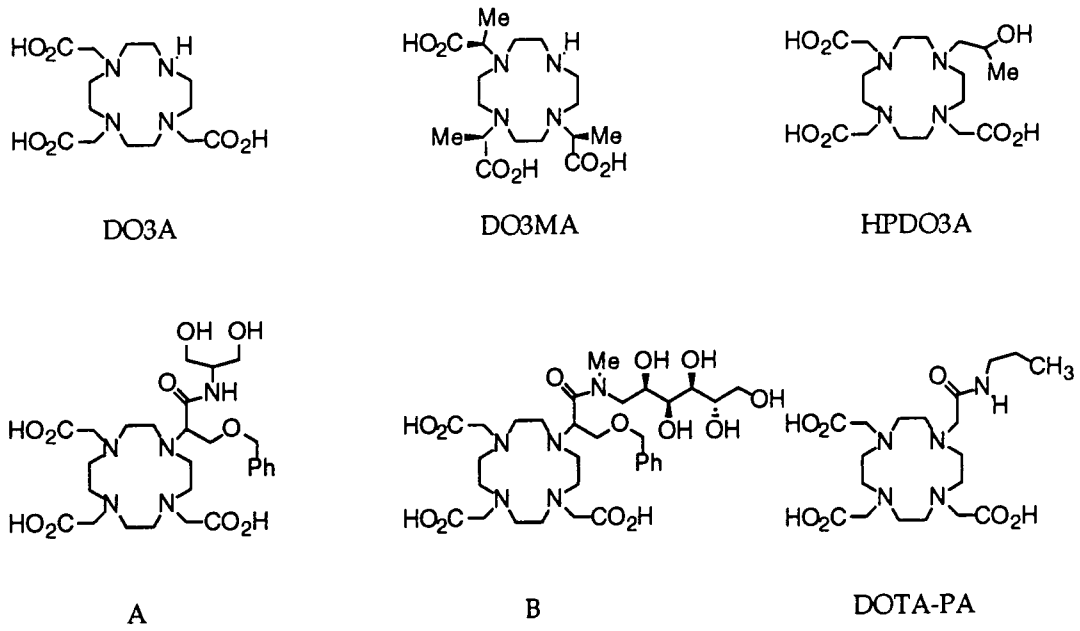

Figure 2.1 : *Examples of ligands for gadolinium MRI.*

Whilst all the neutral gadolinium complexes shown have a high thermodynamic stability, it should be noted that the two seven coordinate complexes [Gd.DO3A] and [Gd.DO3MA] are the least kinetically stable with respect to acid catalysed dissociation, whilst the eight coordinate complex [Gd.HP-DO3A] shows better kinetic stability.

2.3 LIGAND FUNCTIONALISATION

2.3.1 Amide Functionalised Ligands

The amide carbonyl oxygen is an effective ligand for cations of high charge density such as Li^+ and Ca^{2+} (Gd^{3+} and Y^{3+} also have a high charge density). This is due to its appreciable ground state dipole moment ($HCONMe_2$ has a dipole moment of 3.82 debye) which allows it to act as a good σ^- donor.[11] Bearing in mind the kinetic stability of neutral gadolinium complexes (Table 2.1), and the related yttrium complex [Y.DOTA-BMA] (Section 1.8.3), it would appear that for *in vivo* use, any neutral complex of yttrium should be eight coordinate with an amide (or perhaps an alcohol) ligating group.

This rationale, coupled with the fact that further functionalisation of the macrocycle (e.g. introduction of a reactive group to permit antibody conjugation) could easily be effected at the nitrogen of the amide donor (e.g. as for B, Figure 2.1), led to the decision that one amide should be introduced into the target ligand for yttrium.

2.3.2 Phosphonic Acid Functionalised Ligands

Although all the ligands proposed so far for yttrium contain pendent ligating carboxylate arms to satisfy the positive charge of the metal centre, there are alternatives.

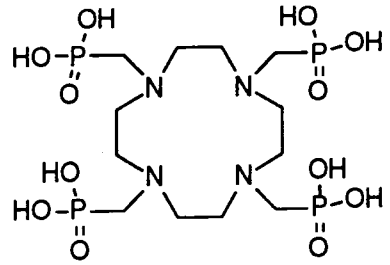

Figure 2.2 : *DOTP*

Currently under investigation for use with lanthanides is DOTP, a phosphonic acid derivative of DOTA.[12,13,14] Despite ^{1}H NMR suggesting that lanthanide DOTP complexes are non-fluxional, and hence have an increased complex rigidity compared to DOTA, DOTP was found to have a greatly increased rate of complexation, although its complex stabilities have been shown to be smaller.[15] There is also a pronounced tendency for this ligand, with its two basic sites per phosphorus, to form protonated metal complexes of diminished stability, thereby facilitating acid mediated metal decomplexation. Because of this, and the anionic nature of an yttrium complex incorporating four methylphosphonic acid arms, phosphonic acids are an inappropriate alternative to carboxylic acids.

2.3.3 Phosphinic Acid Functionalised Ligands

The second alternative, and one which has been exploited in the work of others,[16,17] is the use of phosphinic acids (-PRO(OH)) rather than carboxylic acids (-CO(OH)). There are two basic differences in the chemistry of these two systems that are of particular importance. Firstly, the phosphinate moiety is more difficult to protonate on the oxygen than is the carboxylate, i.e. it possesses a lower pK_a which may mean that enhanced complex kinetic stability with respect to acid catalysed dissociation will result. This can be seen in the pK_a of the monoanionic complexes of $[Y.DOTA]^-$, and its methylphosphinate analogue $[Y.12N_4P_4Me_4]^-$.[18] This is obviously of prime importance when dealing with the radionuclide ^{90}Y *in vivo.*

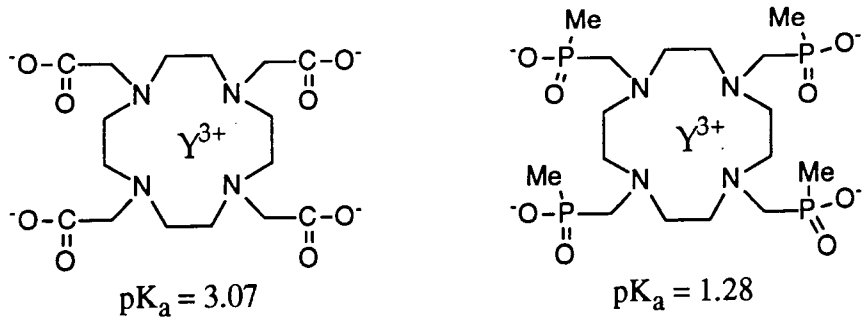

$pK_a = 3.07$ $pK_a = 1.28$

Figure 2.3 : *pK_as of $[Y.DOTA]^-$ and $[Y.12N_4P_4Me_4]^-$*

The second important difference is the pentavalency of phosphorus which, by varying the nature of the alkyl or aryl P-substituent, permits control over complex lipophilicity, and provides the opportunity for a site of further functionalisation, including perhaps conjugation to an antibody.

2.4 LIGAND CONJUGATION TO AN ANTIBODY

The purpose of forming these stable yttrium complexes is to allow radiolabelling of an antibody for radioimmunotherapy. This means that additional functionalisation of the ligand is necessary to permit conjugation to an antibody.

A ligand can essentially be functionalised in four places. Functionalisation can take place at the phosphorus atom of the phosphinic acid, although this requires extensive preparation of an initial phosphinate ester.[17] The arm of the carboxylic acid donor can be functionalised, or a more time consuming and tedious synthesis requiring a cyclisation step will permit the introduction of functionality into the carbon backbone of the $12N_4$ ring.[19]

The fourth, and perhaps the most direct approach to functionalising the ligand is through a pendent amide. A suitable functional group can be readily incorporated through selective choice of the R' or R" moieties on the nitrogen of the amide (See Figure 2.4). Because of the simplicity of this approach, this was the technique employed.

2.5 CHOICE OF LIGAND

In summary, to achieve complex neutrality and subsequent further derivatisation, it would appear that a likely target ligand for yttrium is a mono-amide tri-phosphinic or tri-carboxylic acid derivative of $12N_4$, such as those depicted below.

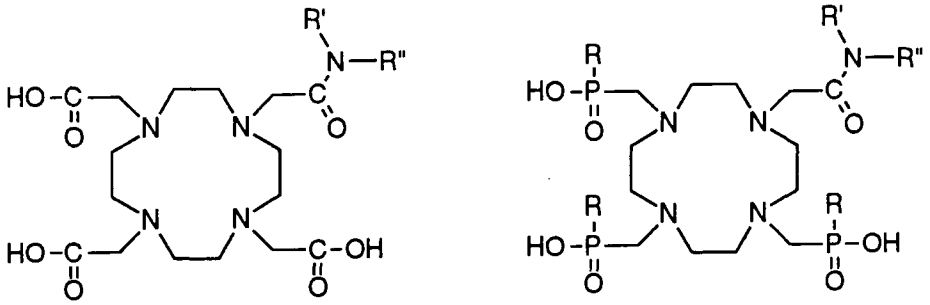

R, R', R" = alkyl, aryl

Figure 2.4 : *Proposed ligands for yttrium*

There are two principal approaches to the formation of a mono-amide tri-phosphinic or carboxylic acid derivatised ligand; initial tri-substitution of the ring by acid functionalities, followed by reaction at the fourth site by an amide (Scheme 2.1 (a) & (b)), or initial selective mono-substitution of the cycle by an amide followed by addition of three acid groups (Scheme 2.1 (c) & (d)).

Synthetic routes (a) and (c) do not take advantage of any protection procedures, relying simply on the addition of the correct ratio of reagents followed by careful separation of the various mono, di, tri, or tetra substituted products. Although effective, yields are low and purification can be laborious.[20]

Alternatively, a higher yielding protection scheme can be employed, selectively and precisely protecting either one (route (b)) or three (route (d)) of the four ring nitrogens. A particularly interesting and useful example of the mono-protection of the tetra aza ring (route (b)), is in the formation of the previously unknown 1-formyl-1,4,7,10-tetraazacyclododecane [21] by the partial hydrolysis of the known 1,4,7,10-tetraazactricyclo[5.5.1.0] tridecane.[22] This ingenious protection

scheme permits the addition of acid functionalities to the remaining three ring nitrogens, followed by a simple acid hydrolysis to remove the formyl protecting group (Scheme 2.2).

Similarly, a metal complex of $12N_4$ can be formed which incorporates three of the four ring nitrogens, leaving the fourth site free for functionalisation (route (d)).[23]

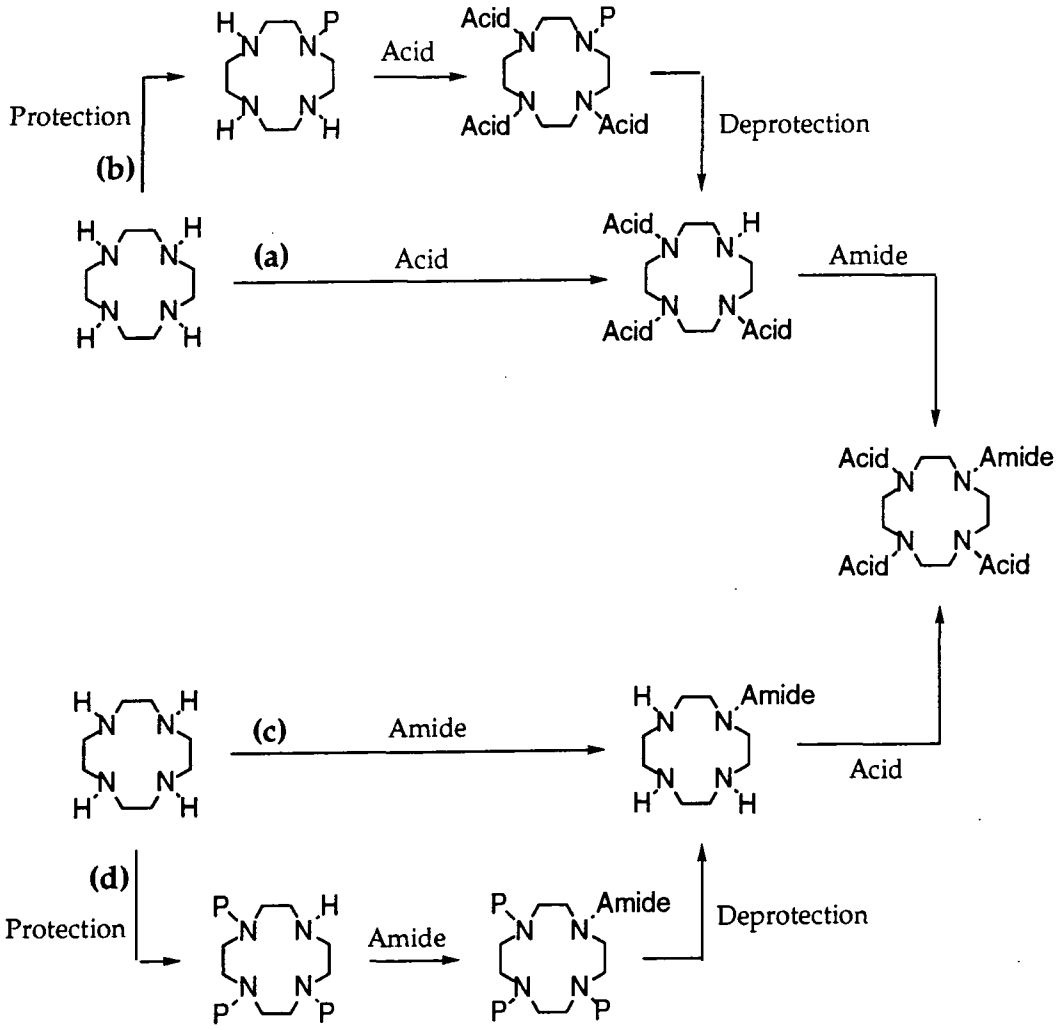

Scheme 2.1 : *Selective functionalisation of the cycle.*

P = Protecting group, Amide = $CH_2CONR'R''$, Acid = CH_2CO_2H or CH_2PRO_2H.

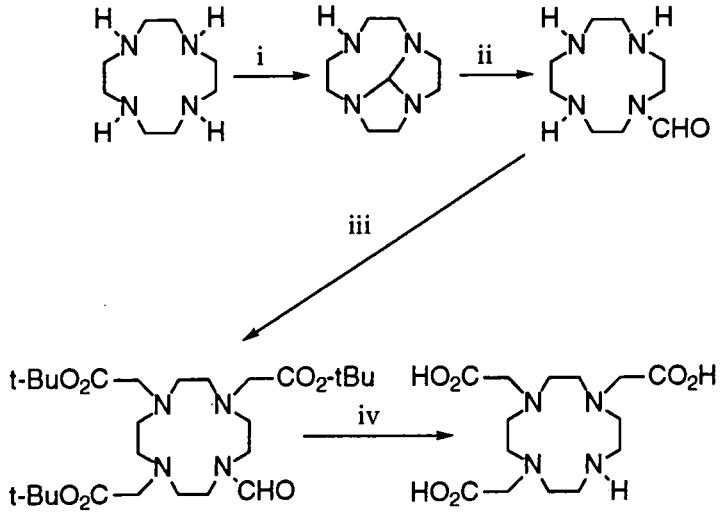

Scheme 2.2 : *Formyl ring protection. Reagents : (i) $(CH_3)_2NCH(OCH_3)_2$, cyclohexane; (ii) H_2O; (iii) $BrCH_2CO_2$-tBu, Toluene, NaOH,H_2O; (iv) H_2SO_4.*

Synthesis and testing of both carboxylic and phosphinic acid functionalised ligands will enable us to compare the relative merits of the two ligand systems showing if indeed an enhanced complex kinetic stability can be observed for the phosphinic derivatives.

2.6 LIGAND SYNTHESIS

2.6.1 Macrocycle Synthesis

A modified version of Stetter and Frank's general synthesis of tetraazamacrocycles[24] was employed to synthesise the twelve-membered ring 1,4,7,10-tetraazacyclododecane ($12N_4$).

In place of sodium ethoxide employed by Stetter and Frank in the cyclisation step (ii), potassium carbonate was used as it was found to give a cleaner reaction by

reducing the major side reaction; oligomerisation.[20] Potassium carbonate, although not a strong base, is able to deprotonate both of the tosylamides of (1) (in DMF the potassium cation is highly solvated, leaving CO_3^{2-} to act as a strong base) which then undergo S_N2 displacement reactions with $TsO(CH_2)_2OTs$ yielding the tetratosylated cycle (2). Subsequent detosylation of (2) with concentrated sulphuric acid followed by acid-base work up yielded the tetraamine (3) as its free amine white powder (Scheme 2.3).

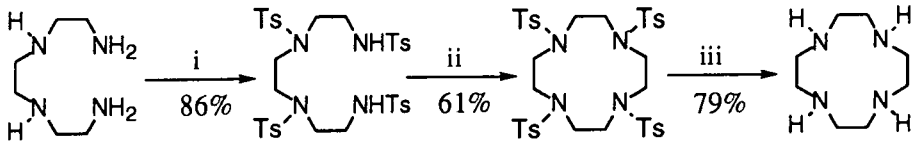

(1) (2) (3)

Scheme 2.3 : *Synthesis of $12N_4$. Reagents : (i) TsCl, K_2CO_3, H_2O; (ii) $TsO(CH_2)_2OTs$, K_2CO_3, DMF; (iii) c.H_2SO_4.*

2.6.2 Amide Functionalisation of the Macrocycle

Choice of the pendent amide side arm to functionalise the cycle was dictated by the need for further functionalisation at a site on one of the amide nitrogens substituents. For reasons of simplicity, and because of its ease of further derivatisation, it was decided that one of these substituents would possess a primary amine which would permit reaction with molecules exhibiting such functionalities as acid chlorides, active esters or α-haloamides.

Two different amides (5) and (6) were used. The bifunctional amide (5) possesses a primary amine group protected as its sulphonamide. Once attached to the macrocycle, deprotection could be undertaken to allow further functionalisation of the free amine group. Because of its enhanced sensitivity to acid deprotection (HBr, AcOH),[25] p-methoxy benzenesulphonamide was used in preference to

tosylamide for primary amine protection of (**5**), negating the need for the forcing conditions of concentrated sulphuric acid, and its associated amide hydrolysis.

Monoprotection of 1,4-diaminobutane by its use in large excess yielded the amine (**4**), which subsequently underwent a low temperature Schotten-Baumann acylation (the low temperature reduced competitive amine alkylation) to give (**5**) as a white powder. Similarly, a low temperature Schotten-Baumann acylation of diisobutylamine with bromoacetylbromide gave the α-bromoamide (**6**) to serve as a comparison to (**5**).

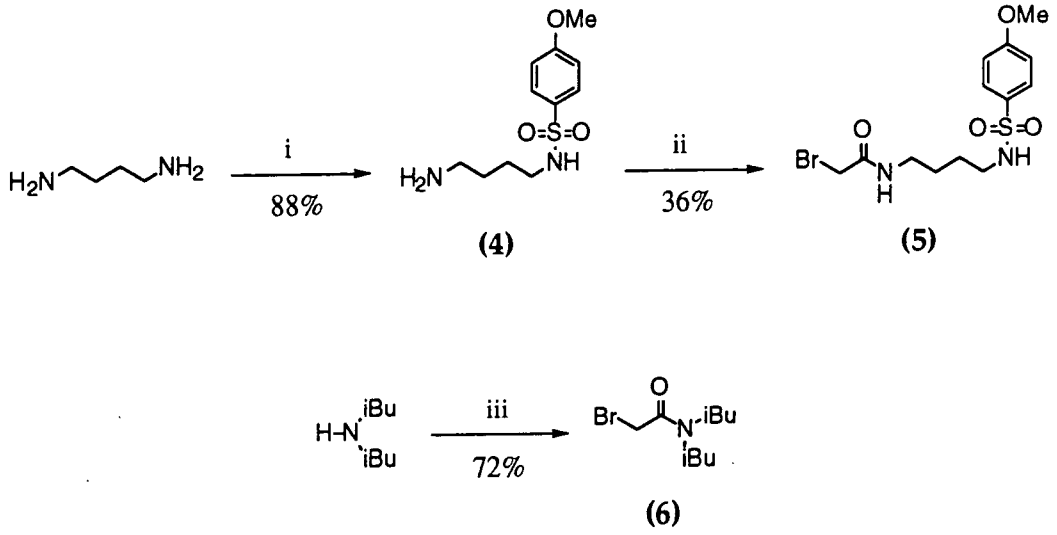

Scheme 2.4 : *Synthesis of α-bromoamide side arms.*

Reagents : (i) p-$MeOC_6H_4SO_2Cl$, CH_2Cl_2; (ii) $BrCH_2COBr$, $C_2H_4Cl_2$, NaOH, H_2O; (iii) $BrCH_2COBr$, $C_2H_4Cl_2$, NaOH, H_2O.

Following the discovery that chromium hexacarbonyl would form metal complexes with a selection of cyclic and acyclic tetraamines,[23] the reaction of molybdenum hexacarbonyl and $12N_4$ (**3**) in dibutyl ether analogously formed the air sensitive, yet relatively stable (under argon) $[Mo(CO)_3 12N_4]$ complex, (**7**), (Scheme 2.5).

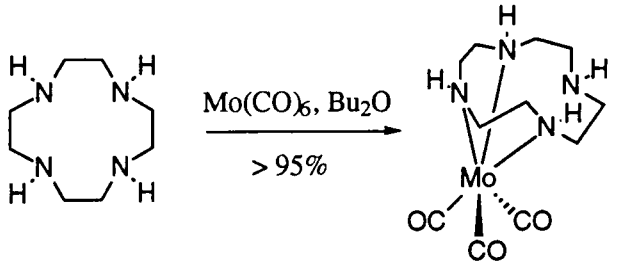

(3) (7)

Scheme 2.5 : *Synthesis of the [Mo(CO)$_3$12N$_4$] complex.*

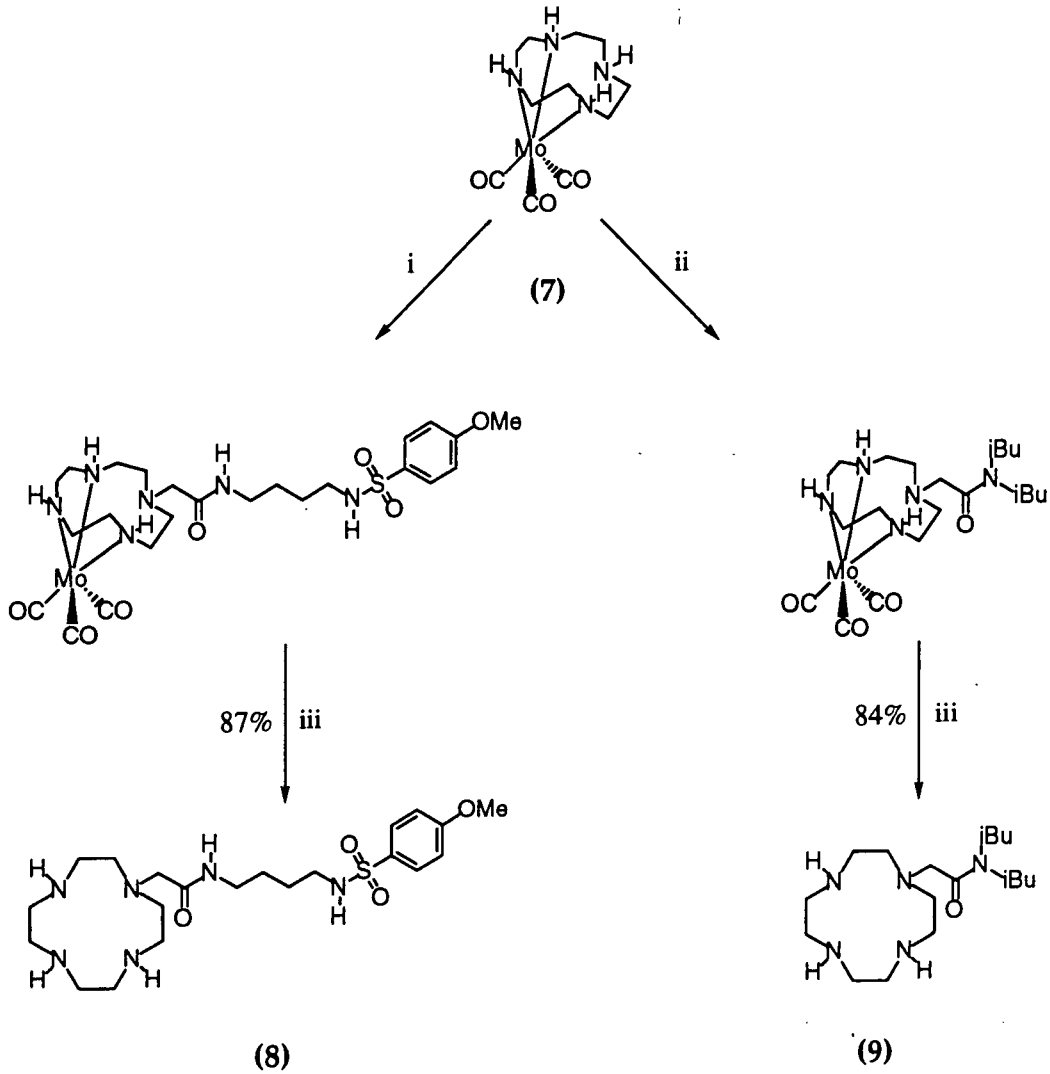

(8) (9)

Scheme 2.6 : *Monoalkylation of 12N$_4$ with pendent amides (5) and (6).*

Reagents : (i) (5), K$_2$CO$_3$, DMF; (ii) (6), K$_2$CO$_3$, DMF; (iii) 10% HCl, air.

Owing to its unusual ring nitrogen protection scheme, whereby three of the four ring nitrogens are protected, selective monoalkylation of **(7)** at the remaining fourth uncoordinated site was possible using **(5)** or **(6)** and potassium carbonate as a strong base in DMF (Scheme 2.6).

Subsequent molybdenum deprotection of the resulting mono-alkylated protected cycles merely required their 10 % HCl solutions to be stirred overnight in contact with air, to give after acid / base work up, the free amines **(8)** and **(9)** in high yield.

2.6.3 Carboxylate Functionalisation of the Macrocycle

Unlike the synthesis of the tetracarboxylic acid substituted cycle DOTA,[26] chloroacetic acid was not used to alkylate the three ring nitrogens of **(8)** and **(9)**. Instead, for ease of purification, conversion of these monoalkylated species to their respective tricarboxylic acid derivatives proceeded through the intermediacy of the tricarboxylate esters **(10)** and **(12)** (Scheme 2.7). After extensive column chromatography, reasonable yields (60%) of these pure esters were obtained, which after subsequent base (KOH) or acid (HBr, glacial acetic acid, phenol) ester hydrolysis yielded the carboxylic acids **(11)** and **(13)**. In the acid hydrolysis of **(10)**, the reaction proceeded with concomitant deprotection of the primary amine of the amide side chain (NB. Sulphuric acid was not used for ester hydrolysis or deprotection because amide hydrolysis may also occur).

2.6.4 Phosphinate Functionalisation of the Macrocycle

As in the carboxylic acid functionalisation of the $12N_4$ ligands, there are two different routes for the synthesis of phosphinic acid functionalised ligands. Either direct reaction of the monosubstituted ligand with a suitable alkylphosphinic acid in the presence of aqueous formaldehyde under acidic conditions, or as in the preferred synthesis of carboxylic acids functionalised ligands (Section 2.6.3), via the intermediacy of a phosphinate ester. Choice of the direct route, although yielding the product in one step, results in contamination by $HOCH_2RPO_2H$. For this reason the two step synthesis via the ester was chosen, whereby condensation of the monoamide substituted ligands **(8)** or **(9)** with paraformaldehyde in anhydrous THF yielded an intermediate iminium ion which was trapped by a dialkoxyphosphine ($RP(OEt)_2$) to give the corresponding monoamide-trimethylenephosphinate ester functionalised ligands **(14)** and **(17)** (Scheme 2.8). Exclusion of water through the use of anhydrous reagents and molecular sieves was found to be essential to prevent the formation of

hydroxymethylphosphinate esters $HOCH_2PRO_2Et$. Attempts to increase the yield of the reaction by deliberately promoting the Arbusov reaction by the addition of anhydrous tetrapentylammonium chloride or bromide failed to produce any noticeable improvements in the reaction products.[17]

Direct base (KOH) or acid (HBr, AcOH, PhOH) hydrolysis of the phosphinate esters **(14)** and **(17)** yielded the phosphinic acids **(15)**, **(16)**, and **(18)**. Again deprotection of the tosylamide was observed as **(14)** underwent acid hydrolysis to **(15)**.

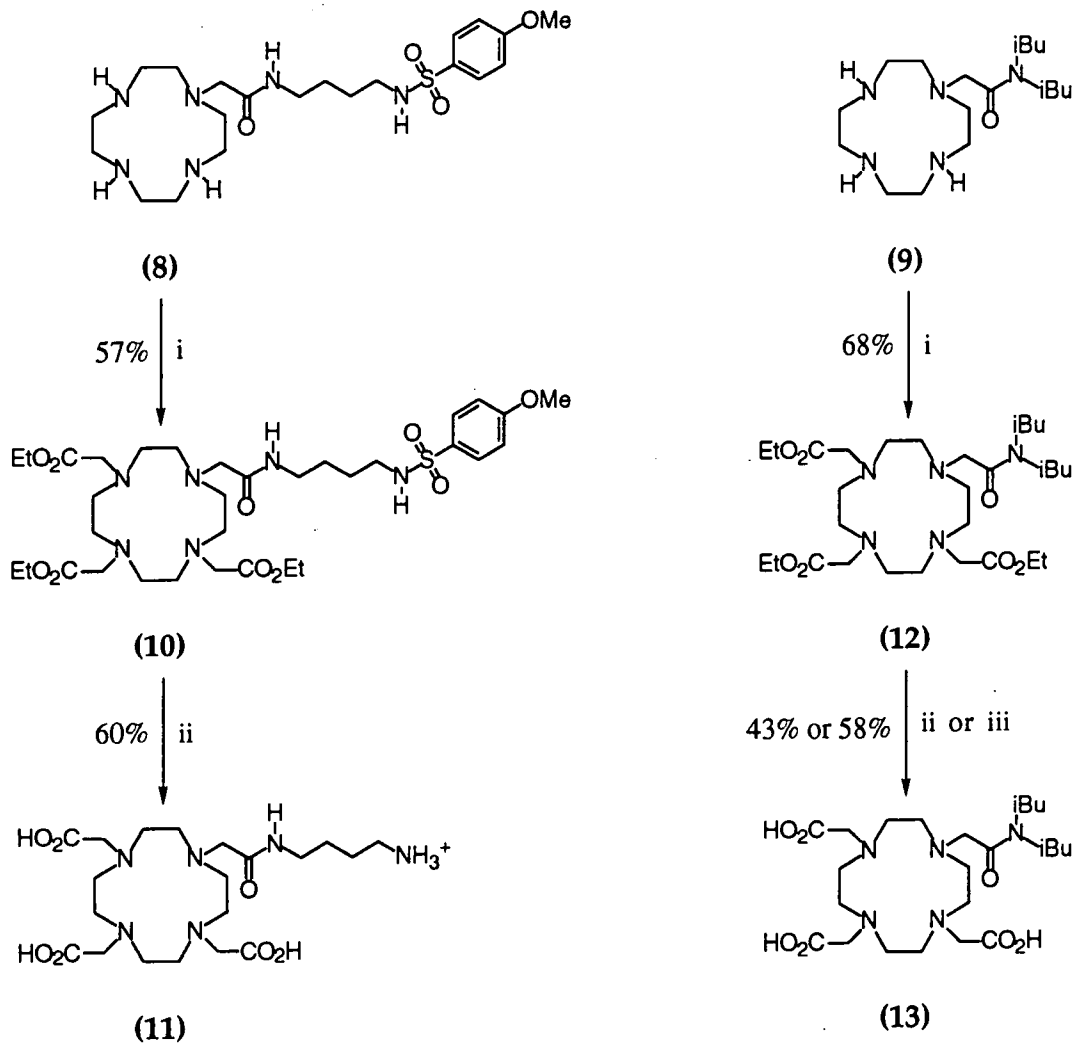

Scheme 2.7 : *Synthesis of monoamide tricarboxylic acid ligands.*

Reagents : (i) $BrCH_2CO_2Et$, K_2CO_3, EtOH; (ii) HBr, AcOH, PhOH; (iii) KOH, H_2O.

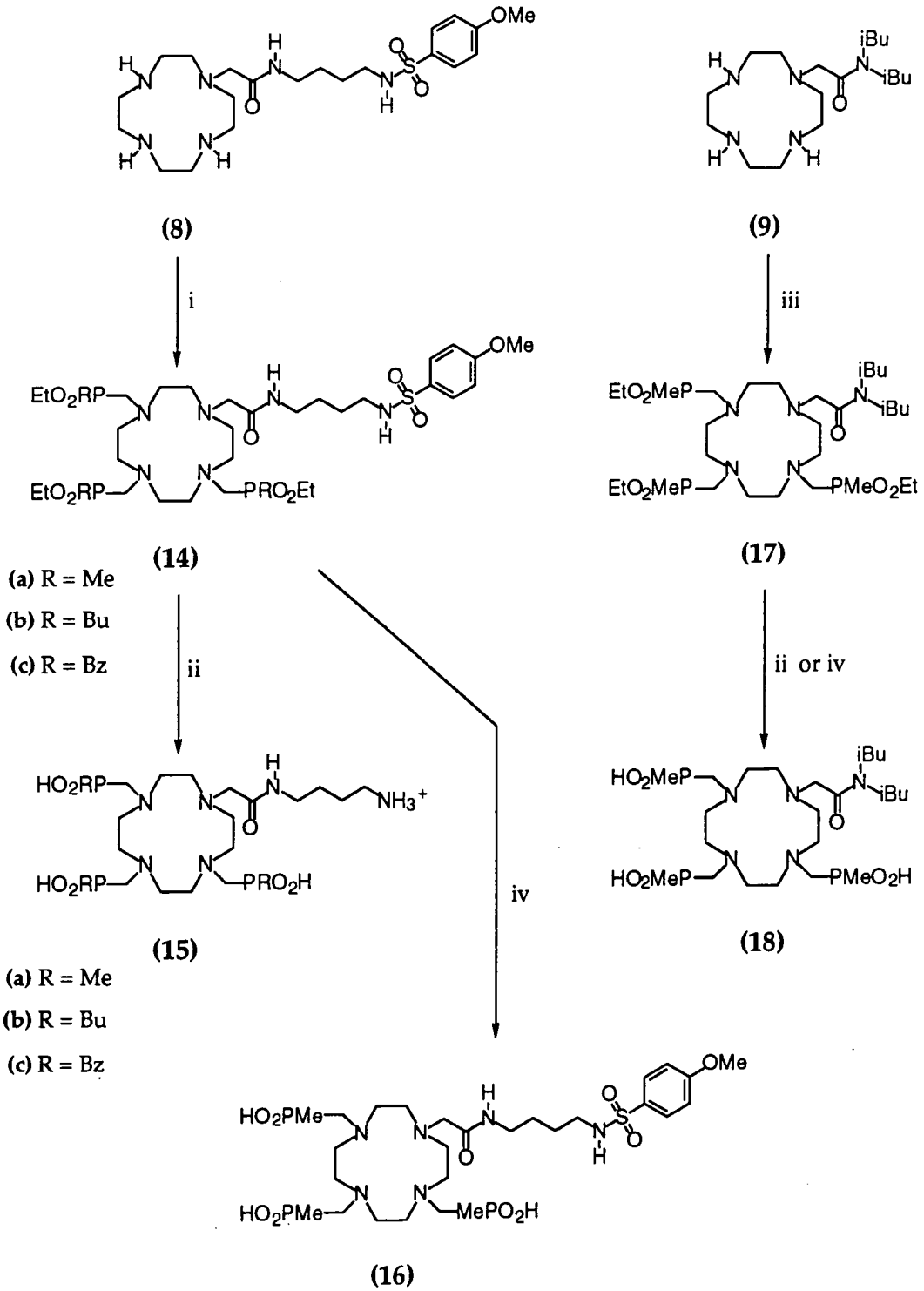

Scheme 2.8 : *Synthesis of monoamide triphosphinic acid ligands.*

(i) $RP(OEt)_2$, $(CHOH)_n$, THF; (ii) HBr, AcOH, PhOH;

(iii) $MeP(OEt)_2$, $(CHOH)_n$, THF; (iv) KOH, H_2O.

2.7 COMPLEX SYNTHESIS

Yttrium complexes of ligands **(13)** and **(16)** and a gadolinium complex of **(15a)** were formed by dissolving either Y_2O_3 or Gd_2O_3 in water at pH = 1.5, and heating at reflux overnight to effectively dissolve the metal oxide. Subsequent raising of the solution pH to 6, and continuation of heating, permitted complexation to occur. An indium complex of **(16)** was also formed at room temperature in pH 5.5 acetate buffer. Although no crystal structures of these amide complexes were obtained, its is expected that like $[Y.DOTA]^-$,[27] and the DOTA-monoamide complex [Gd.A], [6] (Figure 2.1) the complex structures will adopt a distorted square antiprismatic structure capped with a water molecule (Figure 2.5).

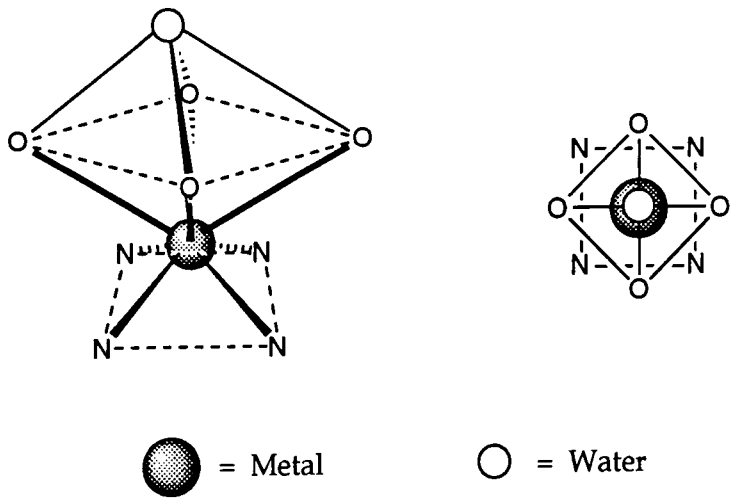

Figure 2.5 : *Distorted square antiprismatic complex structure showing four ring nitrogens, three acidic donors, an amide oxygen donor, and one coordinating water.*

For these monoamide triphosphinic acid complexes, there are 32 possible stereoisomers. For each complex three stereogenic centres exist giving eight possible stereoisomers, RRR, SSS, RRS, RSS, RSR, SRS, SRR and SSR. Through a combination of ring inversion, and phosphinate arm rotation, each of these eight

stereoisomers can exist in four structural arrangements, giving a total of 32 possible stereoisomers (Unpublished work from S. Aime and M. Botta (Turin)).

2.8 COMPLEX CHARACTERISATION

On complexation, a number of different changes in the properties of the ligand can be observed by I.R. and NMR. In I.R., both the acid and amide carbonyl stretching frequencies are reduced as their overall bond order decreases due to donation to the metal centre. This effect was observed for all of the complexes made, and can be taken as an indication of complexation. For instance in the case of [Y.(**16**)], there is an amide carbonyl shift of 53 cm^{-1} from 1679 cm^{-1} for the free ligand to 1626 cm^{-1} for the complex. Similar shifts ranging from 18 cm^{-1} to 49 cm^{-1} were observed for [Y.(**13**)], [In.(**16**)], and [Gd.(**15a**)]$^{+}$.

Similarly, observation of the acid and amide carbonyl shifts using ^{13}C NMR gives information on the nature and extent of complexation. Generally, there was an 8 - 9 ppm shift to higher frequency of the carbonyl resonance on complexation. This was seen with [Y.(**16**)] for example where the amide carbonyl shifted from 175.6 ppm for the free ligand to 183.9 ppm for the corresponding yttrium complex.

Both ^{31}P and ^{89}Y have a nuclear spin of 1/2, and therefore should exhibit coupling. The complex [Y.(**16**)] did indeed show yttrium-phosphorus coupling in its ^{31}P NMR spectrum. The free ligand exhibited two resonances at 38.68 ppm and 39.23 ppm in the ratio 2:1 corresponding to the two slightly different environments of the phosphorus atoms of the ligand. Following complexation, the two resonances were split by coupling to yttrium with a coupling constant $J_{Y\text{-}P}$ of 5 Hz. (Figure 2.6). This compares well with the reported value of 5.1 Hz for $[Y\{S_2P(OEt)_2\}_4]^{-}$.[28]

All of this spectral data is consistent with simultaneous metal coordination of both the acid groups and the amide carbonyl oxygen.

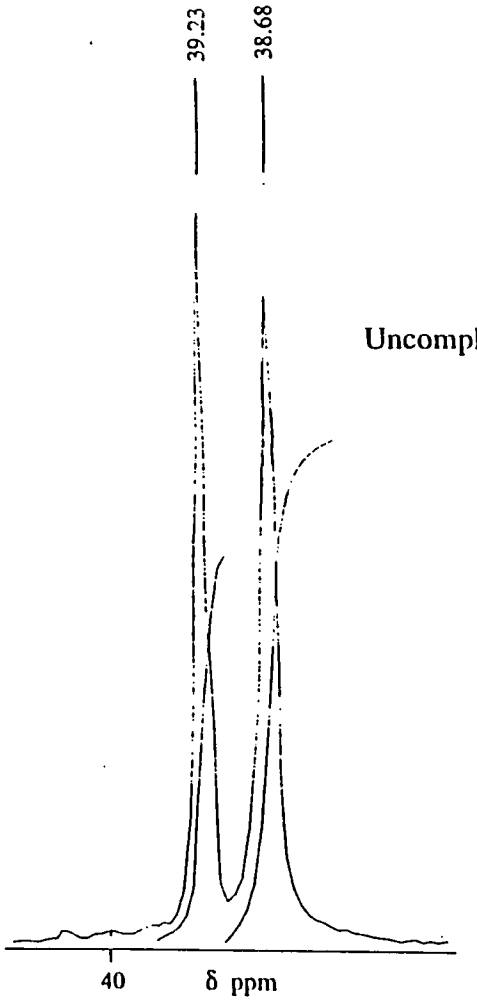
39.23
38.68
Uncomplexed
40
δ ppm

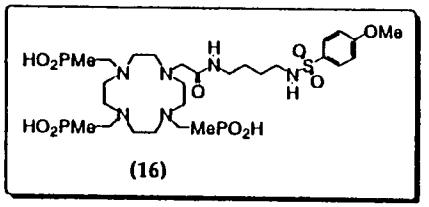
HO2PMe
HO2PMe
MePO2H
OMe
(16)

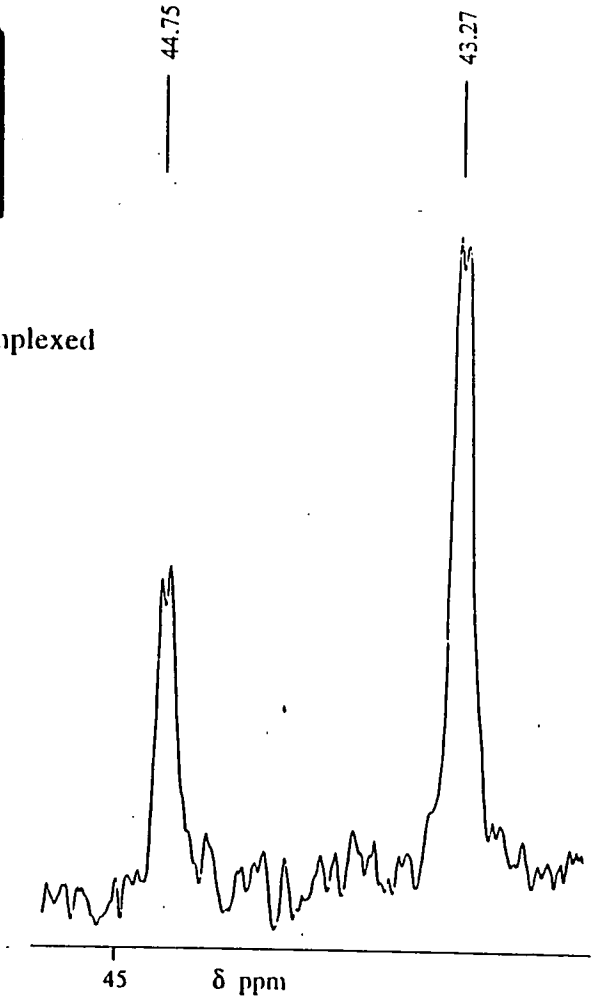
44.75
43.27
Complexed
45
δ ppm

Figure 2.6

2.9 YTTRIUM COMPLEX N.M.R.

Despite being hampered by the long relaxation time required between pulses (30 seconds), ^{89}Y NMR spectra were acquired for [Y.(**13**)], [Y.(**16**)], and other related yttrium complexes (see Figure 2.7 for ligand structures, and Table 2.2 for chemical shift data).

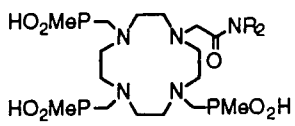

$P_3Me_3NBu_2$ - R = Bu
$P_3Me_3NBz_2$ - R = Bz

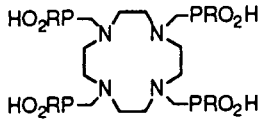

P_4Me_4 - R = Me
P_4Bu_4 - R = Bu
P_4Ph_4 - R = Ph
P_4Bz_4 - R = Bz

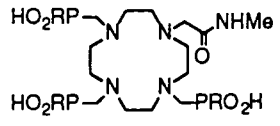

P_3Me_3NHMe - R = Me
P_3Bu_3NHMe - R = Bu

Synthesised by K. Pulukkody & C. J. Broan

Figure 2.7

In the case of [Y(**16**)], the low concentration of the solution meant no coupling information could be seen, (although a doublet of triplets was expected). However, for the two tetraphosphinic acid complexes $[Y.P_4Bz_4]^-$ and $[Y.P_4Me_4]^-$, a quintet of lines was observed with J_{YP} of 5 Hz. This was the predicted splitting pattern with yttrium being split four times by the four equivalent phosphorus atoms.

Complex	δ_Y
[Y.DOTA]	+111.8
$[Y.P_4Bz_4]^-$	+152.8
$[Y.P_4Me_4]^-$	+156.8
$[Y.P_3Me_3NBu_2]$	+168.3
$[Y.EDTA]^-$	+123.5
$[Y.DTPA]^{2-}$	+81.6
[Y.(**13**)]	+111.3
[Y.(**16**)]	+152.0

Table 2.2 : *^{89}Y Chemical shift data*

Although the ligands thus far are presumed to be eight coordinate in solution, yttrium is capable of assuming a nine-coordinate geometry, with the ninth coordination site being taken up by the solvent, a water molecule. Indeed X-ray crystallography has shown both $[Eu.DOTA]^-$,[29] and $[Y.DOTA]^-$ [27] to have a ninth coordinating water molecule. It was therefore quite possible that on going from H_2O to D_2O, $[Y.DOTA]^-$ would exhibit a solvent isotope effect in its ^{89}Y NMR . If indeed this were the case, it was suggested that the extent of the effect would be a reflection of the ability of the ligand to shield bound yttrium from the solvent. It was hoped therefore that $[Y.DOTA]^-$ having one coordinating water molecule would show a considerable effect, whilst the analogous phosphinic acid functionalised complexes would not, due to the shielding of yttrium by the alkyl or aryl groups on phosphorus (a tetrabenzylphosphinic acid functionalised yttrium complex was shown crystallographically to have no coordinating water).

Although small, there is a precedent for a solvent isotope effect of this nature; the solvent isotope effect for the Y^{3+} aquo-ion is 4.3 ppm.[28] Unfortunately, no solvent isotope effect was observed for $[Y.DOTA]^-$, or even for $[Y.EDTA]^{2-}$, thus precluding any conclusions being made concerning the solvation state of complexed yttrium.

2.10 KINETICS OF ASSOCIATION

Suitable complexing agents for use in radioimmunotherapy must label rapidly under conditions mirroring those required for conjugation to an antibody (Section 1.8.1). The forward rate of ^{90}Y uptake by a number of ligands was assessed, comparing **(15a)** and **(11)** to four other ligands prepared independently (see Figure 2.7 for structures).

Each ligand to be tested was incubated with the highest purity yttrium-90 possible, samples were removed at set time intervals, and any unbound yttrium

scavenged by a large excess of DTPA at pH 5.5. Anion exchange chromatography permitted separation of $[Y.DTPA]^{2-}$, and the neutral or monoanionic yttrium complexes, allowing the extent of yttrium association to be determined (Table 2.3).

The choice of solution pH and temperature was found to be a crucial factor in determining the extent of yttrium association as the extent of radiolabelling was dramatically reduced on changing from a solution of pH 6.5 to pH 5.5 or by a temperature change from 37°C to 20°C.

t /min	LIGAND					
	DOTA	P_4Me_4	P_3Me_3 NHMe	P_3Me_3 NBu_2	(15a)	(11)
1	54.4	8.8	2.0	5.9	17.4	3.4
2	80.5	18.3	4.1	12.0	36.2	8.9
5	98.5	55.2	12.6	35.2	78.5	23.6
10	99.7	85.3	24.7	61.1	90.2	42.8
15		-	35.8	78.7	97.4	59.9
20		92.6	45.4	86.8		67.6
30		93.4	58.4	90.2		81.3
60			79.8			91.8

Tests performed at the MRC Radiobiology Unit.

Table 2.3 : *Percentage ^{90}Y uptake by charged and uncharged ligands.*
[Ligand] = 5 μmol dm^{-3}, pH 6.5, 37°C, 0.2 mol dm^{-3} NH_4OAc.

With the exception of P_3Me_3NHMe all the ligands tested gave a radiolabelling yield in excess of 90% within 60 minutes, with DOTA, the tetraphosphinic acid P_4Me_4, and the monoamide phosphinate **(15a)** looking very promising.

2.11 KINETICS OF DISSOCIATION

It is now generally accepted that the relative rate of complex dissociation at low pH (kinetic stability) rather than the 1:1 ML thermodynamic stability constant is a more accurate guide to complex stability *in vivo*. With a view to use in radioimmunotherapy or magnetic resonance imaging, the rate of dissociation of a number of yttrium and gadolinium complexes (Figure 2.7) was determined over the pH range 1-2 (Table 2.4).

Complex	k_{obs} x 10^6 s			Half life (hours)		
pH	1.0	1.5	2.0	1.0	1.5	2.0
$[Gd.DOTA]^-$	3.2	0.9	0.05	60	214	3929
$[Y.DOTA]^-$	15.0	1.9	0.3	13	102	583
$[Gd.P_4Me_4]^-$	10.4	4.6	1.1	19	42	171
$[Y.P_4Me_4]^-$	21.0	9.6	3.1	9	20	62
$[Gd.P_3Me_3NBu_2]$	1.3	0.5	0.2	153	389	943
$[Y.P_3Me_3NBu_2]$	1.9	0.7	0.3	102	276	721
$[Gd.P_3Me_3NBz_2]$	4.3	1.6	1.0	45	118	192
$[Y.P_3Me_3NBz_2]$	4.3	1.6	1.0	145	380	989
$[Gd.P_3Bu_3NHMe]$	4.1	1.5	0.45	47	127	427
$[Gd.P_4Bu_4]^-$	36.9	20.1	7.08	5.2	9.6	27.2
$[Gd.P_4Ph_4]^-$	77.7	36.4	14.7	2.5	5.3	13.1
$[Gd.P_4Bz_4]^-$	23.9	9.1	2.8	8.1	21.1	69.0

Tests performed at the MRC Radiobiology Unit.

Table 2.4 : *Kinetics of dissociation of ^{90}Y and ^{153}Gd complexes at 310K.*

It is evident from these results that the tetraphosphinic acid ligands P_4R_4 do not form complexes with yttrium or gadolinium which are quite as stable as those of DOTA. It must be noted however, that the kinetic stability of these tetraphosphinic

acid complexes shows a less steep dependence on pH, perhaps associated with their reduced tendency to protonate compared to that of a carboxylic acid. Generally it was found that gadolinium complexes were less sensitive to acid-catalysed dissociation than their yttrium analogues.

The use of monoamide triphosphinic acid ligands which form neutral complexes with yttrium and gadolinium was vindicated by these studies. Markedly increased kinetic stability over the anionic tetra phosphinic acid complexes was observed, with a less steep pH dependence. Such kinetic stability was predicted to arise owing to the reduced tendency of neutral complexes to protonate, giving more labile protonated species.

The neutral complexes tested showed promising kinetic stability, and in accordance with these results it was hoped that the complexes formed by **(15)**, **(16)** and **(18)** would also exhibit an acceptable stability *in vivo*, as well as an efficient radiolabelling when used in radioimmunotherapy.

2.12 COMPLEX BIODISTRIBUTION

As well as satisfying the preliminary requirements for radioimmunutherapy, the ligands thus far mentioned also have considerable potential in MRI, with gadolinium complexes of related ligands being used as paramagnetic contrast agents in MRI. Current MRI agents in clinical use, e.g. $[Gd.DTPA]^{2-}$, and $[Gd.DOTA]^{-}$ are excreted predominantly through the kidneys. Consequently, neither is suitable for targeting specific organs such as the liver.

The biodistribution of gadolinium complexes of **(11)**, **(13)**, **(15 a, b, c)** and **(18)** as well as others synthesised by K. Pulukkody in Durham, were tested in mice to define the structural and charge properties which determine the mode of clearance of a complex from the body, to perhaps give an insight into the design of more tissue

specific complexes. A selection of the results is shown in Table 2.5, and represented graphically in Figures 2.8 and 2.9.

Gd Complex	% Dose ^{153}Gd in Whole Tissue						
	Blood	Kidneys	Liver	Gall Bladder	Stomach	Small Intestine	Large Intestine
$[Gd.DOTA]^-$	13.8	6.7	1.8	0.09	0.33	1.4	0.63
$[Gd.P_4Bz_4]^-$	3.7	2.3	14.3	3.10	1.40	45.3	0.37
[Gd.(**13**)]	17.5	7.5	3.2	0.03	0.42	1.8	1.00
[Gd.(**18**)]	15.9	5.7	1.7	0.13	0.41	2.1	0.91
$[Gd.(\mathbf{11})]^+$	17.3	8.4	1.7	0.03	0.44	1.7	0.90
$[Gd.(\mathbf{15a})]^+$	17.0	9.0	2.0	0.02	0.45	1.8	1.10
$[Gd.(\mathbf{15b})]^+$	17.3	12.5	2.5	0.02	0.47	2.0	0.89
$[Gd.(\mathbf{15c})]^+$	20.6	12.5	2.7	0.03	0.39	2.2	1.0

Tests performed at the MRC Radiobiology Unit.

Table 2.5 : *5 minute biodistribution of ^{153}Gd radiolabelled complexes in mice.*

There are two principal excretion routes from the body for the complexes: via the kidneys (renal clearance), or via the liver and the gut (hepatobiliary clearance). The excretion route taken by a specific complex is indicated by a larger dose of ^{153}Gd found in that organ. Thus, renally cleared complexes show a higher dose of radiation in the kidneys (see Table 2.5), whilst hepatobiliary cleared complexes show high doses in the liver, gall bladder and at later time intervals, in both the small and large intestines (also in the stomach due to reflux back from the intestine). Looking at Figures 2.8 and 2.9 plotted from Table 2.5, it is obvious that only $[Gd.P_4Bz_4]^-$ exhibits significant hepatobiliary clearance. "Total gut" (from Figures 2.8 & 2.9) refers to the combined value for the stomach, and the small and large intestines.

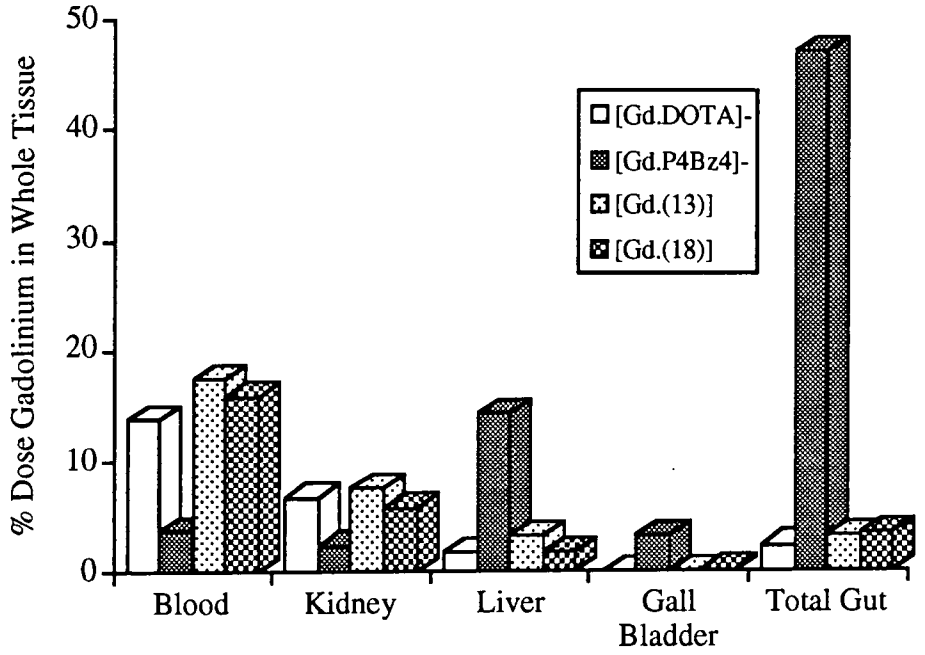

Figure 2.8

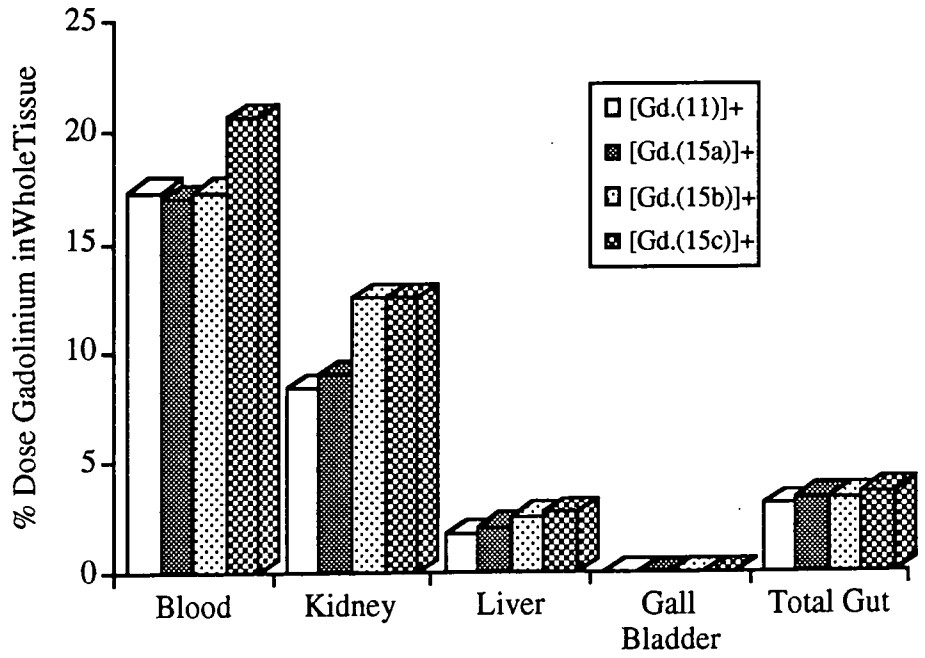

Figure 2.9

It should be noted also, that the blood radiation level for $[Gd.P_4Bz_4]^-$ is substantially lower than the others. The reason for this is that at the low dose of complex given, the liver is capable of removing complexes from the blood stream faster than the kidneys. At higher concentrations of complex however, the receptor sites in the liver becomes saturated, and more of the complex is excreted by the kidneys.

Very generally, it was expected that hydrophilic complexes would pass through the kidneys, whilst more lipophilic complexes would be excreted by the liver. From the results given in Table 2.5, along with other information not shown here, but reported elsewhere,[30] it was found that both complex charge and lipophilicity played important roles in determining complex biodistribution. Cationic complexes (e.g. $[Gd.(\mathbf{11})]^+$ and $[Gd.(\mathbf{15\ a, b, c})]^+$) and neutral complexes (e.g. [Gd.(**13**)] and [Gd.(**18**)]) were found to show predominantly renal clearance, although some more lipophilic neutral complexes did show a small degree of hepatobiliary clearance. Hydrophilic anionic complexes such as $[Gd.DOTA]^-$ also exhibited renal clearance, but lipophilic anionic complexes such as $[Gd.P_4Bz_4]^-$ exhibited hepatobiliary clearance.

The link between complex lipophilicity and the extent of hepatobiliary clearance can be explained in terms of plasma protein binding. Hydrophilic complexes which do not bind to plasma proteins are non-specifically filtered out in the kidneys. As complex lipophilicity increases, plasma protein binding increases reducing the free fraction available for renal filtration thus increasing the amount of complex which can be taken up by liver cells and excreted into the bile (hepatobiliary excretion).

It should be noted that the anionic nature of a complex also plays a crucial role in determining hepatobiliary excretion. It is thought that anionic complexes are taken up by the same carrier system that transports bilirubin IXα, (the dicarboxylic acid breakdown product of heme), and various anionic dyes such as bromosulfophthalein to the liver.[31] This carrier system involves membrane proteins,

and thus in addition to being anionic, the complex must also exhibit some degree of lipophilicity so as to bind to these proteins. This would explain why the anionic lipophilic complex $[Gd.P_4Bz_4]^-$ exhibits hepatobiliary clearance whilst the anionic hydrophilic complex, $[Gd.DOTA]^-$, does not.

With the exception of $[Gd.(\mathbf{15b})]^+$, all complexes in Table 2.5 were shown to be stable with respect to gadolinium dissociation *in vivo*, in that they met the standard set by $[Gd.DOTA]^-$ of < 0.15 % of the injected dose in the liver, and < 0.1 % in the skeleton after 24 hours [30] (data not shown). The deposition of gadolinium by $[Gd.(\mathbf{15b})]^+$ may be simply due to a lack of kinetic stability, or may possibly be explained by the very low concentrations of complex used in these studies. At such low concentrations, there is a comparatively high concentration of cations with which to catalyse complex dissociation. However, at the high concentrations of complex required for MRI, the extent of dissociation would be limited by the concentration of cations in the plasma. This has indeed been found to be the case for $[Gd.DTPA]^{2-}$ which shows much greater complex dissociation at low complex concentration.[30]

From these results, it seems evident that all of the ligands synthesised, with the exception of **(15b)**, are suitable for use *in vivo*, and we have come a step closer to designing more specific complexes.

2.13 GADOLINIUM MAGNETIC RESONANCE IMAGING

As previously stated, the ligands designed for yttrium-90 based radioimmunotherapy may also find use as their gadolinium complexes, as contrast agents in magnetic resonance imaging.

Magnetic resonance imaging (MRI) is a diagnostic imaging technique which relies on the detection of NMR signals of water protons in the body. A gradient magnetic field (rather than a static field used in laboratory based NMR) is applied across the body which causes water protons to resonate at slightly differing

frequencies depending on their position in the gradient field, thus allowing spatial information about the subject to be obtained.

Paramagnetic compounds such as gadolinium ($S = {}^{7}/_{2}$) catalyse proton relaxation in aqueous solutions as the water oxygen atom is coordinated to the metal ion (Gd^{3+}). This causes a perturbation in signal intensity which can be utilised to increase the signal intensity and obtain a more intense image. Free gadolinium ions are however highly undesirable in the body because of a poor acute tolerance (LD_{50} *ca* 0.1 mmol kg^{-1}). Gadolinium therefore must be administered as a stable complex. This is where the ligands synthesised earlier are useful. The biodistribution experiments (section 2.12) have shown the ligands to form gadolinium complexes which are stable *in vivo*, and thus to be possible candidates for MRI.

In general there are two distinct mechanisms for the relaxation of water protons in the presence of the paramagnetic ion Gd^{3+}: inner sphere and outer sphere relaxation. The inner sphere contribution to the relaxation arises from the dipolar interactions between Gd^{3+} and the proton nuclei of the water molecule directly coordinated to the metal ion. The number of water molecules coordinated to the metal ion is denoted q. These dipolar interactions are modulated by the molecular reorientation (τ_R), electron spin relaxation (τ_S) and chemical exchange (τ_M) times. The latter chemical exchange process, which is a measure of the mean residence lifetime of the water molecule at the coordinating site of the metal, is sufficiently fast for Gd^{3+} to provide a means of transferring the relaxation effect to the bulk water. The outer sphere relaxation process involves the electron-nuclear magnetic dipolar coupling which occurs when solvent water molecules approach the metal complex during their translational diffusion.

The large quantity of structural and dynamic information on the solvent relaxation rates of Gd(III) complexes can only be obtained through a magnetic field dependent study. Experimentally this can be done with a field-cycling relaxometer developed by S. H. Koenig and R. D. Brown III,[32] which allows the relaxation rate to be determined in a range of magnetic fields corresponding to Larmor frequencies

0.01 to 50 MHz. What is obtained is a Nuclear Magnetic Relaxation Dispersion (NMRD) profile.

An NMRD study was carried out on the gadolinium complex of **(15a)** at 5, 25, and 35 °C (Figure 2.10 & Table 2.6) and its profile compared to the theoretical one for no water coordination (solid lines in Figure 2.11 represent q = 0, i.e. only outer sphere contribution). The results were also compared to those obtained for the tetrabenzylphosphinic acid complex $[Gd.P_4Bz_4]^-$ which has been shown crystallographically and by NMRD studies to be a complex with q = 0 (Figure 2.11).

Parameter	Temperature / °C		
	5	25	35
τ_{S0} / 10^{-11} s	9.50	8.03	8.47
τ_V / 10^{-11} s	2.54	1.41	1.54
τ_M / 10^{-8} s	18.0	10.0	7.06
τ_R / 10^{-11} s	15.5	9.2	6.80
q	1.00	1.00	1.00
r / Å	3.47	3.47	3.47
a / Å	4.00	4.00	4.00
D / 10^{-5}	1.00	2.20	3.00

Unpublished data from S. Aime, and M. Botta (Turin).

Table 2.6 : *NMRD parameters for [Gd.(15a)]$^+$*

τ_{S0} = electron spin relaxation time at zero field, τ_V = correlation time characterising the time dependence of the interaction responsible for the relaxation process, τ_M = the chemical exchange time of the water molecules, τ_R = molecular reorientation time proportional to molecular size, q = number of coordinating water molecules, r = distance between the water protons and the unpaired electron spin, a = the molecular radius, and D = the diffusion coefficient of the complex.

It was found for $[Gd.(\mathbf{15a})]^+$ that q = 1, i.e. that there was one bound water molecule in the complex. This is in contrast to the tetrabenzylphosphinic acid

Figure 2.10

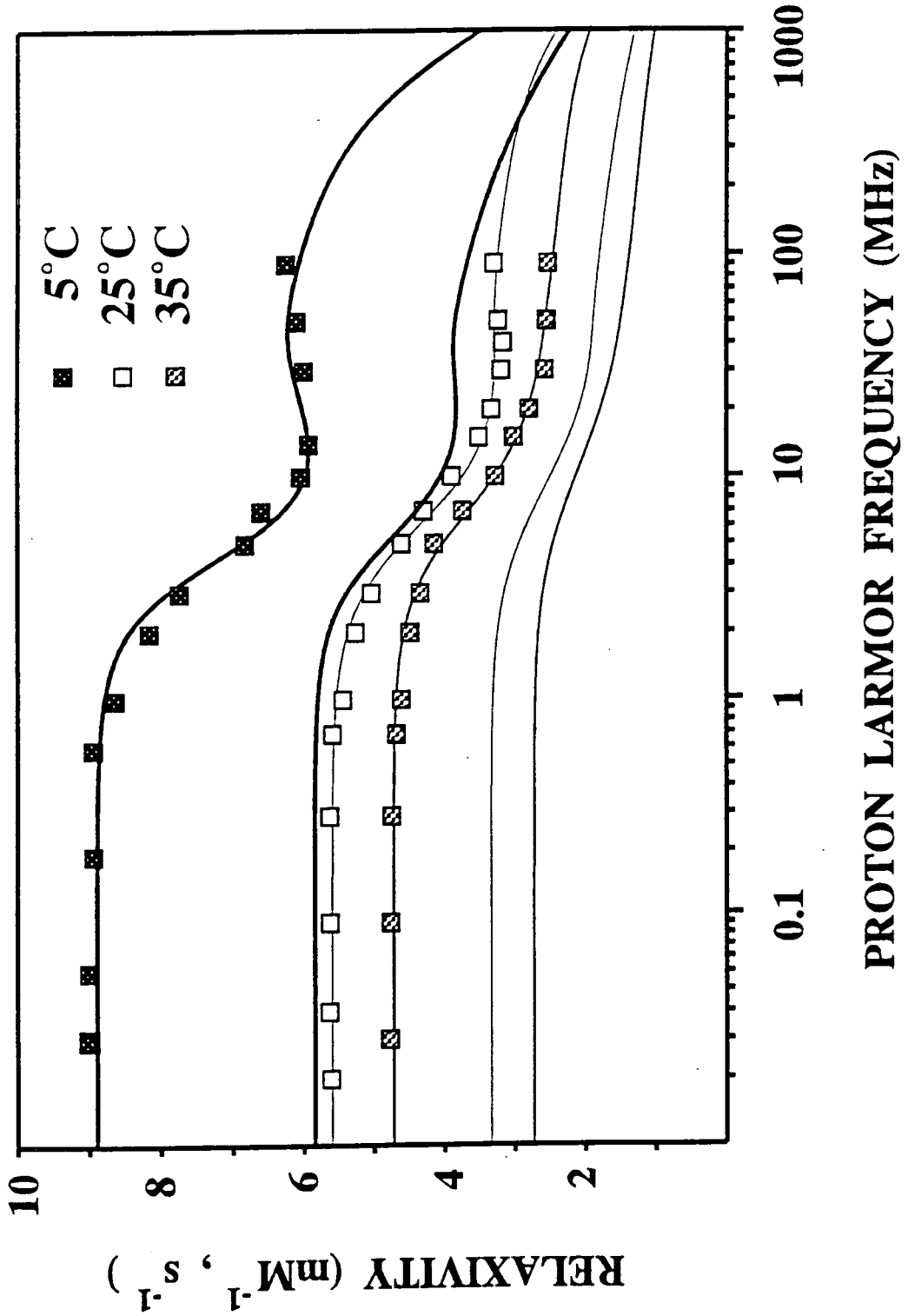
5°C
25°C
35°C
10
8
6
4
2
RELAXIVITY (mM-1, s-1)
0.1
1
10
100
1000
PROTON LARMOR FREQUENCY (MHz)

Figure 2.11

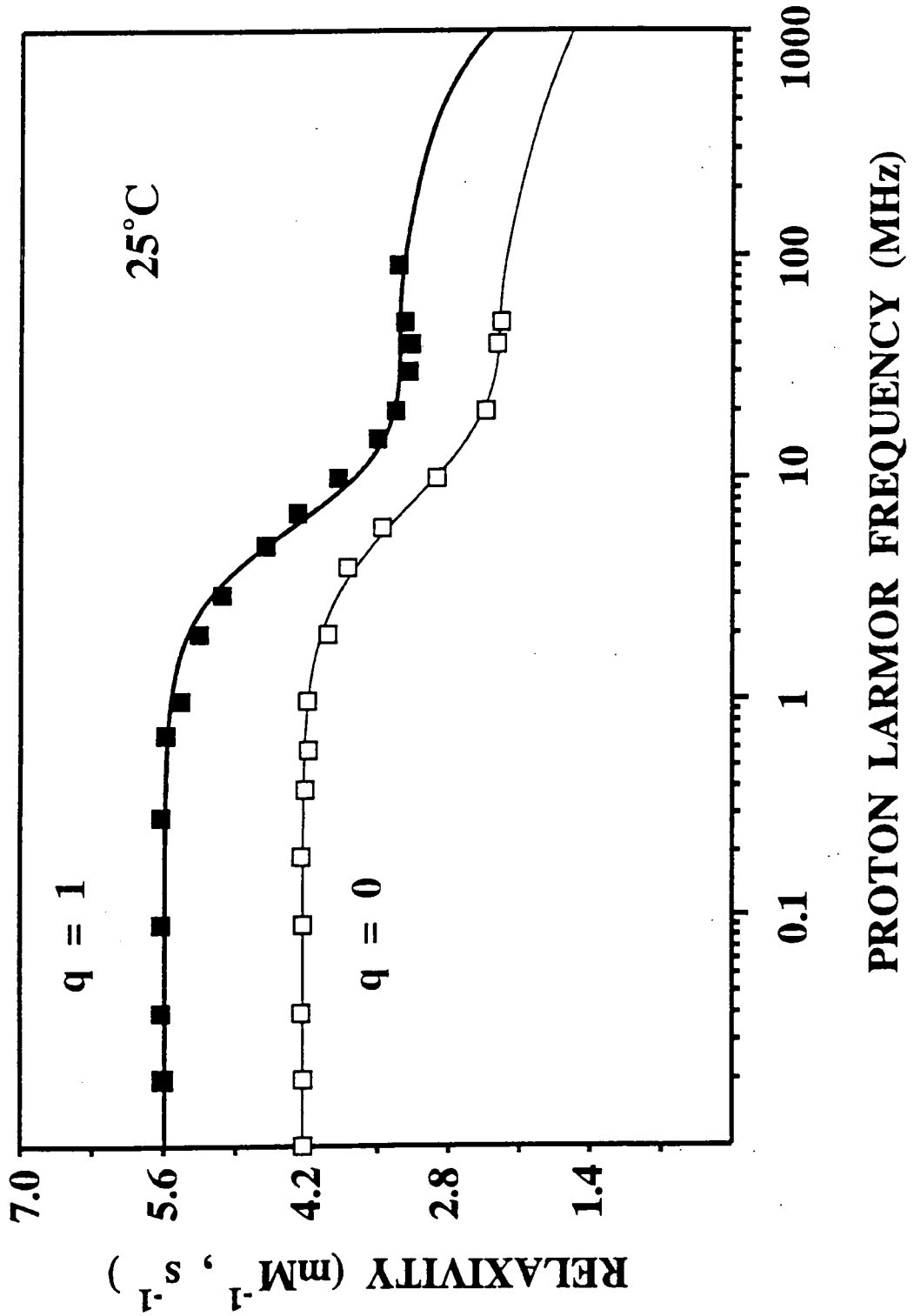
RELAXIVITY (mM^{-1}, s^{-1})
7.0
5.6
4.2
2.8
1.4
0.1
1
10
100
1000
PROTON LARMOR FREQUENCY (MHz)
25°C
q = 1
q = 0

complex $[Gd.P_4Bz_4]^-$ which had q = 0, presumably because the four bulky benzyl groups totally shield the gadolinium ion from the water.

The complex Gd.DOTA-PA (see Figure 2.1) is very similar to $[Gd.(\mathbf{15a})]^+$, in that they both possess a pendent amide, and three acidic groups; phosphinic acids in the case of **(15a)**, and carboxylic acids in the case of DOTA-PA. NMRD profiles have been reported for both [Gd.DOTA-PA] and $[Gd.DOTA]^-$.[10] Like $[Gd.(\mathbf{15a})]^+$, both showed the presence of just one inner sphere water molecule, suggesting that an amide functional group, like a carboxylate or a phosphinate does, as predicted, occupy a site in the gadolinium coordination sphere, thereby preventing an increase in inner-sphere water molecules.

2.14 CONCLUSIONS

A number of ligands suitable for the complexation of yttrium and gadolinium have been synthesised with a view to producing neutral yttrium complex conjugates for radioimmunotherapy, and perhaps for use in MRI. The use of pendent phosphinic acids on the ligands has been shown to produce complexes which are kinetically slightly less stable than their carboxylic acid analogues, although the complexes are still of sufficient stability for use *in vivo*. The monoamide triphosphinic acid ligands which were designed specifically to form neutral complexes have however shown excellent stability, whilst I.R. and NMR studies (including an NMRD profile) have all shown that the pendent amide takes part in binding to the complexed cation. Ligand **(15a)** appears particularly promising, with further ligand functionalisation being possible at the pendent NH_3^+ site to give a desired bifunctional complexing agent. Chapter 3 will concentrate on the functionalisation of ligand **(15a)** (to form a bifunctional complexing agent), specifically dealing with the attachment of functional groups with which to bind to antibody fragments.

2.15 REFERENCES

1 J. P. L. Cox, K. J. Jankowski, R. Kataky, D. Parker, N. R. A. Beeley, B. A. Boyce, M. A. W. Eaton, K. Millar, A. T. Millican, A. Harrison, and C. Walker, *J. Chem. Soc., Chem. Commun.*, 1989, 797

2 K. Kumar and M. F. Tweedle, *Pure Appl. Chem.*, 1993, **65**, 515.

3 A. Chang, A. C. Francesconi, M. F. Malley, K. Kumar, J. Z. Gougoutas, M. F. Tweedle, D. W. Lee, and L. J. Wilson, *Inorg. Chem.*, 1993, **32**, 3501.

4 X. Wang, T. Jin, V. Comblin, A. Lopez-Mut, E. Merciny, and J. F. Desreux, *Inorg. Chem.*, 1992, **31**, 1095.

5 K. Kumar, C. A. Chang, and M. F. Tweedle, *Inorg. Chem.*, 1993, **32**, 587.

6 S. Aime, P. L. Anelli, M. Botta, F. Fedeli, M. Grandi, P. Paoli, and F. Uggeri, *Inorg. Chem.*, 1992, **31**, 2422.

7 R. Harder, and S. J. Chabarek, *J. Inorg. Nucl. Chem.*, 1959, **11**, 197.

8 T. Moeller, and L. C. Thompson, *J. Inorg. Nucl. Chem.*, 1962, **24**, 499.

9 W. P. Cacheris, S. K. Nickle, and A. D. Sherry, *Inorg. Chem.*, 1987, **26**, 958.

10 A. D. Sherry, R. D. Brown III, C. F. G. C. Geraldes, S. H. Koenig, K. Kuan, and M. Spiller, *Inorg. Chem.*, 1989, **28**, 620.

11 K. E. Matthes, D, Parker, H. J. Buschmann, and G. Ferguson, *Tet. Lett.*, 1987, **28(45)**, 5573.

12 I. Lázár, D. C. Hrncir, W. Kim, G. E. Kiefer, and A. D. Sherry, *Inorg. Chem.*, 1992, **31**, 4422.

13 C. F. G. C. Geraldes, A. D. Sherry, and W. P. Cacheris, *Inorg. Chem.*, 1989, **28**, 3336.

14 M. P. Pasechnik, S. P. Solodovnikov, E. I. Matrosov, S. A. Pisareva, Y. M. Polikarpov, and M. I. Kabachnik, *Bull. Acad. Sci. USSR, Div. Chem. Sci.*, 1988, **37**, 1866.

15 C. F. G. C. Geraldes, A. D. Sherry, and G. E. Kiefer, *J. Magn. Reson.*, 1992, **97**, 290.

16 E. Cole, D. Parker, G. Ferguson, J. F. Gallagher, and B. Kaitner, *J. Chem. Soc., Chem. Commun.*, 1991, 1473.

17 C. J. Broan, E. Cole, K. J. Jankowski, D. Parker, K. Pulukkody, B. A. Boyce, N. R. A. Beeley, K. Millar, and A. T. Millican, *Synthesis*, 1992, **1/2**, 63.

18 E. Cole, R. C. B. Copley, J. A. K. Howard, D. Parker, G. Ferguson, J. F. Gallagher, B. Kaitner, A. Harrison, and L. Royle, *J. Chem. Soc. Dalton Trans.*, 1994, 1619.

19 M. L. Garrity, G. M. Brown, J. E. Elbert, and R. A. Sachleben, *Tet. Lett.*, 1993, **34(35)**, 5531.

20 J. P. L. Cox, Ph. D. Thesis, University of Durham, 1989.

21 D. D. Dischino, E. J. Delaney, J. E. Emswiler, G. T. Gaughan, J. S. Prasad, S. K. Srivastava, and M. F. Tweedle, *Inorg. Chem.*, 1991, **30**, 1265.

22 T. J. Atkins, U. S. Patent No 4,085,106, April 18, 1978.

23 J. Yaouanc, N. Le Bris, G. Le Gall, J. Clement, H. Handel, and H. des Abbayes, *J. Chem. Soc., Chem. Commun.*, 1991, 206.

24 H. Stetter, and W. Frank, *Angew. Chem., Int. Ed. Engl.*, 1976, **15**, 686.

25 K. Kitagawa, K. Kitade, Y. Kizo, T. Akita, S. Funakoshi, N. Fujii, and H. Yajima, *J. Chem. Soc., Chem. Commun.*, 1979, **47**, 3146.

26 J. F. Desreux, *Inorg. Chem.*, 1980, **19(5)**, 1319.

27 C. A. Chang, L. C. Francesconi, M. F. Malley, K. Kumar, J. Z. Gougoutas, M. F. Tweedle, D. W. Lee, and L. J. Wilson, *Inorg. Chem.*, 1993, **32**, 3501., and D. Parker, K. Pulukkody, F. C. Smith, A. Batsanov, and J. A. K. Howard, *J. Chem. Soc. ,Dalton Trans.*, 1994, 689.

28 "Multinuclear NMR", ed. J. Mason, Plenum Press, 1987.

29 M-R. Spirlet, J. Rebizant, J. F. Desreux, and M-F. Loncin, *Inorg. Chem.*, 1984, **23**, 359.

30 A. Harrison, C. A. Walker, K. A. Pereira, D. Parker, L. Royle, K. Pulukkody, and T. Norman, *Magn. Reson Imag.*, 1993, **11**, 761.

31 R. B. Lauffer, *Chem. Rev.*, 1987, **87**, 901.

32 S. H. Koenig, and R. D. Brown III, "Relaxometry of Tissue in NMR Spectroscopy of Cells and Organisms" Vol. 2, ed R. M. Gupta, F. L. Boca Raton, CRC Press, 1987, 75-114.

Chapter 3

Bifunctional Complexing Agents

3.1 INTRODUCTION

This chapter is primarily concerned with the synthesis of bifunctional complexing agents with which to radiolabel antibody fragments, (see Section 1.6.5) with yttrium-90. Ligand **(15a)** (Scheme 2.8) satisfied the criteria laid out in Chapter 1 (Section 1.8.1) for the metal complexing component of a bifunctional complexing agent, and was accordingly chosen as the foundation of any proposed synthesis.

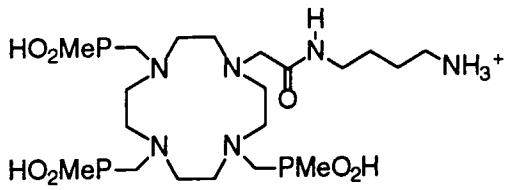

(15a)

3.2 LIGAND CONJUGATION TO AN ANTIBODY

3.2.1 Reactive Antibody Sites

There are only two practical sites for linkage of a ligand to the polypeptide chains of an antibody fragment; at the ε-amino sites of lysine residues, of which there are up to ninety in a typical monoclonal antibody, or at the site of a free thiol (Section 1.9).

Although readily accessible, the inherent problem with effecting Fab' conjugation via ε-amino sites of lysine residues lies in the fact that some of them may be found close to, or at the antigen binding site of the Fab'. Hence attachment of a metal complex at one of these sites will severely impair the specificity of antigen binding, resulting in a diminution of the 'immunoreactivity' of the Fab'. Using recombinant antibody methods however, a free cysteine thiol residue can be introduced into the C_H1 domain of an antibody (Figure 1.10),[1] effectively negating

the problems experienced with lysine, and permitting site specific derivatisation of the antibody fragment away from its antigen binding site. It should also be noted that unlike the functionalisation of a Fab' at its ε-amino sites, the use of the cysteine thiol dictates the introduction of one metal complex only. For this reason, it was decided to attach a ligand at a free thiol introduced into the C_H1 domain.

3.2.2 Thiol Selective Agents

There are really only two possible candidates with which to target a free thiol in the presence of ε-amino lysine residues; vinylpyridines, and maleimides (Figure 3.1).

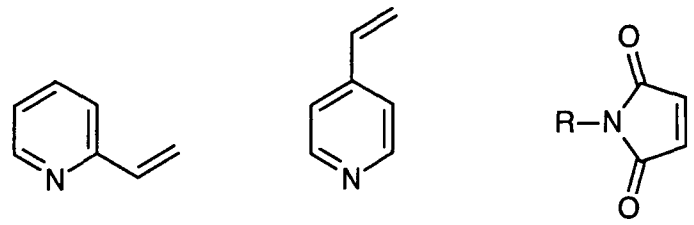

(a) (b) (c)

Figure 3.1 : *Thiol selective agents (a) 2-vinylpyridine, (b) 4-vinylpyridine, and (c) maleimide.*

Although their use is compromised by a slow rate of reaction with thiol groups, previous work in the pH range 5-9 has shown vinylpyridines to be substantially more reactive towards the thiol group of cysteine than towards primary amines which showed less than 3 % reaction over a period of two hours.[2]

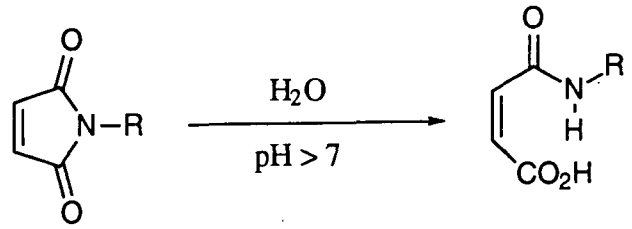

Scheme 3.1 : *Maleimide hydrolysis to a maleamic acid.*

Maleimides on the other hand exhibit a comparatively greater rate of reaction with thiols, but show only moderate selectivity for thiols over primary amines, and tend to undergo slow hydrolysis to maleamic acids at a pH in excess of 7 (Scheme 3.1).

3.3 BIFUNCTIONAL COMPLEXING AGENT DESIGN

Both 2-vinylpyridines [2,3,4] and maleimides [5,6,7] have been used with some success in the conjugation of antibodies to ligands. However, because of their speed of reaction with thiols, and ease of synthesis, maleimides were chosen for this work to form part of a bifunctional complexing agent with which to bind a Fab'.

If we can furnish ligand **(15a)** with a pendent maleimide, it should be possible to attach it to an antibody fragment via the free thiol of the cysteine residue (Scheme 3.2).

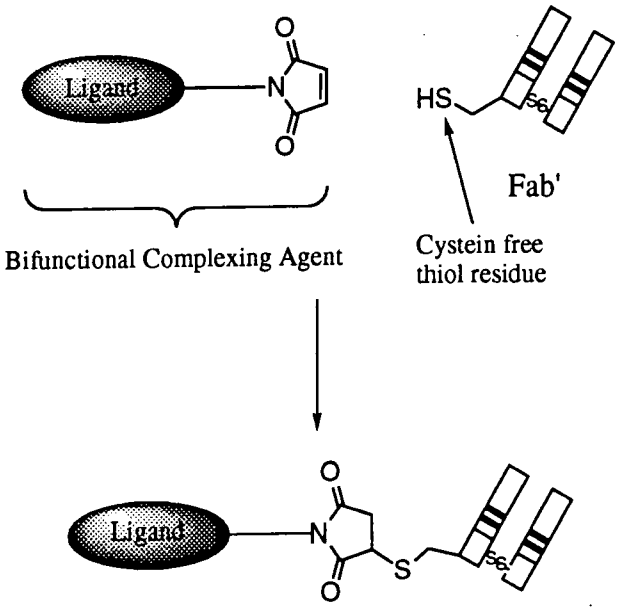

Scheme 3.2 : *A bifunctional complexing agent incorporating a maleimide to bind to the cysteine residue in the C_H1 domain of a Fab'.*

As radiolabelling of the ligand is usually done after it has been attached to the antibody fragment, the metal binding site should ideally remain easily accessible for complexation. If the ligand is directly attached to the antibody fragment with little distance between the two, the ligand can become engulfed within the comparatively large three dimensional structure of the Fab', sterically hindering the approach path of an aquo yttrium-90 species, and reducing overall labelling efficiency. To reduce this effect, a spacer group should be incorporated into the bifunctional complexing agent between the ligand **(15a)** and the maleimide functionality.

As intended, any functionalisation of ligand **(15a)** will occur at the primary amine site of the aminoalkyl chain of the amide. Thus, incorporation of a maleimide onto this primary amine site requires a maleimide reagent which possesses a functional group capable of reacting with the primary amine.

A range of maleimides are commercially available, coming in one of two forms; either with an attached carboxylic acid functional group (maleimido carboxylate) or as an active ester of the carboxylic acid form (see Figure 3.2).

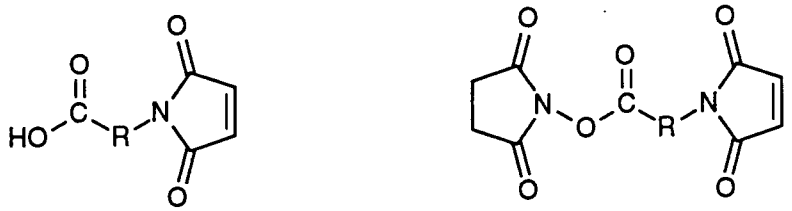

Figure 3.2 : *(a) Maleimido carboxylates, and (b) N-hydroxysuccinimide active esters*

The carboxylic acid derivative of the maleimide can be converted into its reactive acid chloride, or coupled to the amine of **(15a)** using a coupling agent such as dicyclohexylcarbodiimide (DCC), whilst the active ester form can be used directly to react with the pendent amine of **(15a)**.

The use of maleimide active esters for the coupling of biomolecules such as antibody fragments is not without precedent. Indeed, as far back as 1976 Kitagawa

and Aikawa used the maleimide active ester meta-maleimidobenzoyl N-hydroxysuccinimide to couple insulin via a primary amine to the enzyme β-D-galactosidase through a free thiol group.[8] Since then, a variety of maleimide active esters have been used to couple a range of biomolecules for use in the preparation of sensitive enzyme immunoassays.[9,10] This use of active esters is analogous to the proposed coupling of a Fab' to the ligand **(15a)**. In both cases, the maleimide reacts with a free thiol group of an antibody fragment, whilst the active ester functionality reacts with a primary amine (Scheme 3.3).

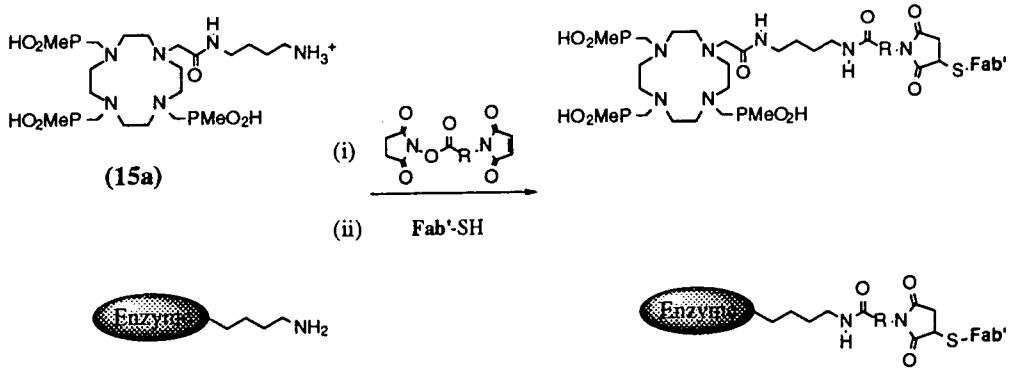

Scheme 3.3 : *The coupling of an antibody fragment to ligand (15a) or to an enzyme using a maleimide active ester.*

3.4 MALEIMIDE SYNTHESIS

It was previously noted that maleimides underwent slow ring-opening hydrolysis at a pH of 7 or over. The stability of a number of maleimide active esters was accordingly tested at 30°C in pH 7 phosphate buffer in order to choose the most suitable candidate for use in immunoassays.[11] Nine different active esters were tested, showing maleimide hydrolysis ranging between 10 and 93% over a period of 6 hours. Active esters with R = CH_2, $(CH_2)_3$, $(CH_2)_5$, or CH_2cyclohexyl,

(see Figure 3.2) were shown to possess the greatest stability, whilst the use of aromatic R groups considerably reduced maleimide stability.

Unfortunately, commercially available maleimides are very expensive at £80 and £1000 per gram for the maleimido carboxylates and the active ester derivatives respectively. Laboratory scale synthesis of these maleimides however is relatively simple, requiring two steps for the synthesis of the maleimido carboxylate from maleic anhydride, and an extra step to form the active ester.

In view of the reported maleimide stabilities, the synthesis of maleimidohexanoate, R = $(CH_2)_5$ was brought about following the standard literature synthesis.[12] Initial ring opening of maleic anhydride by 6-aminohexanoic acid yielded the maleamic acid **(19)** in reasonable yield which, on heating in acetic anhydride subsequently underwent ring cyclisation via an anhydride intermediate, to give on careful crystallisation the maleimide **(20)** (Scheme 3.4). In an analogous manner, the maleamic acid N-(4-carboxycyclohexylmethyl)-maleamic acid also underwent cyclisation to the maleimide N-(4-carboxycyclohexylmethyl)-maleimide **(21)**. In both cases, incomplete cyclisation and a mixture of products, resulting in a black viscous oil in the case of **(20)**, severely hampered product crystallisation, and led in part to the low yields (approx. 15 %) of pure material reported.

In an investigation into possible primary amine protecting groups for use in peptide chemistry, Keller and Rudinger [13] explored the possibility that an amino group may be protected as a maleimide in a similar manner to protection as a phthalimide. During their studies, it was confirmed that ring opening could be effected under mildly basic conditions but, more importantly, they also found that on treatment with 1 mol dm^{-3} acetic acid at 40°C, the maleamic acid **(19)** showed complete conversion back to 6-aminohexanoic acid. In our cyclisation of the maleamic acids to the maleimides **(20)** and **(21)**, acetic anhydride was used, but was later hydrolysed to acetic acid by heating in water at 70°C for 3 hours. This may perhaps go some way to explain the mixture of products observed from the cyclisation step, particularly as ethylene-1,2-dicarboxylic acid was formed, as much

of the unreacted maleamic acid would undergo acid hydrolysis back to the amino acid (Scheme 3.4).

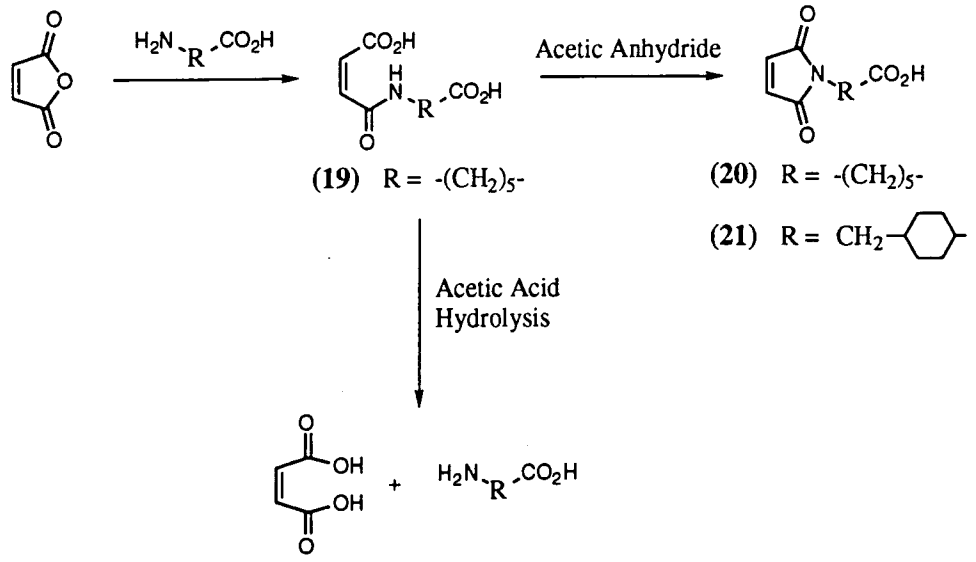

Scheme 3.4 : *Synthesis of maleimido carboxylic acids, showing unwanted acetic acid hydrolysis of the maleamic acid*

Conversion of the maleimides, 4-maleimidobutyric acid (R = $(CH_2)_3$) (purchased from Sigma), and 6-maleimidohexanoic acid (R = $(CH_2)_5$) **(20)** to their respective succinimidyl active esters **(22)** and **(23)** followed the synthesis laid out by Keller and Rudinger[13] using DCC to couple N-hydroxysuccinimide to the maleimido carboxylic acid in DMF (Scheme 3.5).

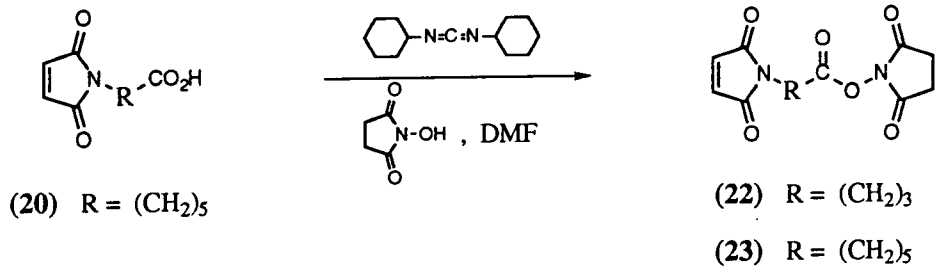

Scheme 3.5 : *The synthesis of succinimidyl maleimido carboxylates using DCC*

Reasonable conversion to the active esters resulted, although purification using a silica column still gave products which contained up to 20 % unreacted acid (this would not interfere in the next step as it is merely the product of ester hydrolysis).

It should also be noted that, although not attempted, an alternative active ester synthesis has been reported.[12] This required initial conversion of the maleimido carboxylic acid to its acid chloride, and conversion of N-hydroxysuccinimide to its sodium salt. Addition of the two reagents resulted in a 76% yield of the required active ester.

3.5 MONO-MALEIMIDE - BIFUNCTIONAL COMPLEXING AGENT

3.5.1 Synthesis

Incorporation of a maleimide functionality onto the pendent amine of ligand **(15a)** proceeded as proposed upon the addition of excess active ester succinimidyl 4-maleimidobutyrate **(22)**, to a DMSO solution of the ligand **(15a)** and N-methylmorpholine (ligand was an HBr salt) (Scheme 3.6).

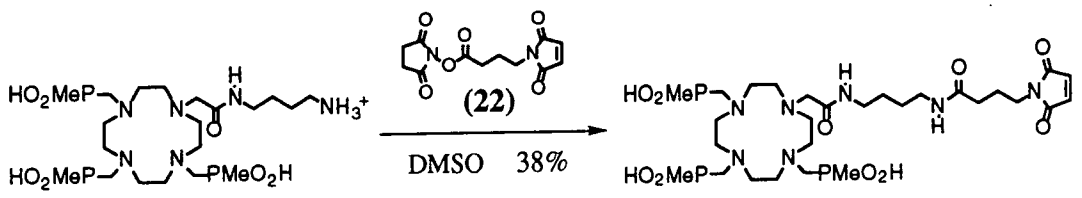

(15a) **(24)**

Scheme 3.6 : *Synthesis of a mono-maleimide bifunctional complexing agent*

Because of the relatively slow rate of reaction of the active ester with **(15a)**, competitive ester hydrolysis was a problem. Therefore an excess of the ester was required, and the utmost care was taken to ensure the use of anhydrous solvents and

reagents. After overnight reaction, analytical HPLC indicated approximately 60% conversion of the ligand, and approximately 25% hydrolysis of the active ester to 4-maleimidobutyric acid. Purification required preparative HPLC, giving the product as its tri TFA salt in 38% yield, contaminated with approximately 20% 4-maleimidobutyric acid which eluted at the same time from the column. Attempts to remove excess acid using a diethyl ether wash failed to improve product purity.

3.5.2 Stability and Biodistribution Results

Because the mono-maleimide **(24)** was designed for use *in vivo* as its yttrium complex, the kinetic stability of its yttrium complex was tested at pH 1.0, 1.5, and 2.0, and compared to the yttrium complex of C-functionalised DOTA mono-maleimide (Table 3.1).

Complex	k_{obs} x 10^6 s				Half life (hours)		
	pH 1.0	1.5	2.0		1.0	1.5	2.0
[Y.**(24)**]	6.56	2.11	0.52		29	91	370
[Y.DOTA mono-maleimide]$^-$	2.72	0.76	0.14		71	254	1368

Tests performed at the MRC Radiobiology Unit.

Table 3.1 : *The rates of dissociation and half lives of two mono-maleimides under acidic conditions*

The figures in Table 3.1 are approximate, but do show that the neutral complex [Y.**(24)**], though less inert than [Y.DOTA-mono-maleimide]$^-$, is still remarkably stable at pH 1.0 (compares well with the results for yttrium complexes given in Table 2.4), and at pH 1.5, the half life of the complex, 91 hours, exceeds the physical half life of ^{90}Y (64 hours).

Although a very good indicator, kinetic stability measurements need to be backed up by actual *in vivo* testing. The mono-maleimide **(24)** was designed not only to complex yttrium, but also to couple to an antibody fragment (Fab'). The Fab' conjugates of [Y.(**24**)] and [Y.DOTA-mono-maleimide]$^-$, from now on referred to as [Y.(**24**)]-B72.3 and [Y.DOTA]$^-$-B72.3 respectively (B72.3 is the antibody from which the specific Fab' used was derived), were accordingly formed, and their biodistributions examined in mice after 48 hours.

In comparing the two Fab' conjugates, it is was found that the % dose per gram of blood was higher for [Y.(**24**)]-B72.3, not because of any stability differences, but merely because of the size of the initial injected dose. It was therefore more informative to compare ratios of doses, rather than absolute values (i.e. % dose in tissue). The ratios of tissue dose to the blood dose for various tissues is given in Table 3.2.

Tissue	^{90}Y Tissue : Blood Ratio	
	[Y.(24)]-B72.3	[Y.DOTA]$^-$-B72.3
Brain	0.024 ± 0.004	0.028 ± 0.006
Femur	0.193 ± 0.021	0.176 ± 0.022
Kidneys	0.304 ± 0.059	0.322 ± 0.116
Liver	0.702 ± 0.198	0.740 ± 0.244
Lungs	0.371 ± 0.058	0.348 ± 0.020
Muscle	0.083 ± 0.018	0.072 ± 0.016
Spleen	0.393 ± 0.090	0.374 ± 0.066

Tests performed at the MRC Radiobiology Unit.

Table 3.2 : *The ratios of the amount of yttrium-90 found in various tissues compared to that in the circulating blood 48 hours post injection into mice.*

Complex instability is accompanied by a deposition of ^{90}Y in the bones (e.g. the femur). A stable complex will therefore exhibit a low value for the ratio of femur to blood (see Tables 3.2 and 3.3), and an unstable complex will give a higher value. The ratios of femur to blood for [Y.(**24**)]-B72.3 and $[Y.DOTA]^-$-B72.3 were found to be 0.19 and 0.18 respectively indicating high complex stability for both complexes. In comparison, $[Y.DTPA]^{2-}$-B72.3 gave a ratio of 1.7, showing once again the kinetic instability of acyclic complexing agents compared to macrocyclic agents. The marrow of the femur is perfused by blood, hence much of the radioactivity detected in the femur may not be attributed to ^{90}Y decomplexation and subsequent bone deposition, but merely due to stable complex in the circulating blood. For this reason the marrow was removed (leaving the shaft), and new ratios calculated. Once again the ratios showed both [Y.(**24**)]-B72.3 and $[Y.DOTA]^-$-B72.3 to be very stable *in vivo*, whilst the DTPA complex was shown to be unstable. The results can be seen in Table 3.3.

	[Y.(24)]-B72.3	$[Y.DOTA]^-$-B72.3	$[Y.DTPA]^{2-}$-B72.3
Femur : Blood	0.193 ± 0.021	0.176 ± 0.022	1.7
Shaft : Marrow	0.14	0.16	2.17
Shaft : Blood	0.058 ± 0.016	0.058 ± 0.010	-

Tests performed at the MRC Radiobiology Unit.

Table 3.3

The biodistribution experiments conducted on the two Fab' conjugates indicated high complex stability but no significant difference in stability between the two, yet the kinetic stability studies clearly indicated [Y.(**24**)] to be slightly less stable than its DOTA analogue.

In vivo, the circulating antibody conjugates will be exposed mainly to conditions in which the pH is in the range 6 to 7.5. Bearing in mind the half lives reported in Table 3.1, after 48 hours a negligible amount of complex will have

dissociated. Therefore there presumably reaches a point where additional kinetic stability at low pH has no beneficial effects on *in vivo* stability as the amount of dissociation will be so small. Both macrocyclic complexes satisfy the kinetic stability requirement, but the DTPA complex does not reach this point of minimum kinetic stability, and is accordingly found to dissociate at an appreciable rate *in vivo*.

These kinetic and *in vivo* tests clearly show **(24)** to be a good bifunctional complexing agent, forming stable yttrium-90 - Fab' conjugates.

3.6 TRI-MALEIMIDES

3.6.1 Reasons for Synthesis

Compared to an intact antibody (IgG), an antibody fragment will penetrate more deeply, localise faster, and clear more rapidly from the body. Yttrium complexes such as [Y.**(24)**]-B72.3 bearing one Fab' (see Section 3.5.2), have however been shown to clear too rapidly from the body to allow sufficient time for tumour localisation, and have therefore resulted in lower than expected tumour to non-tumour ratios. Whilst still using antibody fragments, it was predicted that a decrease in the clearance rate could be obtained if the ligand (e.g. **(15a)**) were functionalised not with one Fab' as in [Y.**(24)**]-B72.3, but with two, three, or perhaps even four antibody fragments. This increase in overall size, it was hoped, would as for an intact antibody reduce the clearance rate, whilst at the same time increase tumour binding avidity as the complex would now bear multiple antigen binding sites rather than just the one.

In an attempt to bear out these predictions, compounds bearing one, two, three, and four maleimides were synthesised by Celltech Ltd., and duly conjugated to Fab', to give the mono-Fab', di-Fab', tri-Fab', and the tetra-Fab' moieties respectively. Tumour binding studies and *in vivo* experiments did indeed reveal a progressive

improvement in the strength of tumour binding, and in the tumour to non-tumour ratios on proceeding from the mono-Fab' through to tri-Fab', although the tetra-Fab' showed only a modest improvement over the tri-Fab'.

As a result of the difficulties associated with tetra-Fab' purification, the tri-Fab' was chosen as the most suitable candidate for future research.

3.6.2 Design and Synthesis

There are two alternative routes to the synthesis of a ligand bearing three maleimides. The first is to produce a ligand exhibiting three pendent primary amine sites to permit the addition of three maleimide moieties. The second alternative is to produce a tri-maleimide functionalised molecule which could then be attached to a ligand. Because of the difficulties associated with producing a tri-functionalised ligand, and because the synthesis of ligand **(15a)** was already established, it was decided to synthesise a tri-maleimide, and attach **(15a)** to it via the pendent primary amine.

Previous research into the synthesis of nine and twelve membered C-functionalised azacycles [5,7] utilised a mono-protected tetraamine (Figure 3.3).

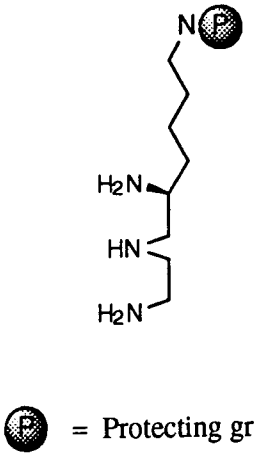

Figure 3.3 : *The mono-protected tetraamine. Starting molecule for tri-maleimide synthesis*

The addition of maleimide moieties to this tetraamine could take place at the three free amine sites perhaps as for the synthesis of **(24)** from **(15a)** (see section 3.5.1), leaving, after removal of the protecting group, a primary amine site free for conjugation to the ligand **(15a)**. The choice of protecting group for the fourth amine site is of utmost importance. Maleimides are susceptible to base hydrolysis, hence any protecting group should be labile under mild acidic conditions. The ideal choice it seemed was a BOC protecting group. This could easily be removed in 20 minutes with 90 % trifluoroacetic acid at room temperature.

The synthesis of the tetraamine was completed following the procedures laid out by Cox *et al.*,[7] (Scheme 3.7).

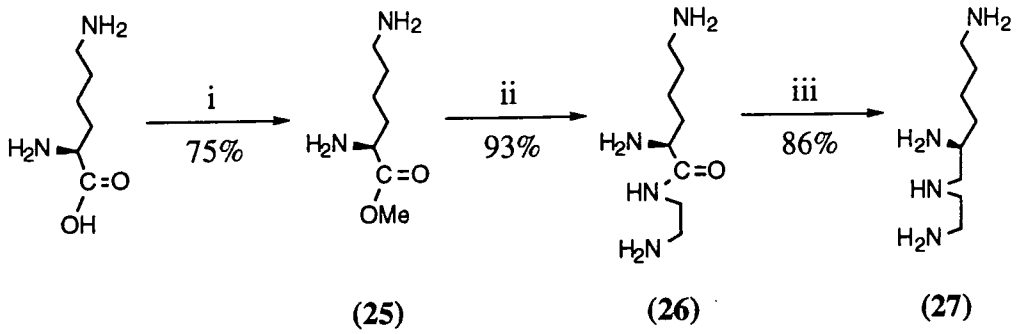

(25) **(26)** **(27)**

Scheme 3.7 : *Tetraamine synthesis starting from lysine. (i) CH_3COCl, MeOH; (ii) $H_2N(CH_2)_2NH_2$; (iii) BH_3-THF*

After esterification of (+)-(2S)-lysine, the dihydrochloride salt **(25)**, was treated with excess neat ethylenediamine, and the resulting amide **(26)** reduced with borane-THF to yield the tetraamine **(27)**. After protection of the diethylenetriamine subunit of **(27)** as its copper (II) complex, (log K_{ML} of the analogous diethylenetriamine copper complex is 16.1) the ε-amino group was selectively BOC protected, and the copper protecting group then removed by bubbling H_2S through its solution (copper sulfide results) to give the mono-protected tetraamine **(28)** in 66% yield (Scheme 3.8).

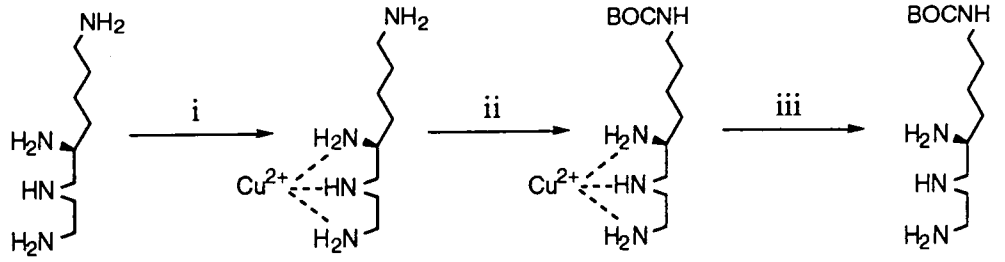

(27) (28)

Scheme 3.8 : *Mono-protection of the tetraamine. (i) Cu^{2+}; (ii) BOCON; (iii) H_2S*

Conversion of the tetraamine **(28)** to the tri-maleimide can be brought about by functionalisation at the three free amine sites. Attempted syntheses included the use of (a) a maleimide active ester (as in the conversion of **(15a)** to **(24)** (Scheme 3.6)), (b) a maleimide acid chloride, (c) the coupling agent DCC to couple **(28)** to a maleimido carboxylate, and (d) a hydroxybenzotriazole (HOBT) maleimide active ester formed in situ using the water soluble coupling agent EDC and a maleimido carboxylate (Scheme 3.9).

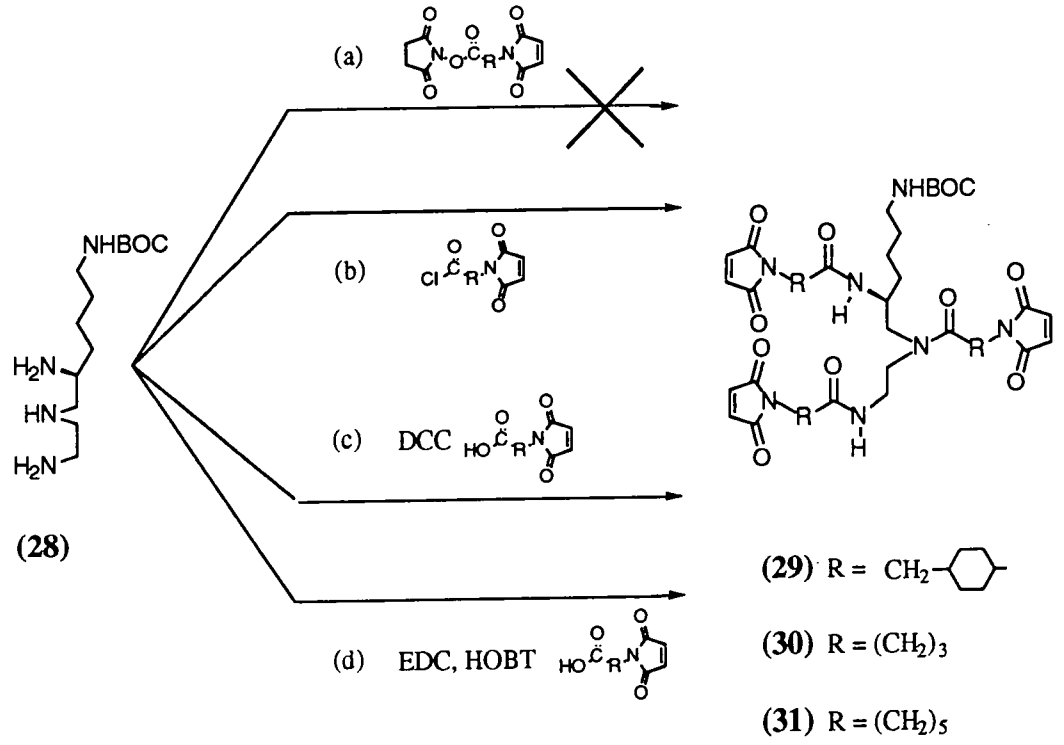

Scheme 3.9 : *Various routes to tri-maleimides*

All attempts to functionalise **(28)** using an active ester (route (a)) failed. Solvents used for the reaction included DMF, acetonitrile, dichloromethane, and a pH 6.9 DMSO / phosphate buffer, yet on all occasions the only identifiable products were the starting ester, and the products of ester hydrolysis. The slow rate or lack of reaction may in part be due to the steric crowding around the amine sites, leading to competitive ester hydrolysis. For this reason, a maleimidocarboxylate was converted to the more reactive acid chloride using oxalyl chloride or thionyl chloride, and added to **(28)**. Immediate reaction occurred, although HPLC purification resulted in a poor yield of the tri-maleimide (approx. 15%), and a large amount of an unidentified maleimide associated compound. Two other routes (c) and (d) also resulted in the desired product. Route (c) used dicyclohexylcarbodiimide (DCC) to directly couple the maleimido carboxylate to the amine sites, whilst in the case of route (d), the hydroxybenzotriazole maleimide active ester was formed in situ to give on reaction with **(28)**, the desired product.

Because the three maleimides of a tri-maleimide are in close proximity to one another, it was suggested that on conjugation, steric crowding may result between antibody fragments. This could perhaps lead to incomplete reaction at all the maleimide sites giving a mixture of tri, di, and mono Fab' products. In an attempt to alter the ratios of products, and determine if indeed steric crowding was a problem, tri-maleimides with differing length maleimide side chains were synthesised **(29)**, **(30)**, and **(31)** (Scheme 3.9), and conjugated to antibody fragments (see Chapter 5).

3.7 TRI-MALEIMIDE FUNCTIONALISED LIGANDS

Two different approaches were attempted to couple the tri-maleimide (**31**) to the ligand (**15a**). Prior to coupling, TFA removal of the BOC protecting group from the fourth amine of the tri-maleimide (**31**) was monitored by HPLC at 302 nm, clearly showing quantitative conversion of (**31**) (T_R 20.5 min.), to the amine (T_R 15.7 min.) (Scheme 3.10). Both the ligand (**15a**) and the deprotected tri-maleimide exhibit a primary amine. To couple the two together, a bifunctional linker molecule (e.g. (**32**) Scheme 3.10) must be inserted.

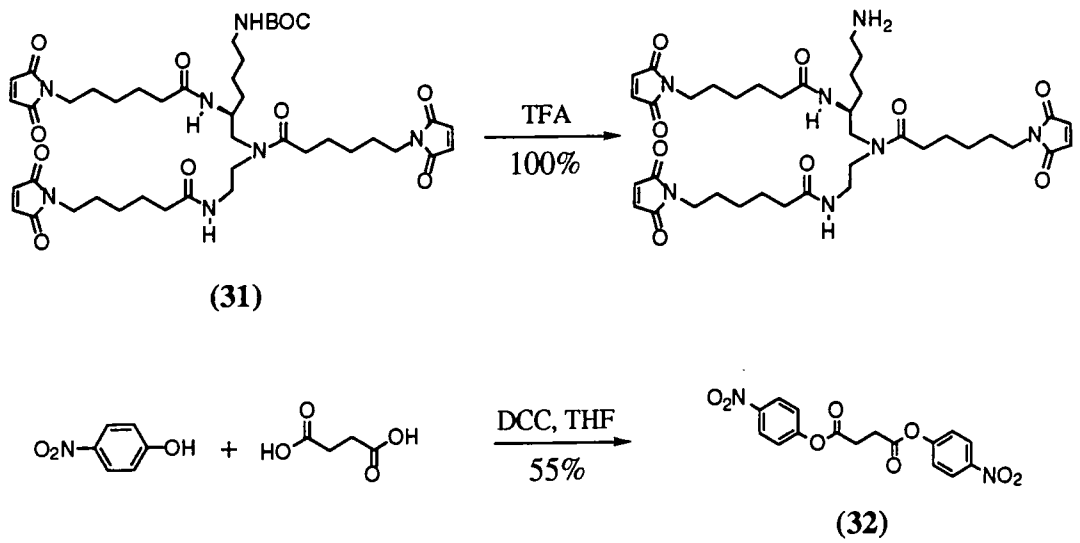

Scheme 3.10 : *Tri-maleimide deprotection, and the synthesis of a bifunctional linker.*

Two slightly differing syntheses (Schemes 3.11 & 3.12) gave the required product (**34**). Reaction of (**15a**) with the bis paranitrophenol active ester (**32**) gave the active ester (**33**), which on addition of the deprotected tri-maleimide gave the maleimide functionalised ligand (**34**).

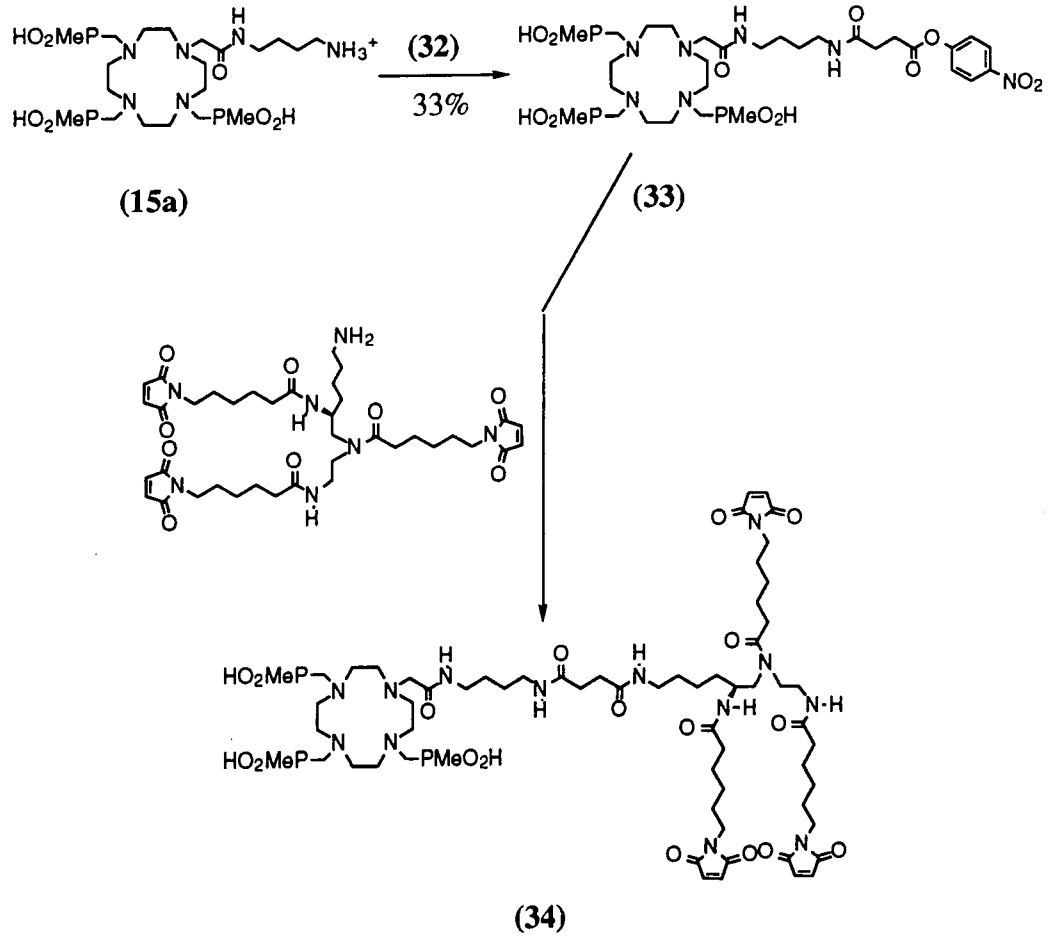

Scheme 3.11 : *Route 1 to the tri-maleimide functionalised ligand*

Alternatively, route 2 required initial reaction of the deprotected tri-maleimide with succinic anhydride. Analytical HPLC clearly showed quantitative conversion of this deprotected tri-maleimide (T_R = 13.2 min.) to the carboxylic acid functionalised tri-maleimide **(35)** (T_R = 12.7 min.). Addition of oxalyl chloride to **(35)** gave the acid chloride which after immediate addition of **(15a)** then gave **(34)**. Both routes gave the product in very poor yield after HPLC purification. Subsequent conjugation to Fab', and gel electrophoresis, confirmed the existence of **(34)** (see Chapter 5).

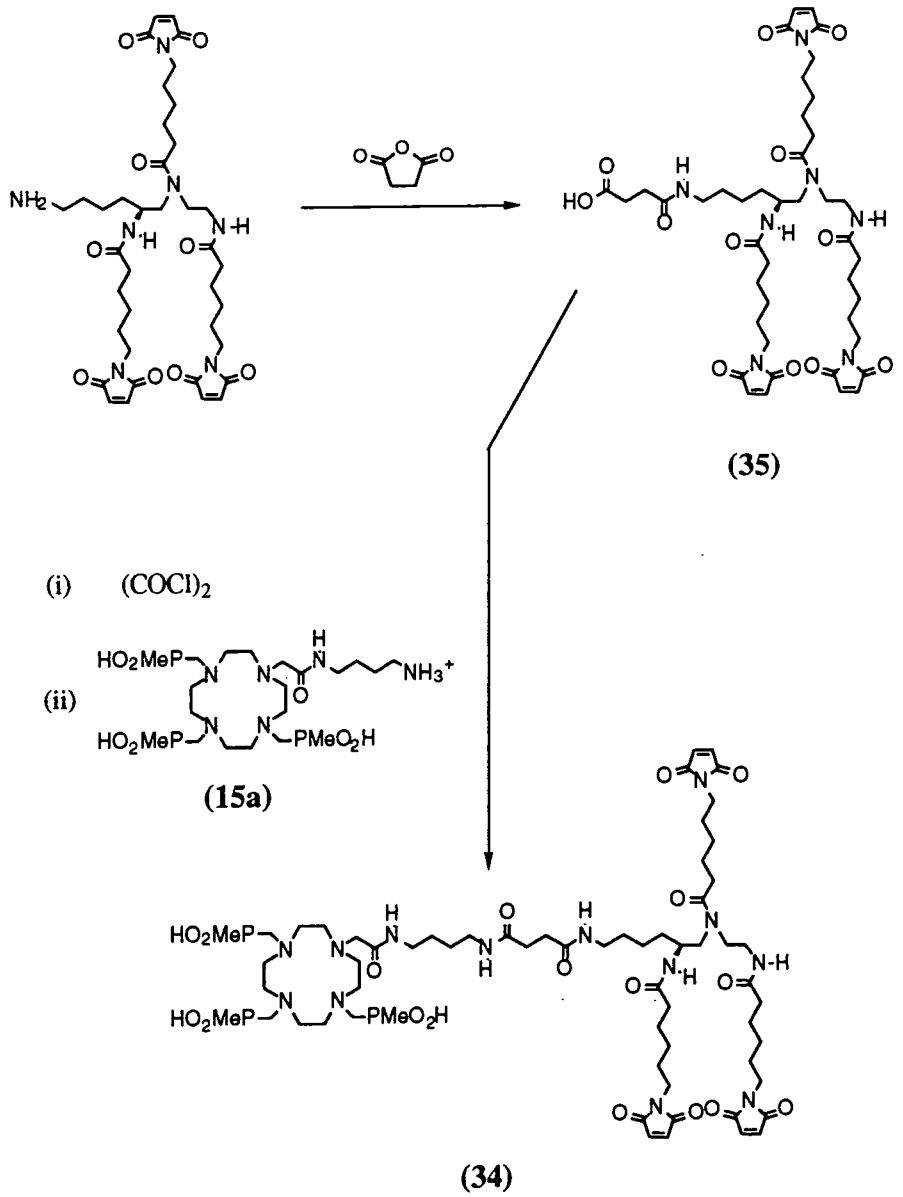

Scheme 3.12 : *Route 2 to the tri-maleimide functionalised ligand*

3.8 NITROIMIDAZOLES

3.8.1 Mode of Action

As a result of out-growing their blood supply, oxygen deprived ('hypoxic') cells develop in the majority of rapidly proliferating solid human tumours. Because

cellular oxygen essentially serves to 'fix' radiation-induced free radical damage, particularly at the DNA level, viable hypoxic cells are considerably more resistant to the lethal effects of ionising radiation, and it is this fact which can influence tumour control by radiation.

Hypoxic cells contain a much higher concentration of reductase enzymes than normoxic cells and, as a result, have been shown to selectively retain a class of compound called nitroimidazoles which are reduced, and then are unable to diffuse out of the cell.

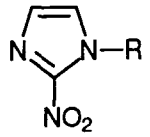

Figure 3.4 : *A nitroimidazole*

Nitroimidazoles have also shown promise in acting as radiosensitizers, in that they serve to make a hypoxic cell more susceptible to radiation induced damage by acting as an oxygen mimic.[14] This combination of tumour localisation, and radiosensitisation, makes nitroimidazoles a reasonable choice for conjugation to a radiolabelled ligand (a technetium labelled nitroimidazole for the imaging of regional hypoxia in ischaemic heart disease is discussed in section 1.10.1).

3.8.2 Conjugation to a Ligand

The nitroimidazole chosen contained an aminoalkyl side chain and, as before, **(15a)** was the choice of ligand. As for the coupling of **(15a)** to the BOC deprotected trimaleimide (Scheme 3.11), both molecules possess a primary amine through which coupling can occur. As before, **(15a)** was converted to its paranitrophenol active ester **(33)** using the bis active ester **(32)**. Addition of 1-aminopropyl-2-nitroimidazole to the active ester **(33)**, and subsequent HPLC purification gave in 73% yield the nitroimidazole-ligand conjugate **(36)** which on yttrium complexation

will form a neutral complex-conjugate which should be able to passively diffuse into cells (Scheme 3.13).

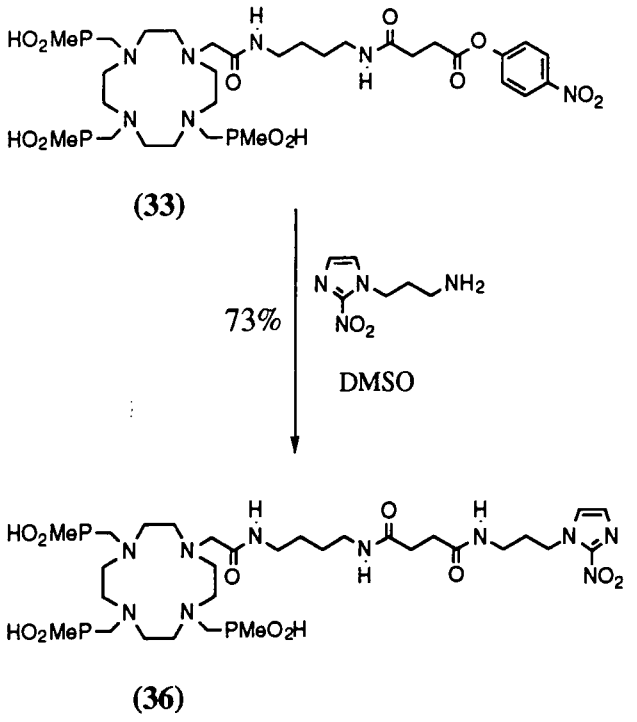

Scheme 3.13

The biodistribution of [^{153}Gd.(**36**)] - 0.1 μmol kg^{-1} was examined in mice, both in the absence and presence of a large excess of misonidazole (300 μmol kg^{-1}). Misonidazole (Figure 3.5) is a well established nitroimidazole which has shown activity in many different tumour types, especially in rodents, and is accordingly added to avoid the premature reduction of the small tracer amounts of [^{153}Gd.(**36**)] in the blood-stream.

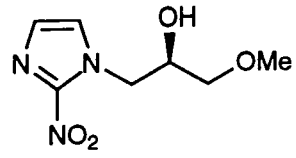

Figure 3.5 : *Misonidazole*

In both cases, there did not appear to be any significant accumulation of [^{153}Gd.(**36**)] in tissues such as the eyes, oesophagus, liver or salivary glands which

are expected to be hypoxic. This may simply be due to the inability of the conjugate to selectively accumulate in the target tissues, or it may be due to its premature reduction even in the presence of a large excess of misonidazole. The complex cleared via the usual renal route, and after 24 hours more than 99% of the ^{153}Gd activity had cleared from the body, consistent with the excellent *in vivo sta*bility of the conjugate (**36**).

3.9 CONCLUSIONS

The mono-maleimide (**24**) has been shown to form stable complexes both *in vitro*, and more importantly *in vivo*, whilst the tri-maleimide (**34**), as yet untested, is hoped to show the same *in vivo* stability, whilst exhibiting improved tumour binding, and tumour to non-tumour ratios.

Although the nitroimidazole conjugate (**36**) was found to show no hypoxic cell localisation properties, other groups have had some success with nitroimidazole conjugates.[15] It may be that (**36**) needs to be in a higher concentration, and the use of nitroimidazoles cannot be totally discounted for further study.

3.10 REFERENCES

1 D. J. King, "*Advances in the Applications of Monoclonal Antibodies in Clinical Oncology*", University of London Royal Postgraduate Medical School Conference Abstracts, 1989.

2 J. R. Morphy, D. Parker, R. Kataky, M. A. W. Eaton, A. T. Millican, R. Alexander, A. Harrison, and C. Walker, *J. Chem. Soc. Perkin Trans. 2*, 1990, 573.

3 J. P. L. Cox, K. J. Jankowski, R. Kataky, D. Parker, N. R. A. Beeley, B. A. Boyce, M. A. W. Eaton, K. Millar, A. T. Millican, A. Harrison, and C. Walker, *J. Chem. Soc., Chem. Commun.*, 1989, 797.

4 J. R. Morphy, D. Parker, R. Kataky, A. Harrison, M. A. W. Eaton, A. Millican, A. Phipps, and C. Walker, *J. Chem. Soc., Chem. Commun.*, 1989, 792.

5 A. S. Craig, I. M. Helps, K. J. Jankowski, D. Parker, N. R. A. Beeley, B. A. Boyce, M. A. W. Eaton, A. T. Millican, K. Millar, A. Phipps, . K. Rhind, A. Harrison, and C. Walker, *J. Chem. Soc., Chem. Commun.*, 1989, 794.

6 C. J. Broan, E. Cole, K. J. Jankowski, D. Parker, K. Pulukkody, B. A. Boyce, N. R. A. Beeley, K. Millar, and A. T. Millican, *Synthesis*, 1992, 63.

7 J. P. L. Cox, A. S. Craig, I. M. Helps, K. J. Jankowski, D. Parker, M. A. W. Eaton, A. T. Millican, N. R. A. Beeley, and B. A. Boyce, *J. Chem. Soc. Perkin Trans. 2*, 1990, 2567.

8 T. Kitagawa, and T. Aikawa, *J. Biochem.*, 1976, **79**, 233.

9 S. Yoshitake, M. Imagawa, Y. Niitsu, I. Urushizaki, M. Nishiura, R. Kanazawa, H. Kurosaki, S. Tachibana, N. Nakazawa, and H. Ogawa, *J. Biochem*, 1982, **92(5)**, 1413.; T. Kohno, K. Yamaguchi, and E. Ishikawa, *J. Biochem.*, 1990, **108(5)**, 741.; S. Hashida, and E. Ishikawa, *J. Biochem.*, 1990, **108**, 960.; and S. Hashida, K. Tanaka, N. Yamamoto, T. Uno, K. Yamaguchi, and E. Ishikawa.

10 M. J. O'Sullivan, E. Gnemmi, D. Morris, G. Chieregatti, A. D. Simmonds, M. Simmons, J. W. Bridges, and V. Marks, *Anal. Biochem.*, 1979, **100**, 108.

11 S. Hashida, M. Imagawa, S. Inoue, K. Ruan, and E. Ishikawa, *J. Appl. Biochem.*, 1984, **6**, 56.

12 S. Yoshitake, Y. Yamada, E. Ishikawa, and R. Masseyeff, *Eur. J. Biochem.*, 1979, **101**, 395.

13 O. Keller, and J. Rudinger, *Helv. Chim. Acta.*, 1975, **58**, 531.

14 "Chemistry of Antitumour Agents", ed. D. E. V. Wilman, Blackie & Son Ltd., 1990.

15 R. J. DeRocco, A. Bauer, B. L. Kuczynski, J. P. Pirro, K. Linder, R. K. Narra, and A. D. Nunn, *J. Nucl. Med.*, 1992, **33**, 865.

Chapter 4

DNA Intercalation

4.1 INTERCALATORS

4.1.1 Nature and Mode of Binding

Intercalators are typically planar fused-ring polyaromatic molecules bearing a cationic charge on an aromatic ring, and / or on a pendent group. They are capable of binding tightly yet reversibly to double helical DNA, and exhibit many properties which make their use in medicine, particularly in the treatment of cancers of prime importance.

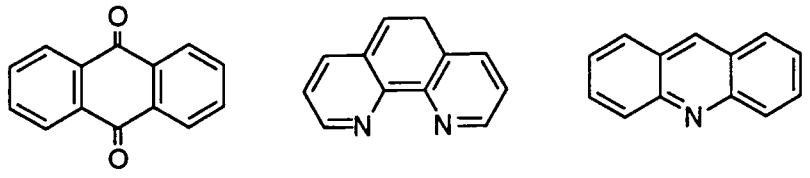

Anthraquinone Phenanthroline Acridine

Figure 4.1 : *Some common intercalators*

Intercalators get their name from the Latin '*intercalare*' which means to insert. Accordingly, binding to DNA is through the insertion of the aromatic plane of an intercalating molecule between the aromatic planes of two stacked DNA base pairs. For intercalation, the planar part of the molecule must possess a minimum surface area of 28 $Å^2$ with an optimum of three to four rings.[1] Upon intercalation the general structure of the DNA remains intact, but because of the resulting helix unwinding, and the increased separation of adjacent base pairs from 3.4 Å to approximately 7 Å (to maintain a spacing of approximately 3.4 Å between the aromatic planes) required to incorporate the intercalator, a slight lengthening of the helix occurs.

Experimentally determined DNA association constants[1] for intercalators are in the range 10^5-10^7 M^{-1} and can be attributed to a number of factors, including π-π stacking of the aromatic rings, hydrogen bonding, and electrostatic forces.[2] There

are however few studies to indicate the relative importance of these factors, and no firm guidelines exist whereby one can confidently relate intercalator structure to DNA binding strength.[3]

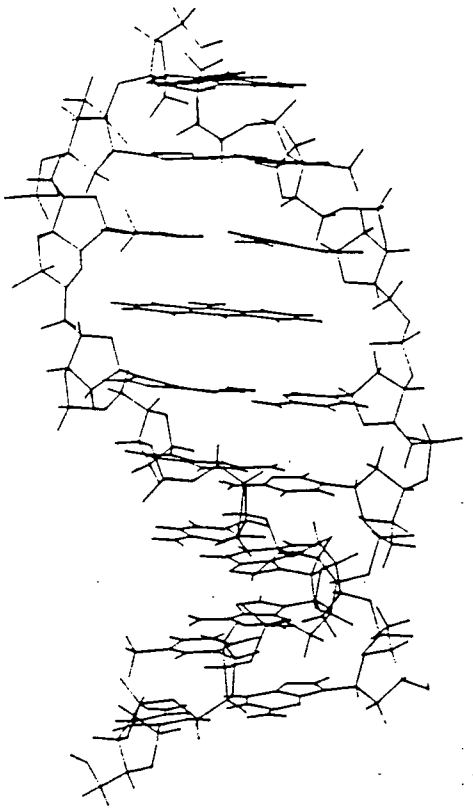

Figure 4.2 : *Insertion of the intercalator 9-amino acridine into the DNA double helix*

4.1.2 Applications

The primary use of intercalating compounds is in the treatment of cancer. Here, changes in the DNA structure impair replication, or induce strand breaking to relieve the torsional strain caused by intercalation. Intercalating agents such as anthracyclines can also directly affect strand breakage through their redox properties,[4] whilst the cytotoxicity of others can be attributed to their ability to induce cross-linking in DNA. Generally, intercalators which are most widely used can be put into four main categories; actinomycins, anthracyclines such as Daunomycin and

Adriamycin, acridines such as Amsacrine, and anthraquinones such as Mitoxantrone (see Figure 4.3).

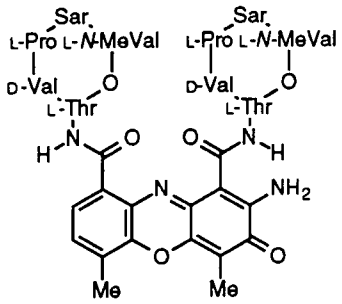

Actinomycin D

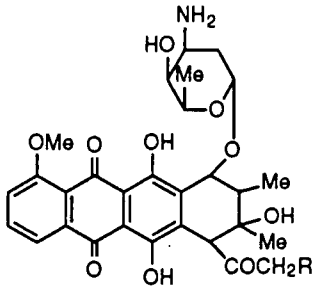

Daunomycin R = H
Adriamycin R = OH

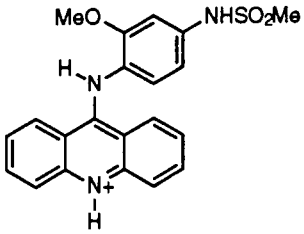

Amsacrine

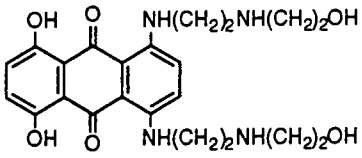

Mitoxantrone

Figure 4.3 : *Some commonly used intercalating drugs for the treatment of cancer*

Actinomycin D is used in the treatment of Wilm's tumour in children, whereas the anthracycline antibiotics Daunomycin and Adriamycin are used in the treatment of leukaemia, and as a broad spectrum anti-cancer drug respectively. Acridines were one of the first classes of intercalating drugs, and nowadays Amsacrine is used in the treatment of acute leukaemias and malignant lymphomas whilst Mitoxantrone, an example of the anthraquinone class of intercalators, has been used in the treatment of breast cancer.

One strategy for the control of tumour gene expression involves the use of synthetic oligonucleotides which bind to specific regions of DNA or RNA thus inhibiting transcription and translation of genetic information. The covalent

attachment of intercalating agents to oligonucleotides has been used to increase the binding affinity to the oligonucleotide's complementary sequence, and thus enhance inhibition of gene replication.[5] A similar use of intercalators includes attachment of an intercalating agent to a synthetic oligonucleotide attached in turn to a metal complex capable of causing DNA cleavage.[6,7,8,9] The intercalator anchors the oligonucleotide to a specific region of DNA, thus permitting sequence specific cleavage of DNA, in effect allowing the metal complex to act as a chemical nuclease in a similar manner to restriction enzymes.

4.2 THE USE OF INTERCALATORS IN THIS WORK

To be at its most effective, radiation produced during the radioimmunotherapy of cancer must hit the chromosomal DNA of the tumour stem cells. Although antibody fragments are capable of specifically binding an yttrium-90 labelled macrocycle to the surface of a cancer cell, the cell's DNA is but a small part of the whole cell, and as a result, much of the emitted radiation will pass through the cell causing unwanted damage of a less severe nature. Ideally, an yttrium-90 labelled macrocycle would bind not to the surface of the tumour cell, but to its DNA. Obviously this would require the labelled molecule to first pass through the cell wall on its way to the nucleus. With the advent of a new breed of antibody fragments (specifically one named A33) which are capable of penetrating the cell wall, this has become a distinct possibility.

It is postulated that, if a suitable DNA intercalating agent is covalently attached to a molecule bearing an yttrium-90 labelled macrocycle and A33 antibody fragments, targeting not only of tumour cells, but of their DNA would become possible. A molecule of the nature shown in Figure 4.4 is therefore required.

As a consequence of being able to bind directly to a tumour cell's DNA, it may be possible to reduce the dose of injected drug needed for effective

radioimmunotherapy as there is a significantly increased chance that emitted radiation will interact with the DNA and cause cell death.

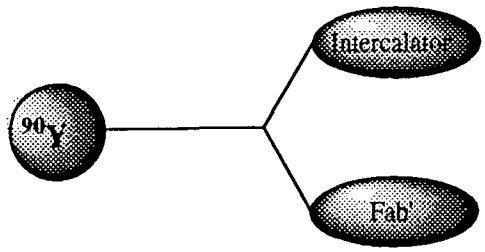

Figure 4.4

4.3 CHOICE OF INTERCALATOR

There are numerous different classes of intercalating agents available, many of which have been found to be potent drugs in the treatment of cancers and other diseases. A precise correlation between a drug's structural charactersitics and its potency has not been shown, only that potency is in some cases linked to the strength of binding. For this work the choice of intercalator was not of crucial importance; it was not based on an effectiveness against cancer, but merely on an ability to bind to DNA, and as a result, any anti-cancer properties exhibited would be an added bonus.

The main criteria for the choice of an intercalating agent were ease of functionalisation, ease of NMR spectra interpretation, a chemically robust nature, and a reasonable amount of relevant background work. With this in mind, there were two logical choices, acridines, and to a lesser extent anthraquinones (see Figure 4.1).

Acridines are probably the most thoroughly studied class of intercalating agents and, of those which have found their way into drug use, the majority are functionalised at the 9 position with an amino group (e.g. Amsacrine (Fig. 4.3)). The simplest acridine of this class is 9-amino acridine (Figure 4.5).

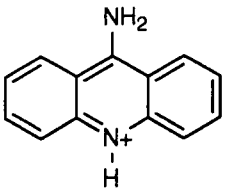

Figure 4.5 : *9-amino acridine*

It was decided therefore that initial attempts to conjugate an intercalating agent to an yttrium-90 radiolabelled macrocycle would concentrate on the use of the ligand **(15a)** covalently attached to an acridine via a 9-amino group. The final goal however, was to form a macrocycle-acridine conjugate, leaving a site free for further maleimide derivatisation to permit subsequent Fab' conjugation.

4.4 9-AMINO ACRIDINE SYNTHESIS

The starting material for the synthesis of most 9-amino acridines is 9-chloro acridine **(37)**. This was formed in a one step cyclisation from N-phenyl anthranilic acid using phosphorus oxychloride,[10] and was converted to the more reactive 9-methoxy acridine **(38)**, and 9-phenoxy acridine **(39)** species (Scheme 4.1).

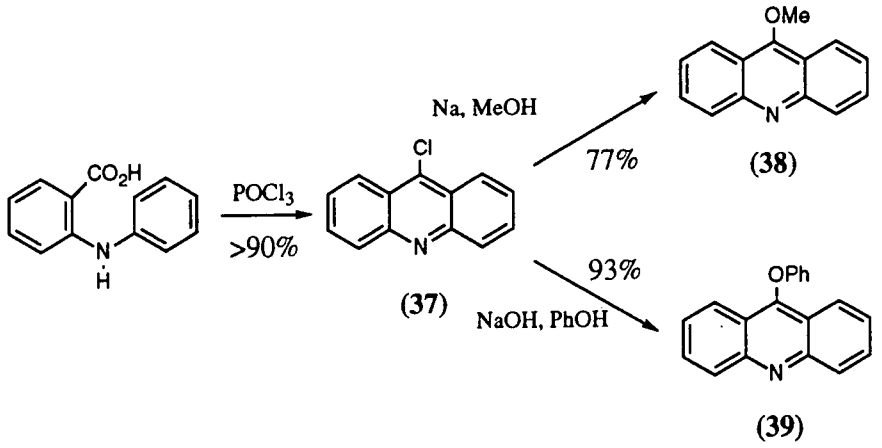

Scheme 4.1 : *Synthesis of 9-chloro, 9-methoxy and 9-phenoxy acridines*

There are two principal routes to the synthesis of amino acridines: reaction of an amine salt with a 9-alkoxy or 9-phenoxy acridine,[11] or reaction of a free amine with 9-chloro acridine **(37)** in phenol proceeding through a 9-phenoxy acridine intermediate.[12] Both routes are essentially mechanistically the same; the 9-phenoxy acridine (or 9-methoxy acridine) being the reactive species, and the reaction requiring a catalysing proton source, the amine salt or phenol respectively (Scheme 4.2).

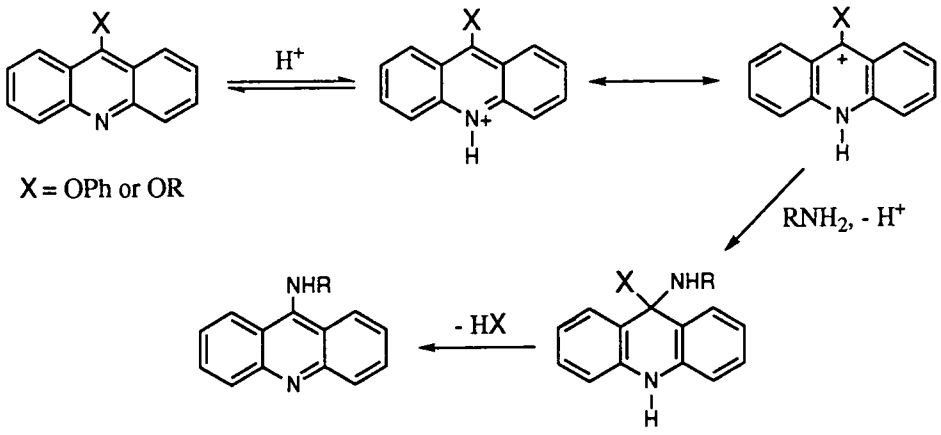

Scheme 4.2 : *The synthesis of 9-amino acridines*

4.5 AMINO ACRIDINE FUNCTIONALISED LIGANDS

Initial attempts to form an acridine-ligand conjugate concentrated simply on the joining together of the two halves, without incorporation of a site for further maleimide derivatisation. The possession of a pendent primary amine made ligand **(15a)** an ideal choice with which to form an amino acridine. Accordingly, **(15a)** was taken, and to it added 9-methoxy acridine **(38)** in methanol. Unfortunately, no reaction was observed. It was suggested that as **(15a)** possessed phosphinic acid side arms, and was used as its hydrobromide salt, 9-methoxy acridine may have been acid-hydrolysed to 9-acridanone, or that the reaction's progress may somehow have been swamped out by an excess of acid. For this reason, in an attempt to neutralise

excess acid, triethylamime was added to **(15a)**, removed under reduced pressure, and the resulting ligand added to 9-chloro acridine **(37)** in phenol. Yet again no reaction was observed (Scheme 4.3).

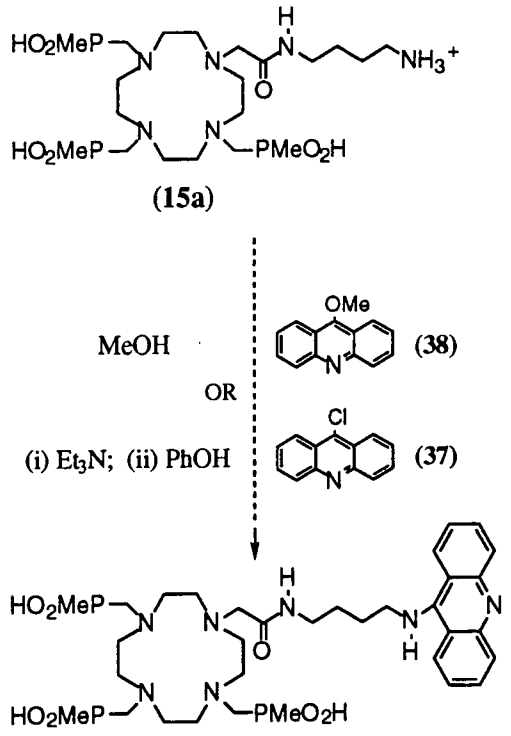

Scheme 4.3 : *Failed syntheses of an acridine-ligand conjugate*

The synthesis of an amino acridine in the presence of ligand **(15a)** had failed (Scheme 4.3). It was decided therefore to start with an amino acridine which could then be linked to **(15a)**. 9-Phenoxy acridine **(39)** was reacted with 3-bromo propylamine hydrobromide to give the amino acridine **(40)** (Scheme 4.4).

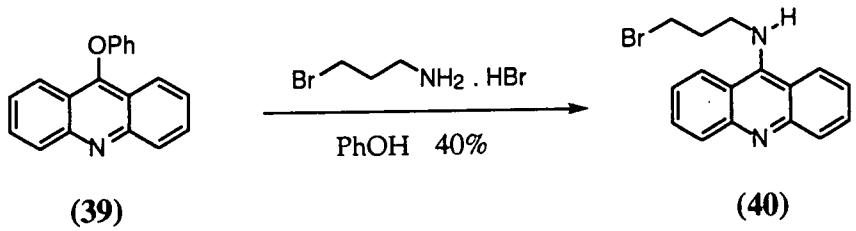

Scheme 4.4

It was hoped that this could then be reacted with **(15a)** to yield an acridine-ligand conjugate with a free secondary amine site for subsequent maleimide derivatisation (Scheme 4.5).

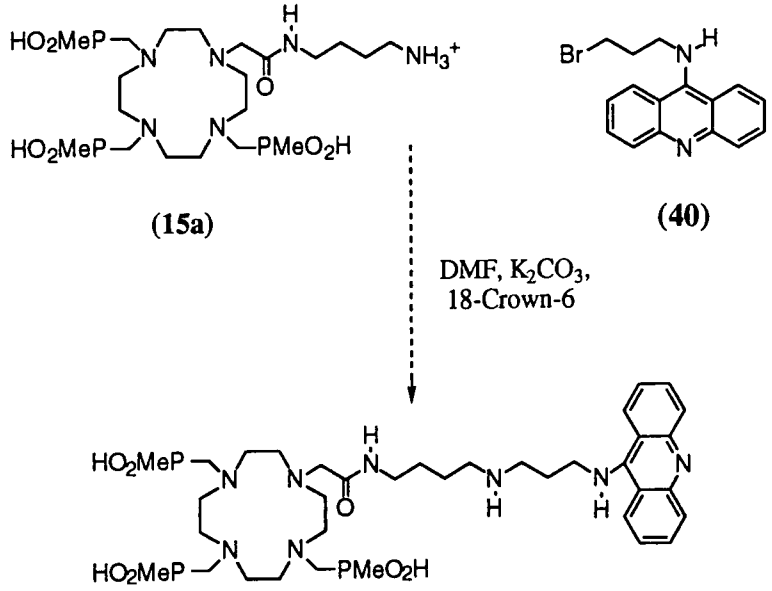

Scheme 4.5 : *Failed coupling of ligand (15a) and the amino acridine (40)*

The reaction was attempted on a number of occasions at temperatures ranging from 45°C to 90°C using either potassium or caesium carbonate as the base, and in some instances using 18-crown-6. In all cases, HPLC indicated a large number of acridine associated products, none of which were found to be the desired product. Failure of the reaction again may have been due to the presence of acidic groups, or due in part to decomposition or base hydrolysis of **(40)**, although this does not explain the large number of products observed.

To see if it was indeed the acidity of **(15a)** which was the cause of the lack of reaction, it was decided to conjugate its parent ester **(14a)** to the amino acridine **(40)**, and then hydrolyse the resulting conjugate to the phosphinic acid using HBr in glacial acetic acid (Scheme 4.6).

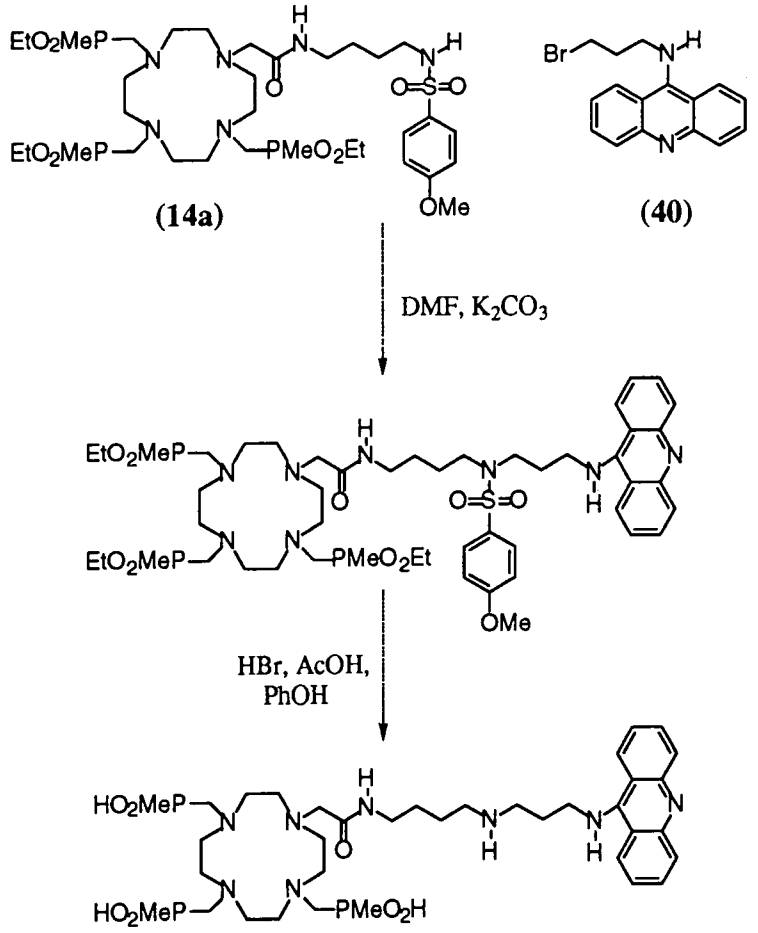

Scheme 4.6 : *Failed synthesis of an acridine-ligand conjugate*

Again, HPLC gave none of the desired product, just a variety of unidentifiable acridine derivatives. To determine whether the lack of reaction was due to the unreactivity of the sulphonamide **(14a)** or due to the instability of the amino acridine **(40)**, the sulphonamide **(14a)** was converted to its more reactive sodium salt using sodium ethoxide, and again added to **(40)**. Once more no reaction was observed.

It appeared that the use of the pre-formed amino acridine **(40)** was one cause of the problem, and it was accordingly decided to revert back to the idea of forming the amino acridine during the main coupling reaction. This time however, instead of using the phosphinic acid functionalised ligand **(15a)** to form an amino acridine (as in Scheme 4.3), it was decided to use a phosphinate ester functionalised with a

primary amine site which would then hopefully form an amino acridine when added to 9-chloro acridine (**37**), and be amenable to conversion to the desired phosphinic acid functionalised ligand.

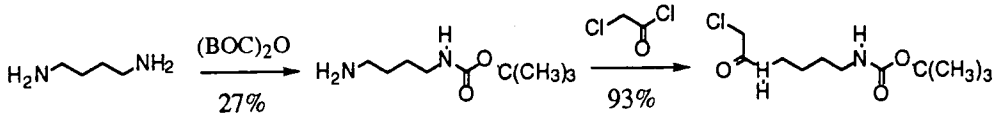

(**41**) (**42**)

Scheme 4.7

The primary amine site to which the acridine was to be attached was synthesised separately (Scheme 4.7), and attached in its BOC amine protected form to the phosphinate ester (**14a**) using potassium carbonate in DMF to give (**43**) (Scheme 4.8).

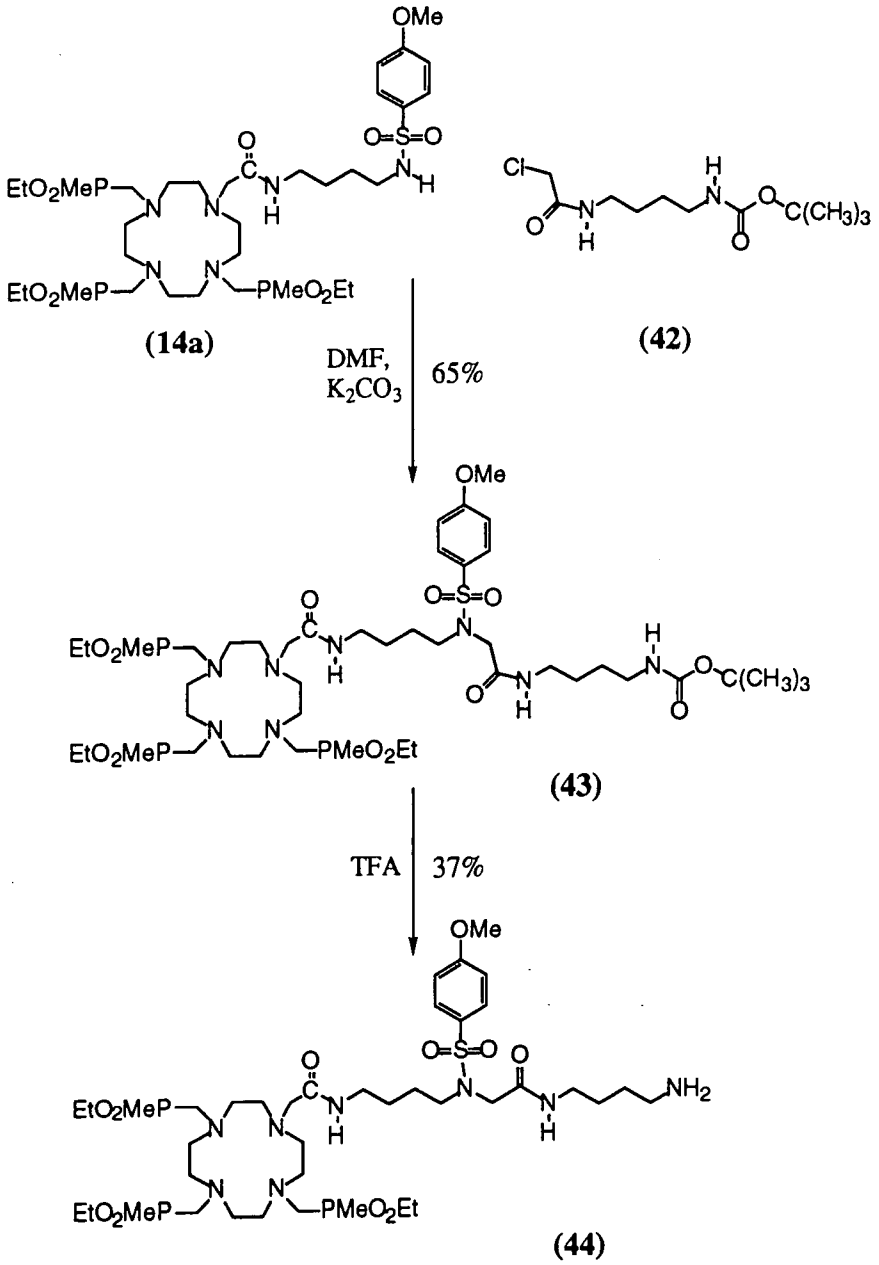

Scheme 4.8 : *The successful synthesis of the primary amine functionalised phosphinate ester (44)*

Using trifluoroacetic acid, BOC deprotection of the amine (**43**) proceeded quantitatively, to give the crude amine salt (**44**), which following HPLC purification was extracted as its free amine from a saturated aqueous potassium carbonate solution.

Reaction of the free amine (**44**) with 9-chloro acridine (**37**) in phenol gave after preparative HPLC, the amino acridine (**45**) in 62% yield (Scheme 4.9). It was hoped then that subsequent treatment of this amino acridine with HBr, AcOH, PhOH would hydrolyse the phosphinate esters to the desired phosphinic acids, and in the process remove the p-methoxy-benzenesulphonyl protecting group from the secondary amine site leaving it free for maleimide derivatisation. However, HPLC indicated complete decomposition of (**45**) to a large number of products, presumably due to the thermal and chemical instability of the amino acridine to acid catalysed hydrolysis.[13]

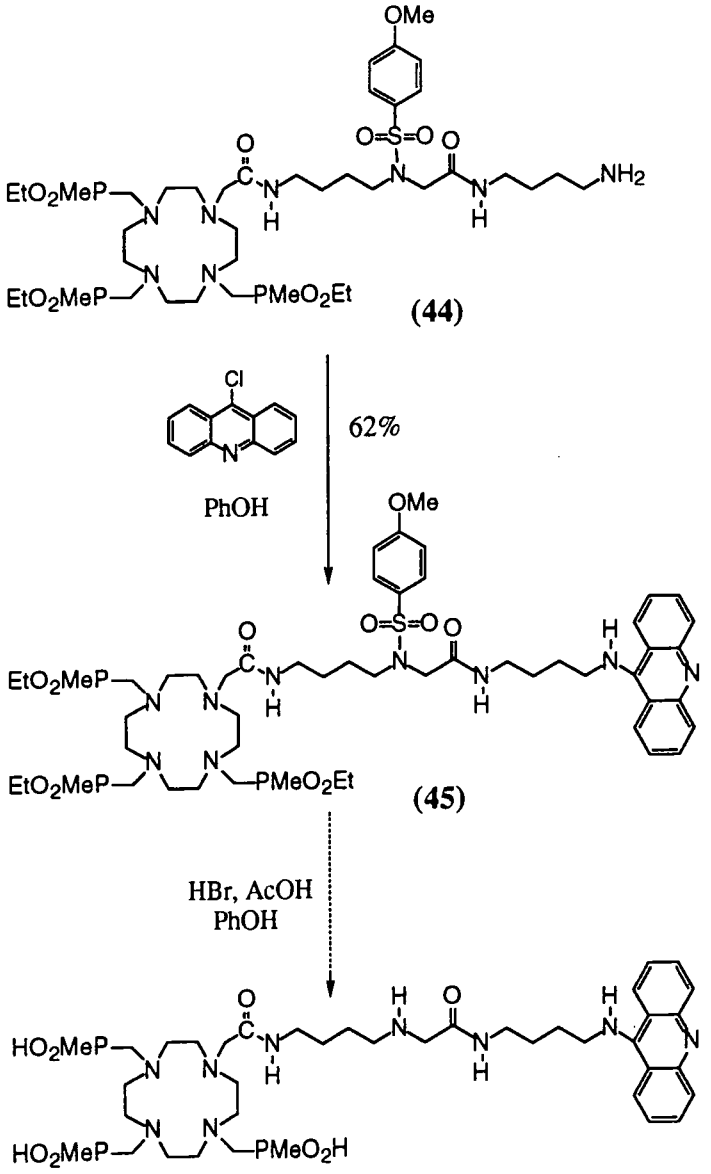

Scheme 4.9 : *Amino acridine synthesis, and unsuccessful deprotection*

4.6 ACRIDINE AMIDE FUNCTIONALISED LIGANDS

It became apparent that the use of amino acridines was inherently flawed by their instability towards acid hydrolysis during exposure to HBr in glacial acetic acid. It was therefore decided to look at some other means of conjugating a macrocycle to an acridine moiety. The solution appeared to lie not in the use of amino acridines, but in acridine amides, whereby linkage to the acridine ring system was achieved via an amide functionality. Acridine-9-carboxylic acid was readily available, and following prolonged heating in neat thionyl chloride yielded the acid chloride, acridine-9-carbonyl chloride **(46)** as a yellow solid.[14] Immediate addition of an amine resulted in rapid production of an acridine amide (Scheme 4.10).

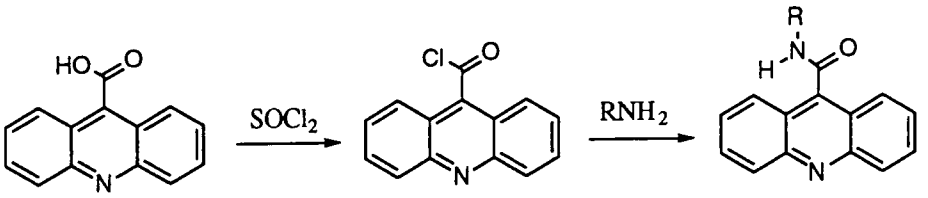

(46)

Scheme 4.10 : *Synthesis of acridine amides*

Starting again with the ligand **(15a)**, it was predicted that unlike the formation of amino acridines (Scheme 4.3), formation of acridine amides would be unaffected by the presence of such an acidic molecule. The acridine acid chloride **(46)** was duly formed, and to it added a solution of **(15a)** and N-methylmorpholine in DMF (Scheme 4.11). Subsequent HPLC purification of the products did indeed give, albeit in low yield (14%), the desired acridine labelled ligand **(47)**.

Building on the successful conjugation of the macrocycle **(15a)** to acridine (Scheme 4.11), it was decided to attach as their amides, acridine and the intercalator anthraquinone to **(44)**, which after removal of the p-methoxy benzenesulphonyl protecting group should leave a secondary amine site free for maleimide derivatisation (Schemes 4.12 & 4.13). As for acridine-9-carboxylic acid,

anthraquinone-2-carboxylic acid can also be converted to its acid chloride (**48**) using thionyl chloride.

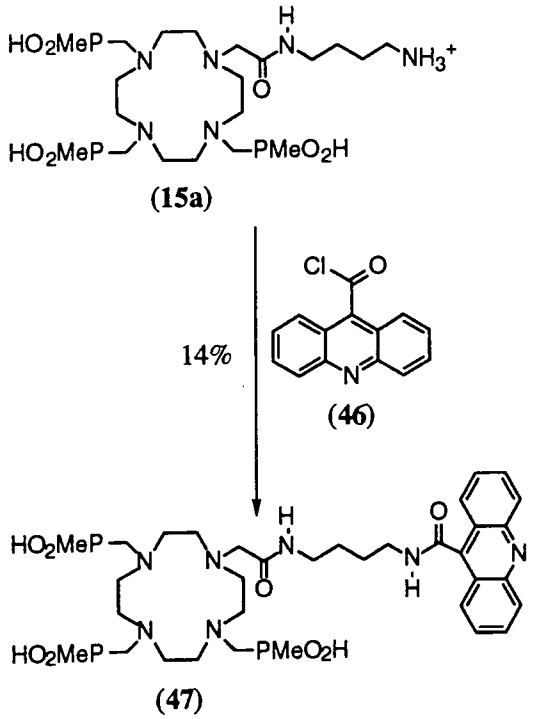

Scheme 4.11 : *Successful synthesis of the acridine amide (47)*

Conjugation of the acridine and anthraquinone moieties to the amine (**44**) proceeded well to give after HPLC purification, the two amides (**49**) and (**51**) in 50% and 42% yields respectively. As expected, hydrolysis of the phosphinate ester (**49**) to the phosphinic acid (**50**) proceeded well with concomitant amine deprotection to give after HPLC purification, the desired product (**50**) in 72% yield. A doubling in the overall yield of the phosphinic acid (**50**) from the amine (**44**) was achieved when (**49**) was used as its crude without initial HPLC purification.

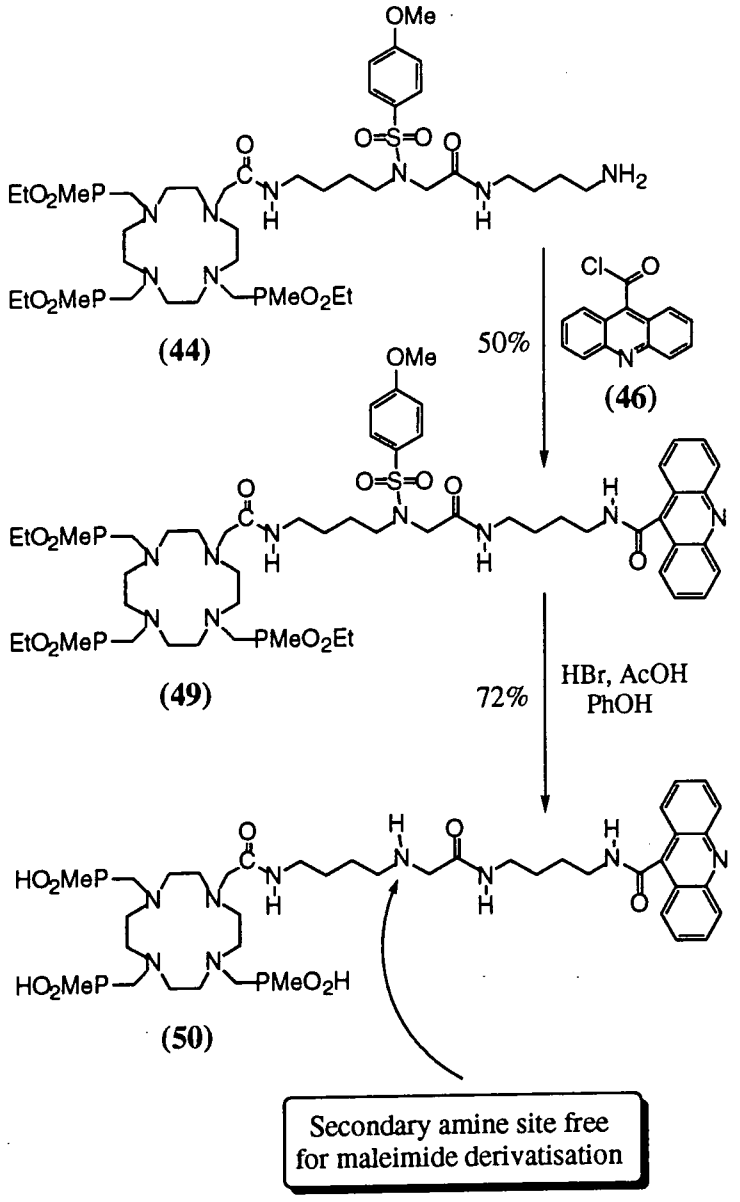

Scheme 4.12 : *Successful synthesis of the acridine amide (50) bearing a free secondary amine site for maleimide derivatisation*

Treatment of the anthraquinone amide (**51**) with HBr, AcOH, PhOH, unlike the corresponding acridine derivative, did not appear to give the desired phosphinic acid product. Indeed HPLC indicated a number of products, which on isolation of the main components did not yield any identifiable compounds.

A model reaction was attempted to try to determine the fate of the anthraquinone amide (**51**). A simple anthraquinone butylamide was taken, and as before, treated with HBr in glacial acetic acid with phenol to scavenge any bromine. After 1 day, analysis of the resulting products showed the presence of approximately 25% of an insoluble compound, perhaps anthraquinone-2-carboxylic acid, the amide hydrolysis product, indicating that (**51**) may similarly have undergone amide hydrolysis.

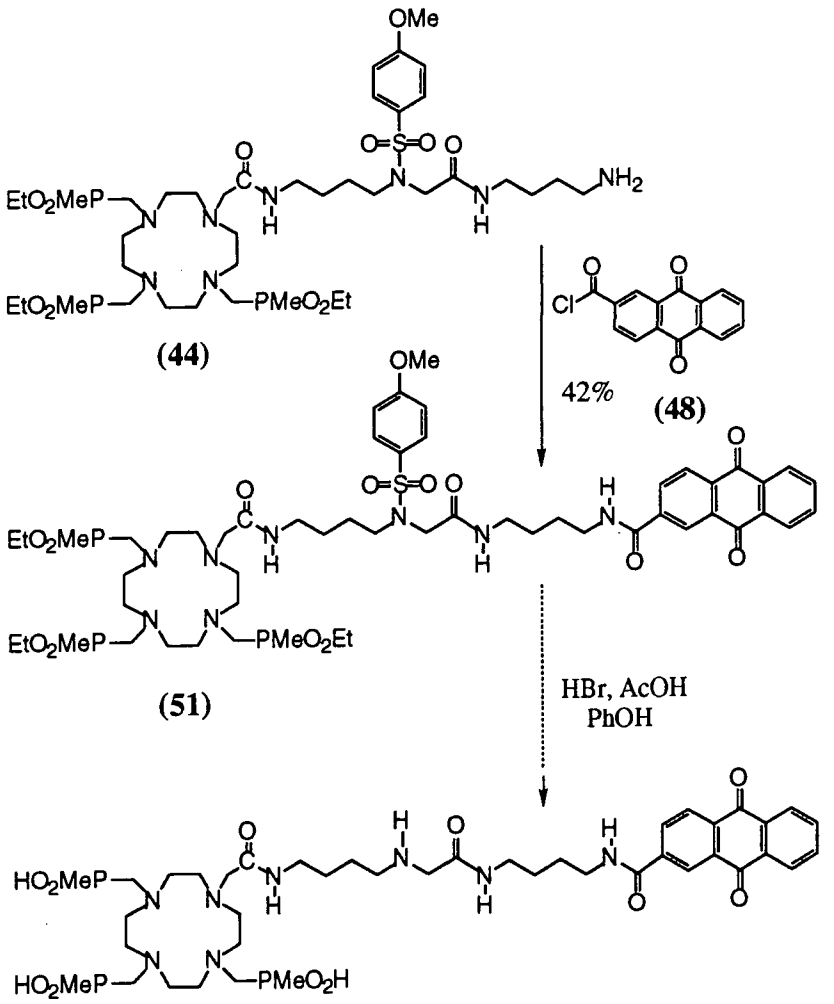

Scheme 4.13 : *Successful synthesis of the anthraquinone amide (51), but unsuccessful deprotection of the amine site*

4.7 D.N.A. BINDING

4.7.1 Tests

The purpose of attaching acridine and anthraquinone intercalating moieties to the ligand was to facilitate tumour DNA binding. There are a number of physical measurements which can be done to test the strength and degree of this binding, be it intercalation, or some other mode of DNA binding. Intercalation results in changes in the viscosity, sedimentation coefficient, and electrophoretic mobility of DNA.[15] Changes can also be observed in the ^{31}P NMR of the phosphodiester backbone of DNA as well as in the ^{1}H NMR of the aromatic region of the intercalator.[16]

One of the simplest indications of intercalation is a change in the U.V. spectrum of an intercalator on addition of DNA. Many researchers working primarily on acridine based intercalating agents, have on addition of DNA, observed small shifts to higher wavelength in the U.V. spectra of intercalating agents, as well as extinction coefficient reductions.[17,18] It was accordingly decided to test the DNA binding ability of the acridine conjugate **(49)**. The phosphinate ester **(49)** rather than the phosphinic acid **(50)** was chosen for testing for reasons of simplicity and charge. The target complex-intercalator conjugate will indeed be a phosphinic acid functionalised ligand, but as its yttrium complex. Moreover, the free secondary amine site introduced into the backbone of **(50)** will in the final conjugate be maleimide functionalised. The combination of these two facts means that the complex-intercalator conjugate will exhibit overall charge neutrality. The phosphinate ester **(49)** is also charge neutral, whereas the phosphinic acid **(50)** is not.

The DNA chosen for the intercalation test was Calf Thymus (Type XV) DNA. A 10^{-5} mol dm^{-3} solution of the intercalator **(49)** was made up in pH 7.4, 0.05 mol dm^{-3} sodium phosphate buffer, and to it added one equivalent of 50 x 10^{-5} mol dm^{-3} DNA, also made up in the same buffer. The DNA-phosphate concentration (i.e. the concentration of binding sites) was calculated from the extinction coefficient

6600 mol^{-1} dm^3 cm^{-1} at 260 nm. The U.V. spectrum of the solution was recorded, and another equivalent of DNA added. This process was repeated until approximately 15 equivalents of DNA had been added. The spectra were then overlaid to determine the extent of the red shift produced on intercalation. No shift was observed for (**49**), or indeed for the anthraquinone derivative (**51**). The experiment was then repeated using two simple amino acridines (Figure 4.6), and the red shifts observed recorded in Table 4.1. On this occasion, shifts although small (approx. 2 nm), were observed.

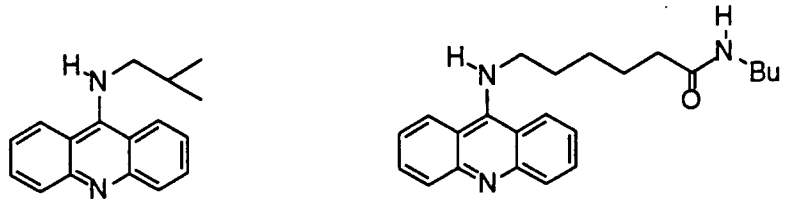

I II

Figure 4.6 : *Amino acridines used in DNA binding study*

Intercalator	λ_{free} / nm	λ_{bound} / nm	Red Shift / nm
I	410	412.9	2.9±0.3
II	417.4	418.8	1.4±0.3

Table 4.1 : *Red shifts observed on addition of 10-15 equivalents of calf thymus DNA to I & II in pH 7.4, 0.05 mol dm^{-3} phosphate buffer at 20°C*

The results obtained for the amino acridines I and II were in accordance with other reported amino acridine derivatives which have shown shifts ranging from 0 to 7 nm.[18,19]

4.7.2 DNA Binding Strength

The question arose as to whether the apparent absence of a U.V. red shift for **(49)**, was indicative of a lack of DNA binding, or simply of a much weaker binding. It became evident that the reason no DNA binding could be detected lay in the lack of charge on the endocyclic nitrogen of acridine. The presence of the amino group in 9-amino acridines (e.g. I & II Figure 4.6) dramatically increases the pKa of the ring nitrogen from 5.60 [20] for acridine, to one in the range 9.5 - 10. This essentially means that at physiological pH 7.4, amino acridines will exist as mono cations, protonated on the ring nitrogen, whilst the acridine amide **(49)** with a pKa of approximately 4.2 [21] remains unprotonated. The existence of such a cationic acridine species leads to an electrostatic attraction to the polyanionic phosphodiester backbone of DNA, producing the largest contribution to DNA binding affinity, and hence producing the observed red shifts. Indeed, as far back as 1946, an extensive study of the antibacterial activity of over a hundred acridines revealed that protonation of the aromatic ring nitrogen was a requisite for bacteriostasis, and most likely efficient DNA binding.[21]

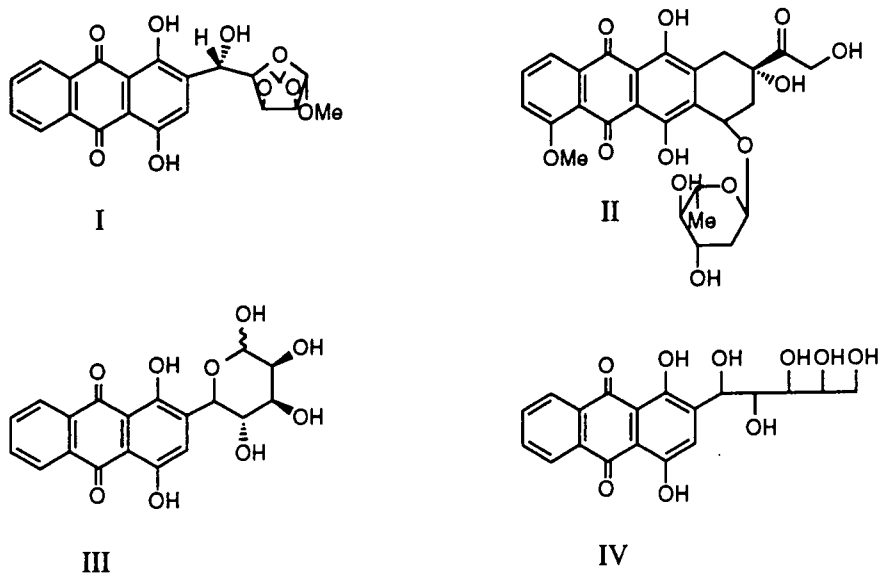

Figure 4.7 : *Neutral intercalating species*

Because of their inactivity, there are few reports on the DNA binding strengths of neutral intercalators However, two groups working on the kinetics of interaction of anthraquinone based intercalators with DNA have shown intercalation, albeit weak, to exist for neutral intercalators (Figure 4.7).[22,23]

The binding constants for I - IV were found to be 2.7 x 10^4, 1.0 x 10^5, 3.6 x 10^4, and 3.0 x 10^4 M^{-1} respectively, 10 - 100 times smaller than the corresponding derivatives bearing a charged pendent amino group. It therefore seems likely that both the acridine amide (**49**), and the anthraquinone amide (**51**), do in fact bind to DNA, particularly as the anthraquinones (**51**), I, II, and IV are all substituted in the 2 position. As a consequence of there being no electrostatic contribution to the DNA binding of (**49**) and (**51**), binding constants will be slightly lower, with no detectable red shift in the U.V. There may however be one distinct advantage in a charge neutral intercalator, in that it should lead to reduced membrane interactions, and superior *in vivo* transport properties compared to those of the cationic analogue.[23]

4.8 CATIONIC ACRIDINE INTERCALATORS

4.8.1 Charged Chromophore

In an attempt to increase DNA binding affinity, it was decided to try once again to form a cationic ligand-amino acridine conjugate. Synthesis involved the initial formation of the carboxylate functionalised amino acridine (**52**) from the reaction between methoxy acridine (**38**), and 6-aminohexanoic acid, followed by its conversion to the acid chloride (**53**) (Scheme 4.14). The first step gave (**52**) in 53% yield as a yellow precipitate from a methanol solution, whilst once converted to its acid chloride, (**53**) had to be used immediately owing to it rapidly becoming insoluble, presumably due to polymerisation or cyclisation.

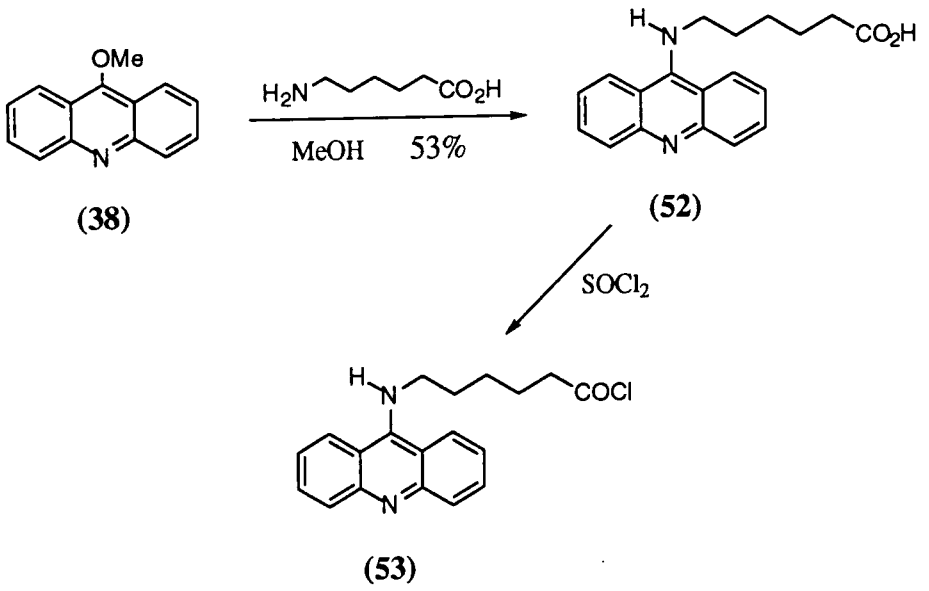

Scheme 4.14

Addition of the acid chloride (**53**) to the amine functionalised ligand (**44**) was carried out in dichloromethane containing an excess of N-methylmorpholine, to give after HPLC purification, the amino acridine (**54**) in 49% yield (Scheme 4.15). Subsequent ester hydrolysis and concomitant detosylation of the secondary amine of (**54**) resulted not in the desired product, but in a large number of unidentified compounds. Separation of the principal components showed no sign of the desired product. It was presumed, that as for HBr, AcOH, PhOH treatment of (**45**) (Scheme 4.9), unwanted hydrolysis of the amino acridine had occurred.

DNA intercalation studies of (**54**) did, as predicted for a charged acridine moiety, show a U.V. red shift of 1.6 nm from 414.3 nm to 415.9 nm, on addition of up to 20 equivalents of calf thymus DNA. The shift became progressively larger, as more DNA was added (Figure 4.8). Although a reduction in the extinction coefficient of the acridine chromophore does occur on intercalation of DNA, much of the reduction in intensity observed in Figure 4.8 was due merely to a reduction in concentration, as progressively more DNA solution was added to (**54**).

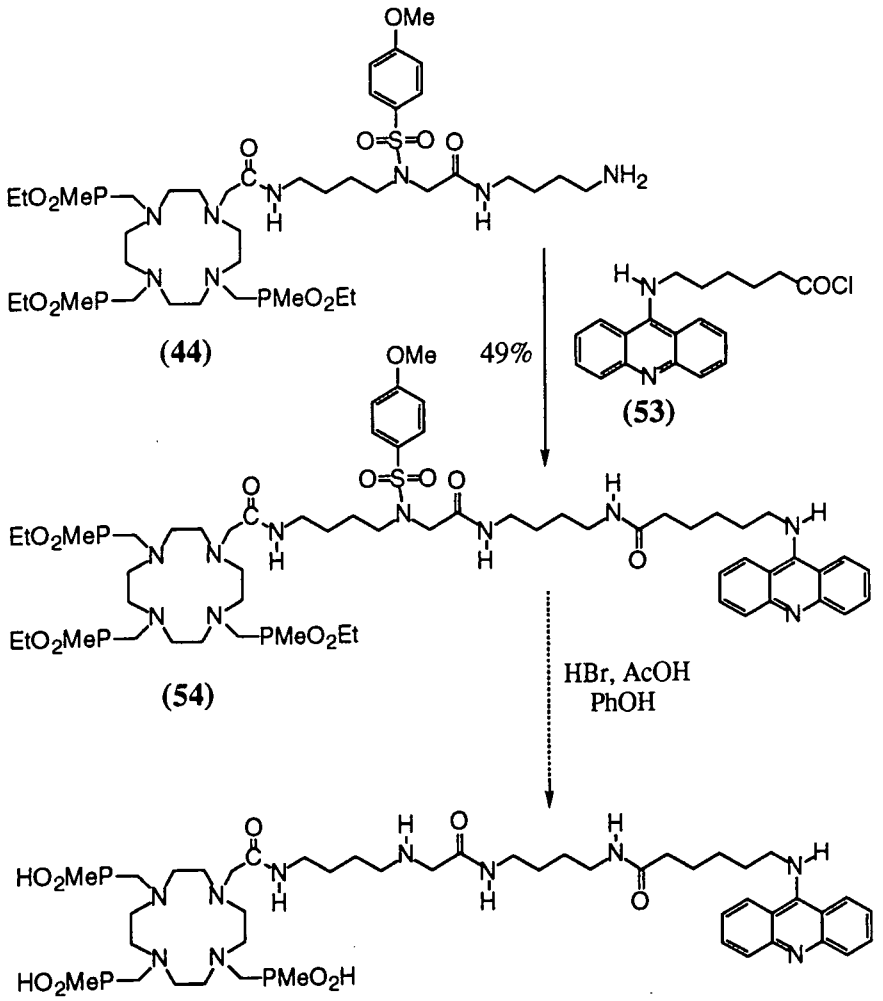

Scheme 4.15 : *Successful synthesis of the ligand-amino acridine conjugate (54) but failed ester hydrolysis, and amine deprotection*

4.8.2 Charged Side-chains

So far, discussion has been limited to intercalating agents which are charge neutral, or which possess a cationic charge on their aromatic ring system. The charge neutral ligands produced (e.g. **(50)** Scheme 4.12) may be ideal as their distribution properties are predicted to be better than their charged analogues, although it is uncertain as to whether their efficacy may be compromised by their weak intercalation to DNA.

The cationic amino acridines however, although showing strong DNA binding, were ruled out because of the difficulties encountered during the final detosylation step (Scheme 4.15).

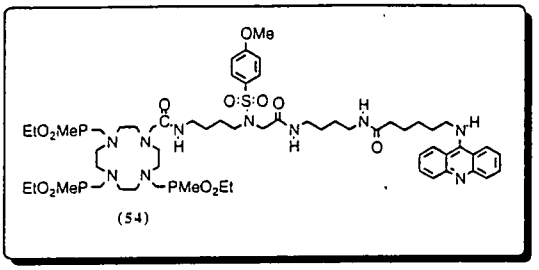

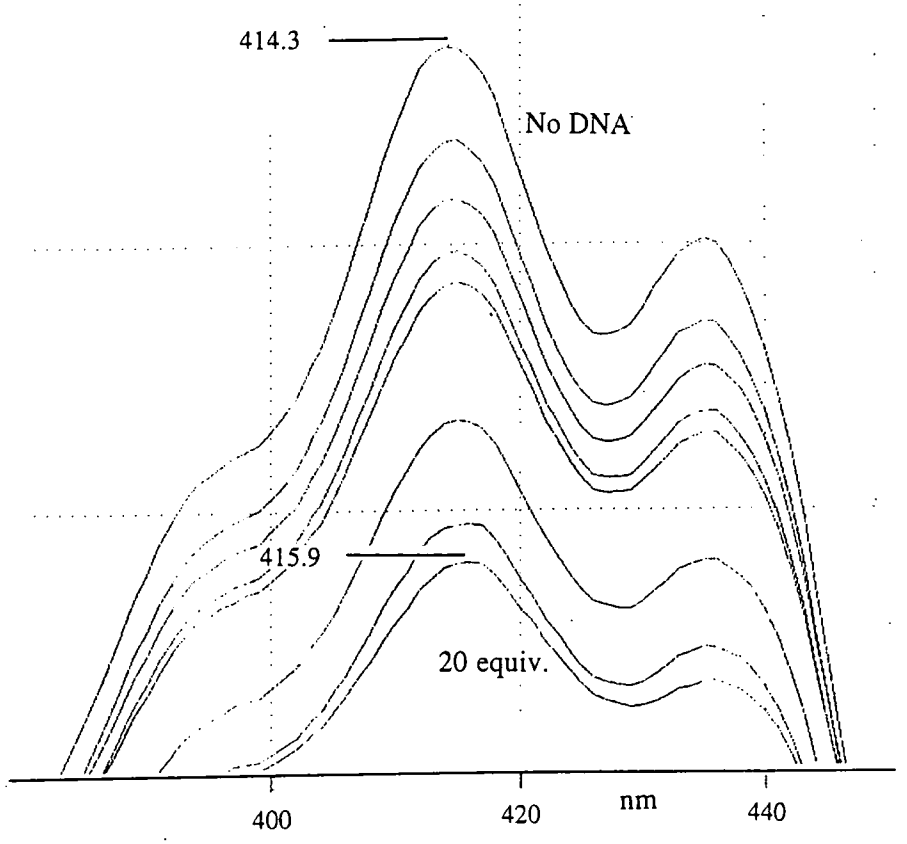

Figure 4.8 : *U.V. red shift for (54) on addition of 20 equiv. of DNA at pH 7.4*

There is however another class of charged intercalator, which although cationic in nature does not possess a charge on the ring system. Incorporation of functional groups such as amines into the pendent arms of a potential intercalating

agent permits as for amino acridines, electrostatic interaction with the anionic phosphodiester backbone of DNA, or more specific hydrogen bonding to DNA bases. These effects result in an increase in DNA intercalation strength.

Ametantrone (I) is an example of an anthraquinone based intercalating agent bearing pendent cationic charges which has proven potency in anti-cancer chemotherapy,[24] and acridine-4-carboxamide (II) is also a pendent-monocation which has shown considerable activity against leukaemia[25] (Figure 4.9).

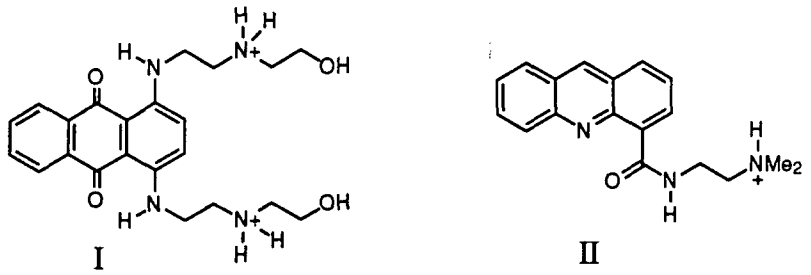

Figure 4.9 : *Cationic intercalators Ametantrone (I) and Acridine-4-carboxamide (II)*

Recent preliminary reports on examples of charged pendent arm acridines have shown intercalation for di [26] and tri (III)[14] intercalators, and for an acridine-oligonucleotide conjugate (IV) (Figure 4.10).[27] Compound III showed strong intercalation of all three chromophores, and was therefore considered interesting as the two acridine units used were in the form of acridine amides substituted in the 9-position (cf. **(50)** Scheme 4.12). The intercalating ability of the acridine-oligonucleotide conjugate (IV) also proved interesting as yet again, the acridine was in the form of an acridine amide, substituted in the 9-position. Acridine-4-carboxamide (II), although not substituted in the 9-position, is also an acridine amide which shows intercalation.

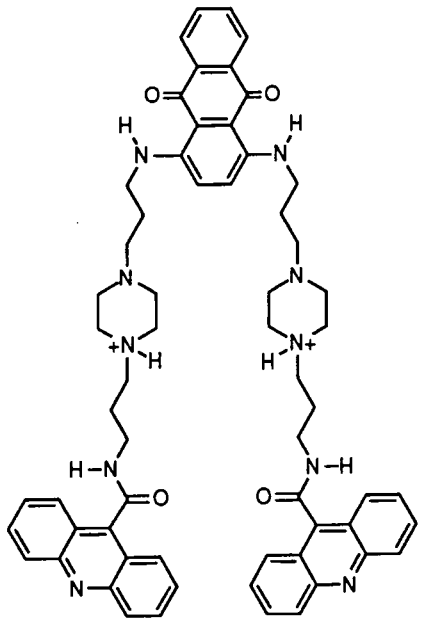

III

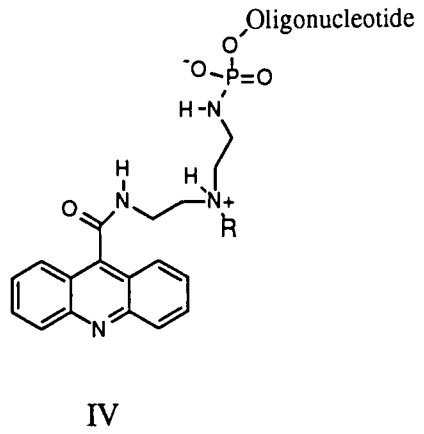

IV

Figure 4.10 : *Pendent charged 9-acridine amide intercalators*

With these encouraging results in mind, an acridine amide similar to **(49)** but incorporating a tertiary amine site (will protonate) in the linker between the acridine and the ligand was synthesised (Scheme 4.17). In an identical manner to the synthesis of the BOC protected amine **(42)** (Scheme 4.7), the BOC protected amine **(56)** was formed (Scheme 4.16).

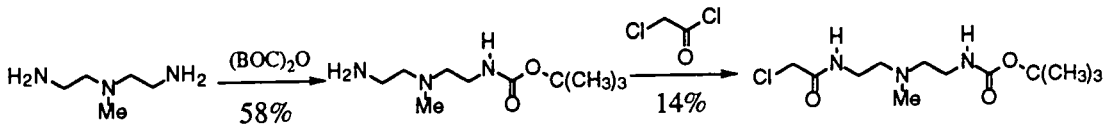

(55) **(56)**

Scheme 4.16

Subsequent addition of **(56)** to **(14a)** was carried out in exactly the same manner as for the synthesis of **(46)** (Scheme 4.8), and the acridine amide **(58)** formed, by the subsequent addition of the acid chloride **(46)** (as in Scheme 4.12).

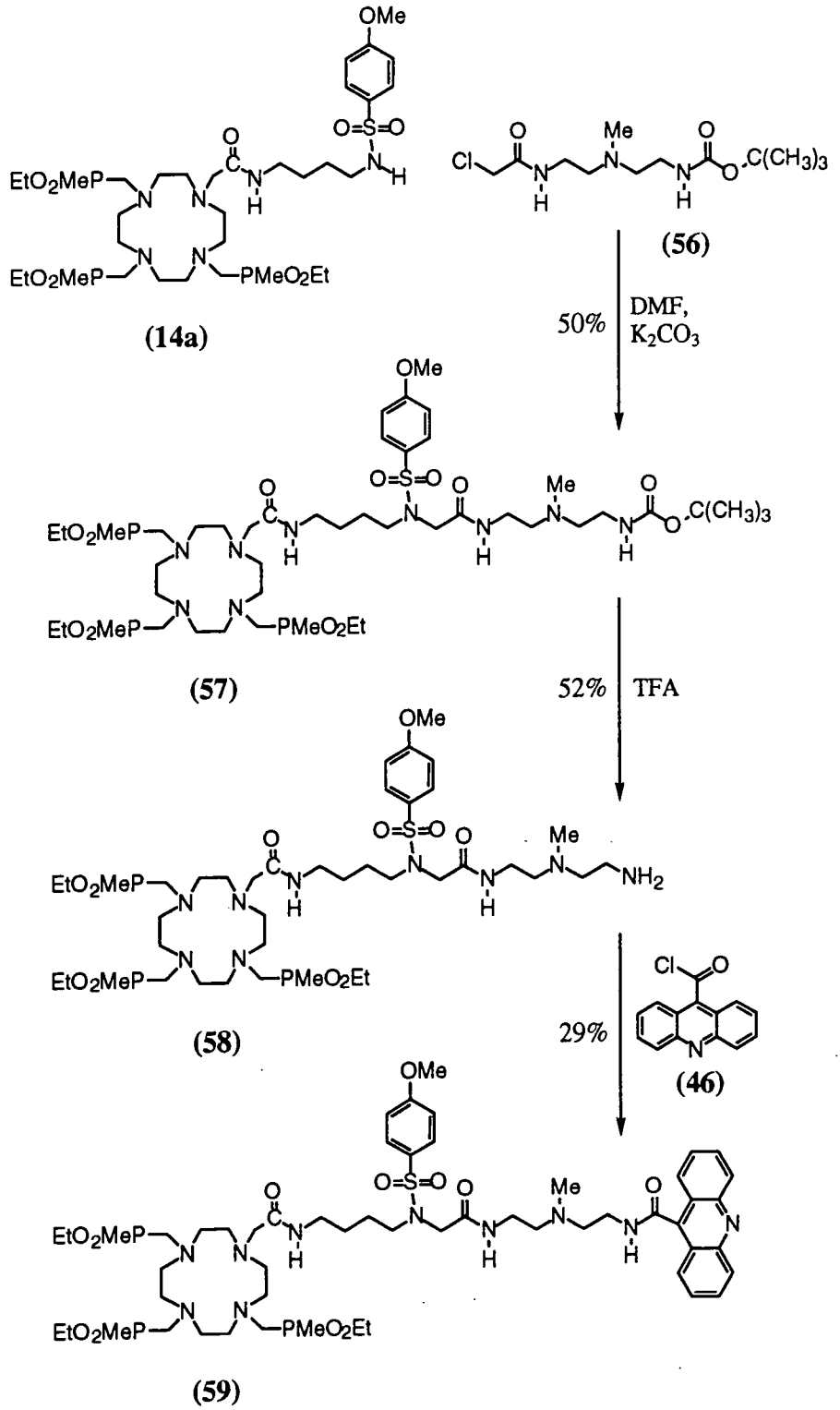

Scheme 4.17 : *Synthesis of the charged pendent arm acridine amide (59)*

Owing to the small quantity of **(59)** produced, subsequent phosphinate ester hydrolysis and detosylation was not attempted. The DNA binding properties of **(59)** were however tested to determine the extent, if any, of intercalation.

No red shift was observed for **(59)** on addition of up to 20 equivalents of calf thymus DNA. Although disappointing, the result was the expected one, as the intercalation strength was predicted to be one or two orders of magnitude smaller than the cationic amino acridines which themselves only gave a red shift of approximately 2 nm (Table 4.1). The red shift for **(59)** therefore, would be too small to detected. For definitive proof of intercalation, tests such as DNA helix unwinding angle, and sedimentation coefficient changes would have to be performed. These were beyond the scope of my work, and although interesting were not performed.

4.9 MALEIMIDE DERIVATISATION

4.9.1 Mono-maleimide

As discussed in Section 4.2, the purpose of the attachment of a DNA intercalating agent to a complex-antibody conjugate, was to bind the complex to a tumour cell's DNA once the antibody fragment (Fab') had taken the complex inside the cell. The ligand-acridine conjugate **(50)** therefore required maleimide derivatisation at the free secondary amine site on the backbone connecting the ligand and acridine. The maleimide is able to react selectively in the presence of amines, with a free thiol of a Fab', thereby permitting conjugation to the molecule. As for the synthesis of the mono-maleimide-ligand conjugate **(24)** (Chapter 3 Scheme 3.6), initial attempts to functionalise **(50)** with a single maleimide moiety concentrated on the use of a maleimide active ester **(22)** in DMSO. All attempts, including the use of a model of **(50)** (Figure 4.11) failed to produce any of the desired maleimide derivatised product, and only slow hydrolysis of the active ester **(22)** was observed.

It was suspected that the electron withdrawing effect of the adjacent amide functionality of **(50)** was reducing the nucleophilicity of the amine site, thus halting the desired reaction.

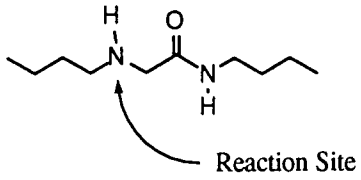

Figure 4.11 : *Model of (50)*

The addition of the more reactive maleimide acid chloride to **(50)** in a DMF / dichloromethane solution did however, cleanly form the mono-maleimide derivative **(60)** (Scheme 4.18), which after HPLC purification gave a yield of 93%. Both NMR and electrospray mass spectrometry confirmed the existence of **(60)**.

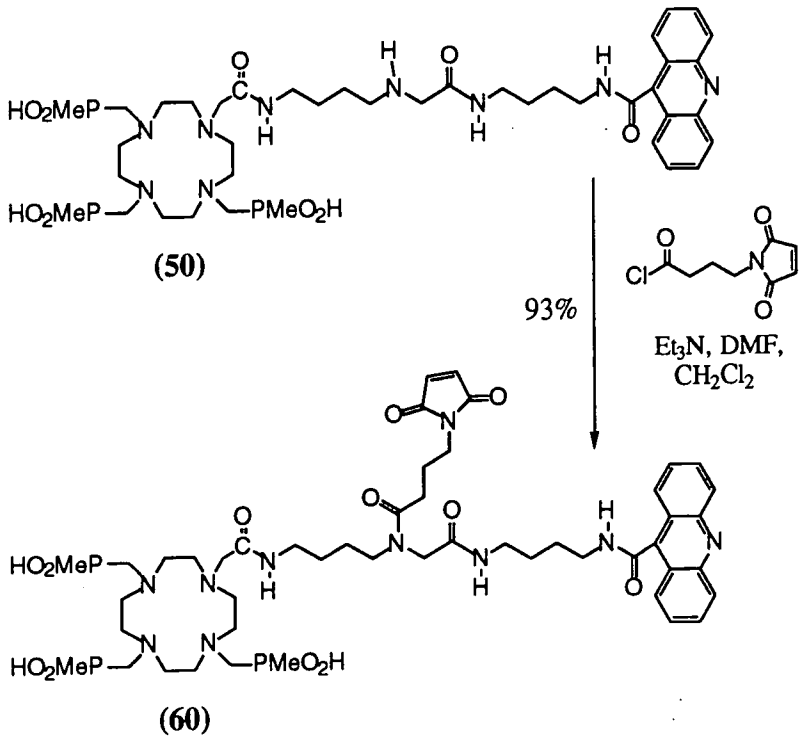

Scheme 4.18 : *Synthesis of the mono maleimide derivative (60)*

The ^1H NMR of **(60)** was unusual, in that the expected singlet due to the two equivalent protons of the maleimide appeared as two distinct resonances in roughly a 2:1 ratio. Indeed, the singlet and the triplet due to the protons on either side of the newly formed amide (see Figure 4.12), also showed in the same 2:1 ratio, chemical shift non-equivalence of approximately 65 Hz, giving instead, two singlets and two triplets. Even though **(60)** had eluted from the HPLC column as one clean peak, and mass spectrometry had confirmed its existence, it initially appeared that two maleimide species were present. Repetition of the reaction using **(50)** and also its model (Figure 4.11), always showed one product by HPLC, yet the unusual 2:1 non-equivalence of the same three sets of resonances was always observed. The answer to the problem was established by a V.T. ^1H NMR experiment. As the temperature was increased from 5-35°C, careful measurements of the resonance shifts showed a slight coalescence of the three sets of anisochronous resonances of 3.2 Hz, and 7.6 Hz, for the triplet and the CH_2 singlet respectively. This suggested that rotation around the newly formed amide C-N bond of **(60)** was conformationally locked due to hydrogen bonding between the amide carbonyl oxygen, and the proton of the adjacent amide (Figure 4.12).

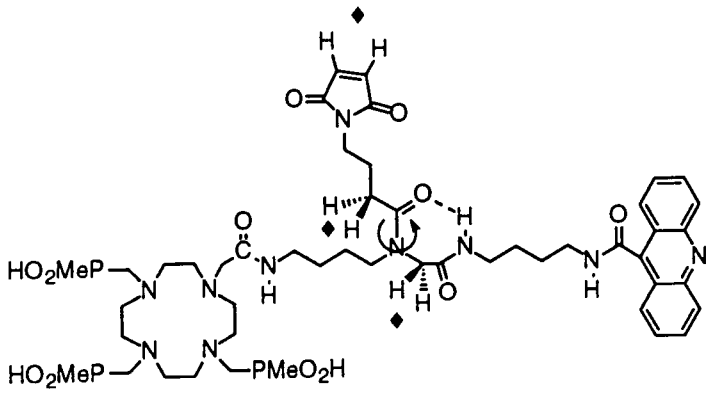

(60)

♦ = Site of observed chemical shift non-equivalence

Figure 4.12 : *The locked conformation of (60), showing restricted C-N bond rotation*

This locked conformation essentially introduced an inequivalency of the maleimide protons, and of the protons at other two sites, as well as at other sites whose splitting was obscured in the ^1H NMR spectrum.

4.9.2 Tri-maleimide

For the same reasons expressed in Chapter 3 (Section 3.6.1), it was desirable to functionalise the ligand-acridine conjugate **(50)** with three antibody fragments, thus requiring the addition of three maleimides.

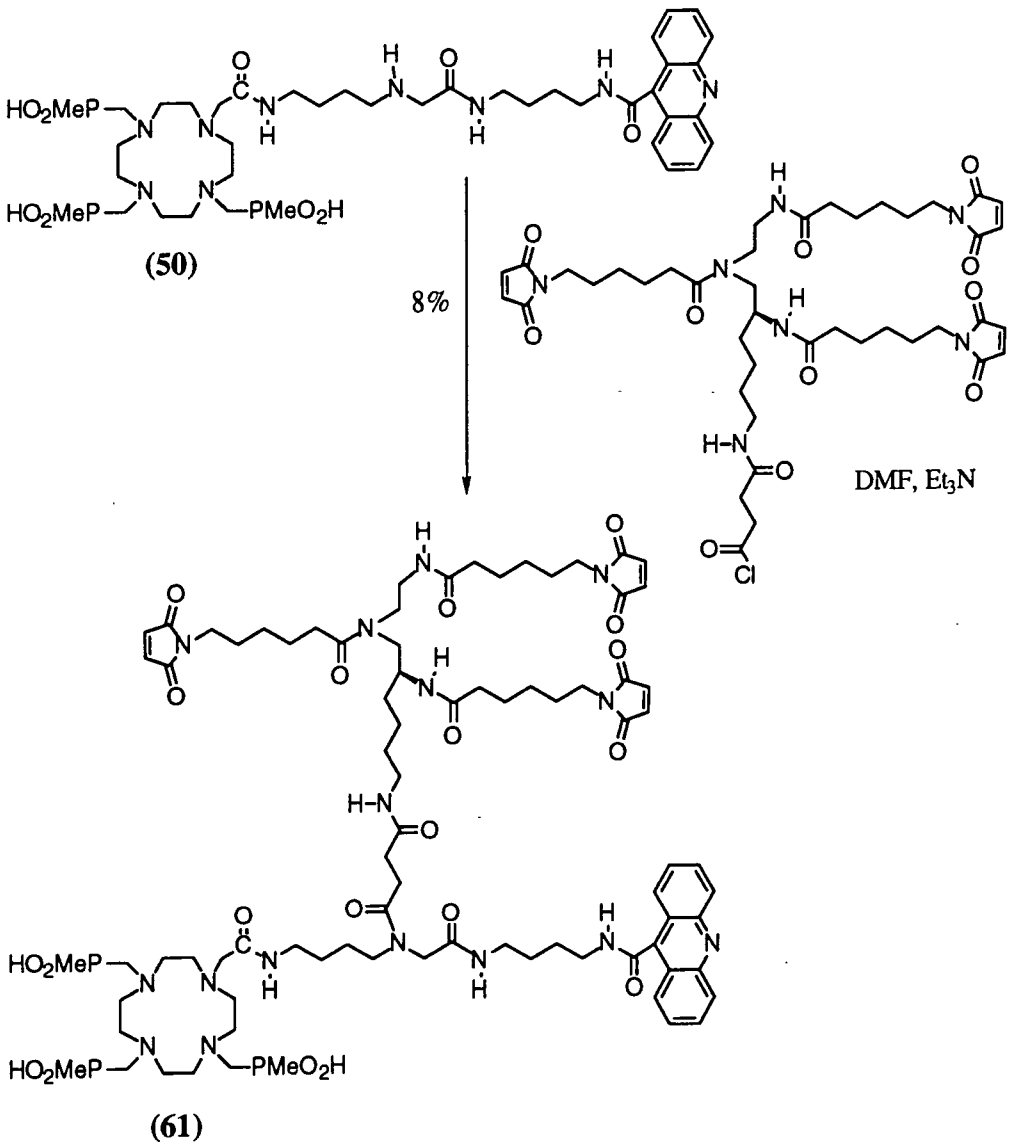

Scheme 4.19 : *Synthesis of the tri-maleimide-acridine-ligand conjugate (61)*

It was suggested that the antibody fragment responsible for cell internalisation (A33), is most effective when surface antigen cross-linking is achieved. Thus, a tri-Fab', being capable of cross-linking three antigen sites should be more suitable for cell internalisation than the mono-Fab', Fab'-**(60)** which is incapable of cross-linking.

To determine however if a mono-Fab' was capable of cell internalisation, tests were carried out on amongst others, Fab'-**(60)** to discover their effectiveness (see Chapter 5, Section 5.8).

Synthesis of the tri-maleimide-acridine functionalised ligand **(61)** was effected as for the synthesis of the tri-maleimide **(34)** (Chapter 3, Scheme 3.12). The carboxylic acid functionalised tri-maleimide **(35)** was converted to its acid chloride by the addition of oxalyl chloride, and added immediately to a DMF solution of **(50)** and triethylamine. HPLC purification gave the desired product **(61)**, albeit in very low yield (Scheme 4.19).

4.10 CONCLUSIONS

The use of antibody fragments in conjunction with intercalators does in principle present a novel and improved technique for accurate radioimmunotherapy of cancer. It however waits to be seen if indeed intercalators will show any positive improvements over merely Fab' labelled ligands.

Although DNA intercalation is yet to be proven, the use of uncharged acridine amides may in principle allow better conjugate biodistribution. For charged pendent arm intercalators, intercalation should also be possible, but has not been proven yet *in vitro*. Along with the tests carried out at Celltech Ltd., (see Chapter 5), more accurate biological tests are required to determine the extent, if any of intercalation. This use of intercalators is still in its infancy, and may take time to prove its effectiveness.

4.11 REFERENCES

1 U. Pindur, M. Haber, and K. Sattler, *J. Chem. Educ.*, 1993, **70(4)**, 263.

2 E. C. Long, and J. K. Barton, *Acc. Chem. Res.*, 1990, **23(9)**, 271.

3 M. Cory, D. D. McKee, J. Kagan, D. W. Henry, and J. A. Miller, *J. Am. Chem. Soc.*, 1985, **107**, 2528.

4 R. W. Bates, Ph.D Thesis, University of Oxford, 1993.

5 J. Chen, D. V. Carlson, H. L. Weith, J. A. O'Brien, M. E. Goldman, and M. Cushman, *Tet. Lett.*, 1992, **33(17)**, 2275.

6 J. Sun, J. François, R. Lavery, T. Saison-Behmoaras, T. Montenay-Garestier, N. T. Thuong, and C. Hélène, *Biochemistry*, 1988, **27**, 6039.

7 J. François, T. Saison-Behmoaras, M. Chassignol, N. T. Thuong, J. Sun, and C. Hélène, *Biochemistry*, 1988, **27**, 2272.

8 J. François, T. Saison-Behmoaras, M. Chassignol, N. T. Thuong, J. Sun, and C. Hélène, *J. Biol. Chem.*, 1989, **264(10)**, 5891.

9 D. S. Sigman, *Biochemistry*, 1990, **29(39)**, 9097.

10 A. Albert, and B. Ritchie, *Org. Syntheses Collective*, 1955, **3**, 53.

11 D. J. Dupré, and F. A. Robinson, *J. Chem. Soc.*, 1945, 549.

12 H. J. Barber, J. H. Wilkinson, and W. G. H. Edwards, *Chem. Ind.*, 1947, **66**, 411.

13 "Heterocyclic Compounds - Acridines", ed. R. M. Acheson, Interscience Pulishers, 2nd edition, 1973, pg 124.

14 S. Takenaka, S. Nishira, K. Tahara, H. Kondo, and M. Takagi, *Supramol. Chem.*, 1993, **2**, 41.

15 L. S. Lerman, *J. Mol. Biol.*, 1961, **3**, 18.

16 W. D. Wilson, F. A. Tanious, R. A. Watson, H. J. Barton, A. Strekowski, *Biochemistry*, 1989, **28**, 1984.

17 B. E. Bowler, K. J. Ahmed, W. I. Sundquist, L. S. Hollis, E. E. Whang, and S. J. Lippard, *J. Am. Chem. Soc.*, 1989, **111(4)**, 1299.

18 S. C. Zimmerman, C. R. Lamberson, M. Cory, and T. A. Fairley, *J. Am. Chem. Soc.*, 1989, **111**, 6805.

19 E. S. Canellakis, Y. H.Shaw, W. E. Hanners, and R. A. Schwartz, *Biochim. Biophys. Acta*, 1976, **418**, 277.

20 A. Albert, S. D. Rubbo, and R. Goldacre, *Nature*, 1941, **147**, 332.

21 A. Albert, and R. J. Goldacre, *J. Chem. Soc.*, 1946, 706.

22 V. Rizzo, N. Sacchi, and M. Menozzi, *Biochemistry*, 1989, **28**, 274.

23 F. Barceló, D. J. Mincher, M. R. Crampton, J. R. Brown, and G. Shaw, *Anti-Cancer Drug Design*, 1991, **6**, 37.

24 M. B. Gandecha, J. R. Brown, and M. R. Crampton, *Biochem Pharmacol.*, 1985, **34(6)**, 733.

25 "Chemistry of Antitumour Agents", ed. D. E. V. Wilman, Blackie & Son Ltd, London, 1990, pg. 25.

26 S. Takenaka, T. Ihara, and M. Takagi, *J. Chem. Soc., Chem. Commun.*, 1990, 1485.

27 K. Shinozuka, Y. Seto, and H. Sawai, *J. Chem. Soc., Chem. Commun.*, 1994, 1377.

Chapter 5

Antibody Conjugation

5.1 INTRODUCTION

Each year, there are estimated to be over 400,000 new cases of colorectal cancer diagnosed world-wide. In its early stages, surgery and chemotherapy can lead to greater than 80% five year survival. However, in later stages, when cancer has spread, there is only about a 50% five year survival following treatment. For this reason, this work is concerned specifically with the radioimmunotherapy of colorectal cancer.

The mono and tri-maleimide functionalised ligands reported in Chapters 3 and 4 were formed to permit antibody fragment (Fab') conjugation to a metal complex for radioimmunotherapy. This chapter is concerned primarily with the techniques of Fab' conjugation and purification, as well as subsequent conjugate testing.

5.2 ANTIBODIES USED

Chimeric monoclonal antibody fragments (Fab'), rather than whole antibodies were used for reasons laid out in Chapter 1 (Section 1.6). Two different antibody fragments were available for the targeting of antigens found specifically in colorectal cancers. These were B72.3 and A33, both of which have been shown to bind with high specificity to antigenic tumour associated glycoproteins (TAG-72 in the case of B72.3). The monoclonal antibody A33 has distinct advantages over B72.3, in that unlike the antigen TAG-72, which is only present in 80% of colorectal cancers,[1] the antigen for A33 is homogeneously present in all colorectal cancers. Moreover, in clinical studies using ^{131}I-radiolabelled whole antibodies, tumour to non-tumour ratios for B72.3 were less than ten,[2] whereas for A33 the ratios were consistently found to be much higher.[3] The antibody A33 also has the unusual property of cell internalisation, although one potential limitation of the use of A33 is the expression of its antigen in non-cancerous colonic mucosa.

5.3 FAB' PREPARATION

5.3.1 Thiol Reduction

Antibody fragment conjugation to a maleimide is achieved through a thiol group. Both B72.3 and A33 may be modified to contain only one thiol in the form of a cysteine residue in the hinge region of the antibody fragment (see Scheme 3.2). However, before conjugation to a maleimide is possible, the thiol in the hinge region must be reformed immediately prior to use. This was achieved by incubation with β-mercaptoethylamine (β-ME), a reducing agent which is able to convert a disulfide or SO_xH back to a thiol. However, as a Fab' contains five disulfide bridges, a selective reduction must be carried out, whilst leaving the disulfide bridges intact.

Typically, to 0.9 ml of Fab' (B72.3 or A33) at a concentration of approximately 5 mg ml^{-1} in 0.1 M acetate-citrate-EDTA [pH 6.0 buffer], was added 0.1 ml of 50 mM β-ME in the same buffer. The solution was then incubated in a water bath at 37°C, for exactly 30 minutes, at which point, to remove any excess β-ME, it was loaded onto a prepacked Sephadex G-25M PD-10 column equilibrated in the same buffer. The column was eluted with buffer, and 1 ml fractions collected.

Beer-Lambert $A = \varepsilon.c.l$

(A = absorbance, c = concentration, ε = extinction coefficient, l = cell path-length)

$c = A/\varepsilon.l$ (l = 1 cm)

$c = A/\varepsilon$ (ε = 1.14 $cm^{-1}mg^{-1}ml$ at 280 nm)

$[Fab'] = A_{280}/\varepsilon$ / mg ml^{-1}

Fab' RMM = 50,000

$[Fab'] = A_{280} / 50{,}000.\varepsilon$ / μM

Scheme 5.1 : *Calculation of antibody concentration*

The antibody concentration in each eluted fraction was then calculated from absorbance measurements at 280nm (A_{280}) of diluted samples (approx. 30 fold) of each 1 ml fraction (Scheme 5.1). Typically the fourth, and to a lesser extent the fifth eluted fractions contained the bulk of the reduced antibody fragment, which was stored on ice in an attempt to inhibit aerial oxidation of the thiol group.

5.3.2 Thiol Assay

The extent of Fab' reduction (thiol reformation), varies from one incubation to another, and affects the degree of maleimide coupling that is possible. Too much reduction leads to cleavage of intra disulfide bridges, and can cause aggregation of antibodies. Too little reduction on the other hand leads to a wastage of Fab'. Ideally, incubation should affect reformation of just one thiol (the cysteine residue) per Fab'. The extent of this reduction can be determined using a thiol assay. Values in the range 0.9 to 1.1 thiols per Fab' are acceptable for use in conjugation.

For the assay, three 100 µl solutions (Test, Blank, and Control) were prepared, incubated for exactly 10 minutes, and their U.V. spectra measured at either 324 nm or 280 nm (Table 5.1).

Solution	Fab' /µl	PBS /µl	DTDP / µl	λ / nm
Test	30	60	10	324
Blank	0	90	10	324
Control	30	70	0	280

(DTDP = 4, 4' -Dithiodipyridine 5 mM in ethanol.)

Table 5.1

When added to DTDP, a Fab' thiol will liberate an equivalent of thiopyridine (Scheme 5.2). Knowing the extinction coefficient ε of thiopyridine at 324 nm ($\varepsilon = 19800\ cm^{-1}\ M^{-1}$), its concentration, and hence the concentration of thiol can be calculated for the Test and Blank solutions.

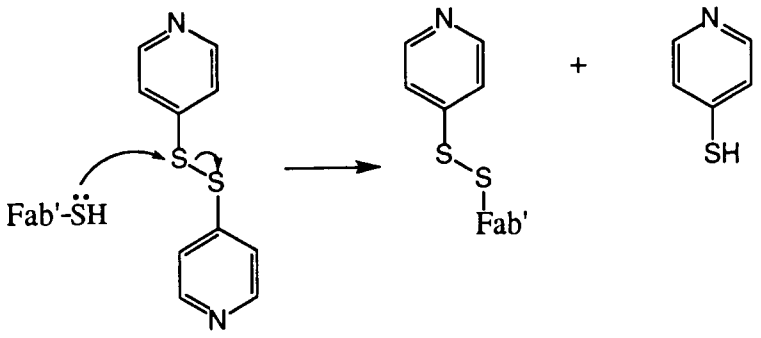

Scheme 5.2

Measurement of the absorbance of the Control solution at 280 nm then permits the overall concentration of Fab' to be calculated (see Scheme 5.1). Knowing both the thiol concentration and the concentration of Fab' present, the average number of thiols per Fab' can be determined (Scheme 5.3).

From the Test and Blank at 324 nm.

$$[\text{Fab' Thiol}] = \frac{[A_{324}\,(\text{Test}) - A_{324}\,(\text{Blank})]}{19800} \times 10^6 \quad / \mu M$$

From the Control at 280 nm.

$$[\text{Fab'}] = A_{280}\,(\text{Control}) / 50{,}000.\varepsilon \quad / \mu M$$

Therefore,

$$\text{Thiols per Fab'} = \frac{[\text{Fab' Thiol}]}{[\text{Fab'}]}$$

Scheme 5.3 : *Determination of the average number of free thiols per Fab'*

5.4 FAB' CONJUGATION TO TRI-MALEIMIDES

5.4.1 Nature of Products

Initial attempts to conjugate antibody fragments to maleimides concentrated on the tri-maleimides **(29)**, **(30)**, and **(31)** (Figure 5.1).

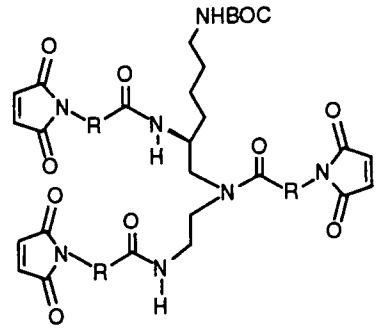

(29) R = CH_2-⬡ **(30)** R = $(CH_2)_3$ **(31)** R = $(CH_2)_5$

Figure 5.1 : *The tri-maleimides used in the coupling reactions*

Contrary to expectations, conversion of a tri-maleimide to its tri-Fab' could not be brought about by the simple addition of 3 or more equivalents of reduced Fab'. Indeed, addition of too much Fab' appeared to reduce the amount of tri-Fab' formed, with both the di-Fab' and the mono-Fab' also being formed. The proportion of each of the three products was found to be highly dependent on the ratio of Fab' to tri-maleimide used. If the ratio was too small, then as expected, very little tri-Fab' was observed. On the other hand, if the ratio of Fab' to tri-maleimide was too large, then again very little tri-Fab' was formed.

The reason why complete tri-maleimide conversion to the tri-Fab' could not be obtained is unclear. Partial maleimide hydrolysis, or reaction with trace amines could account for the presence of the di and mono-Fab' species. In addition, steric inhibition of conjugation may also be involved. Compared to the distance between

maleimide moieties of a tri-maleimide, an antibody fragment with a mass of 50,000 Da is very large. Thus, steric crowding may result when trying to form a tri-Fab'. It was for this reason that the three different tri-maleimides **(29)**, **(30)**, and **(31)** were prepared, in an attempt to ascertain if a difference in the ratio of products could be observed on changing the effective distance between the three maleimide moieties.

5.4.2 'One Pot Route'

Two different routes to the formation of tri-Fab' species were attempted. On all occasions, addition of reduced Fab' to a tri-maleimide resulted in a mixture of tri, di, and mono Fab' species, as well as unreacted Fab'. Differing ratios of Fab' to tri-maleimide were used in an attempt to optimise the amount of tri-Fab' formed.

Typically, following a '1-pot route', solutions containing reduced Fab' (approx. 70 μM) and the tri-maleimide (1 mM in dry DMF), were made up in ratios ranging from 1:1 to 8:1, and incubated at 37°C for a minimum of 2 hours. For example, a 3:1 ratio may contain approximately 2 μl of tri-maleimide (1 mM), and 100 μl of reduced Fab'. The percentage of tri-Fab', di-Fab', and mono-Fab' was then determined by analytical HPLC (0.2 M sodium phosphate buffer, pH 7.0, 1 ml $min.^{-1}$, 273 nm) using a Dupont Bioseries Zorbax GF250 gel filtration column. Using this technique, the three major products could be easily resolved with retention times for the tri, di, and mono Fab' species of 8.4 min., 8.9 min., and 9.9 min. respectively. The area under each peak could then integrated to give the percentage of each product.

5.4.3 'Two Pot Route'

In addition to the problem of steric inhibition of conjugation, re-oxidation of the Fab' thiol group may also occur, effectively reducing the Fab' concentration available for conjugation. It was proposed that if a mono-Fab' of a tri-maleimide was

formed, and subsequently reacted with a fresh batch of reduced Fab', then perhaps approach of the Fab' to the maleimide moiety may be less sterically hindered, and moreover, less Fab' oxidation should occur during the second step, as the reaction time should be reduced. It should also be noted that, in related work with tetra-maleimides, the formation of a tetra-Fab' species was not possible using the 1-pot route, but was possible using the 2-pot route. Although more wasteful of the tri-maleimide linker, this second alternative technique was tried.

To a sample of reduced Fab' (approx. 70 μM) was added a 10 fold excess of the tri-maleimide linker (10 mM in dry DMF). This was incubated at 37°C for 1 hour, followed by a further incubation of 30 minutes with a 3 fold excess (over Fab') of N-ethylmaleimide (also in acetate-citrate-EDTA, [pH 6.0 buffer]) to cap any unreacted free Fab' thiols. The solution was then desalted using a Sephadex PD10 column as before (Section 5.3.1), and the fourth eluted fraction of Fab'-Linker (approx. 50 μM) retained. Immediately, using a freshly prepared batch of reduced Fab', various ratios of Fab' : Fab'-Linker from 1:1 to 4:1 were mixed and once again incubated for a minimum of 2 hours. The extent of reaction was, as for the 1-pot route, determined by analytical HPLC.

5.4.4 Large Scale Tri-Fab' Synthesis

Large scale preparation of the B72.3 tri-Fab' of **(30)** and the A33 tri-Fab' of **(31)** was carried out on approximately 30 mg of Fab' starting material with a view to determining *in vivo* tumour binding ability of the resulting tri-Fab's. However, on all occasions, the coupling efficiency was inexplicably reduced by approximately 10% compared to that of the small scale tests (Table 5.2 & 5.3). Purification was brought about either using preparative HPLC (same type of column as for analytical), or using a 2 metre long, gravity fed S200 column, eluting with 0.1 M KOAc, 0.2 M KCl, 2 mM EDTA, pH 6.0 buffer over an 18 hour period. After purification, the overall yield of tri-Fab' was approximately 20%.

5.5 RESULTS OF FAB' CONJUGATION

5.5.1 Coupling Efficiency

The ratio of tri, di, and mono Fab' products observed for each incubation was found to be dependent on the ratios of reagents used, and varied from one incubation to another. In general however, there appeared to be no observable difference in relative ratios of the products on changing from B72.3 to A33 Fab'. The tri maleimide bearing cyclohexylmethyl side-chains **(29)**, appeared to be the poorest linker, whilst little or no difference in product ratios was observed with the use of the C_3, and C_5 side-chain tri-maleimides **(30)**, and **(31)** respectively. As predicted, the 'two-pot route' to Fab' cross-linking did indeed prove itself to be the more successful of the two techniques, showing improvements of 5-15% in the amount of tri-Fab' produced, although admittedly being more time and reagent consuming.

Tri-maleimide	Fab' : Linker	%		
		Tri-Fab'	Di-Fab'	Mono-Fab'
Cyclohexyl methyl **(29)**	3:1	18.0	45.1	36.9
	4:1	15.4	40.1	44.5
	5:1	16.3	33.4	50.3
	6:1	9.5	34.5	56.0
C_3 **(30)**	2:1	5.0	35.0	60.0
	3:1	16.5	48.1	35.4
	4:1	34.5	29.5	36.0
	5:1	35.7	32.9	31.4
	6:1	28.8	28.9	42.3
C_5 **(31)**	4:1	24.8	39.9	35.3
	5:1	39.3	36.3	24.4
	6:1	24.4	40.0	35.1
	7:1	22.2	31.8	46.0

Table 5.2 : *Cross-linking results from 1-pot reactions using B72.3 or A33 Fab'*

It should be noted that, ideally, a large percentage of the tri-Fab' product is required, with a small amount of the neighbouring di-Fab', so that purification of the desired tri-Fab' is made easier. It appeared that for the three tri-maleimides tested, and for others run at Celltech, a ratio of 5:1 gave the optimum product distribution. Changing from a C_3 **(30)** to a C_5 **(31)** tri-maleimide did not appear to affect product distribution, although the use of a cyclohexylmethyl tri-maleimide **(29)** did give very poor Fab' conjugation. This could have been as a result of steric crowding, but is more likely to be due to an overall loss of activity of the maleimides due to competitive base hydrolysis, or amine coupling.

Using the 2-pot route, results were found to be consistently better.

Tri-maleimide	Fab' : Fab'-Linker	%		
		Tri-Fab'	Di-Fab'	Mono-Fab'
C_3 **(30)**	2:1	32.4	38.8	28.8
	3:1	39.1	29.0	31.9
	4:1	34.8	24.7	40.5
	5:1	30.1	22.1	47.8

Table 5.3 : *Cross-linking results from 2-pot reactions using B72.3 Fab'*

For both the one and two pot routes, incubation times in excess of 2 hours gave negligible improvement in product ratios, whereas a slight improvement was seen when initial Fab' concentrations were increased prior to coupling.

5.5.2 Gel Electrophoresis of Products

Although HPLC gives an accurate measurement of the percentage of each component of Fab' conjugation, as molecular weight increases, HPLC peak separation decreases. As a consequence, small amounts of high molecular weight (greater than 150,000 Da) aggregates may not be revealed. Gel electrophoresis however, is a

convenient technique to detect high molecular weight components, and although no accurate percentages can be assumed, it is very useful in determining purity. Reducing and non-reducing conditions can also be employed on the gel to determine the nature of components from their reduced products.

Gel electrophoresis was performed on the products of Fab' conjugation using the 'SDS Page' system on a 4 / 20 Mini Polyacrylamide gradient gel. Samples were run under both reducing (β-mercaptoethanol) and non-reducing conditions, and compared to both low and high molecular weight standards.

A sample for electrophoresis was prepared as follows. To 20 µl of approx. 3 mg ml^{-1} sample was added 5 µl of 5 x concentrate reducing or non-reducing sample buffer. The solution was then heated in a boiling water bath for 3-4 minutes prior to loading 5-10 µl into a well of the gel. Molecular weight marker proteins were also loaded in non-reducing conditions in another well to serve as molecular weight standards. The gel was then run in tank buffer at a constant current of 40 mA with a varying voltage of approximately 100-200V. Staining of the completed gel was brought about using a Coomassie Brilliant Blue R based stain for about 1 hour, followed by subsequent destaining of the gel by 7.5 % aqueous acetic acid solution.

Gel electrophoresis of the products of Fab' conjugation to a tri-maleimide clearly showed three distinct well separated bands due to tri, di, and mono Fab' species, as well as much smaller slow moving bands corresponding to high molecular weight (greater than 150,000 Da) aggregates.

High Molecular Weight Markers		Low Molecular Weight Markers	
212K	Myosin	94K	Phosphorylase b
170K	α-Macroglobulin	67K	Albumin
116K	β-Galactosidase	43K	Ovalbumin
76K	Transferrin	30K	Carbonic Anhydrase
53K	Glutamic dehydrogenase	20K	Trypsin Inhibitor
		14K	α-Lactalbumin

5.6 IMMUNOREACTIVITY COMPETITION ASSAY

Since conjugation of antibody fragments involves chemical modification of the antibody (at the cysteine thiol), it is feasible that its binding ability and specificity (immunoreactivity) to its antigen could be impaired. To test this out, the binding of the C_3 (**30**) B72.3 tri-Fab' was compared to the independently produced B72.3 tri-Fab' of CT998 and to the whole antibody B72.3 IgG. To do this, a binding competition assay was performed. This entailed competitive binding between a whole antibody-Horseradish peroxidase conjugate (B72.3-HRPO), and various concentrations of either one of the two B72.3 tri-Fab's, or the IgG, to microtitre plates coated with bovine submaxillary mucin (which contains the B72.3 antigen). The extent of B72.3-HRPO conjugate binding to the mucin, and hence the amount of tri-Fab' or IgG bound to the mucin, was determined using a hydrogen peroxide containing developing solution (B72.3-HRPO acts on H_2O_2), the results of which were analysed by at 650nm (A_{650}). The less tri-Fab' or IgG bound to the mucin, the more B72.3-HRPO conjugate present and hence the greater the observed A_{650}. From absorbance data at various concentrations of tri-Fab' or IgG, the relative immunoreactivity of each conjugate was determined

Initial sample concentration of the two tri-Fab's was 95 $\mu g\ ml^{-1}$, whilst the IgG concentration was 207 $\mu g\ ml^{-1}$. For sample preparation, to 350 µl of each of the three samples was added 350 µl of 1/2500 B72.3-HRPO. Using a clean non-coated ELISA plate (Figure 5.2) 150 µl of 1/5000 B.72.3-HRPO was placed in all wells, except those of column 1. 300 µl of the prepared samples were then placed in the remaining six wells of column 1 (IgG in rows A and B, C_3 (**30**) tri-Fab' in rows C and D, and CT998 tri-Fab' in rows E and F). A 150 µl sample of solution was then taken from each well of column 1, and transferred to its adjacent well in column 2. This process was repeated from column 2, so that doubling dilutions were achieved from column 1 through to 11 (No transfer was made to wells in column 12).

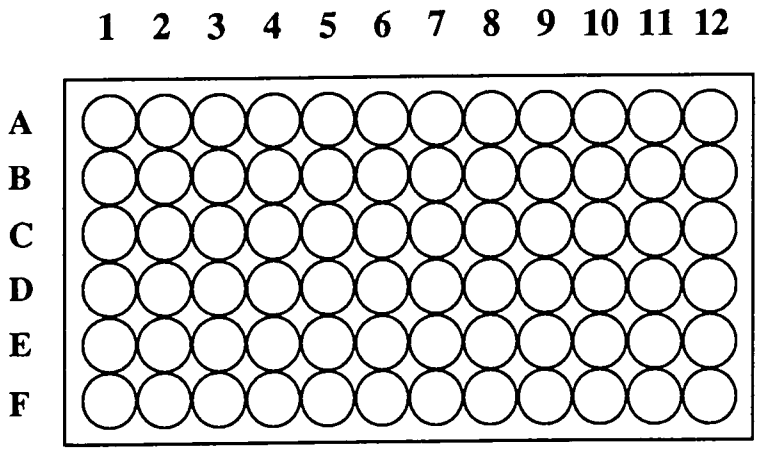

Figure 5.2 : *The wells of an ELISA plate used in an immunoassay*

Next, an identical plate with all wells coated with bovine submaxillary mucin was taken, and 100 µl removed from each of the wells of the original plate, and transferred to their corresponding coated wells in the mucin coated plate. The plate was then left for 1 hour to permit binding, followed by washing to remove all unbound species. To each well was then added 100 µl of substrate reaction mixture, and the plate left for 5 minutes to allow development of a blue colour. The plate was then placed into an auto-plate reader and the absorbance of each well measured at 650 nm. The absorbance due to the wells of column 12 containing only B72.3-HRPO, gave a 100% maximum mucin binding reference. Absorbance due to the other wells gradually increased on going from column 1 to 11, as the amount of sample used decreased, and hence the binding due to the B72.3-HRPO conjugate increased.

A graph of the results was then plotted (Figure 5.3). It can be seen, that to compete for 50% of available binding sites, an IgG must be much more concentrated than a tri-Fab'. From the graph, the relative immunoreactivities of the two tri-Fab's were compared to the whole antibody IgG.

$$\text{Immunoreactivity (tri-Fab')} = \frac{\text{µg/ml at 50\% binding for IgG}}{\text{µg/ml at 50\% binding for tri-Fab'}}$$

However, when 50% binding was observed for the B72.3-HRPO conjugate, we assumed 50% binding by a tri-Fab'. What actually occurred was that 50% of the binding sites were taken up by the tri-Fab'. As each tri-Fab' will in theory bind to three independent sites, and B72.3 IgG being divalent will bind to two sites, then when 50% of the binding sites are taken up by B72.3-HRPO, there are actually one and a half times fewer bound tri-Fab' moieties than B72.3-HRPO. For this reason, when comparing the immunoreactivity of a tri-Fab' with that of a whole IgG using this method, the lower term of the equation should be replaced by μg/ml at 60% binding for tri-Fab' to take the nature of tri-Fab' binding into consideration.

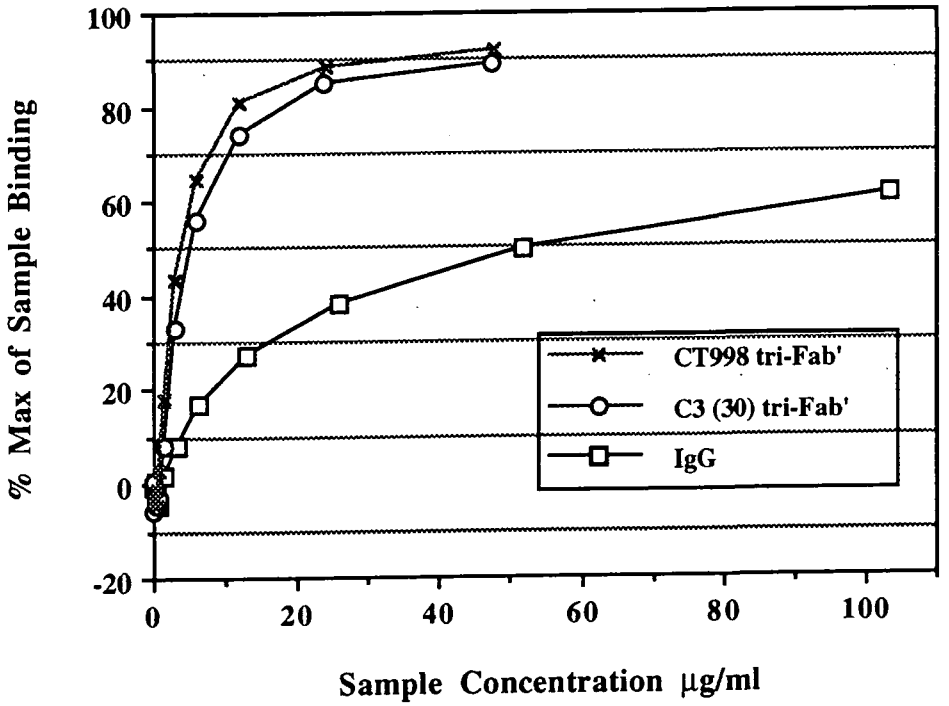

Figure 5.3

Using the equation and the graph, for the C_3 **(30)** tri-Fab' we divide 52 μg/ml by 7 μg/ml, showing the C_3 **(30)** tri-Fab' to be 7.4 times more immunoreactive than B72.3 IgG and 1.35 times less immunoreactive than the CT998 tri-Fab'. This clearly showed that not only is immunoreactivity maintained after conjugation, but more importantly, the use of a Fab' fragment rather than a whole antibody appeared not to

have any detrimental effects on binding. Indeed, as part of the tri-Fab', each Fab' became effectively 2.5 times more immureactive than the IgG. In a similar immunoassay, the C_5 **(31)** A33 tri-Fab' was formed, and again compared to CT998 A33 tri-Fab', and to A33 IgG. Results were very similar to those for the C_3 **(30)** B72.3 tri-Fab', in that C_5 **(31)** A33 tri-Fab' was found to be 8.3 times more immunoreactive than IgG, and 1.28 times less than the CT998 A33 tri-Fab'.

In an 'Off-rate' experiment which measured the rate at which antibody species were washed off an antigen coated plate, and hence gave their relative binding strengths, the half life (i.e. the time taken for half the species to be washed off the plate) of the tri-Fab' CT998 was found to be 2-3 times greater than that of the IgG.[4] Thus, in accordance with the results of the immunoassay, the use of the three antibody fragments of the tri-Fab' gave an increased avidity for binding sites compared to a single antibody.

5.7 FAB' LABELLING OF A TRI-MALEIMIDE-LIGAND CONJUGATE

The purpose of forming the tri-Fab's discussed in Section 5.4, was to optimise conditions for coupling, tri-Fab' purification and analysis, so that the more important Fab' conjugation to ligand-tri-maleimide conjugates could be achieved. Accordingly, this was attempted on a small scale with **(34)** (Figure 5.4).

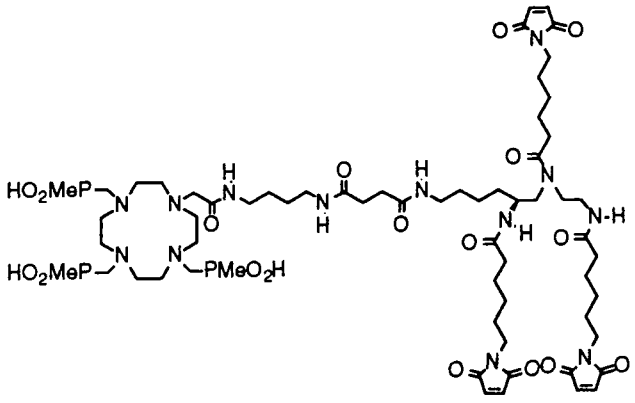

Figure 5.4 : *The ligand-tri-maleimide conjugate (34)*

Preparation of the tri-Fab' conjugate of **(34)** was carried out as described for the simple tri-Fab's of Section 5.4, and formation was confirmed both by analytical HPLC and gel electrophoresis. The optimised percentage of tri-Fab' was however very low (5%), with about 25% di-Fab' produced. This was presumably due to a loss of maleimide activity. Indeed, when the ^{1}H NMR of the tri-maleimide **(34)** was re-run after one month storage, the singlet integral for the maleimide double bond was vastly reduced, confirming the suspicion that maleimide hydrolysis, or more likely reaction with amine had occurred.

The A33 tri-Fab' of the ^{90}Y radiolabelled tri-maleimide-ligand conjugate CT998 (Figure 5.5), synthesised at Celltech, has enjoyed considerable success in the treatment of colorectal tumours implanted in animals.

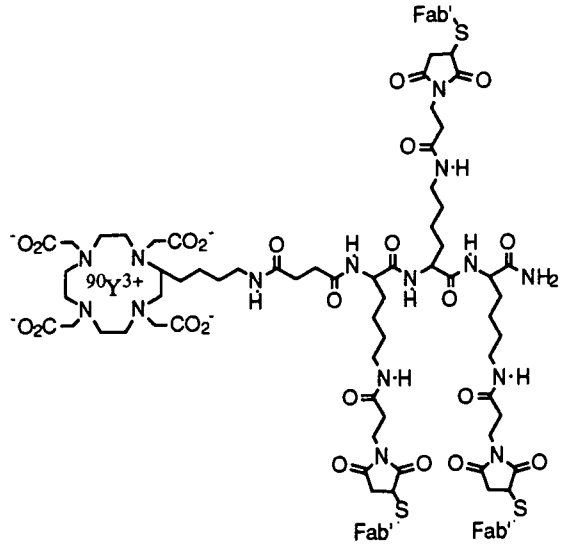

Figure 5.5

Indeed, complete tumour regression has been observed for animals treated with this conjugate, whereas animals which remained untreated exhibited rapid tumour growth (see Figure 5.6). These results do indeed appear very promising, and are being pursued in a clinical trial.

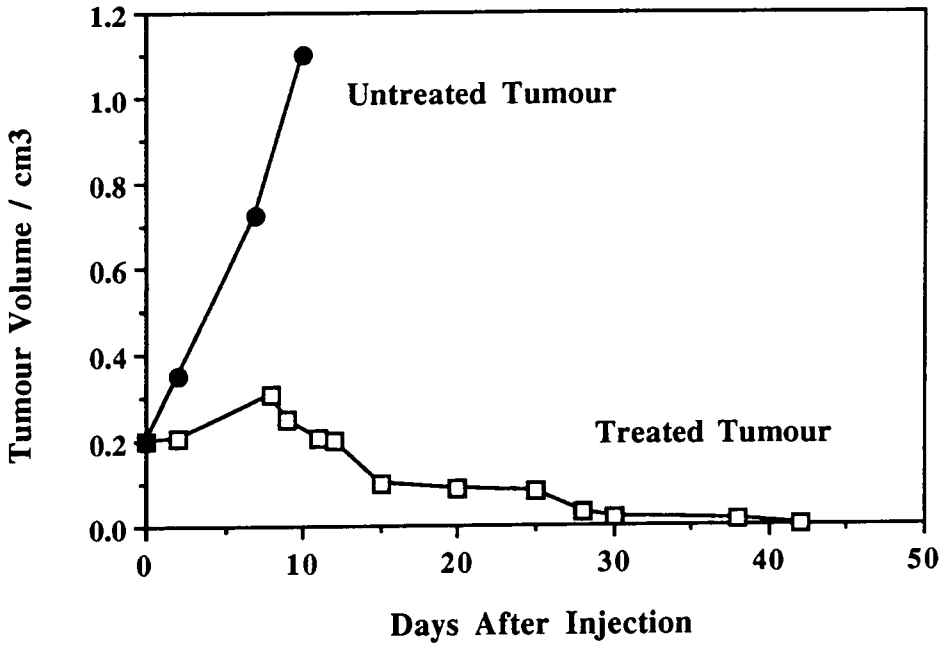

Figure 5.6 : *Tumour therapy with an ^{90}Y radiolabelled A33 tri-Fab'*

5.8 TUMOUR BIODISTRIBUTION RESULTS

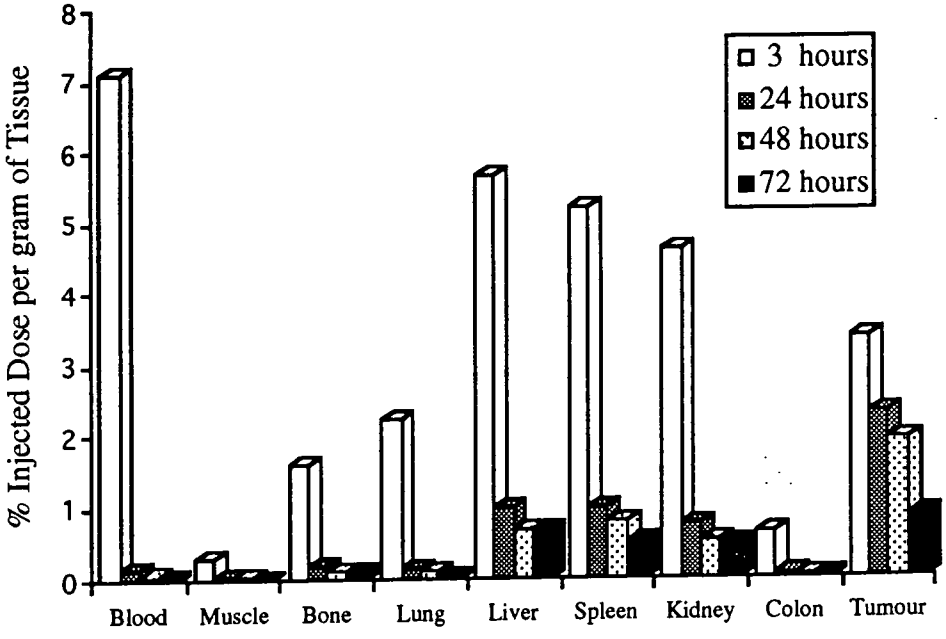

Figure 5.7 : *Biodistribution of ^{125}I radiolabelled C_5 (31) A33 tri-Fab'*

The A33 tri-Fab' of **(31)** was radiolabelled with ^{125}I and injected into nude mice bearing SW1222 xenografts. It can be seen in Figure 5.7, that at later time points the conjugate clears from the blood and other organs much more quickly than it does from the tumour, thus showing its selectivity for the tumour. In must be noted that the high levels of radiolabel found in the liver, spleen and kidneys are due to dehalogenation of the conjugate (when labelled with a stable ^{111}In metal complex levels in the three organs are much lower).

5.9 USE OF INTERCALATORS

The use of an intercalator to bind an ^{90}Y radiolabelled Fab' conjugate to tumour cell DNA was discussed in Chapter 4. The use of such an intercalating agent however, is dependent on the radiolabelled conjugate's ability to penetrate the tumour cell wall, and bind to the DNA.

In an attempt to discover if the use of an intercalator in conjunction with a radiolabelled A33 mono-Fab' would effect more efficient cell death than a purely radiolabelled mono-Fab', *in vitro* tumour cell killing studies were carried out on four ^{111}In radiolabelled conjugates, with and without an intercalator (Figure 5.8). The Fab' conjugated compounds Fab'-**(24)** and Fab'-**(60)** were formed by adding approximately 7 equivalents of the ligands **(24)** and **(60)** to Fab' solutions and allowing the mixtures to incubate at 37°C. After 1 hour, the solutions were purified by gel chromatography, to give Fab' conjugates suitable for testing. ^{111}In, rather than ^{90}Y was used because of its short emission range (0.48 mm - 20 nm). For efficient cell killing by ^{111}In, Auger electrons must be emitted close to the cell nucleus as their range is less than a cell diameter.[5] Thus, any resulting cell death can be attributed to high energy Auger emissions from internalised radiolabelled conjugate. It was postulated that in order to effect efficient cell internalisation, surface antigen cross-linking may have to be achieved (see Section 4.9.2).[4] This

hypothesis means that a tri-Fab' bearing three antigen binding sites should be more suitable for this purpose than an IgG bearing two binding sites, which in turn should be more suitable than a mono-Fab'.

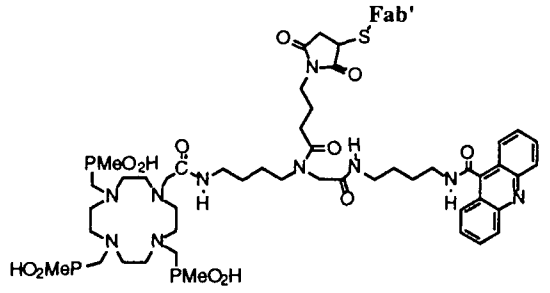

Fab'-(**60**)

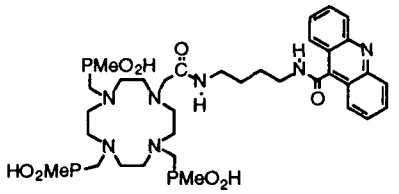

(**47**)

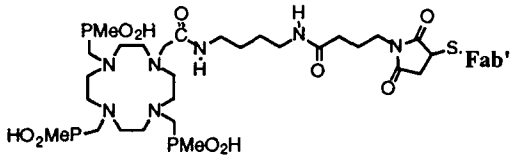

Fab'-(**24**)

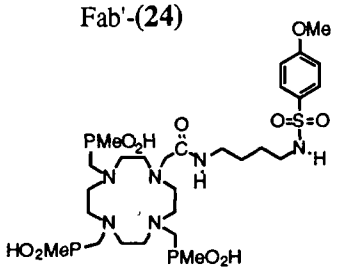

(**16**)

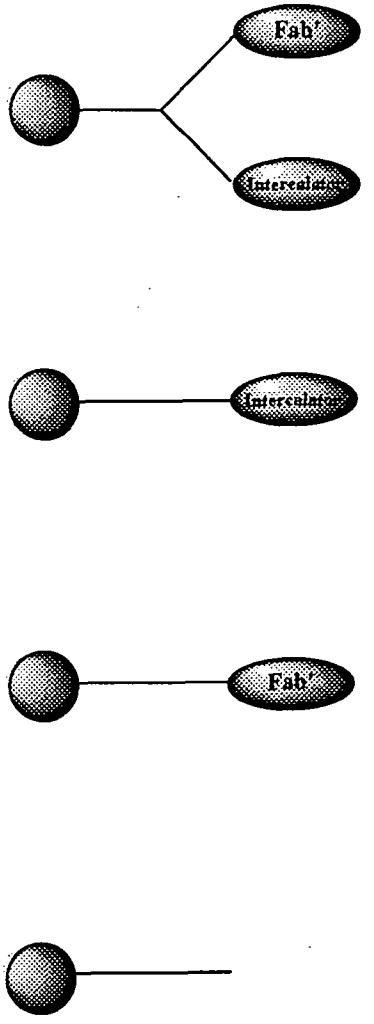

Figure 5.8

Research at the Sloan-Kettering Cancer Centre in New York showed *in vitro* cell killing by ^{111}In radiolabelled A33 IgG.[4] However, researchers at Celltech have been unable to reproduce these results. No cell death was observed, perhaps due to a lack of cell internalisation or simply to the short emission range of any internalised ^{111}In. It should be noted then, that even if cell internalisation does occur for

^{111}In-A33, little tumour cell killing may be observed without an intercalator to bind the radiolabelled conjugate to the DNA. Thus, even though cell internalisation may be less likely with a mono-Fab', it remains to be seen if the use of an intercalator in conjunction with an A33 Fab' (e.g. ^{111}In-Fab'-(**60**)) will exhibit cell killing properties.

5.10 CONCLUSIONS

A simple technique to effect Fab' conjugation and purification was found and exploited to form mono and tri-Fab' conjugates. It was however, found not to be possible to cleanly form a tri-Fab', without associated production of di, and mono-Fab' impurities. The nature of the tri-maleimide used for conjugation appeared to have little effect on the nature of products produced, but it did become apparent that maleimides should be handled with care, to guard against unwanted maleimide base hydrolysis or reaction with amines.

Compared to a single antibody, the tri-Fab's produced showed a significant improvement in immunoreactivity and in antigen binding strength, resulting in a greatly increased residence lifetime at the antigen binding site. It would also appear that the combination of this improved tumour binding affinity, the better tumour to non-tumour ratio and the faster clearance rate observed for tri-Fab' conjugates compared to a single antibody, should lead to significant success in radioimmunotherapy. Preliminary experiments in animals have shown this to be the case (see Sections 5.7 & 5.8).

The use of intercalators to bind to tumour cell DNA is in the process of being tested *in vitro*, although no results are as yet available for the four ^{111}In complexes of Figure 5.8. It is most likely that the use of an intercalator in conjunction with an A33 tri-Fab' which is capable of antigen cross-linking (e.g. the A33 tri-Fab' of (**61**)) is required for efficient tumour cell killing, although this remains to be established.

5.11 BUFFERS AND SOLUTIONS USED

0.1 M Acetate-Citrate-EDTA pH 6.0 buffer

Sodium acetate	41.02 g
Na_4 EDTA	2.10 g
H_4 EDTA	1.62 g
Citric acid	1.50 g
Water	5 litres

PBS pH 7.4 buffer

NaCl	9.00 g
Na_2HPO_4	5.96 g
NaH_2PO_4	1.25 g
EDTA	372 mg
Water	1 litre

Antibody conjugate Buffer

Tris	6.05 g
NaCl	2.92 g
Casein	1.00 g
Tween 20	0.1 ml
HCl	pH to 7.0
Water	to 500 ml

5 x Concentrate Sample Buffer

Glycerol	25.0 ml
Upper-Tris	6.25 ml
SDS	7.5 g
Bromophenol Blue	4 drops
Water	to 50 ml
(β-Mercaptoethanol for reducing sample buffer	12.5 ml

Tank Buffer

Tris	7.5 g
Glycine	36 g
10% SDS	25 ml
Water	to 2.5 litres

Brilliant Blue R Stain

Methanol	800 ml
Acetic acid	140 ml
Water	to 2 litres
Brilliant Blue R-250	0.5 g

Upper Tris pH 6.8

Tris	3.0 g
10 w/v SDS	2 ml
HCl	to pH 6.8
Water	to 50 ml

Substrate Reaction Mixture

Substrate Buffer	30 ml
0.44% v/v H_2O_2	300 µl
TMB	0.3 mg

1/2500 B.72.3-HRPO antibody conjugate

5 µl of B72.3-HRPO + 12.5 ml of antibody conjugate buffer.

5.12 REFERENCES

1 D. Colcher, P. Horan-Hand, M. Nuti, J. Schlom, *Proc. Nat. Acad. Sci. U.S.A.*, 1981, **78**, 3199.

2 Unpublished work from Celltech Ltd.

3 S. Welt, C. R. Divgi, F. X. Real, S. D. Yeh, P. Garin-Chesa, C. L. Finstad, J. Sakamoto, A. Cohen, E. R. Sigurdson, N. Kememy, E. A. Carswell, H. F. Oettgen, and L. J. Old, *J. Clin. Oncol.*, 1990, **8(11)**, 1894.

4 Private communication from Celltech.

5 R. W. Howell, D. V. Rao, D. Y. Hon, V. R. Narra, and K. S. R. Sastry, *Radiation Research*, 1991, **126**, 282.

Chapter 6

Experimental

6.1 SOLVENTS AND INSTRUMENTATION

6.1.1 Solvents

All reactions, except those employing HBr in glacial acetic acid or water as the solvent, were done under dry nitrogen. Most of the solvents used were either distilled before use from the appropriate drying agent, or used from Sure-Seal bottles. Triethylamine and N-methylmorpholine were distilled from calcium hydride, methanol from magnesium methoxide, tetrahydrofuran from sodium benzophenone, and toluene from sodium. Water refers to that purified by the 'Purite$_{STILL}$ plus' system.

6.1.2 Instrumentation

HPLC analysis was performed using a Varian 9010 / 9065 Polychrom system, whilst preparative HPLC was performed on a Varian Vista 5500 / 9050 system using unless otherwise stated, Rainin's reverse phase column Dynamax C18 (21.4 x 250 mm) at 10 ml / min. The solvents employed for HPLC were:

A = H_2O / 0.1% trifluoroacetic acid B = CH_3CN / 0.1% trifluoroacetic acid

Column chromatography was carried out using neutral alumina Merck Art 1077 (0.063-0.200 mm) which had previously been treated with ethyl acetate, or using gravity silica (Merk Art 7734). Alumina t.l.c was performed using Merck Art 5554 plates.

Infra red spectra were run as a thin film on a Perkin Elmer 1600 Series FTIR and U.V. spectra were run on a Kontron Instruments Uvikon 930. ^{1}H and ^{13}C spectra were recorded on either a Brüker AC250 or on a Varian XL200, 250 or VXR-400. The Brüker AC250 operating at 62.90 MHz was used for obtaining ^{31}P spectra whilst ^{89}Y NMR spectra were run on a Brüker AMX 500 at 24.5 MHz with a 90° pulse, and a 30 second delay.

Mass spectra were recorded with a VG 7070E mass spectrometer running in either DCI or FAB mode with ammonia as the impingent gas for DCI, and glycerol as the matrix for FAB analyses. A VG electrospray mass spectrometer was also used.

Biodistribution studies were performed as previously reported.[1]

6.2 KINETICS OF ASSOCIATION

Incubations were effected at 310 K and pH 6.5 (0.2 mol dm^{-3} NH_4OAc) with a ligand concentration of 5 μmol dm^{-3}. Typically, a 1 μl aliquot (67 μCi) of high quality $^{90}Y^{3+}$ (Amersham) was added to a solution containing 25 μl of a 50 μmol dm^{-3} solution of the ligand, 125 μl of a 0.4 mol dm^{-3} solution of NH_4OAc, and 99 μl of MilliQ water, giving an overall volume of 250 μl. 10 μl sample was removed at various time intervals up to 1 hour, and added to a solution containing 5 μl of 500 μmol dm^{-3} DTPA (500 fold excess) and 85 μl of 0.15 mol dm^{-3} NH_4OAc (pH 6.8). Under these conditions dissociation is stopped, and any dissociated ^{90}Y is immediately scavenged by the DTPA. (Bound ^{90}Y has been shown in control experiments to be stable for at least 24 hours, with respect to trans-complexation by DTPA, in the pH range 5 - 6.5).

Samples were analysed by anion exchange HPLC (Poros Q/M : eluent 0.15 mol dm^{-3} NH_4OAc, pH 6.8 run at 2 cm^3 per minute). T_R $[^{90}Y.DTPA]^{2-}$ = *ca* 2 min., whilst the other complexes tested elute with T_R = *ca* 1 min. A Beckman 170 radioisotope detector was used to detect ^{90}Y and ^{153}Gd in HPLC association and dissociation measurements.

6.3 KINETICS OF DISSOCIATION

75 µl samples of a 40 mmol dm^{-3} preformed yttrium-90 or gadolinium-153 complex solution were added to 1.5 cm^3 solutions of pH 1.0, 1.5, and 2.0 glycine buffers (0.1 mol dm^{-3}). This gave a final concentration of the complex of 2 mmol dm^{-3}. Samples were incubated at 37°C and fractions (20 µl) removed at regular time intervals and added to a fifty fold excess (4 µl of 500 mmol dm^{-3}) of DTPA to scavenge any dissociated cations. These samples were diluted in HPLC running buffer (0.15 mol dm^{-3} NH_4OAc, pH 6.8) to 100 µl, and the extent of dissociation determined by HPLC using a Poros Q/M column at 2 cm^3 min^{-1}.

6.4 SYNTHETIC PROCEDURES

6.4.1 Chapter 2

1,3,6,8-tetrakis-(4-tolylsulphonyl)-3,6-azaoctane-1,8-diamine - **(1)**.

To triethylenetetramine (10.00 g, 68.38 mmol), and mesh potassium carbonate (14.58 g, 308.1 mmol) in 400 cm^3 of water at 80°C was added tosylchloride (57.49 g, 301.6 mmol) in small portions over a period of 3 hours. The temperature was maintained overnight, followed by a cooling of the solution to effect precipitation. The solids were filtered off, washed with methanol, water, and diethylether, followed by drying in vacuo to yield the title compound **(1)**, as a white powder (14.72 g, 86%). mp 209 - 211°C.

1,4,7,10-tetrakis-(toluene-p-sulphonyl)-1,4,7,10-tetra-azacyclododecane - **(2)**.

To a stirred solution of **(1)** (44.43 g, 58.23 mmol) and mesh potassium carbonate (16.72 g, 121.0 mmol) in 700 ml of anhydrous DMF under nitrogen was added ethylene glycol ditosylate (21.84 g, 59.28 mmol, in 100 cm^3 of dry DMF) dropwise

over a period of 3 hours. The solution was left overnight at room temperature, followed by 3 hours at 70°C and evaporation of the solvent under vacuum. The resulting residue was taken up into 100 cm^3 of water and 100 cm^3 of dichloromethane, and the aqueous layer extracted (2 x 50 cm^3) with dichloromethane. The organic fractions were combined, dried (K_2CO_3) and the solvent evaporated under vacuum. The resulting residues were shaken vigorously in hot toluene (500 cm^3), and allowed to cool yielding a white precipitate which was filtered off, washed (40 cm^3 cold toluene) and dried in vacuo to yield the title compound (27.80 g, 61%). $\delta_H(CDCl_3)$ 2.40 (12 H, s, CH_3), 3.37 (16 H, s, NCH_2), 7.30, 7.64 (16 H, m, ArH).

1,4,7,10-tetra-azacyclododecane - **(3)**.

(2) (15.62 g, 19.80 mmol) was refluxed in 25 cm^3 of concentrated sulphuric acid under nitrogen at 110°C for approximately 40 hours to give a black solution. To the cooled solution was slowly added water (20 cm^3), potassium hydroxide pellets (to pH ≥ 13) and ethanol (150 cm^3). Solids were removed by filtration and the solvent removed under vacuum to yield yellow residues which were acidified to pH < 2 with 1 mol. dm^{-3} HCl. To this was added dichloromethane (30 cm^3) and the aqueous layer extracted (2 x 30 cm^3) with dichloromethane. The organic fractions were discarded, the pH of the aqueous layer increased to ≥13 (KOH pellets), and the free amine extracted into chloroform (5 x 20 cm^3) to yield on drying and evaporation of the solvent, the title compound as a white solid (2.71 g, 79%). $\delta_H(CDCl_3)$ 2.02 (16 H, s, CH_2), 1.56 (4 H, s, NH). $\delta_C(CDCl_3)$ 44.8 (8 C, CH_2).

N-(4-Aminobutyl)-4-methoxybenzenesulfonamide - **(4)**.

4-Methoxy benzenesulphonyl chloride (7.62 g, 36.9 mmol) was added to a stirred solution of 1,4-diaminobutane (22.46 g, 254.8 mmol) in dichloromethane (400 cm^3) over a period of 45 minutes. The solution was stirred under nitrogen overnight, the solvent removed under reduced pressure, and the residues taken up in $KOH_{(aq)}$ to raise the pH to 13. The aqueous phase was extracted exhaustively with chloroform, the

organic fractions combined, dried ($MgSO_4$) and the solvent removed under reduced pressure to yield the title compound as a thick pale yellow oil (8.38 g, 88%). I.R. (aromatic C=C) 1597 cm^{-1}, 1498 cm^{-1}, (NH_2) 1578 cm^{-1}, (S=O) 1320 cm^{-1}, 1154 cm^{-1}. Found: M^+, 258.103. $C_{11}H_{18}N_2O_3S$ requires M^+, 258.104. δ_H(DMSO) 1.37 (2 H, p, J 6.8 Hz, $CH_2CH_2NH_2$), 1.39 (2 H, p, J 6.5 Hz, $CH_2CH_2NHSO_2$), 2.48 (2 H, t, J 6.5 Hz, CH_2NH_2), 2.72 (2 H, t, J 6.6 Hz, CH_2NHSO_2), 3.4-4.0 (3 H, br s, NH_2, NH), 3.84 (3 H, s, CH_3O), 7.12 (2 H, d, J 8.8 Hz, $CHCSO_2$), 7.77 (2 H, d, J 9.1 Hz, $CHCOCH_3$), δ_C(DMSO) 26.9 (1 C, $CH_2CH_2NH_2$), 30.7 (1 C, $CH_2CH_2NHSO_2$), 41.5 (1 C, CH_2NH_2), 42.8 (1 C, CH_2NHSO_2), 55.8 (1 C, CH_3O), 114.5 (2 C, $CHCSO_2$), 128.9 (2 C, $CHCOCH_3$), 132.6 (1 C, CSO_2), 162.3 (1 C, $COCH_3$).

N-(4-Bromoacetamidobutyl)-4-methoxybenzenesulfonamide - **(5)**.

To a solution of the mono-hydrochloride salt of **(4)** (8.38 g, 28.4 mmol) and sodium hydroxide (2.28 g, 57.0 mmol, in 6 cm^3 of water) in 1,2-dichloroethane (300 cm^3) was added bromoacetylbromide (5.71 g, 28.3 mmol in 100 cm^3 $C_2H_4Cl_2$) dropwise, maintaining a temperature of <-10°C. The solution was stirred at <-10°C for a further 1 hour, allowed to warm to room temperature, and stirred overnight. The organic phase was washed (NaOH 0.1 mol. dm^{-3}, 2 x 25 cm^3; HCl 0.1 mol. dm^{-3}, 2 x 25 cm^3, and water 3 x 25 cm^3), dried ($MgSO_4$) and the solvent evaporated, to yield on standing, the crude yellow solid (approx. 75%). The solid was shaken vigorously in hot toluene (100 cm^3), the cloudy solvent decanted off, cooled (0°C), and any precipitated solids filtered off. These were washed with a small quantity of cold toluene, and dried *in vacuo*. The process was repeated from the addition of hot toluene until the solution no longer became cloudy on shaking with the crude solid residue. Yield (3.90 g, 36%). m.p. 75-77°C. Found: M^++1, 379.025. $C_{13}H_{19}N_2SO_4Br$ requires M^++1, 379.033. Found: N 7.40%, C 41.3%, H 5.05%. $C_{13}H_{19}N_2SO_4Br$ requires: N 7.39%, C 41.2%, H 5.05%. I.R. (CO) 1650 cm^{-1}. $\delta_H(CDCl_3)$ 1.48 (4 H, m, $(CH_2)_2CH_2NH$), 2.84 (2 H, q, CH_2NHCO), 3.17 (2 H, q, CH_2NHSO_2),

3.69 (2 H, s, CH_2Br), 3.80 (3 H, s, OCH_3), 5.77 (1 H, t, CONH), 6.92 (2 H, t, J 8.4 Hz, $CHCSO_2$), 7.07 (1 H, t, SO_2NH), 7.74 (2 H, d, J 8.3 Hz, $CHCOCH_3$). $\delta_C(CDCl_3)$ 26.0 (1 C, CH_2CH_2NHCO), 26.2 (1 C, $CH_2CH_2NHSO_2$), 28.8 (1 C, CH_2Br), 39.2 (1 C, CH_2NHCO), 42.4 (1 C, CH_2NHSO_2), 55.3 (1 C, OCH_3), 113.9 (2 C, $CHCSO_2$), 128.7 (2 C, CHCO), 130.9 (1 C, CSO_2), 162.4 (1 C, $COCH_3$), 166.2 (1 C, CO).

2-Bromo-N,N-diisobutylethanamide - **(6)**.

To a solution of diisobutylamine hydrochloride (33.14 g, 0.20 mol) and sodium hydroxide (16 g, 0.4 mol in 20 cm^3 of water) in 1,2-dichloroethane (150 cm^3) was added bromoacetylbromide (40.37 g, 0.20 mol in 25 cm^3 of 1,2-dichloroethane) dropwise maintaining a temperature of <-10°C. The solution was stirred at <-10°C for a further 1 hour, allowed to warm to room temperature and stirred overnight. The organic phase was washed (NaOH 0.1 mol. dm^{-3}, 2 x 25 cm^3; HCl 0.1 mol. dm^{-3}, 2 x 25 cm^3 and water 3 x 25 cm^3), dried ($MgSO_4$), and the solvent evaporated to yield a colourless viscous oil (36.03 g, 72%). Found: M^++1, 250. $C_{10}H_{20}NBrO$ requires M^++1, 250. Found: C 47.7%, H 8.2%, N 5.45%. $C_{10}H_{20}NBrO$ requires C 48.0%, H 8.00%, N 5.60%. I.R. (CON) 1655 cm^{-1}. $\delta_H(CDCl_3)$ 0.02 (6 H, d, J 6.6 Hz, CH_3), 0.08 (6 H, d, J 6.4 Hz, CH_3), 1.15 (2 H, n, J 7.0 Hz, CH), 2.32 (4 H, d, J 7.6 Hz, NCH_2), 3.07 (2 H, s, $BrCH_2$).

Molybdenum tricarbonyl-1,4,7,10-tetraazacyclododecane complex - **(7)**.[2]

1,4,7,10-tetraazacyclododecane (1.64 g, 6.21 mmol), and molybdenum hexacarbonyl (1.64 g, 6.21 mmol) were refluxed in dibutylether under argon at 160°C for 2 hours. The bright yellow solids were filtered off under argon, and dried *in vacuo*, to give the title compound (2.08 g, 95%). This was used directly in the next step.

4-(4-Methoxyphenylsulfonamido)butylcarbomylmethyl-1,4,7,10-tetraazacyclo dodecane - **(8)**.

To the molybdenumtricarbonyl-12N_4 complex **(7)** (3.55 g, 10.1 mmol) in degassed DMF (50 cm^3) under argon was added **(5)** (3.83 g, 10.1 mmol), and a slight excess of mesh potassium carbonate (1.79 g, 13.0 mmol) and the solution heated for 1-2 hours at 80°C. The solvent was removed under reduced pressure (10^{-2} mmHg), and the black residue taken up into 10% v/v HCl and left open to the air overnight. The pH was adjusted to 14 (KOH pellets) and the suspension filtered to give a yellow aqueous solution which was exhaustively extracted with dichloromethane, the organic fractions combined, dried (K_2CO_3), and the solvent removed to give a pale yellow oil (4.13 g, 87%). Found: M^++1, 471.268. $C_{21}N_6SO_4H_{38}$ requires M^++1, 471.276. $\delta_H(CDCl_3)$ 1.42 (4 H, br, $(CH_2)_2CH_2NHSO_2$), 2.10-3.03 (23 H, m, CH_2N ring, CH_2NHCO, NH ring, $(CH_2)(CH_2)NCH_2CO$), 3.12 (2 H, q, CH_2NHSO_2), 3.71 (3 H, s, OCH_3), 6.82 (2 H, d, J 8.8 Hz, $CHCSO_2$), 7.60 (2 H, d, J 8.80 Hz, $CHCOCH_3$), 7.92 (1 H, t, SO_2NH). $\delta_C(CDCl_3)$ 26.0 (2 C, $(CH_2)_2CH_2NH$), 37.8 (1 C, CH_2NHCO), 42.0 (1 C, CH_2NHSO_2), 44.4 (2 C, $CH_2CH_2NCH_2CO$), 46.0 (4 C, $(CH_2)_2NHCH_2CH_2NCH_2CO$), 52.5 (2 C, CH_2NCH_2CO), 55.1 (1 C, OCH_3), 58.2 (1 C, NCH_2CO), 113.5 (2 C, $CHCSO_2$), 128.3 (2 C, $CHCOCH_3$), 131.8 (1 C, CSO_2), 161.9 (1 C, $COCH_3$), 171.2 (1 C, CO).

1-(Diisobutylcarbamoylmethyl)-1,4,7,10-tetraazacyclododecane - **(9)**.

Synthesis was as described for **(8)** using the molybdenum tricarbonyl-12N_4 complex **(7)** (1.75 g, 4.97 mmol), 2-bromo-N,N-diisobutylethanamide **(6)** (1.24 g, 4.97 mmol) and fine mesh potassium carbonate (0.96 g, 6.94 mmol) to yield a colourless oil (1.43 g, 84%). Found: M^++1, 342.317. $C_{18}H_{39}N_5O$ requires M^++1, 342.324. $\delta_H(CDCl_3)$ 0.73 (6 H, d, J 7.2 Hz, CH_3), 0.77 (6 H, d, J 7.0 Hz, CH_3), 1.82 (2 H, m, CH), 2.40-3.10 (23 H, m, NCH_2 ring, NH, NCH_2CH), 3.40 (2 H, s, NCH_2CO). $\delta_C(CDCl_3)$ 19.7 (2 C, CH_3), 19.8 (2 C, CH_3), 26.0 (1 C, CH), 27.3

(1 C, CH), 45.3, 45.4, 46.7, 51.6, 52.4, 54.2, 55.2 (11 C, NCH_2 ring, NCH_2CO, NCH_2CH), 170.6 (1 C, CON).

Triethyl 10-[4-(4-Methoxyphenylsulfonamido)butylcarbamoylmethyl]-1,4,7,10-tetraazacyclododecane-1,4,7-triyltriacetate - **(10)**.

To a stirred solution of **(8)** (0.18 g, 0.38 mmol) in anhydrous ethanol (10 cm^3) under nitrogen was added mesh potassium carbonate (0.19 g, 1.34 mmol) and ethylbromoacetate (0.19 g, 1.14 mmol), and the solution refluxed at 80°C for 18 hours. The solvent was evaporated off, the residue taken up in dichloromethane, filtered, and the filtrate evaporated to yield a yellow oil. Purified by alumina column chromatography (gradient elution 0-5% methanol in dichloromethane) to yield the title compound, a pale yellow oil (0.16 g, 57%). Found: M^+, 728. $C_{33}H_{56}N_6O_{10}S$ requires M^+, 728. $\delta_H(CDCl_3)$ 1.23 (9 H, m, J 7.0 Hz, OCH_2CH_3), 1.54 (4 H, br, $(CH_2)_2CH_2NH$), 1.80-3.80 (28 H, m, NCH_2), 3.84 (3 H, s, OCH_3), 4.0-4.3 (6 H, m, OCH_2), 6.2-6.6 (1 H, br s, NHCO), 6.97 (2 H, d, $CHCSO_2$), 7.84 (2 H, d, $CHCOCH_3$), 8.23 (1 H, t, SO_2NH). $\delta_C(CDCl_3)$ 14.0 (3 C, OCH_2CH_3), 25.7, 26.3 (2 C, $(CH_2)_2CH_2NHSO_2$), 38.5 (1 C, CH_2NHCO), 42.6 (1 C, CH_2NHSO_2), 46.5-57.5 (12 C, CH_2 ring,CH_2CO_2, NCH_2CON), 55.4 (1 C, OCH_3), 61.0 (3 C, OCH_2), 113.8 (2 C, $CHCSO_2$), 129.0 (2 C, $CHCOCH_3$), 131.7 (1 C, CSO_2), 162.1 (1 C, COMe), 171.6 (1 C, CON), 172.5 (1 C, CO_2), 173.0 (2 C, CO_2).

10-[(4-Aminobutyl)carbamoylmethyl)]-1,4,7,10-tetraazacyclododecane-1,4,7-triyl triacetate - **(11)**.

To the stirred ester **(10)** (144 mg, 0.20 mmol) was added an equivalent mass of phenol and 40% v/w HBr in glacial acetic acid (20 cm^3). The solution was refluxed at 100°C overnight, and allowed to cool. The product was precipitated out by the addition of excess diethyl ether to yield the title compound, an off-white solid as its trihydrobromide salt (84 mg, 60%). Compound too hygroscopic for microanalysis. m.p. > 210°C. Found: M^++1, 472.261. $C_{20}H_{38}N_6O_7$ requires M^++1, 472.265.

$\delta_H(D_2O)$ 1.40-2.85 (4 H, m, $(CH_2)_2CH_2NH_3^+$), 2.96 (2 H, t, $CH_2NH_3^+$), 2.50-4.25 (26 H, m, CH_2 ring, CH_2CO_2, CH_2CON, CH_2NHCO).

Triethyl 10-(diisobutylcarbamoylmethyl)-1,4,7,10-tetraazacyclododecane 1,4,7-triyl triacetate - **(12)**.

As for **(10)** using **(9)** (0.15 g, 0.43 mmol), mesh potassium carbonate (0.18 g, 1.33 mmol) and ethylbromoacetate (0.21 g, 1.24 mmol) to yield the title compound, a pale yellow oil (0.18 g, 68%). Found: M^++1, 600. $C_{30}H_{57}N_5O_7$ requires M^++1, 600. $\delta_H(CDCl_3)$ 0.82 (6 H, d, J 6.6 Hz, CH_3), 0.89 (6 H, d, J 6.5 Hz, CH_3), 1.24 (6 H, t, J 7.1 Hz, CH_2CH_3), 1.25 (3 H, t, J 7.1 Hz, CH_2CH_3), 1.91 (2 H, m, CH), 2.15-3.90 (28 H, m, NCH_2), 4.05-4.30 (6 H, m, OCH_2). $\delta_C(CDCl_3)$ 13.9 (1 C, OCH_2CH_3), 14.0 (2 C, OCH_2CH_3), 19.7 (2 C, CH_3). 19.9 (2 C, CH_3), 26.1 (1 C, CH), 27.2 (1 C, CH), 46-56 (14 C, NCH_2), 60.8 (2 C, OCH_2), 61.0 (1 C, OCH_2), 170.9 (1 C, CON), 173.0 (2 C, CO_2), 173.3 (1 C, CO_2).

10-(Diisobutylcarbamoylmethyl)-1,4,7,10-tetraazacyclododecane-1,4,7-triyl triacetic acid - **(13)**.

Hydrolysis of the ester **(12)** to the carboxylic acid was brought about by dissolving it in an excess (> 3 fold) of 1mol dm^{-3} KOH solution and leaving it for 18 hours. The solution was concentrated, and salts removed by gel filtration using an Amberlite XAD16 column, to yield the colourless ligand (58%). Alternatively the ligand can be obtained as its trihydrobromide salt as for **(11)** using the ester **(12)** (120 mg, 0.20 mmol) to yield an off-white solid (65 mg, 43%). Compound too hygroscopic for accurate microanalysis. I.R. (CO_2H) 1735 cm^{-1}, (CONH) 1674 cm^{-1}. Found: M^++1, 516.333. $C_{24}H_{45}N_5O_7$ requires M^++1, 516.340. $\delta_H(D_2O$; pD=2) 0.82 (12 H, 2xd, CH_3), 1.8-2.1 (2 H, m, CH), 2.7-4.4 (28 H, m, CH_2). $\delta_H(D_2O$; pD=8) 0.76 (12 H, m, CH_3), 1.70-1.90 (2 H, m, CH), 2.00-3.23 (26 H, m, NCH_2), 3.23-3.48 (2 H, br, NCH_2CH).

Triethyl 10-[4-(4-methoxyphenylsulfonamido)butyl carbamoylmethyl]-1,4,7,10-tetraazacyclododecane-1,4,7-triyltrimethylene tri(methylphosphinate) - **(14a)**.

Diethoxymethylphosphine (1.12 g, 8.23 mmol), followed immediately by paraformaldehyde (0.28 g, 9.33 mmol) were added to anhydrous THF (30 cm^3) containing **(8)** (0.97 g, 2.06 mmol) at 100°C under nitrogen. The solution was refluxed for 18 hours at 100°C with azeotropic removal of water by 4Å molecular sieves, followed by filtration (to remove excess paraformaldehyde) and evaporation of the solvent to yield a pale yellow oil. Purification by alumina column chromatography (gradient elution 0-5% methanol in dichloromethane) afforded the title compound as a pale yellow gum (1.41 g, 82%). T.l.c. R_f 0.60 (10% MeOH in CH_2Cl_2 on alumina). Found M^++1, 831.377. $C_{33}H_{65}N_6O_{10}SP_3$ requires M^++1, 831.377. $\delta_H(CDCl_3)$ 1.2-1.3 (9 H, 2xt, J 6.6 Hz, CH_2CH_3), 1.47 (13 H, m + 2xd, ^2J 13.0 Hz, $(CH_2)_2CH_2NHSO_2$, PCH_3), 2.20-3.30 (26 H, m, NCH_2), 3.15 (2 H, q, CH_2NHSO_2), 3.79 (3 H, s, OCH_3), 4.00 (6 H, 2xp, J 6.8 Hz, OCH_2), 6.78 (1 H, t, CONH), 6.88 (2 H, d, J 8.6 Hz, $CHCSO_2$), 7.72 (2 H, d, $CHCOCH_3$), 7.91 (1 H, t, $NHSO_2$). $\delta_C(CDCl_3)$ 13.1 (3 C, ^1J 89 Hz, PCH_3), 15.9 (3 C, ^3J 5.6 Hz, OCH_2CH_3), 26.1, 25.9 (2 C, $(CH_2)_2CH_2NHSO_2$), 37.8 (1 C, CH_2NHCO), 41.8 (1 C, CH_2NHSO_2), 53.4-55.4 (12 C, CH_2 ring, NCH_2P, NCH_2CO), 54.8 (1 C, OCH_3), 59.4 (3 C, ^2J 6.7 Hz, OCH_2), 113.2 (2 C, $CHCSO_2$), 128.1 (2 C, $CHCOCH_3$), 131.7 (1 C, CSO_2), 161.6 (1 C, $COCH_3$), 1 C, CO). $\delta_P(CDCl_3)$ 52.0-52.2 (br m).

Triethyl 10-[4-(4-methoxyphenylsulfonamido) butylcarbamoylmethyl]-1,4,7,10-tetraazacyclododecane-1,4,7-triyltrimethylenetributylphosphinate) - **(14b)**.

As for **(14a)**, using **(8)** (0.21 g, 0.45 mmol), diethoxybutyl phosphine (0.36 g, 2.02 mmol) and paraformaldehyde (0.08 g, 2.66 mmol). Yielded a pale yellow gum (331 mg, 78%). T.l.c. R_f 0.70 (10% MeOH in CH_2Cl_2 on alumina). Found: M^++1, 958. $C_{42}H_{83}N_6SO_{10}P_3$ requires M^++1, 958. $\delta_H(CDCl_3)$ 0.87 (9 H, t, J 6.6 Hz, butyl CH_3), 1.26 (9 H, t, OCH_2CH_3), 1.32-1.68 (16 H, br m, $PCH_2(CH_2)_2$,

(CH_2)$_2$$CH_2NHSO_2$), 1.68-1.80, (6 H, m, PCH_2CH_2), 2.32-3.42 (28 H, m, NCH_2), 3.81 (3 H, s, OCH_3), 4.03 (6 H, m, OCH_2), 6.60 (1 H, br s, CONH), 6.91 (2 H, d, $CHCSO_2$), 7.73 (2 H, d, $CHOCH_3$), 8.22 (1 H, s, $NHSO_2$). $\delta_P(CDCl_3)$ 54.1-54.6 (br m).

Triethyl 10-[4-(4-Methoxyphenylsulfonamido) butylcarbamoylmethyl] -1,4,7,10-tetraazacyclododecane - 1,4,7-triyltrimethylenetri (benzyl phosphinate) - **(14c)**.

As for **(14a)**, using **(8)** (0.23 g, 0.49 mmol). diethoxybenzyl phosphine (0.41 g, 1.93 mmol) and paraformaldehyde (0.08 g, 2.66 mmol). Yielded a pale yellow gum (298 mg, 58%). T.l.c. R_f 0.50 (10% MeOH in CH_2Cl_2 on alumina). Found: M^++1, 1059. $C_{51}H_{77}N_6O_{10}SP_3$ requires M^++1, 1059. $\delta_H(CDCl_3)$ 1.00-1.32 (9 H, m, OCH_2CH_3), 1.32-1.56 (4 H, br m, (CH_2)$_2$$CH_2NHSO_2$), 2.30-3.40 (34 H, m, NCH_2 ring, NCH_2P, NCH_2CO, CH_2NHCO, PCH_2C, CH_2NHSO_2), 3.76 (3 H, d, OCH_3), 3.79-4.17 (6 H, m, OCH_2), 6.40-6.80 (2 H, br s, CONH, SO_2NH), 6.86 (2 H, d, J 10 Hz, $CHCSO_2$), 7.05-7.40 (15 H, m, ArH), 7.71 (2 H, d, J 10 Hz, CHCOMe). $\delta_P(CDCl_3)$ 49.1, 49.7 (2:1).

10-[(4-Aminobutyl)carbamoylmethyl]-1,4,7,10-tetraazacyclododecane - 1,4,7-triyltrimethylenetri(methylphosphinic acid) trihydrobromide salt - **(15a)**.

Method as for **(11)** using **(14a)** (160 mg, 0.19 mmol). Yield (140 mg, 89%). Compound too hygroscopic for accurate microanalysis. I.R. (CONH) 1674 cm^{-1}. Found: M^++1, 577. $C_{20}H_{47}N_6O_7P_3$ requires M^+, 576. $\delta_H(D_2O$; pD=4) 1.47 (9 H, d, ^2J 14.4 Hz, PCH_3), 1.60 (4 H, m, (CH_2)$_2$$CH_2NH_3^+$), 2.98 (2 H,t, CH_2NHCO), 3.05-3.75 (24 H, m, CH_2 ring, NCH_2P, $CH_2NH_3^+$), 4.00 (2 H, s, NCH_2CO). $\delta_C(D_2O)$ 16.9 (3 C, ^1J 89 Hz, PCH_3), 26.5, 27.5 (2 C, $CH_2CH_2NH_3^+$, CH_2CH_2NHCO), 41.3, 41.5 (2 C, $CH_2NH_3^+$, CH_2NHCO), 52-56 (11 C, CH_2 ring, NCH_2P), 57.6 (1 C, NCH_2CO), 167.8 (1 C, NHCO).

10-[(4-Aminobutyl)carbamoylmethyl]-1,4,7,10-tetraazacyclododecane - 1,4,7-triyltrimethylenetri(butylphosphinic acid) trihydrobromide salt - **(15b)**.

Method as for **(11)**, using **(14b)** (188 mg, 0.20 mmol). Yield (150 mg, 80%). Found: M^++1, 703.423. $C_{29}H_{65}N_6P_3O_7$ requires M^++1, 703.421. $\delta_H(CD_3OD)$ 0.96 (9 H, t, J 6.74 Hz, CH_3), 1.30-2.50 (22 H, m, $P(CH_2)_3$, $(CH_2)_2CH_2NH_3^+$), 2.90-4.50 (28 H, m, NCH_2).

10-[(4-Aminobutyl)carbamoylmethyl]-1,4,7,10-tetraazacyclododecane-1,4,7-triyltrimethylenetri(benzylphosphinic acid) trihydrobromide salt. **(15c)**.

Method as for **(11)**, using **(14c)** (166 mg, 0.16 mmol). Yield (138 mg, 84%). Compound too hygroscopic for accurate microanalysis. Found: M^+, 804.366. $C_{38}H_{59}N_6P_3O_7$ requires M^+, 804.362. $\delta_H(CD_3OD)$ 1.55-1.90 (4 H, br, $(CH_2)_2CH_2NH_3^+$), 2.70-4.10 (34 H, m, NCH_2, PCH_2C), 7.20-7.55 (15 H, m, ArH).

10-[4-(4-Methoxyphenylsulfonamido)butylcarbamoylmethyl]-1,4,7,10-tetra-aza cyclododecane-1,4,7-triyltrimethylenetri(methylphosphinic acid) - **(16)**.

Base hydrolysis of the ester **(14a)** as for **(13)** and purified by reverse phase HPLC (t=0min. 90% A 10% B, t=30min. 25% A 75% B, 254nm T_R 16.9 min.). I.R. (CONH) 1626 cm^{-1}. Found M^++1, 747.282. $C_{27}H_{53}N_6O_{10}SP_3$ requires M^++1, 747.283. $\delta_H(D_2O)$ 0.82-1.09 (9 H, 2xd, PCH_3), 1.15 (4 H, br s, $(CH_2)_2CH_2NHSO_2$), 1.90-2.70 (24 H, br m, CH_2N ring, NCH_2P, NCH_2CO), 2.87 (4 H, br s, CH_2NHSO_2, $CH2NHCO$), 3.60 (3 H, s, OCH_3), 6.80 (2 H, d, $CHCSO_2$), 7.43 (2 H, d, $CHCOCH_3$). $\delta_C(D_2O$; pD=14) 19.5 (2 C, ^1J 89 Hz, PCH_3), 19.8 (1 C, ^1J 89 Hz, PCH_3), 28.9 (1 C, CH_2CH_2NHCO), 31.1 (1 C, $CH_2CH_2NHSO_2$), 41.5 (1 C, CH_2NHCO), 47.4 (1 C, CH_2NHSO_2), 53.4-61.0 (12 C, NCH_2 ring, CH_2P, NCH_2CO), 58.0 (1 C, OCH_3), 116.3 (1 C, $CHCSO_2$), 130.8 (1 C, $CHCOCH_3$), 137.9 (1 C, CSO_2), 163.0 (1 C, $COCH_3$), 175.6 (1 C, CONH). $\delta_P(D_2O$; pD=4) 43.0, 35.4 (1:2).

Triethyl 10-(diisobutylcarbamoylmethyl)-1,4,7,10-tetraazacyclododecane-1,4,7-triyltrimethylenetri(methylphosphinate) - **(17)**.

Synthesis as for **(14a)** using diethoxymethyl phosphine (0.81 g, 5.95 mmol), paraformaldehyde (0.25 g, 8.32 mmol) and **(9)** (0.50 g, 1.47 mmol) yielding the title compound as a pale yellow gum (0.58 g, 56%). Found: M^++1, 702.426. $C_{30}H_{66}N_5O_7SP_3$ requires M^++1, 702.426. $\delta_H(CDCl_3)$ 0.80 (6 H, d, J 6.5 Hz, CH_3), 0.86 (6 H, d, J 6.5 Hz, CH_3), 1.25 (9 H, t, J 7.1 Hz, CH_2CH_3), 1.49 (9 H, d, ^{2}J 13.7 Hz, PCH_3), 1.91 (2 H, m, CH), 2.20-3.80 (28 H, m, NCH_2), 4.01 (6 H, p, OCH_2). $\delta_C(CDCl_3)$ 13.6 (3 C, ^{1}J 90 Hz, PCH_3), 16.7 (3 C, J 5.4 Hz, OCH_2CH_3), 20.0 (4 C, CH_3), 26.3, 27.6 (2 C, CH), 50-57 (14 C, NCH_2), 60.1 (3 C, ^{2}J 6.1 Hz, OCH_2), 170.5 (1 C, CON). $\delta_P(CDCl_3)$ 52 (br m).

10-(Diisobutylcarbamoylmethyl)-1,4,7,10-tetraazacyclododecane-4,7,10-triyl trimethylenetri(methylphosphinic acid) - **(18)**.

An excess of 1mol dm^{-3} aqueous KOH solution was added to the phosphinate ester **(17)**, and the solution shaken to dissolve all of the compound. The solution was left overnight, the pH lowered to 5 by addition of acetic acid, and the solution passed down a H^+ cation exchange resin column. The solvent was removed to yield the title compound, as a clear very pale yellow solid (43%) Found: M^++1, 618.330. $C_{24}H_{54}N_5O_7P_3$ requires M^++1, 618.331. m.p. > 200°C. $\delta_H(D_2O)$ 0.55-0.85 (12 H, m, CH_3), 0.92-1.22 (9 H, m, PCH_3), 1.68-1.95 (2 H, m, CH), 2.25-3.50 (20 H, m, NCH_2 ring, NCH_2CH), 2.92-3.17 (6 H, br m, NCH_2P), 3.17-3.35 (2H, br s, CH_2CON). $\delta_P(D_2O$; pD=4) 27.8, 26.6 (2 : 1).

Yttrium complex - $[Y.(13)]^+$.

To **(13)** (142 mg, 0.28 mmol) in 10 cm^3 of water at pH 1.5 (HCl) was added yttrium oxide (31 mg, 0.14 mmol). The solution was heated at 110°C for 18 hours after which the pH was raised to 6 (aqueous KOH) and the solution heated at reflux for a further 45 minutes. The solution was concentrated, and salts removed by gel filtration using

an Amberlite XAD16 column, to yield the colourless complex (137 mg, 72%). Found: M^+, 601.215. $C_{24}H_{42}N_5O_7Y$ requires M^+, 601.214. m.p. > 200°C. $\delta_H(D_2O)$ 0.78 (6 H, d, J 6.9 Hz, CH_3), 0.82 (6 H, d, J 6.9 Hz, CH_3), 1.75-2.04 (2 H, m, CH), 2.08-4.10 (28 H, m, NCH_2). $\delta_C(D_2O)$ 22.0, 22.2 (4 C, CH_3), 28.9, 29.7 (2 C, CH), 48.0, 48.1 (2 C, NCH_2CH), 55-60-(8 C, CH_2 ring), 64.5-66.5 (1 C, NCH_2CON), 68.7 (3 C, NCH_2CO_2), 177.8 (1 C, CON), 183.0 (3 C, CO_2). $\delta_Y(D_2O)$ +111.3 ppm.

Gadolinium Complex - [Gd.(**15a**)]$^+$.

Synthesis as for [Y.(**13**)]$^+$ using (**15a**) (33.3 mg, 0.037 mmol) and Gd_2O_3 (8.0 mg, 0.022 mmol) to yield the colourless complex (27.0 mg, 73%). Sample found to be ninhydrin positive. I.R. (CONH) 1648 cm^{-1}, (NH_3^+) 1572 cm^{-1} (cf (CONH free ligand) 1674 cm^{-1}).

Yttrium complex - [Y.(**16**)].

Synthesis as for [Y.(**13**)]$^+$ using (**16**) (289 mg, 0.39 mmol), and yttrium oxide (53 mg, 0.23 mmol). Yield (367 mg, 85%). m.p. > 200°C. I.R. (CONH) 1626 cm^{-1} (cf (CONH) 1679 cm^{-1} free ligand.). Found (FAB): M^+, 832.160. $C_{27}H_{50}N_6O_{10}P_3SY$ requires M^+, 832.158. $\delta_H(D_2O)$ 1.24-1.60 (13 H, m, PCH_3, $(CH_2)_2CH_2NHSO_2$), 2.19-2.70 (16 H, br m, CH_2 ring), 2.20-2.93 (2 H, m, CH_2NHCO), 2.93-3.64 (12 H, br m, CH_2NHCO, CH_2NHSO_2, NCH_2P, NCH_2CO), 3.77 (3 H, s, OCH_3), 7.01 (2 H, d, J 8.6 Hz, $CHCSO_2$), 7.68 (2 H, d, J 8.6 Hz, $CHCOCH_3$). $\delta_C(D_2O)$ 18.8 (3 C, ^1J 106 Hz, PCH_3), 26.1 (1 C, CH_2CH_2NHCO), 28.6 (1 C, $CH_2CH_2NHSO_2$), 42.4 (1 C, CH_2NHCO), 44.9 (1 C, CH_2NHSO_2), 51-62 (12 C, CH_2 ring, NCH_2P, NCH_2CO), 56.2 (1 C, OCH_3), 117.4 (2 C, $CHCSO_2$), 131.7 (2 C, $CHCOCH_3$), 132.8 (1 C, CSO_2), 165.3 (1 C, $COCH_3$), 183.9 (1 C, CONH). $\delta_P(D_2O)$ 44.63 : 43.13 : 42.91 ratio 1:1:1. J_{Y-P} 5.1 Hz. $\delta_Y(H_2O)$ +151.9 ppm.

Indium complex - [In.(**16**)].

(16) (46.5 mg, 0.0627 mmol) and indium chloride (13.9 mg, 0.0627 mmol) were dissolved in pH 5.5 acetate buffer to form the complex. Purification as for $[Y.(\mathbf{13})]^+$. Yield (43%). m.p. > 200°C. I.R. (CONH) 1636 cm^{-1} (cf (CONH) 1654 cm^{-1} free ligand.). Found (FAB): M^+, 858. $C_{27}H_{50}N_6O_{10}P_3SIn$ requires M^+, 858. $\delta_H(D_2O)$ 1.40-1.60 (13 H, m, PCH_3, $(CH_2)_2CH_2NHSO_2$), 2.60-3.60 (30 H, br m, CH_2 ring, CH_2NHCO, CH_2NHSO_2, NCH_2P, NCH_2CO), 3.92 (3 H, s, OCH_3), 7.18 (2 H, d, $CHCSO_2$), 7.83 (2 H, d, $CHCOCH_3$).

6.4.2 Chapter 3

N-(5-carboxypentyl) maleamic acid - (**19**).

To 300 cm^3 of diglyme containing dissolved maleic anhydride (26.84 g, 0.274 mol), was added 6-aminohexanoic acid (35.90 g, 0.274 mol). The suspension was stirred at room temperature for 3 hours followed by slow heating over 1 hour to 150°C to effect complete solvation of all solids. The solution was allowed to cool slowly to room temperature, and left overnight at -10°C to afford pale brown solids. The precipitate was filtered off, washed (diglyme then water), and dried *in vacuo* to yield the title compound as a pale brown powder (33.6 g, 54% yield). (Can be recrystallised from hot acetone to yield a white powder). m.p. 159-160°C. Found: N 5.99%, C 52.39%, H 6.59%. $C_{10}H_{15}NO_5$ requires: N 6.11%, C 52.19%, H 6.75% Found: M^++1, 230. $C_{10}H_{15}NO_5$ requires M^++1, 230. δ_H(DMSO) 1.32 (2 H, p, $CH_2(CH_2)_2CO_2H$), 1.48 (4 H, m, $CH_2CH_2CH_2CH_2CO_2H$), 2.21 (2 H, t, J 7.2 Hz, CH_2CO_2H), 3.19 (2 H, q, J 6.5 Hz, CH_2NH), 6.20, 6.27, 6.41, 6.47 (2 H, 4xs, CH=CH), 9.21 (1 H, t, NH). δ_C(DMSO) 24.4 (1 C, $CH_2(CH_2)_2CO_2H$), 26.2 (2 C, $CH_2CH_2CH_2CH_2CO_2H$), 28.3 (1 C, CO_2H), 33.8 (1 C, CH_2NH), 132.0, 133.6 (2 C, CH=CH), 165.5, 165.8 (2 C, COCH=CHCO), 174.7 (1 C, CH_2CO_2H).

6-Maleimidohexanoic acid - **(20)**.

(19) (33.57 g, 0.146 mol) and sodium acetate (6.5 g), were heated overnight in 75 cm^3 of acetic anhydride under nitrogen at 50°C. The solution was then poured into 600 cm^3 of water, heated at 75°C for 2-3 hours, concentrated to 150 cm^3, and left at -10°C overnight to yield a white powder which was filtered off and retained. The remaining solution was acidified to pH 1-2 (H_2SO_4), extracted with EtOAc (6 x 50 cm^3), and the EtOAc removed to yield a brown crude oil. This was then taken up into $CHCl_3$ / 5% AcOH, filtered through a 1" plug of alumina, and the solvents removed to give a pale yellow oil. This was then heated / melted in 10 cm^3 of EtOAc / 5% AcOH, and left at -10°C to yield yet more of the title compound. Yield 5.2 g, 17%, m.p. 81-84°C (cf. lit. 89-90°C [3]), R_f 0.64 (MeOH / $CHCl_3$ 1:1 on alumina). Found: N 6.20%, H 5.90%, C 56.68%. $C_{10}H_{13}NO_4$ requires N 6.63%, H 6.20%, C 56.86%. $\delta_H(CDCl_3)$ 1.36 (2 H, m, $CH_2(CH_2)_2CO_2H$), 1.63 (4 H, m, $CH_2CH_2CH_2CH_2CO_2H$), 2.36 (2 H, t, J 7.4 Hz, CH_2CO_2H), 3.53 (2 H, t, J 7.1 Hz, CH_2N), 6.72 (2 H, s, CH=CH), 11.5 (1 H, br s, CO_2H). $\delta_C(CDCl_3)$ 23.9 (1 C, $CH_2(CH_2)_2CO_2H$), 26.0 (1 C, $CH_2CH_2CO_2H$), 28.0 (1 C, CH_2CH_2N), 33.6 (1 C, CH_2CO_2H), 37.4 (1 C, CH_2N), 133.9 (2 C, CH=CH), 170.8 (2 C, COCH), 179.5 (1 C, CO_2H).

N-(4-Carboxycyclohexylmethyl)-maleimide - **(21)**.[4]

A solution of N-(4-carboxycyclohexylmethyl)-maleamic acid (7.72 g, 30.2 mmol), and sodium acetate (1.20 g) was heated for 2 hours at 50°C in acetic anhydride (20 cm^3) under nitrogen. The solution was then poured into 250 cm^3 of water and heated at 70°C for 2-3 hours until a clear brown solution was obtained (complete decomposition of remaining anhydride). The solution was concentrated to 50 cm^3 and left overnight to yield white crystals which were filtered off, washed with cold water, and dried *in vacuo* (0.8 g, 11%· cf lit. 34%). m.p. 143-145°C. $\delta_H(CDCl_3)$ 0.85 - 2.35 (10 H, m, cyclohexyl H), 3.38 (2 H, d, J 6.84 Hz, NCH_2), 6.70 (2 H, s, HC=CH). $\delta_C(CDCl_3)$ 28.0 (1 C, $CH_2CH_2CHCO_2H$), 29.6 (2 C, CH_2CHCO_2H), 36.3 (1 C,

$CHCH_2N$), 42.5, 43.6 (2 C, $CHCO_2H$, NCH_2), 134.0 (2 C, C=C), 171.0 (2 C, $COCH$=CH), 180.0 (1 C, CO_2H).

Succinimidyl 4-maleimidobutyrate - **(22)**.

To a solution of 4-maleimidobutyric acid (0.664 g, 3.66 mmol) and N-hydroxy succinimide (0.417 g, 3.66 mmol) in DMF (10 cm^3) at 0°C was added a solution of DCC (0.923 g, 4.48 mmol) in 20 cm^3 of DMF also at 0°C. The solution was stirred under nitrogen at 0°C for four hours and then at room temperature overnight. The solvent was removed and the residues purified by silica chromatography using 70% ethyl acetate and 30% hexane as the solvent to yield a white solid, (0.964 g, 95%). Silica T.l.c. R_f 0.4 (70% ethyl acetate and 30% hexane). Found: N 9.92%, C 51.61%, H 4.64%. $C_{12}H_{12}N_2O_6$ requires: N 10.00%, C 51.42%, H 4.31%. $\delta_H(CDCl_3)$ 1.93 (2 H, p, J 7.20 Hz, $CH_2CH_2CO_2$), 2.57 (2 H, t, J7.50 Hz, CH_2CO_2), 2.76 (4 H, s, CH_2CON), 3.54 (2 H, t, J 6.91Hz, CH_2N), 6.65 (2 H, s, CH). $\delta_C(CDCl_3)$ 23.27 (1 C, $CH_2CH_2CO_2$), 25.34 (2 C, CH_2CON), 28.08 (1 C, CH_2CO_2), 36.37 (1 C, CH_2N), 133.96 (2 C, CH), 167.70, 169.09, 170.51 (5 C, CO).

Succinimidyl 6-maleimidohexanoate - **(23)**.

As **(22)** using 6-maleimidohexanoic acid (0.504 g, 2.37 mmol), N-hydroxy succinimide (0.272 g, 2.37 mmol), and DCC (0.584 g, 2.83 mmol), to yield a white solid, (0.420 g, 57%). Silica T.l.c. R_f 0.4 (70% ethyl acetate and 30% hexane). $\delta_H(CDCl_3)$ 1.41 (2 H, m, $CH_2(CH_2)_2CO_2$), 1.64 (2 H, m, $CH_2CH_2CO_2$), 1.78 (2 H, p, J 7.9Hz, CH_2CH_2N), 2.61 (2 H, t, J 7.4 Hz, CH_2CO_2) 2.84 (4 H, s, CH_2CON), 3.58 (2 H, t, J 7.1Hz, CH_2N), 6.70 (2 H, s, CH). $\delta_C(CDCl_3)$ 23.99 (1 C, $CH_2(CH_2)_2CO_2$), 25.53 (1 C, $CH_2CH_2CO_2$), 25.75 (1 C, CH_2CH_2N) 27.97 (1 C, CH_2CO_2), 30.70 (2 C, $(CH_2)_2CON$), 37.39 (1 C, CH_2N), 134.01 (2 C, CH), 168.17, 169.16, 170.62 (5 C, CO).

Mono-maleimide functionalised ligand - **(24)**.

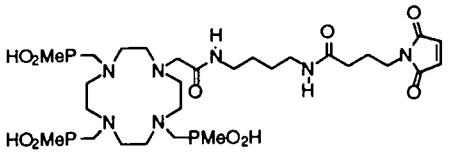

To **(15b)** (29.2 mg, 0.030 mmol), in dry DMSO (0.4 cm^3), was added N-methyl morpholine (18.0 mg, 0.178 mmol) followed by **(22)**. The solution was left under nitrogen overnight , and purified by reverse phase HPLC (t=0min. 90% A 10% B, t=20min. 25% A 75% B, 300nm), to yield a colourless solid T_R 10.7 min., 13.3 mg, 38%. Found: (Electrospray) M^++1, 742. $C_{28}H_{54}N_7O_{10}P_3$ requires M^++1, 742. $\delta_H(D_2O)$ 1.29 (6 H, d, ^2J 14 Hz, PCH_3), 1.33 (3 H, d, ^2J 14 Hz, PCH_3), 1.38 (4H, br, $(CH_2)_2CH_2NH$), 1.75 (2 H, p, 6.8Hz, CH_2CH_2CO), 2.10 (2 H, t, J 6.7 Hz, CH_2CH_2CO), 2.9-3.5 (26 H, m, CH_2N, CH_2NH), 3.43 (2 H, t, CH_2NCO), 3.68 (2 H, br, NCH_2CO), 6.70 (2 H, s, CH=CH).

(2S)-Lysine methylester dihydrochloride - **(25)**.[5]

Acetyl chloride (4 cm^3) was carefully added to a solution of (2S)-lysine dihydrochloride (19.96 g, 91.10 mmol) in anhydrous methanol (200 cm^3) under nitrogen and refluxed at 80°C. The volume of the solvent was reduced to 50 cm^3 under reduced pressure to afford precipitation of a white solid which was filtered off, washed with cold methanol, and dried *in vacuo* (15.93 g, 75%). m.p. 212-213°C. (Lit. value: 214-215°C.) $\delta_H(D_2O)$ 1.47 (2 H, p, $CH_2CH_2NH_3^+$), 1.67 (2 H, p, J 7.7 Hz, CH_2CH_2CH), 1.94 (2 H, m, CH_2CH), 2.96 (2 H, t, J 7.5 Hz, $CH_2NH_3^+$), 3.79 (3 H, s, OCH_3), 4.12 (1 H, t, J 6.5 Hz, CH). $\delta_C(D_2O)$ 24.4 (1 C, CH_2CH_2CH), 29.1 (1 C, $CH_2CH_2NH_3^+$), 32.1 (1 C, CH_2CH), 41.9, 55.5, 56.5, (3 C, $CH_2NH_3^+$, $CHNH_3^+$, OCH_3), 173.4 (1 C, CO_2).

(2S)-N-(2-Aminoethyl)-2,6-diaminohexanamide - **(26)**.[5]

(2S)-Lysine methylester-dihydrochloride **(25)** (8.35 g, 35.8 mmol) was added in small batches to 100 cm^3 of ethylenediamine at 90°C. The solution was heated at 120°C for

18 hours and the ethylenediamine removed by distillation under reduced pressure (10^{-2} mmHg). The residue was taken up into aqueous sodium hydroxide (4 mol. dm^{-3}, 25 cm^3), the solvent evaporated, and the subsequent residue treated with dichloromethane (100 cm^3), filtered, and the solvent removed under reduced pressure to yield a clear viscous pale yellow oil (6.28 g, 93%). Found: M^++1, 189. $C_8H_{20}N_4O$ requires M^++1, 189. $\delta_H(D_2O)$ 1.15-1.75 (6 H, m, $(CH_2)_3CH$), 2.63 (2 H, t, CH_2NH_2), 2.68 (2 H, t, CH_2NH_2), 3.22 (2 H, t, CH_2NH), 3.30 (1 H, t, CH). $\delta_C(CDCl_3)$ 21.9 (1 C, CH_2CH_2CH), 31.1 (1 C, $CH_2CH_2NH_2$), 34.0 (1 C, CH_2CH), 40.1, 40.3, 40.8, 54.0 (4 C, CH_2NH_2, CH, CH_2NH), 174.9 (1 C, CO).

(5S)-3-Azanonane-1,5,9-triamine - **(27)**.[5]

(2S)-N-(2-Aminoethyl)-2,6-diaminohexanamide **(26)** (6.20 g, 32.9 mmol) was heated to reflux in 1.0 mol. dm^{-3} borane-THF complex (100 cm^3) overnight. Excess borane was quenched (100 cm^3 of methanol) and solvents evaporated to leave residues which were refluxed in 6 mol. dm^{-3} HCl (70 cm^3) for 3 hours. Evaporation of the solvent, entraining in methanol (4 x 25 cm^3), followed by adjustment of the pH to 13 (KOH solution) and exhaustive extraction into chloroform gave upon evaporation of the chloroform, the free amine as a bright clear viscous yellow oil (4.94 g, 86%). Found: M^++1, 175. $C_8H_{22}N_4$ requires M^++1, 175. $\delta_H(D_2O)$ 1.00-1.50 (6 H, CH_2), 2.10-2.90 (9 H, CH_2N, CH). $\delta_C(D_2O)$ 25.6 (1 C, CH_2CH_2CH), 35.0 (1 C, $CH_2CH_2NH_2$), 37.5 (1 C, CH_2CH), 43.0, 43.7 (2 C, $(CH_2)_3CH_2NH_2$, NCH), 52.6, 54.1, 58.0, (3 C, $CH_2NHCH_2CH_2$).

(5S)-N-(5,9-Diamino-7-azanonyl)-t-butyloxycarbonamide - **(28)**.

To a stirred solution of (5S)-3-Azanonane-1,5,9-triamine **(27)** (0.92 g, 5.27 mmol) in 12 ml of water at 50°C was added $CuCO_3.Cu(OH)_2$ (0.70 g, 3.15 mmol) and the solution maintained at 50°C for 30 minutes to give a deep blue solution. To the now cooled solution was added triethylamine (8 cm^3), 1,4-dioxane (12 cm^3) and BOCON (1.30 g, 5.27 mmol), and the solution stirred for 4 hours at room temperature. H_2S

was bubbled through the solution for 15 minutes to give a dark brown precipitate (copper sulfide). The solution was then basified (pH 14), and any solids removed by filtration. Evaporation of the filtrate yielded a residue which was then taken up into water and dichloromethane, the aqueous layer then being exhaustively extracted with dichloromethane. The organic fractions were combined, dried (K_2CO_3), and the solvent evaporated to give a thick yellow oil (0.96 g, 66%). $\delta_H(CDCl_3)$ 0.7-1.6 (20 H, m, NH_2, NH, $(CH_2)_3CH$, CH_3), 2.0-2.2 (1 H, m, CH), 2.20-2.65 (6 H, m, $CH_2CH_2NHCH_2$), 2.81 (2 H, br, CH_2NHCO), 5.18 (1 H, s, CONH). $\delta_C(CDCl_3)$ 22.8 (1 C, CH_2CH_2CH), 27.9 (3 C, CH_3), 29.6 (1 C, CH_2CH_2NH), 35.3 (1 C, $(CH_2)_3CH_2CH$), 39.7 (1 C, CH_2NHCO), 41.2 (1 C, CH), 50.4, 52.0, 55.9 (3 C, CH_2NH_2, CH_2NH), 78.1 (1 C, $(CH_3)_3C$), 155.6 (1 C, CO).

Cyclohexylmethyl tri-maleimide - **(29)**.

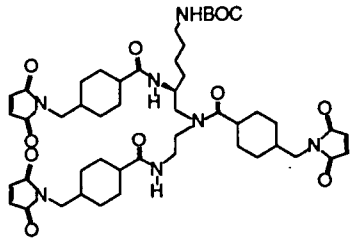

Conversion of the maleimido carboxylic acid **(21)** (314 mg, 1.33 mmol) to the acid chloride N-(4-chloroformylcyclohexylmethyl)-maleimide was brought about by the addition of a large excess of thionyl chloride and heating for 2 hours in a small quantity of anhydrous toluene. The solvent was removed under reduced pressure and the crude oil used immediately. I.R. (CO maleimide) 1715 cm^{-1} , (COCl) 1795 cm^{-1} . $\delta_H(CDCl_3)$ 0.85-2.70 (10 H, m, cyclohexyl H), 3.31 (2 H, d, J 6.8 Hz, NCH_2), 6.66 (2 H, s, HC=CH). $\delta_C(CDCl_3)$ 28.1 (2 C, $CH_2CH_2CHCOCl$), 28.9 (2 C, $CH_2CHCOCl$), 35.9 (1 C, $CHCH_2N$), 42.9 (1 C, CH_2N), 54.5 (1 C, CHCOCl), 133.8 (2 C, C=C), 170.7 (2 C, COCH=CH), 173.1 (1 C, COCl).

To this acid chloride at -10°C in 1 cm^3 of CH_2Cl_2 under nitrogen was slowly added a mixture of **(28)** (93 mg, 0.34 mmol) and triethylamine (120 mg, 1.19 mmol) in 1 cm^3

of CH_2Cl_2. The solution was allowed to warm to RT, and was left overnight and purified by reverse phase HPLC (t=0min. 90% A 10% B, t=20min. 0% A 100% B, 302nm) to give the title compound T_R 17.7 min. as a colourless solid (21%). I.R. (CON) 1639 cm^{-1}, (CO maleimide) 1704 cm^{-1}. $\delta_H(CDCl_3)$ 0.75-1.15 (6 H, m, CH_2CHCH_2N), 1.15-1.53 (15 H, br, CH_3, CH_2CHCH_2N), 1.53-1.88 (15 H, m, $CHCH_2N$, CH_2CHCO, $(CH_2)_3CH$), 1.88-2.13 (6 H, m, CH_2CHCO), 2.13-2.37 (3 H, txt, CHCO), 2.96-3.10 (2 H, br, CH_2NHCO_2), 3.32 (6 H, d, J 6.64 Hz, $CH_2NCOCH=CH$), 3.25-3.50 (7 H, br, $CH_2CH_2NCH_2CH$), 6.70 (4 H, s, CH=CH), 6.72 (2 H, s, CH=CH) $\delta_C(CDCl_3)$ 22.6 (1 C, $CH_2(CH_2)_2NH$), 28.1, 28.6 (6 C, $CH_2CHCH_2NCH=CH$), 28.3 (3 C, CH_3), 29.4 (1 C, $CH_2CH_2NHCO_2$), 29.5 (6 C, CH_2CHCO), 35.4 (1 C, CH_2CHNH), 36.2 (3 C, $CHCH_2NHCOCH=CH$), 39.1 (CH_2NHCO_2), 43.5 (3 C, $CH_2NCOCH=CH$), 44.9, 44.8 (3 C, CHCON), 78.9 (1 C, $(CH_3)_3C$), 133.9 (6 C, CH=CH), 156.5 (1 C, OCONH), 170.9 (6 C, COCH=CH), 173.2, 176.6, 177.9 (3 C, CON, CONH).

C_3 tri-maleimide - **(30)**.

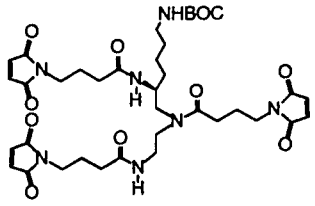

Synthesis and purification as for **(29)** using the acid chloride 4-maleimido butyryl chloride (263 mg, 1.30 mmol) converted from the acid as in **(29)**, triethylamine (120 mg, 1.19 mmol) and **(28)** (96 mg, 0.35 mmol) to give the title compound as a colourless solid (18%). Alternatively, to **(28)** (175 mg, 0.638 mmol) in 5 cm^3 of dry DMF were added dry N-methylmorpholine (290 mg, 2.87 mmol), 1-(3-dimethyl aminopropyl)-3-ethylcarbodiimide.HCl (E.D.C.) (551 mg, 2.87 mmol), 1-hydroxybenzatriazole (388 mg, 2.87 mmol), and 4-maleimidobutyric acid (526 mg, 2.87 mmol). The solution was stirred for 4 days under nitrogen, and purified by

reverse phase HPLC (t=0min. 90% A 10%B, t=25min. 0% A 100% B, 302nm, Hypersil 5 ODS, 5 ml min^{-1}), to yield a colourless solid T_R 13.4 min., 45 mg, 9% yield. I.R. (CON) 1650 cm^{-1}, (CO maleimide) 1703 cm^{-1}. δ_H(400MHz)($CDCl_3$) 1.43 (9 H, s, $(CH_3)_3$), 1.5-1.6 (6 H, m, $(CH_2)_3NHCO$), 1.86, 1.92, 1.93 (6 H, 3xp, CH_2CH_2CO), 2.13, 2.22 (6 H, 2xt, CH_2CO), 3.55 (6 H, m, $CH_2NCOCH=CH$), 3.10+3.4-3.7 (9 H, br m, CH_2NHCO, CH_2NCO), 4.70 (1 H, t, $NHCO_2$), 6.28 (1 H, d, CHN*H*CO), 6.700, 6.702, 6.708 (6 H, 3xs, CH=CH), 7.09 (1 H, t, CH_2NHCO). δ_C(100MHz)($CDCl_3$) 23.1, 23.4, 23.6 (3 C, $(CH_2)_3CH_2NHCO_2$), 27.4 (3 C, CH_3), 28.6, 28.7 (2 C, $NHCOCH_2CH_2$), 29.1 (1 C, $NCOCH_2CH_2$), 31.8, 32.1, 32.4 (3 C, CH_2CO), 36.1, 36.2, 26.3, 37.3, 39.2 (5 C, $(CH_2)_2NCO$, $CH_2CHNHCO$, CH_2NHCO_2), 47.8, 48.8, 49.2 (3 C, $CH_2NCOCH=CH$), 133.1 (6 C,, CH=CH), 155.0 (1 C, CO_2), 169.90, 169.91, 169.94 (6 C, *C*OCH=CH), 171.8, 171.9 (2 C, CONH), 173.0 (1 C, $CON(CH_2)(CH_2)$).

C_5 tri-maleimide - **(31)**.

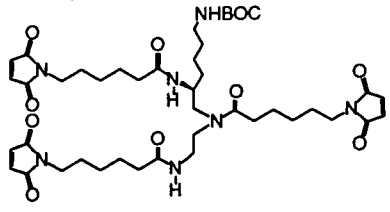

To **(28)** (21.6 mg, 0.079 mmol) in dry THF (5 cm^3) under nitrogen was added DCC (81.2 mg, 0.394 mmol) and **(20)** (74.8 mg, 0.354 mmol). Reverse phase HPLC (t=0min. 90% A 10% B, t=20min. 25% A 75% B, t=20.1min. 0% A 100% B, 302nm) gave the product T_R 20.5 min. in approx. 15% yied. Alternatively synthesis as for **(29)** using the acid chloride of 6-maleimidohexanoic acid **(20)** (298 mg, 1.93 mmol), triethylamine (131 mg, 1.30 mmol) and **(28)** (79 mg, 0.29 mmol). Purified by reverse phase HPLC as before to yield a colourless solid T_R 20.5 min., 38.5 mg, 16%. I.R. (COCl) 1795 cm^{-1}. Found: M^++1, 854. $C_{43}H_{63}N_7O_{11}$ requires M^++1, 854. δ_H(400MHz) ($CDCl_3$) 1.25-1.55 (12 H, m, $(CH_2)_3CH_2NHCO_2$,

$CH_2CH_2CH_2CON$), 1.43 (9 H, s, $(CH_3)_3$), 1.6 (12 H, m, $CH_2CH_2CH_2CH_2CO$), 2.05-2.40 (6 H, m, CH_2CON), 3.0-3.6 (9 H, m, CH_2NH, $CHNH$, CH_2NCOCH_2), 3.49 (6 H, t, $CH_2NCOCH{=}CH$), 5.45 (1 H, br, CH_2NHCO_2), 6.10 (1 H, d, CHNHCO), 6.692, 6.694, 6.708 (6 H, 3xs, CH=CH), 7.0 (1 H, t, $CH_2NHCOCH_2$). $\delta_C(CDCl_3)$ 134.1 (6 C, C=C), 156.0 (1 C, CO_2), 170.8 (6 C, $COCH$), 173.5, 173.9 (2 C, CONH), 175.0 (1 C, $CON(CH_2)(CH_2)$).

Bis para-nitrophenol active ester - **(32)**.

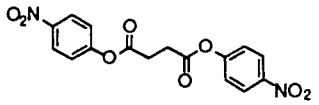

Succinic acid (0.755 g, 6.39 mmol), para-nitrophenol (2.224 g, 15.98 mmol) and DCC (3.957 g, 19.18 mmol) were dissolved in dry THF (60 cm^3) containing 4 Å molecular sieves. The solution was left overnight under nitrogen at room temperature, and any solids filtered off. Purification required flash silica column chromatography, using 20% hexane in dichloromethane as the eluant, to give the product as a white solid, (1.259 g, 55%). $\delta_H(CDCl_3)$ 3.11 (4 H, s, CH_2), 7.35 (4 H, d, CHCO), 8.33 (4 H, d, $CHCNO_2$).

Active ester functionalised ligand - **(33)**.

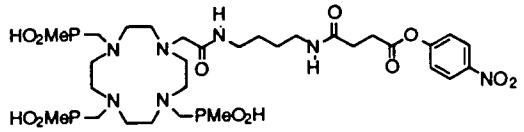

To **(15b)** (118.1 mg, 0.131 mmol) in dry DMSO (0.25 cm^3) were added N-methylmorpholine (92.9 mg, 0.918 mmol) and the bis paranitrophenol active ester **(32)** (118.2 mg, 0.328 mmol). The solution was heated under nitrogen at 50°C to keep all solids in solution, and the progress of the reaction followed by HPLC. This indicated a decline in the proportion of title compound after 1 hour. The reaction was

then stopped by freezing, and the solution was purified by reverse phase HPLC (t=0min. 90% A 10% B, t=20min. 25% A 75% B, 278nm), to yield a colourless solid T_R 16.4 min., 49.9 mg, 33% yield. Found: M^++1, 798. $C_{30}H_{54}N_7O_{12}P_3$ requires M^++1, 798. $\delta_H(D_2O)$ 1.36 (6 H, d, ^2J 15 Hz, PCH_3), 1.40 (3 H, d, ^2J 15 Hz, PCH_3), 1.47 (4 H, p, $(CH_2)_2CH_2NHCO$), 2.64 (2 H, t, CH_2CONH), 2.93 (2 H, t, CH_2CO_2), 3.0-3.6 (26 H, m, CH_2N, CH_2NHCO), 3.68 (2 H, br s, $NHCOCH_2N$), 7.33 (2 H, d, CHCO), 8.30 (2 H, d, $CHCNO_2$).

C_5 tri-maleimide functionalised ligand - **(34)**.

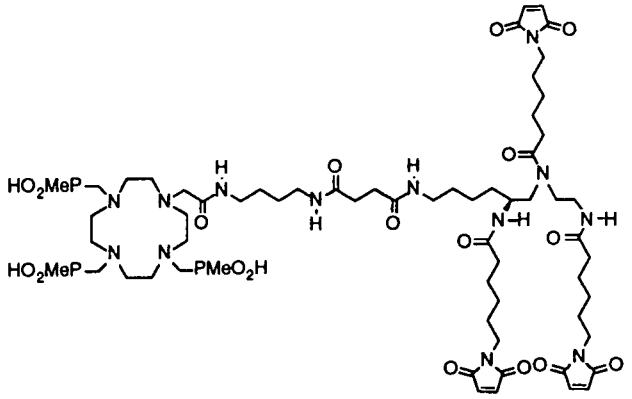

To **(31)** (6.0 mg, 0.007 mmol) was added 0.03 cm^3 of water and 0.27 cm^3 of TFA. The solution was left at RT for 30 min., and the solvent removed to give the BOC deprotected TFA amine salt. To a solution of this in dry DMSO (0.5 cm^3) were added **(33)** (5.0 mg, 0.0044 mmol) and N-methylmorpholine (2.2 mg, 0.022 mmol), and the solution was left overnight at room temperature under nitrogen. Alternatively, oxalyl chloride (0.5 cm^3) was added to **(35)** (7.2 mg, 0.0085 mmol) and 1 drop of DMF added to the solution. After 45 minutes the solvents were removed and the resulting solid acid chloride immediately taken up into dry DMF (0.5 cm^3), and added to **(15b)** (8.8 mg, 0.0098 mmol) followed by triethylamine (17.3 mg, 0.171 mmol). The solution / suspension was left under nitrogen overnight and the DMF removed.

In both cases the solutions were purified by reverse phase HPLC (t=0min. 90% A 10% B, t=20min. 25% A 75% B, 302nm. T_R 12.7 min.) to yield 2-3 mg, approximately 20-25%. $\delta_H(D_2O)$ 1.0-1.6 (37 H, br m, PCH_3, $CH_2(CH_2)_3CH_2CO$,

$NHCH_2(CH_2)_2CH_2NHCO$, $CH(CH_2)_3CH_2NHCO$), 2.05 (4 H, t, $(CH_2)_2CH_2$ CONH), 2.20 (2 H, t, $(CH_2)_2CH_2CON(CH_2)(CH_2)$), 2.45, 2.55 (4 H, 2xm, $CO(CH_2)_2CO$), 2.60-3.60 (43 H, br m, CH_2N), 6.69 (6 H, s, CH=CH).

Carboxylic acid functionalised C_5 tri-maleimide - **(35)**.

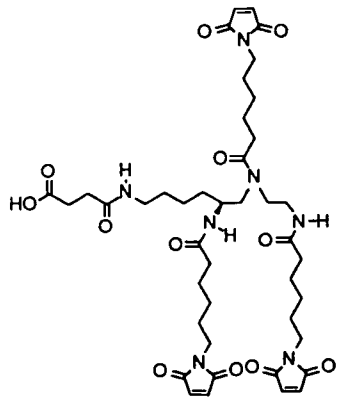

To **(31)** (6.3 mg, 0.0074 mmol) was added 0.04 cm^3 of water and 0.36 cm^3 of TFA. After 30 min. the solvent was removed, and the residues taken up into dry DMF (0.6 cm^3). To this were then added succinic anhydride (0.81 mg, 0.081 mmol) and triethylamine (1.49 mg, 0.0148 mmol). The solution was left at room temperature under nitrogen overnight and the extent of reaction determined by analytical HPLC (t=0min. 90% A 10% B, t=20min. 25% A 75% B, Hypersil 5 ODS 302 nm). BOC deprotected trimaleimide T_R 13.2 min., and after reaction with succinic anhydride T_R 12.7 min.. This showed that a clean and quantitative conversion to the solid product had occurred. δ_H(400MHz) (CD_3CN) 1.25-1.55 (12 H, m, $(CH_2)_3CH_2NH$, $CH_2(CH_2)_2CON$), 1.6 (12 H, m, $CH_2CH_2CH_2CH_2CO$), 2.08 (4 H, t, $(CH_2)_4CH_2CONH$), 2.23 (2 H, t, $(CH_2)_4CH_2CON(CH_2)(CH_2)$), 2.38, 2.51 (4 H, 2xm, $COCH_2CH_2CO$), 3.0-3.6 (9 H, m, CH_2NH, CHNH, CH_2NCOCH_2), 3.49 (6 H, t, CH_2NCOCH=CH), 5.45 (1 H, t, $NHCO(CH_2)_2CO$), 6.48 (1 H, d, CHNHCO), 6.692, 6.694, 6.708 (6 H, 3xs, CH=CH), 6.90 (1 H, t, $NHCO(CH_2)_5$).

2-Nitroimidazole functionalised ligand - **(36)**.

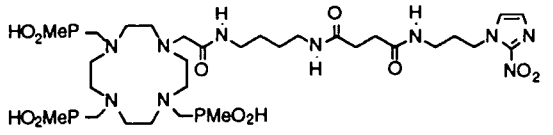

To **(33)** (38 mg, 0.033 mmol), in dry DMSO (0.5 cm^3), under nitrogen was added 1-aminopropyl-2-nitroimidazole (29 mg, 0.170 mmol). The solution was left at room temperature overnight and was subsequently purified by reverse phase HPLC (t=0min. 90% A 10% B, t=20min. 25% A 75% B, 325nm) to yield the title compound as a pale yellow solid, T_R 11.6 min., 39 mg, 73%. $\delta_H(D_2O)$ 1.21 (3 H, d, ^2J 13 Hz, PCH_3), 1.32 (6 H, d, ^2J 13 Hz, PCH_3), 1.37 (4 H, br, $(CH_2)_2CH_2NHCO$), 1.94 (2 H, p, $NCH_2CH_2CH_2NHCO$), 2.36 (4 H, s, $CO(CH_2)_2$), 2.6-3.6 (30 H, m, CH_2N, NCH_2CO, CH_2NHCO), 4.35 (2 H, t, J 7.2 Hz, CH_2NCH), 7.04 (1 H, s, $CHN(CH_2)_3$), 7.33 (1 H, s, $CHNCNO_2$).

6.4.3 Chapter 4

9-Chloro acridine - **(37)**.[6]

To N-phenylanthranilic acid (10g, 47 mmol) in 60 cm^3 of $POCl_3$, were added two drops of conc. H_2SO_4 to stop an explosive start at high temperature (reaction is acid catalysed). The solution was heated to 85°C until a vigorous reaction set in, and immediately removed from the heat. Once boiling had subsided, the solution was heated at 135°C for 2 hours, and excess $POCl_3$ removed by distillation. Once cooled, the solution was poured into a well stirred mixture of conc. NH_3 (40 cm^3), ice (100 g), and $CHCl_3$ (40 cm^3), and stirred until no solids remained. The chloroform layer was separated off, the water layer extracted with chloroform, the organic fractions combined, dried ($CaCl_2$), and the solvent removed to yield almost *quantitatively* a greenish-grey powder. Can be crystalised from EtOH by addition of 0.5% ammonia to yield yellow crystals. m.p. 119-120°C. $\delta_H(CDCl_3)$ 7.52 (2 H, t, J 7.8 Hz, H_6, H_3),

7.72 (2 H, t, J 7.7 Hz, H_7, H_2), 8.15 (2 H, d, J 8.1 Hz, H_5, H_4), 8.29 (2 H, d, J 9.5 Hz, H_8, H_1).

9-Methoxy acridine - **(38)**.[7]

To 9-chloro acridine **(37)** (2.0 g, 9.4 mmol) suspended in methanol (30 cm^3), was added 1.3 equivalents of NaOMe, and the solution heated at 70°C for 2 hours. Precipitated sodium chloride was removed by filtration, and the filtrate was treated with water to give the title compound as a yellow solid (1.51 g, 77%). It was possible to recrystallise some of the product from 50% aqueous methanol to give pale yellow needles. m.p. 103°C. $\delta_H(CD_3OD)$ 4.23 (3 H, s, OCH_3), 7.54, 7.79 (4 H, 2xt, H_6, H_3, H_7, H_2), 8.09, 8.28 (4 H, 2xd, H_5, H_4, H_8, H_1).

9-Phenoxy acridine - **(39)**.

Sodium hydroxide (0.52 g, 0.013 mmol) was dissolved in phenol (8.74 g, 92.8 mmol) at 100°C and 9-chloro acridine **(37)** (2.0 g, 9.36 mmol) added with stirring. After 2 hours the product was precipitated out in excess diethyl ether, and recrystallised from methanol to give a bright yellow powder, 2.34 g, 93%. $\delta_H(CDCl_3)$ 6.77 (2 H, d, CHCO), 6.96 (1 H, t, C*H*$(CH)_2$CO) 7.18 (2 H, t, C*H*CHCO), 7.36, 7.69 (4 H, 2xt, H_6, H_3, H_7, H_2), 8.02, 8.20 (4 H, 2xd, H_5, H_4, H_8, H_1).

9-(γ-Bromopropyl) aminoacridine - **(40)**.

To 9-phenoxy acridine **(39)** (2.08 g, 7.68 mmol) dissolved in phenol (7 g) at 80°C was added 3-bromopropylamine.HBr (1.69 g, 7.72 mmol), and the solution heated at 120°C for 1 hour. The solution was poured into excess diethyl ether to yield a pale yellow precipitate. This was filtered off, and recrystallised from hot methanol as a yellow powder to yield the product (1.217 g, 40%). $\delta_H(CD_3OD)$ 2.55 (2 H, p, C*H*$_2$$CH_2Br$), 3.63 (2 H, t, J 6.3 Hz, CH_2Br), 4.35 (2 H, t, J 7.0 Hz, CH_2NH), 7.59, 8.0 (4 H, 2xt, J 7.7 Hz, H_6, H_3, H_7, H_2), 7.84, 8.55 (4 H, 2xd, J 8.5 Hz, H_5, H_4, H_8, H_1).

N-t-butyloxycarbonyl-1,4-diaminobutane - **(41)**.

To 1,4 diaminobutane (5.57 g, 0.063mol) in 30 ml of 1,4 dioxane under nitrogen was slowly added a solution of $(BOC)_2O$ in 25 cm^3 of 1,4 dioxane. After a further 1 hour, the solution was reduced to 30 cm^3, and 45 cm^3 of water added to precipitate out any N,N bis *t*-butyloxycarbonyl-1,4 diaminobutane. This was filtered off, and the dioxane removed under reduced pressure. The remaining aqueous solution was saturated with NaCl, extracted with EtOAc (5 x 20 cm^3), and the organic solvent removed to yield a colourless oil. This oil was taken up into water, acidified to pH 3 (HCl), washed with EtOAc, and once more saturated with NaCl. The pH was raised to 14 (KOH) and the aqueous layer exhaustively extracted with EtOAc, the fractions combined, dried (K_2CO_3), and the solvent removed to yield a pale yellow oil 1.60 g, 27%. $\delta_H(CDCl_3)$ 1.21 (2 H, s, NH_2), 1.39 (9 H, s, $(CH_3)_3$), 1.41 (4 H, m, $(CH_2)_2CH_2NH_2$), 2.68 (2 H, t, CH_2NH_2), 3.08 (2 H, dt, CH_2NH), 4.85 (1 H, br s, NH).

N-(4-Chloroacetamidobutyl)-t-butyloxycarbonamide - **(42)**.

To **(41)** (3.30 g, 17.5 mmol) in 10 cm^3 of CH_2Cl_2 was added NaOH (0.710 g, 17.5 mmol) in 1 cm^3 of water. To the cooled solution was added chloroacetylchloride (1.98 g, 17.5 mmol) in 10 cm^3 of CH_2Cl_2 maintaining a temperature of <-10°C. After 1 hour the precipitated white product which had formed was filtered off and dried under reduced pressure. The organic layer was washed with water, dried (K_2CO_3) and the solvent removed to yield more of the title compound (4.23 g, 91%). m.p. 98.5-99.5°C. Found: M^++1, 265. $C_{11}H_{21}N_2O_3Cl$ requires M^++1 265. Found: N 10.27%, C 49.58%, H 7.98%. $C_{11}H_{21}N_2O_3Cl$ requires: N 10.58%, C 49.90%, H 7.99%. $\delta_H(CDCl_3)$ 1.44 (9 H, s, $(CH_3)_3$), 1.56 (4 H, m, $(CH_2)_2CH_2NHCO$), 3.14 (2 H, q, J 6.3 Hz, CH_2NHCO_2), 3.33 (2 H, q, J 6.1 Hz, $CH_2NHCOCH_2$), 4.04 (2 H, s, CH_2Cl), 4.71 (1 H, t, $NHCO_2$), 6.78 (1 H, t, $NHCOCH_2$).

(43).

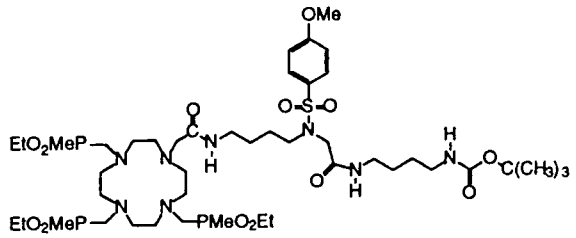

(14a) (244 mg, 0.294 mmol), **(42)** (155.5 mg, 0.587 mmol), and fine mesh potassium carbonate (162.3 mg, 1.175 mmol) were heated overnight at 80°C under nitrogen in dry DMF (2 cm^3). The solvent was removed under reduced pressure, the residues taken up into CH_2Cl_2 (2 cm^3), washed (5 x 1 cm^3 of water), dried (K_2CO_3), and the solvent removed to yield the crude product. This was used directly in the next step without further purification. $\delta_H(CDCl_3)$ 1.24 (9 H, t, J 7.0 Hz, OCH_2CH_3), 1.37 (9 H, s, $(CH_3)_3$), 1.45 (9 H, 2xd, PCH_3), 1.2-1.7 (8 H, m, $(CH_2)_2CH_2NH$), 2.3-3.4 (32 H, br m, CH_2N, CH_2NH), 3.58 (2 H, s, $COCH_2NSO_2$), 3.81 (3 H, s, OCH_3), 3.99 (6 H, p, J 7.1 Hz, OCH_2), 6.42 (1 H, t, $NHCO_2$), 6.91, 8.01 (2 H, 2xt, $NHCOCH_2$), 6.93 (2 H, d, J 9.0 Hz, CHCOMe), 7.68 (2 H, d, J 9.0 Hz, $CHCSO_2$).

(44).

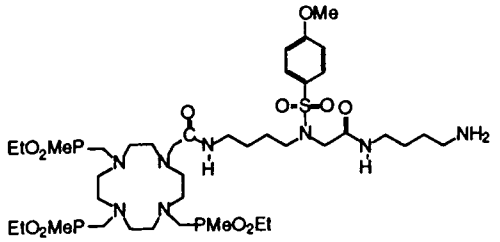

To **(43)** was added 0.9 cm^3 of TFA, and 0.1 cm^3 of water, and the solution left at room temperature for 30 min. to afford amine deprotection. The solvent was removed, and the residues purified by reverse phase HPLC (t=0min. 90% A 10% B, t=30min. 25% A 75% B, 254nm) to give the TFA salt as a colourless solid, T_R 15.2 min. This was then taken up into water, the pH raised to 11 (saturated with K_2CO_3), the solution exhaustively extracted with CH_2Cl_2, and dried (K_2CO_3) to yield on removal of the

solvent, the free amine as a colourless gum 86 mg, 31%. Found: M^++1, 959. $C_{39}H_{77}N_8O_{11}P_3S$ requires M^++1, 959. $\delta_H(CDCl_3)$ 1.24 (9 H, 2xt, J 7.1 Hz, OCH_2CH_3), 1.3-1.6 (6 H, br, $(CH_2)_2CH_2NSO_2$, NH_2), 1.46, 1.47 (9 H, 2xd, ^2J 13.5 Hz, PCH_3), 1.78 (4 H, br, $(CH_2)_2CH_2NH_2$), 2.2-3.3 (32 H, br m, CH_2N, CH_2NH, CH_2NH_2), 3.58 (2 H, br s, $COCH_2NSO_2$), 3.81 (3 H, s, OCH_3), 3.99 (6 H, p, J 7.1 Hz, OCH_2), 6.93 (2 H, d, J 8.8 Hz, CHCOMe), 7.21, 8.02 (2 H, 2xt, NHCO), 7.70 (2 H, d, J 8.8 Hz, $CHCCSO_2$).

(45).

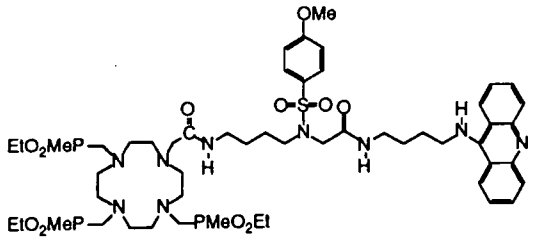

A solution of **(44)** (13.2 mg, 0.0138 mmol), and 9-chloro acridine **(37)** (7.4 mg, 0.036 mmol) was heated in 1 g of phenol at 70°C overnight followed by heating at 120°C for 2 hours. The phenol was removed by warming under vacuum,and the residues purified by reverse phase HPLC (t=0min. 90% A 10% B, t=30min. 25% A 75% B, 353nm) to yield the title compound as a yellow gum T_R 19.6 min., 13.6 mg, 62%. $\delta_H(D_2O)$ 1.23, 1.24, 1.32 (9 H, 3xt, J 7.1 Hz, OCH_2CH_3), 1.4-1.9 (8 H, br, $(CH_2)_2CH_2NHCO$), 1.58, 1.78 (9 H, 2xd, ^2J 14.0Hz, PCH_3), 2.7-3.9 (34 H, br m, CH_2N, CH_2NH), 3.69 (3 H, s, OCH_3), 3.9-4.3 (6 H, m, OCH_2), 6.83 (2 H, d, CHCOMe), 7.47 (2 H, d, $CHCSO_2$), 7.30 (4 H, 2xd, H_5, H_4, H_8, H_1), 7.73, 7.95 (4 H, 2xt, H_6, H_3, H_7, H_2).

Acridine-9-carbonyl chloride - **(46)**.

Acridine-9-carboxylic acid was heated at 80°C under nitrogen for 2 hours in thionyl chloride. The solvent was removed, and the residues azeatroped with dichloromethane

to give the product as a bright yellow solid. This was used immediately in the next step.

(47).

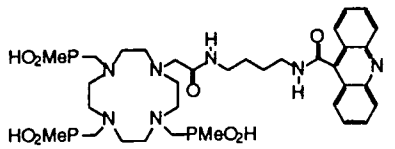

To **(15a)** (8.0 mg, 0.009 mmol) in 0.5 cm^3 of dry DMF under nitrogen was added a 5 fold excess of **(46)** in 0.5 cm^3 of dry DMF followed immediately by an excess of N-methyl morpholine (18.0 mg, 0.178 mmol). After 18 hours the solution was purified by reverse phase HPLC (t=0min. 90% A 10% B, t=30min. 25% A 75% B, 353nm) to yield a yellow solid T_R 13.5 min., 1.5 mg, 14%. $\delta_H(CD_3OD)$ 1.41 (6 H, d, ^2J 14.0 Hz, PCH_3), 1.43 (3 H, d, ^2J 14.0 Hz, PCH_3), 1.6-1.9 (4 H, br m, $(CH_2)_2CH_2NH$), 2.8-4.2 (28 H, br m, CH_2N, CH_2NH), 7.80 (2 H, t, H_5), 8.0-8.4 (6 H, m, H_6, H_7, H_8). $\delta_P(CD_3OD)$ 40.3, 44.4 (1:2).

Anthraquinone-2-carbonyl chloride - **(48).**

Anthraquinone-2-carboxylic acid (6.1 mg, 0.024 mmol) was heated for 1 hour at 80°C in thionyl chloride. The solvent was removed, and the resulting bright yellow solid acid chloride (I.R. (COCl) 1743 cm^{-1}, (CO) 1672 cm^{-1}, (C=C) 1590 cm^{-1}) used immediately in the next step without purification.

(49).

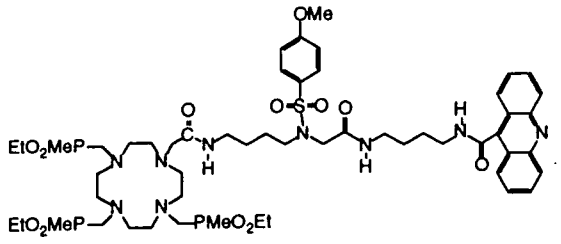

To **(46)** (10.8 mg, 0.039 mmol) in 0.5 cm^3 of CH_2Cl_2 at -10°C under nitrogen was slowly added a solution of the amine **(44)** (12.4 mg, 0.013 mmol) and triethylamine

(13.1 mg, 0.129 mmol). The solution was then left at room temperature overnight under nitrogen, and purified by reverse phase HPLC (t=0min. 90% A 10% B, t=30min. 25% A 75% B, 353nm) to give the product as a yellow gum T_R 19.6 min 10.5 mg, 50%. I.R. (C=C, C=N) 1635 cm^{-1}, (COCl) 1777 cm^{-1}. $\delta_H(CD_3OD)$ 1.33, 1.36 (9 H, 2xt, OCH_2CH_3), 1.2-2.0 (8 H, br, $(CH_2)_2CH_2NH$), 1.64 (6 H, d, ^2J 14.0 Hz, PCH_3), 1.68 (3 H, d, ^2J 14.0 Hz, PCH_3), 2.7-3.8 (30 H, br m, CH_2N, CH_2NH), 3.72 (2 H, t, CH_2NHCOacridine), 3.76 (2 H, s, $COCH_2NSO_2$), 3.88 (3 H, s, OCH_3), 4.12 (6 H, p, OCH_2), 7.09 (2 H, d, J 9.0 Hz, $CHCOMe$), 7.78 (2 H, d, J 9.0 Hz, $CHCSO_2$), 7.96 (2 H, t, CH acridine), 8.36 (6 H, m, CH acridine). $\delta_P(CD_3OD)$ 56.0, 55.7 (1:2).

(50)

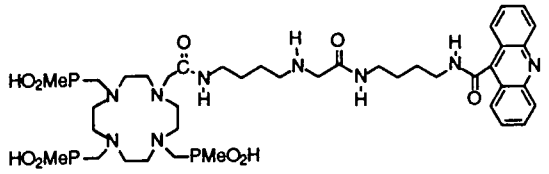

(49) (94.0 mg, 0.081 mmol) was heated at 100°C overnight in 2 cm^3 of 44% v/w HBr in glacial acetic acid containing 8 mg of phenol to stop bromination of the product. The solvent and phenol were removed by warming under vacuum, and the residue purified by reverse phase HPLC (t=0min. 90% A 10% B, t=30min. 25% A 75% B, 353nm) to yield a yellow solid T_R 12.5 min, 45.3 mg, 38%. When **(49)** was not initially purified by HPLC but instead used as its crude, the overall yield for the conversion of **(44)** to **(50)** was doubled from 19% to 38%. $\delta_H(CD_3OD)$ 1.47 (6 H, d, ^2J 14.6 Hz, PCH_3), 1.49 (3 H, d, ^2J 14.6 Hz, PCH_3), 1.5-2.0 (8 H, br, $(CH_2)_2CH_2NH$), 3.05 (2 H, t, $(CH_2NHCOCH_2N(CH_2)(CH_2))$, 2.9-3.7 (28 H, br m, CH_2N ring, CH_2P, CH_2NCH_2CO, CH_2NHCH_2CO, $CH_2NHCOCH_2NH$), 3.72 (2 H, t, J 6.7 Hz, CH_2NHCOacridine), 3.82 (2 H, s, $(CH_2)(CH_2)NCH_2CO$), 3.98 (2 H, s $NHCH_2CO$), 7.96 (2 H, t, J 7.7Hz, H_6, H_3), 8.20-8.45 (6 H, 2xd + t, H_5, H_4, H_8, H_1, H_7, H_2). $\delta_C(CD_3OD)$ 15.9 (2 C, ^1J 97 Hz, PCH_3), 16.1 (1 C, ^1J 97 Hz,

PCH_3), 24.3 (1 C, $CH_2CH_2NHCOCH_2NH$), 27.1 (1 C, CH_2CH_2NHCOacridine), 27.7, 27.9 (2 C, $(CH_2)_2CH_2NHCH_2$), 39.4, 40.1, 40.9 (3 C, CH_2NHCO), 161.5, 162.2 (2 C, $COCH_2$), 166.5 (1 C, COacridine).

(51).

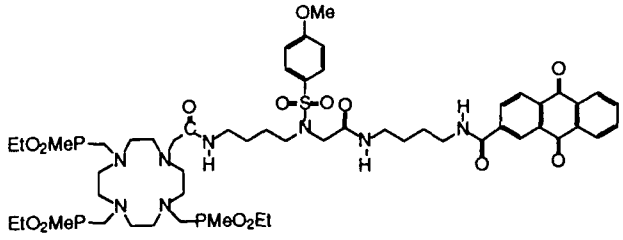

To anthraquinone-2-carbonyl chloride **(48)** (6.5 mg, 0.024 mmol) in 0.3 cm^3 of CH_2Cl_2, was added a solution of **(44)** (7.7 mg, 0.008 mmol) and Et_3N (16.2 mg, 0.161 mmol) in CH_2Cl_2 (0.2 cm^3) at a temperature of -10°C. This was then allowed to warm to room temperature, and left for a further hour. The solution was then purified by reverse phase HPLC (t=0min. 90% A 10% B, t=20min. 25% A 75% B, 278nm) to yield a pale yellow solid T_R 19.0 min., 5.2 mg, 42%. I.R. (CO) 1677 cm^{-1}, (CONH) 1642 cm^{-1}, (C=C) 1590 cm^{-1}. $\delta_H(CDCl_3)$ 1.35 (9 H, 2xt, OCH_2CH_3), 1.50-1.80 (8 H, br, $(CH_2)_2CH_2NHCO$), 1.62 (9 H, 2xd, PCH_3), 2.20-3.80 (32 H, br m, CH_2N, CH_2NH), 3.72 (2 H, s, $COCH_2NSO_2$), 3.86 (3 H, s, OCH_3), 4.18 (6 H, p, OCH_2), 6.98 (2 H, d, CHCOMe), 7.75 (2 H, d, $CHCSO_2$), 7.83 (3 H, m, CH anthraquinone), 8.35 (4 H, m, CH anthraquinone).

9-(ε-Carboxypentyl)-aminoacridine - **(52)**

To 9-methoxy acridine **(38)** (289 mg, 1.38 mmol) in 4 cm^3 of methanol at 60°C was added 6-aminocaproic acid in 0.5 cm^3 of water. The solution was left at 60°C for 2 hours, and the precipitate formed filtered off, washed (water, methanol, ether), and dried under vacuum to yield a yellow powder (226 mg, 53%). m.p. 186-189°C. I.R. (CO^{2-}, aromatic) 1500-1610 cm^{-1}. Found: N 8.19%, C 70.00%, H 6.81%. $C_{19}H_{20}N_2O_2$ requires: N 9.09%, C 74.00%, H 6.54%. Found: M^++1, 309. $C_{19}H_{20}N_2O_3$ requires 309. $\delta_H(CD_3OD)$ 1.52 (2 H, m, $HN(CH_2)_2CH_2$), 1.68 (2 H,

p, $CH_2CH_2CO_2H$), 1.98 (2 H, p, $HNCH_2CH_2$), 2.21 (2 H, t, CH_2CO_2H), 4.12 (2 H, t, CH_2NH), 7.52 (2 H, t, H_6, H_3), 7.78 (2 H, d, H_5, H_4), 7.91 (2 H, t, H_7, H_2), 8.48 (2 H, d, H_8, H_1).

9-(ε-Chloroformylpentyl)-aminoacridine - **(53)**.

(52) (13.4 mg, 0.044 mmol) was heated at 80°C for 1 hour in thionyl chloride (1.5 cm^3). The solvent was removed, and the acid chloride (I.R. (COCl) 1790 cm^{-1}) used *immediately* without purification in the next step.

(54).

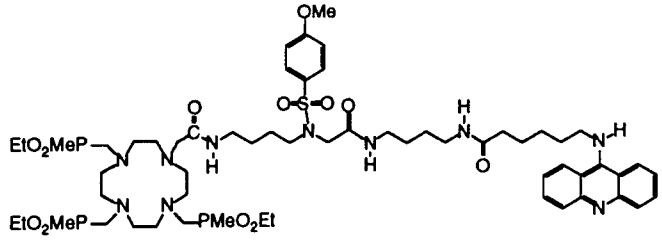

The acid chloride **(53)** (14.2 mg, 0.044 mmol) was taken up into CH_2Cl_2 (1 cm^3) and added immediately to a solution of **(44)** (8.7 mg, 0.009 mmol) and N-methylmorpholine (13.3 mg, 0.136 mmol) in CH_2Cl_2 (1 cm^3). The solution was left at room temperature under nitrogen overnight, and purified by reverse phase HPLC (t=0min. 90% A 10% B, t=30min. 25% A 75% B, 353nm) to yield a pale yellow gum T_R 19.9 min., 7.5 mg, 49%. $\delta_H(CD_3OD)$ 1.33 (9 H, m, OCH_2CH_3), 1.52 (2 H, m, $CH_2(CH_2)_2CONH$), 1.62 (9 H, d, PCH_3), 1.4-1.8 (8 H, m, $(CH_2)_2CH_2NHCO$), 1.70 (2 H, m, $CH_2(CH_2)_3CONH$), 1.95 (2 H, p, CH_2CH_2CONH), 2.33 (2 H, t, CH_2CH_2CONH), 2.6-3.6 (32 H, br m, CH_2ring, CH_2P, CH_2NHCO, $NCH_2CONH(CH_2)_4$, $CH_2CH_2NSO_2$), 3.71 (2 H, s, $COCH_2NSO_2$), 4.07 (2 H, m, CH_2NHAcridine), 4.10 (6 H, p, OCH_2), 7.03 (2 H, d, CHCOMe), 7.72 (2 H, d, $CHCSO_2$), 7.58 (2 H, t, H_6), 7.80 (2 H, d, H_5), 7.95 (2 H, m, H_7), 8.47 (2 H, m, H_8).

N^1-t-butyloxycarbonyl-N^2-methyl-diethylenetriamine - **(55)**.

To N^2-methyldiethylenetriamine (8.900 g, 0.0759 mol) in 1,4-dioxane (15 cm^3) at room temperature was slowly added $(BOC)_2O$ (3.315 g, 0.0152 mol) in 1,4-dioxane (15 cm^3) over a period of 2 hours. All solvents and excess amine were removed by strongly heating at 120°C under vacuum, and the resulting residues taken up into water whereupon any diprotected amine precipitated out and was removed by filtration. The aqueous solution was saturated with NaCl, exhaustively extracted with ethyl acetate, and the organic solvent removed to yield an oily residue. This residue was taken up into water, the pH raised to 14 (KOH), and the solution extracted with ethyl acetate. The organic solvent was dried (K_2CO_3), and removed to yield a yellow oil. 1.929 g, 58%. $\delta_H(CDCl_3)$ 1.28 (2 H, s, NH_2), 1.39 (9 H, s, $(CH_3)_3C$), 2.18 (3 H, s, NCH_3), 2.39, 2.42 (4 H, 2xt, $(CH_2)_2NCH_3$), 2.72 (2 H, t, CH_2NH_2), 3.18 (2 H, q, CH_2NH), 5.08 (1 H, br, CH_2NH).

N^1-t-butyloxycarbonyl-N^2-methyl-N^3-chloromethanecarbonyl-diethylenetriamine - **(56)**.

To **(55)** (1.929 g, 8.875 mmol) in 10 cm^3 of CH_2Cl_2 and 1 cm^3 of NaOH (0.3905 g, 9.763 mmol) at <-10°C was slowly added chloroacetyl chloride (1.103 g, 9.763 mmol) (in 10 cm^3 of CH_2Cl_2) over a period of 1-2 hours maintaining a temperature of <-10°C. The organic layer was separated off, washed once with water (0.5 cm^3), dried (K_2CO_3), and the solvent removed to yield the title compound as a pale yellow solid. Yield 357 mg, 14%. I.R. (CO) 1682 cm^{-1}. Found: M^++1, 294. $C_{12}H_{24}N_3O_3Cl$ requires M^++1, 294. $\delta_H(CDCl_3)$ 1.42 (9 H, s, $C(CH_3)_3$), 2.23 (3 H, s, NCH_3), 2.50, 2.53 (4 H, 2xt, $(CH_2)_2NCH_3$), 3.18 (2 H, t, CH_2NHBOC), 3.34 (2 H, t, $CH_2NHCOCH_2$), 4.04 (2 H, s, $ClCH_2$), 4.95 (1 H, br, NHCOBOC), 7.17 (1 H, br, $NHCOCH_2$). $\delta_C(CDCl_3)$ 28.4 (3 C, $(CH_3)_3$), 36.8, 37.8 (2 C, CH_2Cl, NMe), 41.3 (1 C, CH_2NHCO), 42.7 (1 C, $CH_2NHCOCH_2$), 55.7 (1 C, $CH_2CH_2NHCO_2$), 56.6 (1 C, $CH_2CH_2NHCOCH_2$), 79.6 (1 C, $C(CH_3)_3$), 156.2 (1 C, CO_2), 166.0 (1 C, $COCH_2Cl$).

(57).

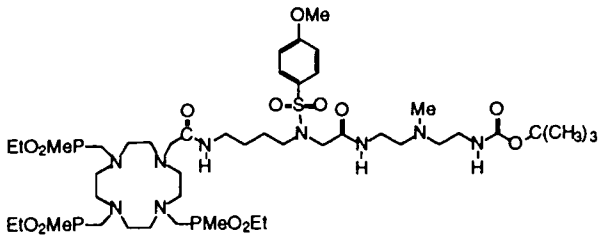

(14a) (45.7 mg, 0.0055 mmol), **(56)** (32.3 mg, 0.110 mmol) and fine mesh potassium carbonate (30.4 mg, 0.220 mmol) were heated overnight at 80°C in dry DMF under nitrogen. The solvent was removed under reduced pressure and the residues taken up into dichloromethane (2 cm^3). The solution was washed twice (5 x 1 cm^3 of water), dried (K_2CO_3) and the solvent removed to yield the crude product (NB More products can be re-extracted from the water washings.). The product can be purified by reverse phase HPLC (t=0min. 90% A 10% B, t=30min. 60% A 40% B, 254nm T_R 25.8 min.), although it was used in the next step without further purification. $\delta_H(CDCl_3)$ 1.33 (9 H, t, OCH_2CH_3), 1.42 (9 H, s, $C(CH_3)_3$), 1.4-1.7 (4 H, br, $(CH_2)_2CH_2NSO_2$), 1.5-1.7 (9 H, 2xd, PCH_3), 2.5-4.0 (38 H, br m, CH_2N, CH_2NH), 2.67 (3 H, s, NCH_3), 3.88 (3 H, s, OCH_3), 4.07 (6 H, p, OCH_2), 6.99 (2 H, d, CHCOMe), 7.70 (2 H, d $CHCSO_2$). $\delta_P(CDCl_3)$ 50.3, 51.5 (2:1).

(58).

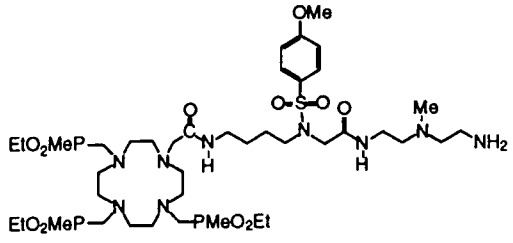

To crude **(57)** was added 0.1 cm^3 of water and 0.9 cm^3 of TFA, and the solution left at room temperature for 30 min.. The solvent was removed, and the residues purified by reverse phase HPLC (t=0min. 90% A 10% B, t=30min. 60% A 40% B, 254nm) to yield the TFA salt T_R 25.8 min. as a colourless oil. Overall yield from **(14a)** 26%.

$\delta_H(CDCl_3)$ 1.22-1.42 (9 H, 2xt, OCH_2CH_3), 1.56 (9 H, 2xd, PCH_3), 1.2-2.1 (2 H, br, NH_2), 1.7-2.1 (4 H, br, $(CH_2)_2CH_2NSO_2$), 2.1-3.7 (35 H, br m, CH_2N, CH_2NH), 2.68 (3 H, s, NCH_3), 3.89 (3 H, s, OCH_3), 4.10 (6 H, p, OCH_2), 6.95, 7.80 (2 H, 2xt, CONH), 7.01 (2 H, d, J 8.8 Hz, CHCOMe), 7.71 (2 H, d, J 8.8 Hz, $CHCSO_2$).

(59).

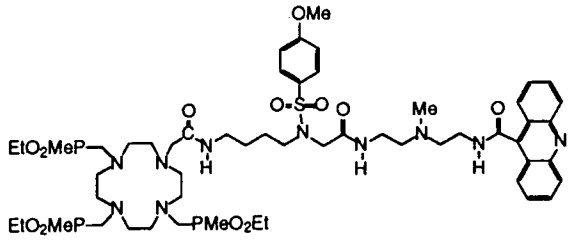

Acridine-9-carbonyl chloride **(46)** (5.6 mg, 0.020 mmol) in 0.5 cm^3 of CH_2Cl_2 was added to a solution of the free amine of **(58)** (5.0 mg, 0.005 mmol) and triethylamine (7.7 mg, 0.076 mmol) in 1 cm^3 of CH_2Cl_2. The solution was left under nitrogen overnight and purified by reverse phase HPLC (t=0min. 90% A 10% B, t=30min. 25% A 75% B, 353nm) to yield the title compound as a yellow solid T_R 20.7 min., 2.6 mg, 29%. $\delta_H(CD_3OD)$ 1.2-1.5 (9 H, m, OCH_2CH_3), 1.5-2.0 (13 H, m, PCH_3, $(CH_2)_2CH_2NSO_2$), 2.5-3.7 (38 H, br m, CH_2N), 2.68 (3 H, s, NCH_3), 3.78 (3 H, s, OCH_3), 4.15 (6 H, m, OCH_2), 7.11 (2 H, d, CHCOMe), 7.70-8.40 (10 H, m, CH Acridine, $CHCSO_2$).

Maleimide-acridine functionalised ligand - **(60).**

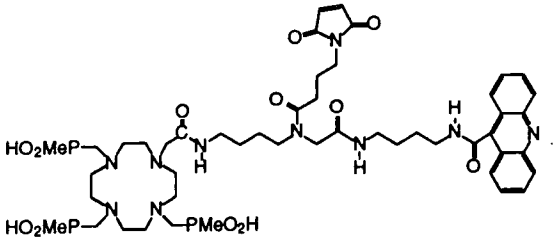

To 4-maleimidobutyric acid (4.9 mg, 0.027 mmol) in toluene (1 cm^3) was added thionyl chloride (0.1 cm^3), and the solution heated at 80°C for 2 hours. The solvents

were removed, and the resulting 4-maleimidobutyryl chloride taken up into dichloromethane (0.05 cm^3) and added to a solution of **(50)** (9.9 mg, 0.007 mmol) and Et_3N (11.5 mg, 0.114 mmol) in 0.5 cm^3 of DMF. The solution was left at room temperature overnight, and a drop of water then added to hydrolyse any remaining acid chloride. The solution was then purified by reverse phase HPLC (t=0min. 90% A 10% B, t=30min. 25% A 75% B, 353nm) to yield a yellow solid T_R 17.3 min., 9.5 mg, 93%. Found: M^++1, 1075. $C_{48}H_{73}N_{10}O_{12}P_3$ requires M^++1, 1075. δ_H(400MHz) (D_2O) 1.42 (6 H, d, PCH_3), 1.48 (3 H, d, PCH_3), 1.32-1.65 (4 H, br, $(CH_2)_2CH_2NCO$), 1.65-1.78 (4 H, m, $(CH_2)_2CH_2NHCO$acridine), 1.82 (2 H, p, $NCH_2CH_2CH_2CO$), 2.28, *2.45* (2 H, 2xt (1:2), $N(CH_2)_2CH_2CO$), 3.05-3.60 (30 H, NCH_2 ring, NCH_2P, $NCH_2(CH_2)_2CO$, $NHCH_2(CH_2)_2CH_2NCO$, $CH_2NHCOCH_2NCO$), 3.72 (2 H, t, CH_2NHCOacridine), 3.78 (2 H, $(CH_2)(CH_2)NCH_2CO$), 3.98, *4.13* (2 H, 2xs (2:*1*), $CONCH_2CO$), 6.76, *6.78* (2 H, 2xs (1:2), CH=CH), 7.99 (2 H, t, H_6, H_3), 8.25-8.40 (6 H, d+t+d, H_5, H_4, H_7, H_2, H_8, H_1). $\delta_P(D_2O$; pD=4) 29.1, 24.8 (1:2)

Tri-maleimide-acridine functionalised ligand - **(61)**.

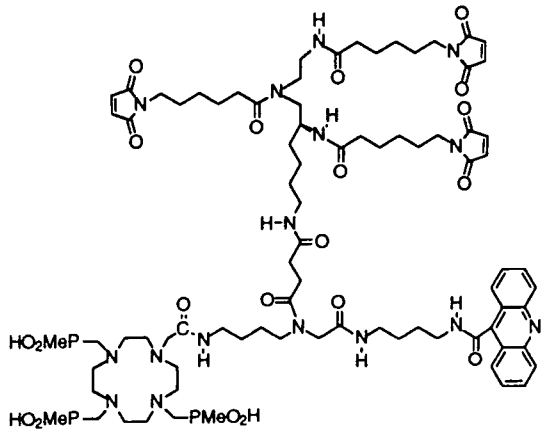

Oxalyl chloride (0.5 cm^3) was added to **(35)** (6.2 mg, 0.0074 mmol) and 1 drop of DMF added to the solution. After 45 minutes the solvents were removed and the resulting acid chloride immediately taken up into dry DMF (0.3 cm^3), and added to **(50)** (10.0 mg, 0.0068 mmol) followed by triethylamine (11.2 mg, 0.111 mmol). The

solution / suspension was left under nitrogen overnight, the DMF removed, and the solids taken up into water to be purified by reverse phase HPLC (t=0min. 90% A 10% B, t=30min. 25% A 75% B, 353nm) to yield the product T_R approx. 17 min. 1.2 mg, 8%. $\delta_H(CD_3OD)$ 1.1-1.9 (41 H, br m, PCH_3, $(CH_2)_2CH_2NHCO$acridine, $(CH_2)_2CH_2N(CO)CH_2$, $CH(CH_2)_3CH_2NHCO$, $CH_2(CH_2)_3CH_2$), 2.1-2.6 (10 H, br m, $CO(CH_2)_2CO$, $(CH_2)_4CH_2CO$), 2.60-4.0 (49 H, br m, CH_2N, CH_2NH, CHNH), 6.80 (6 H, s, CH=CH), 7.75 (2 H, t, H_6, H_3), 7.97.(2 H, t, H_7, H_2), 8.13 (2 H, d, H_5, H_4), 8.23 (2 H, d, H_8, H_1).

6.4.2 Chapter 5

(29) and (30) B72.3 Tri-Fab's, & (29), (30), and (31) A33 Tri-Fab's.

To 0.9 cm^3 of Fab' (B72.3 or A33) at approximately 20 mg ml^{-1} in 0.1M acetate-citrate-EDTA, pH 6.0 buffer was added 0.1 cm^3 of 50 mM β-ME in the same buffer. The solution was mixed and incubated at 37°C for exactly 30 min. and then desalted on a prepacked Sephadex G-25M PD-10 column equilibrated in the same buffer. The concentration of antibody in each eluted fraction was determined by measuring its absorbence at 280nm (A_{280}). A five fold excess of this reduced Fab' was added to the appropriate tri-maleimide, and the solution incubated at 37°C for 2-3 hours. The percentage of tri-Fab' formed was then determined by analytical gel filtration HPLC using a Bioseries Zorbax GF-250 column with 0.2 M sodium phosphate buffer as the eluant. Generally about 30% tri-Fab' was formed which was purified by HPLC using a preparative size gel column, or by gravity gel filtration overnight to give roughly 20% (3-4 mg) of pure product. The prepared triFab's were shown by gel electrophoresis (4 / 20 gradient polyacrylamide gel) to be pure, and to have a molecular mass of approximately 150,000 Da as determined using molecular weight markers whilst running the gel. An immunoassay also showed the tri-Fab's to have greater antigen binding ability than a whole antibody.

(34)-A33 tri-Fab'.

Reduced A33 Fab' was prepared as for the tri-Fab's of **(29)**, **(30)** and **(31)** except used 0.9 cm^3 of A33 Fab' (5 mg ml^{-1}) and 0.1 cm^3 of 50 mM β-ME to give after Fab' purification, a 1 cm^3 fraction of 3.79 mg ml^{-1} Fab'. This was added to the tri-maleimide **(34)** in ratios varying from 7:1 to 1:1 Fab' : **(34)** and incubated overnight at 37°C. The resultant solutions were analysed by gel HPLC showing the presence, albeit small, of the tri-Fab'. This observation was confirmed by gel electrophoresis. No purification was attempted.

Fab'-(24) and Fab'-(60).

To 1.35 ml of 5.0 mg ml^{-1} A33 Fab' was added 0.15 ml of 50 mM β-ME, the solution incubated for 30 minutes, and purified as for the synthesis of the tri-Fab's, to give 2 ml of reduced Fab' (3.29 mg ml^{-1}, 65.8 μM). To **(24)** (0.50 mg, 0.461 μmol) in DMF (30 μl) was added 1 ml of reduced Fab' to give a final ratio of 7:1 for **(24)** : Fab'. The solution was then incubated for 1 hour at 37°C and any unreacted linker **(24)** removed using a prepacked PD-10 Sephadex column to give 1 ml of 2.89 mg ml^{-1} Fab'-**(24)**. Similarly, to **(60)** (0.70 mg, 0.494 μmol) in 30 μl of DMF was added 1 cm^3 of the same reduced Fab', and the solution incubated and purified as before, to give 1 cm^3 of 3.10 mg ml^{-1} Fab'-**(60)**.

6.5 REFERENCES

1 A. Harrison, C. A. Walker, K. A. Pereira, D. Parker, L. Royle, K. Pulukkody, and T. Norman, *Magn. Reson Imag.*, 1993, **11**, 761.

2 J. Yaouanc, N. Le Bris, G. Le Gall. J-C. Clément, H. Handel, and H. des Abbayes, *J. Chem. Soc., Chem. Commun.*, 1991, 206.

3 O. Keller, and J. Rudinger, *Helv. Chim. Acta.*, 1975, **58**, 531.

4 S. Yoshitake, Y. Yamada, E. Ishikawa, and R. Masseyeff, *Eur. J. Biochem.*, 1979, **101**, 395.

5 J. P. L. Cox, A. S. Craig, I. M. Helps, K. J. Jankowski, D. Parker, M. A. W. Eaton, A. T. Millican, K. Millar, N. R. A. Beeley, and B. A. Boyce, *J. Chem. Soc. Perkin Trans. 1*, 1990, 2567.

6 A. Albert, and B. Ritchie, *Org. Syntheses Collective*, 1955, **3**, 53.

7 H. J. Barber, J. H. Wilkinson, and W. G. H. Edwards, *Chem. Ind.*, 1947, **66**, 411.

Appendices

APPENDIX 1

RESEARCH COLLOQUIA, SEMINARS AND LECTURES

Organised by the Department of Chemistry (Aug. 1991 - July 1994)

1991

October 17th — Dr. J. A. Salthouse,* University of Manchester.
Son et Lumière - A demonstration Lecture.

October 31st — Dr. R. Keeley, Metropolitan Police Forensic Science.
Modern Forensic Science.

November 6th — Prof. B. F. G. Johnson,† University of Edinburgh.
Cluster - Surface Analogues.

November 7th — Dr. A. R. Butler, University of St. Andrews.
Traditional Chinese Herbal drugs - a different way of treating disease.

November 13th — Prof. D. Gani,†* University of St. Andrews.
The chemistry of PLP-dependent Enzymes.

November 20th — Dr. M. More O' Ferrall,†* University College, Dublin.
Some Acid-Catalysed Rearrangements in Organic Chemistry.

November 28th — Prof. I. M. Ward, IRC in Polymer Science, University of Leeds.
The SCI Lecture - The Science and Technology of Orientated Polymers.

December 4th — Prof. R. Grigg,†* University of Leeds.
Palladium-Catalysed Cyclisation and Ion-Capture Process.

December 5th — Dr. A. L. Smith, ex Unilever.
Soap, Detergents and Black Puddings.

December 11th — Dr. W. D. Cooper, Shell Research.
Colloid Science - Theory and Practice.

1992

January 22nd — Dr. K. D. M. Harris,† University of St. Andrews.
Understanding the Properties of Solid Inclusion Compounds.

January 29th — Dr. A. Holmes,†* University of Cambridge.
Cycloaddition Reactions in the Service of the Synthesis of Piperidine and Indolizidine Natural Products.

January 30th — Dr. M. Anderson, Shell Research, Sittingborne.
Recent Advances in the Safe and Selective Control of Insect Pests.

February 12th — Dr. D. E. Fenton,†* University of Sheffield.
Polynuclear Complexes of Molecular Clefts as Models for Copper Biosites.

February 13th — Dr. J. Saunders, Glaxo Group Research Limited.
Molecular Modelling in Drug Discovery.

February 19th — Prof. E. J. Thomas,†* University of Manchester.
Applications of Organostannanes to Organic Synthesis.

February 20th — Prof. E. Vogel,* University of Cologne.
The Musgrave Lecture - Porphyrins - Molecules of Interdisciplinary Interest.

February 25th — Prof. J. F. Nixon, University of Sussex.
The Tilden Lecture - Phosphaalkynes - New Building Blocks in Inorganic and Organometallic Chemistry.

February 26th — Prof. M. L. Hitchmann,† University of Strathclyde.
Chemical Vapour Deposition.

March 5th — Dr. N. C. Billingham, University of Sussex.
Degradable Plastics - Myth or Magic ?

March 5th — Dr. S. E. Thomas,†* Imperial College.
Recent Advances in Organo-Iron Chemistry.

March 12th — Dr. R. A. Hann, ICI Imagedata.
Electronic Photography - An Image of the Future.

March 18th — Dr. H. Maskell,†* University of Newcastle.
Concerted or Stepwise Fragmentation in a Diamination Type Reaction.

April 7th — Prof D. M. Knight, Philosophy Department, University of Durham.
Interpreting Experiments - The Beginning of Electrochemistry.

May 13th — Dr. J-C. Gehret, Ciba Geigy, Basel.
Some Aspects of Industrial Agrochemical Research.

October 15th — Dr. M. Glazer, Dr. S. Tarling, Oxford University & Birbeck College.
It Pays to be British ! - The Chemist's Role as an Expert Witness in Patent Litigation.

October 20th — Dr. H. E. Bryndza,* Du Pont Central Research.
Synthesis, Reactions and Thermochemistry of Metal (Alkyl) Cyanide Complexes and Their Impact on Olefin Hydrocyanation Catalysis.

October 22nd — Prof. A. Davies,* University College London.
The Ingold-Albert Lecture - The Behaviour of Hydrogen as a Pseudometal.

October 28th — Dr. J. K. Cockcroft,* University of Durham.
Recent Developments in Powder Diffraction.

October 29th — Dr. J. Emsley, Imperial College, London.
The Shocking History of Phosphorus.

November 4th — Dr. T. P. Kee, University of Leeds.
Synthesis and Co-ordination Chemistry of Silylated Phosphites.

November 5th — Dr. C. J. Ludman,* University of Durham.
Explosions - A Demonstration Lecture.

November 11th — Prof. D. Robins,†* Glasgow University.
Pyrrolizidine Alkaloids - Biological Activity, Biosynthesis and Benefits.

November 12th — Prof. M. R. Truter, University College, London.
Luck and Logic in Host - Guest Chemistry.

November 18th — Dr. R. Nix,† Queen Mary College, London.
Characterisation of Heterogeneous Catalysts.

November 25th — Prof. Y. Vallee. University of Caen.
Reactive Thiocarbonyl Compounds.

November 25th — Prof. L. D. Quin,† University of Massachusetts, Amherst.
Fragmentation of Phosphorous Heterocycles as a Route to Phosphoryl Species with Uncommon Bonding.

November 26th Dr. D. Humber, Glaxo, Greenford.
AIDS - The Development of a Novel Series of Inhibitors of HIV.

December 2nd Prof. A. F. Hegarty, University College, Dublin.
Highly Reactive Enols Stabilised by Steric Protection.

December 2nd Dr. R. A. Aitken,†* University of St. Andrews.
The Versatile Cycloaddition Chemistry of $Bu_3P.CS_2$.

December 3rd Prof. P. Edwards, Birmingham University.
The SCI Lecture - What is Metal ?

December 9th Dr. A. N. Burgess,†* ICI Runcorn.
The Structure of Perfluorinated Ionomer Membranes.

1993

January 20th Dr. D. C. Clary,†* University of Cambridge.
Energy Flow in Chemical Reactions.

January 21st Prof. L. Hall, Cambridge.
NMR - Window to the Human Body.

January 27th Dr. W. Kerr,* University of Strathclyde.
Development of the Pauson-Khand Annulation Reaction : Organocobalt Mediated Synthesis of Natural and Unnatural Products.

January 28th Prof. J. Mann,* University of Reading.
Murder, Magic and Medicine.

February 3rd Prof. S. M. Roberts, University of Exeter.
Enzymes in Organic Synthesis.

February 10th Dr. D. Gillies,† University of Surrey.
NMR and Molecular Motion in Solution.

February 11th Prof. S. Knox,* Bristol University.
The Tilden Lecture - Organic Chemistry at Polynuclear Metal Centres.

February 17th Dr. R. W. Kemmitt,† University of Leicester.
Oxatrimethylenemethane Metal Complexes.

February 18th Dr. I. Fraser, ICI Wilton.
Reactive Processing of Composite Materials.

February 22nd — Prof. D. M. Grant, University of Utah.
Single Crystals, Molecular Structure, and Chemical-Shift Anisotropy.

February 24th — Prof. C. J. M. Stirling,† University of Sheffield.
Chemistry on the Flat-Reactivity of Ordered Systems.

March 10th — Dr. P. K. Baker, University College of North Wales, Bangor.
Chemistry of Highly Versatile 7-Coordinate Complexes.

March 11th — Dr. R. A. Y. Jones, University of East Anglia.
The Chemistry of Wine Making.

March 17th — Dr. R. J. K. Taylor,†* University of East Anglia.
Adventures in Natural Product Synthesis.

March 24th — Prof. I. O. Sutherland,†* University of Liverpool.
Chromogenic Reagents for Cations.

May 13th — Prof. J. A. Pople, Carnegie-Mellon University, Pittsburgh, USA.
The Boys-Rahman Lecture - Applications of Molecular Orbital Theory.

May 21st — Prof. L. Weber, University of Bielefeld.
Metallo-phospha Alkenes as Synthons in Organometallic Chemistry.

June 1st — Prof. J. P. Konopelski, University of California, Santa Cruz.
Synthetic Adventures with Enantiomerically Pure Acetals.

June 2nd — Prof. F. Ciardelli, University of Pisa.
Chiral Discrimination in the Stereospecific Polymerisation of Alpha Olefins.

June 7th — Prof. R. S. Stein, University of Massachusetts.
Scattering Studies of Crystalline and Liquid Crystalline Polymers.

June 16th — Prof. A. K. Covington, University of Newcastle.
Use of Ion Selective Electrodes as Detectors in Ion Chromatography.

June 17th — Prof. O. F. Nielsen, H. C. Ørsted Institute, Copenhagen University.
Low-Frequency IR and Raman Studies of Hydrogen Bonded Liquids.

September 13th — Prof. Dr. A. D. Schlüter, Freie Universität Berlin.
Synthesis and Characterisation of Molecular Rods and Ribbons.

September 13th Dr. K. J. Wynne, Office of Naval Research, Washington.
Polymer Surface Design for Minimal Adhesion.

September 14th Prof. J. M. DeSimone, University of North Carolina, Chapel Hill.
Homogeneous and Heterogeneous Polymerisations in Environmentally Responsible Carbon Dioxide.

September 28th Prof. H. Ila, North Eastern Hill University, India.
Synthetic Strategies for Cyclopentanoids via Oxoketene Dithioacetals.

October 4th Prof. F. J. Feher,† University of California, Irvine.
Bridging the Gap Between Surfaces and Solution with Sessilquioxanes.

October 14th Dr. P. Hubberstey, Nottingham University.
Alkali Metals - Alchemist's Nightmare, Biochemist's Puzzle and Technologist's Dream.

October 20th Dr. P. Quayle,† University of Manchester.
Aspects of Aqueous ROMP Chemistry.

October 21st Prof. R. Adams,†* University of South Carolina.
Chemistry of Metal Carbonyl Cluster Complexes - Development of Cluster Based Alkyne Hydrogenation Catalysts.

October 27th Dr. R. A. L. Jones,†* Cavendish Laboratory.
Perambulating Polymers.

November 10th Prof. M. N. R. Ashfold,† University of Bristol.
High Resolution Photofragment Translational Spectroscopy : A New Way to Watch Photodissociation.

November 17th Dr. A. Parker,†*Laser Support Facility, RAL.
Applications of Time Resolved Resonance Raman Spectroscopy to Chemical and Biochemical Problems.

November 24th Dr. P. G. Bruce,†* University of St. Andrews.
Structure and Properties of Inorganic Solids and Polymers.

November 25th Dr. R. P. Wayne, Oxford University.
The Origin and Evolution of the Atmosphere.

December 1st Prof. M. A. McKervey,†* Queen's University, Belfast.
Synthesis and Applications of Chemically Modified Calixarenes.

December 8th Prof. O. Meth-Cohan,† University of Sunderland.
Friedel's Folly Revisited - A Super Way to Fused Pyridines.

December 16th Prof. R. F. Hudson, University of Kent.
Close Encounters of the Second Kind.

1994

January 26th Prof. J. Evans,† University of Southampton.
Shining Light on Catalysts.

February 2nd Dr. A. Masters,† University of Manchester.
Modelling Water Without Using Pair Potentials.

February 9th Prof. D. Young,†* University of Sussex.
Chemical and Biological Studies on the Coenzyme Tetrahydrofolic Acid.

February 16th Prof. K. H. Theopold, University of Delaware, USA.
Paramagnetic Chromium Alkyls - Synthesis and Reactivity.

February 23rd Prof. P. M. Maitlis,† University of Sheffield.
Across the Border : From Homogeneous to Heterogeneous Catalysis.

March 2nd Dr. C. Hunter,†* University of Sheffield.
Non Covalent Interactions Between Aromatic Molecules.

March 9th Prof. F. Wilkinson, Loughborough University of Technology.
Nanosecond and Picosecond Laser Flash Photolysis.

March 10th Prof. S. V. Ley,* University of Cambridge.
New Methods for Organic Synthesis.

March 25th Dr. J. Dilworth,* University of Essex.
Technetium and Rhenium Compounds with Applications as Imaging Agents.

Apil 28th Prof. R. J. Gillespie, McMaster University, Canada.
The Molecular Structure of some Metal Fluorides and Oxofluorides - Apparent Exceptions to the VSEPR Model.

May 12th Prof. D. A. Humphreys, McMaster University, Canada.
Bringing Knowledge to Life.

† Invited specially for the graduate training programme. *Author's attendance.

APPENDIX 2

CONFERENCES ATTENDED

1.	Stereochemistry at Sheffield, University of Sheffield.	December 18th 1991
2.	North East Graduate Symposium, University of Durham.	April 3rd 1992
3.	XVIII International Symposium of Macrocyclic Chemistry, University of Twente, Enschede, Netherlands.	June 27th - July 2nd 1993
4.	R.S.C. U.K. Macrocycles Group, University of Warwick.	January 5th - 6th 1994

APPENDIX 3

PUBLICATIONS

1. D. Parker, K. P. Pulukkody, T. J. Norman, A. Harrison, L. Royle, and C Walker, *J. Chem. Soc., Chem. Commun.*, 1992, 1442.

2. K. P. Pulukkody, T. J. Norman, D. Parker, L. Royle, and C. J. Broan, *J. Chem. Soc. Perkin Trans. 2*, 1993, 605.

3. A. Harrison, C. A. Walker, K. A. Pereira, D. Parker, L. Royle, K. Pulukkody, and T. J. Norman, *Magn. Reson. Imag.*, 1993, **11(6)**, 761.

4. T. J. Norman, F. C. Smith, D. Parker, A. Harrison, L. Royle, and C. A. Walker, *Supramolecular Chem.*, 1994, (in press).